ISSN 1018-5593

European Commission

technical steel research

Properties and service performance

Application of FeE460, a comparative investigation towards normalized, quenched and tempered, and thermomechanically treated steel types

Report

EUR 15807 EN

STEEL RESEARCH

European Commission

technical steel research

Properties and service performance

Application of FeE460, a comparative investigation towards normalized, quenched and tempered, and thermomechanically treated steel types

J. Vuik, J. Van Wortel

Tno Metaalinstituut
Postbus 541
7300 Am Apeldoorn
The Netherlands

Contract No 7210-KA/607

1 July 1988 to 30 June 1990

Final report

Directorate-General XII
Science, Research and Development

1996

EUR 15807 EN

Cataloguing data can be found at the end of this publication

Luxembourg: Office for Official Publications of the European Communities, 1996

ISBN 92-827-7200-4

Printed in Luxembourg

CONTENTS

1 SUMMARY

In this summary, the items that have been investigated and the main results of the research contract 7210/KA/607-F-1.3/88, "Application of FeE460, a comparative investigation towards normalized, quenched and tempered, and thermo mechanically treated steel types" are described.

The steels mentioned before, have been investigated (in the plate thicknesses 15 and 50 mm) on the items:

- mechanical properties and microstructure after a weld thermal simulation
- cold cracking susceptibility
- mechanical properties of test welds
- mechanical properties after deformation at different temperatures, and
- calculation of the price-effect of application of FeE460 instead of FeE355.

The results of the weld thermal simulation programme established that acceptable hardness values and good Charpy-V notch toughness properties can be obtained with all three steels. PWHT at temperatures of 560° or 590°C reduced the fracture energies of the QT material, and deteriorated the properties of the N and TM material. 530°C is an acceptable PWHT temperature. At high PWHT temperatures, all materials fractured intergranular (at low test temperatures). This has been associated with segregation of P to former austenite grain boundaries. At higher test temperatures the presence of V carbonitrides further reduces the Charpy-V fracture energy for the materials TM and N.

As a result of the cold cracking experiments it appeared that for a very low hydrogen content (less than 3 ml/100 gr) both the QT and TM material could be welded (at 11 kJ/cm) without preheating for both plate thicknesses (15 and 50 mm).
Increasing the hydrogen content resulted in the necessity to pre-heat. The N material required pre-heating for both thicknesses, for all hydrogen levels.
The results of these tests have been compared to BS 5135, the conclusion is that for the high restraint level that was present in the tests, the prediction of BS is not correct. Especially for the QT and TM steels, unsafe predictions can be obtained.

The mechanical properties of the test welds showed that the N material has rather unfavourable Charpy-V and CTOD properties in the HAZ. For this steel, no PWHT is to be advised, and certainly not above 530°C.

The QT material results in very good Charpy-V and CTOD properties, not influenced by PWHT. The behaviour of the TM material is less good than the QT material, but better than the N material. PWHT is only advisable at 530°C.

After deformation at temperatures below AC1, the Re, Rm and A5 values change considerably. For some conditions the values do not meet the DIN 17102 requirements. Especially the Re/Rm value of the TM material reacts very strong on deformation. The Charpy-V fracture energies tend to show a shift of the TT40 towards less favourable values. The effect differs from steel to steel.
Simulating the hot forming process by means of austenitizing treatments showed that the normalized FeE460 is very susceptable to a loss of strength and toughness after such a treatment. This loss in yield strength, Charpy-V fracture energy and CTOD properties showed a clear relationship with the coarsening of the ferrite greain size. Only very high heating and cooling rates, together with reduced peak temperatures led to acceptable results.

The calculation performed on three pressure vessels and one bridge showed that for the pressure vessels, considerable savings can be achieved, depending on the wall thickness, etc. Savings up to 23% have been calculated. For the use of FeE460 in a bridge, less, if any, savings can be expected. This is caused by the fact that for a bridge, fatigue and stability are properties which play an important role. Compared to a bridge, a pressure vessel is much more determined by strength alone.

The general conclusion of the research programme is that FeE460 can be welded and used in a way very similar to FeE355. The strength level is not that much higher that the behaviour of the material is totally different.
Depending on the choice of base material, welding consumables, heat input, PWHT temperature etc. structures can be built with a good resistance to (the initiation of) brittle fracture.
A good choice of base material and consumables makes even welding without pre-heating possible.

From the results of the research programme, it could be concluded that the QT material is to be preferred, especially for application at temperatures below 0°C.
The N material behaves somewhat less good, the properties of the TM material being in between those of the QT and the N material. The mechanical properties of the welded joints tend to get less favourable with increasing vadium contact of the base material. It is therefore recommended to limit the vanadium contact to approx. 0.08%.

It should be emphasized however that the chemical analysis of the base material, and the production routes of the steel producer are the key factors with respect to the mechanical properties of the material after welding, bending etc.. It is therefore possible that in practice, the respective base materials respond different to the manufacturing processes compared to the results presented in this report.

1 RESUMÉ

Dans ce récapitulatif figurant les diférents points étudiés et les principaux résultats du contrat de recherche 7210/KA607-F-1.3/88, "Application of FeE460, a comparative investigation towards normalised, quenched and tempered, and thermo-mechanically treated steel types".

Les types d'acier cités plus haut ont fait l'objet d'études (dans les épaisseurs de plaques de 15 et 50 mm), notamment en ce qui concerne les points suivants:

- propriétés mécaniques et microstructure après simulation thermique d'un soudage;
- propension au fissurage à froid;
- propriétés mécaniques de soudures d'essais;
- propriétés mécaniques après déformation à différentes températures, et,
- calcul de l'impact financier de l'utilisation du FeE460 comme subsituant au FeE355.

Les résultats de programme de simulation d'un soudage ont révélé que les trois types d'acier ont une dureté satisfaisante et une bonne résistance le test Charpy-V. Le traitement thermique post-soudage (PWHT) effectué à des températures de 560°C ou 590°C a entraîné une réduction des énergies de rupture du matériau QT et affecté les propriétés des matériaux N et TM. 530°C s'avère être une température de PWHT satisfaisante. A des tempéatures de PWTH élevées, tous les matériaux se sont fractionnés en grains (à de basses températures de test). Ceci allait de pair avec une ségrégation du P vers les joints préalables de granulation austénitique. A des températures d'essais plus importantes, la présence de carbonne nitruré de V réduit l'énergie de ruputre des matériaux TM et N selon Charpy-V.

Après le déroulement des expériences sur la fissuration à froid, il s'est avéré qu'en présence d'une très faible quantité d'hydrogène (moins de 3 ml/100g) les matériaux QT et TM pouvaient être soudés (à 11 kJ/cm) sans avoir à recourir à un préchauffage pour les deux épaisseurs de plaques (15 et 50 mm). L'augmention du volume d'hydrogène rendait le préchauffage nécessaire.
Quant aux matériaux de type N, ils requiéraient de toute façon un préchauffage pour les deux épaisseurs de plaques et quelque soit le volume d'hydrogène.
Les résultats de ces tests ont été comparés à la norme britannique BS 5135 et l'on peut en conclure que, vues les fortes contraintes utilisées dans les test, la précalculation de la norme britannique ne peut être retenue. Notamment en ce qui concerne les aciers QT et TM, les précalculations peuvent même s'auvérer fausses.

Les propriétés mécaniques des sourdures d'essai ont démontré que le matériau N se comporte de façon plutôt insatisfaisante, en subissant le test Charpy-V et celui du déplacement de l'écartement de l'extrémité de la fissure (CTOD) dans la Z.T.A. En ce qui concerne de ce type d'acier, aucun PWHT nu saurait être recommandé et en tous cas certainement pas à des températures supérieures à 530°C.

Le matériau QT donne de très bons résultats au test Charpy-V et CTOD à condition de ne pas subir l'influence d'un PWHT. Le comportement du matériau TM est moins satisfaisant que celui du matériau QT mais donne de meilleurs résultats que le matériau N. Pour le matériau TM un PWHT ne saurait être recommandé qu'à une temperature de 530°C.

Après déformation à des températures inférieures à ACI, les valeurs Re, Rm et A5 varient considérablement. Dans certaines conditions, les valeurs ne répondent même plus à la norme DIN 17102. Tout particulièrement la valeur Re/Rm du matériau TM réagit très sensiblement en cas de déformation. L'énergie du rupture Charpy-V a une tendance à révéler un glissement de la Température de Transition TT 40 vers des valeurs moins satisfaisante. L'effet est différent selon le type d'acier.

La simulation du processus de formagé à chaud au moyen du traitement par austénitisation a démontré que le FeE460 normalisé a une forte tendance à perdre en résistance et en dureté après un tel traitement. Ce recul de la limite d'élasticité ajouté à la perte d'énergie de rupture Charpy-V et à la perte des propriétés CTOD ont démontré clairement l'interdépendance avec la grossièreté de la taille des grains de ferrite. Seules des vitesses de chauffe et de refroidissement très élevées ainsi qu'une réduction des crêtes thermiques permettent d'obtenir des résultats satisfaisants.

Le calcul effectué sur la base de 3 vases de pressurisation et d'un pont a révélé que des économies considérables pouvaient être réalisées en ce qui concerne les vases de pressurisation en fonction de l'épaisseur des parois, etc. On a calculé des économies de l'ordre de 23 %. En ce qui concerne l'utilisation du FeE460 dans la contruction d'un pont, les économies - si tant est qu'elles soient même réalisables - seront en tous cas beaucoup moins importantes.

Ceci est dû au fait que la fatique et la stabilité d'un pont sont les facteurs déterminants. A l'inverse du pont, le facteur le plus déterminant d'un vase de pressurisation est beaucoup plus sa résistance à des forces.

La conclusion globale de ce programme de recherche est que le FeE460 peut être soudé et utilisé de façon très similaire au FeE355. Le niveau de résistance n'est pas supérieur à un point tel que le comportement du matériau soit à différent. C'est en fonction du choix des matériaux de base, des électrodes à autoconsommation, de l'adduction de chaleur, de la température choisie pour le PWHT, etc. que les structures peuvent être construites tout en offrant une bonne résistance à la rupture fragile. C'est en choissisant le bon matériau de base et les bonnes éléctrodes à autoconsommation qu'il est possibles d'effectuer une soudre sans même recourir à un préchauffage.

On peut conclure des résultats de ce programme de recherche qu'il convient de préférer le matériau QT spécialement en ce qui concerne les utilisations à des températures inférieurs à 0°C.
Le matériau N se comporte de façon moins satisfaisante, les propriétés du matériau TM se situant entre les deux. De toute façon, il convient d'insister sur le fait que l'analyse chimique du matériau de base et les modes de production choisis par les fabricants d'acier sont, dans cette perspective, les facteurs déterminants. C'est pourquoi, dans la pratique, les matériaux de base peuvent répondre respectivement de façon différente aux procédés de fabrication comparés aux résultats tels qu'ils apparaissent dans ce protocole.

1 ZUSAMMENFASSUNG

Die vorliegende Zusammenfassung beschreibt den Gegenstand und die entscheidenden Ergebnisse der Vertragsuntersuchung 7210/KA/607-F-1.3/88 "Application of FeE460, a comparative investigation towards normalised, quenched and tempered, and thermomechanically treated steel types".

Der obengenannte Stahl wurde (für Blechdicken von 15 und 50 mm) einer Untersuchung unterzogen, die sich auf die folgenden Punkte bezog:

- mechanische Eigenschaften und Mirkostrukturen nach einer thermischen Schweisssimulation;
- Kaltrissempfindlichkeit;
- mechanische Eigenschaften von geschweisste Proben;
- mechanische Eigenschaften nach Verformung bei verschiedenen Temperaturen;
- Berechnung des Preis-Leistungsverhältnisses bei der Verwendung von FeE460 anstelle von FeE355.

Die Ergebnisse des thermischen Schweisssimulationsprogramms zeigen, dass sich bei allen drei Stahlsorten akzeptabele Härtegrade und gute Charpy-V Kerbbiege-Eigenschaften erzielen lassen. Spannungsarm glühen bei Temperaturen von 560°C oder 590°C verringerte die Bruchenergie des QT-Werkstoffs und verschlechterte die Eigenschaften der N- und TM-Werkstoffe. 530°C ist eine akzeptabele Spannungsarmglühtemperatur. Bei hohen Spannungsarmglühtemperaturen brachen alle Werkstoffe intergranular (bei niedrigen Testtemperaturen). Dies wurde mit der Anreicherung des Phosphorus bei den ursprünglichen Austenit-Korngrenzen in Zusammenhang gebracht. Bei höheren Testtemperaturen senken die vorhandenen Vanadium-Karbonitride die Charpy-V-Bruchenergie der TM- und N-Werkstoffe zusätzlich.

Die Kaltrissversuche zeigten, dass sich sowohl der QT- als auch der TM-Werkstoff bei einem sehr niedrigen Wasserstoffgehalt (weniger als 3 ml/100 gr) ohne Vorwärmen in beiden Blechdicken (15 und 50 mm) schweissen lassen (bei 11 kJ/cm).
Mit steigendem Wasserstoffgehalt ist Vorwärmen erforderlich. Beim N-Werkstoff war für beide Blechdicken eine Erhitzung erforderlich, und zwar galt dies für beliebige Wasserstoffanteile.
Die Ergebnisse dieser Tests wurden mit denen des BS 5135 verglichen. Aus diesem Vergleich lassen sich folgende Schlüsse ziehen: das hohe Spannungsniveau während der Tests entspricht nicht den Voraussagen des BS. Besonders die Einschätzungen für QT- und TM-Stahl könnten falsch sein.

Die mechanische Eigenschaftsprüfung der geschweissten Proben ergab, dass der N-Werkstoff ziemlich ungünstige Charpy-V und CTOD-Eigenschaften in der Wärmeeinflusszone besitzt. Für diese Stahlsorte ist ein Spannungsarmglühen nicht empfehlenswert. Dies gilt insbesondere für den Temperaturbereich oberhalb von 530°C.
Der QT-Werkstoff weist sehr gute Charpy-V- und CTOD-Eigenschaften auf, die nicht vom Spannungsarmglühen beeinflusst werden. Das Verhalten des TM-Werkstoffs ist schlechter als das des QT-Werkstoffs, allerdings besser als das des N-Werkstoffs. Spannungsarmglühen ist nur bei einer Temperatur von 530°C empfehlenswert.

Nach der Verformung der Teststücke bei Temperaturen unter AC1 ändern sich die Re-, Rm- und A5-Werte erheblich. Unter bestimmten Bedingungen genügen diese Werte noch nicht einmal den Anforderungen der DIN 17102.
Der Re/Rm-Wert des TM-Werkstoffs reagiert besonders stark auf Verformung. Die Charpy-V-Bruchenergien tendieren bei der Unwandlungstemperatur TT40 zu ungünstigeren Werten. Dies wirkt sich unterschiedlich auf die einzelnen Stahlsorten aus.
Die Simulierung des Wärmeverformungsverfahrens mit Hilfe von Austenitisierungsbehandlungen zeigten, dass das normalgeglühte FeE460 sehr empfindlich für Festigkeits- und Zähigkeitsverlust nach einer derartigen Behandlung ist. Der Verlust an Streckspannung, Charpy-V-Bruchenergie und CTOD-Eigenschaften steht in klarem Zusammenhang mit der Ferritkornvergröberung. Nur sehr hohe Erhitzungs- und Abkühlungsraten führten zusammen mit reduzierten Spitzentemperauren zu akzeptabelen Ergebnissen.

Die Berechnungen, die an drei Druckbehältern und einer Brücke durchgeführt wurden, ergaben in Abhängigkeit von der Wandstärke usw. erhebliche Einsparungsmöglichkeiten für die Druckbehälter. Es wurden Einsparungen bis zu 23% berechnet. Bei der Verwendung von FeE460 in einer Brückenkonstruktion sind, wenn überhaupt, weniger Einsparungen zu erwarten.
Der Grund hierfür ist die Tatsache, dass bei einer Brücke Materialermüdung und Stabilität eine wichtige Rolle spielen. Ein Druckbehälter hingegen wird hauptsächlich von der Materialfestigkeit bestimmt.

Allgemein lässt sich aus dem Untersuchungsprogramm der folgende Schluss ziehen: FeE460 lässt sich in ähnlicher Weise wie FeE355 verarbeiten. Die Streckgrenze ist nicht soviel höher, sodass das Materialverhalten vollkommen anders ist.
Abhängig von der Wahl des Ausgangsmaterials, des Schweisszusatzmaterials, der Wärmezufuhr, der

Spannungsarmglühtemperatur usw. lassen sich Strukturen mit einer guten Sprödbruchwiderstand herstellen (auch gegen einsetzenden Sprödbruch beständig).
Die richtige Wahl des Ausgangsmaterials und des Schweisszusatzmaterials ermöglicht sogar ein Schweissen ohne Vorwärmen.

Aufgrund der Untersuchungsergebnisse läge die Vermutung nahe, dass der QT-Werkstoff, insbesondere bei Temperaturen unter 0°C, zu bevorzugen sei. Im Vergleich dazu weist der N-Werkstoff schlechtere Eigenschaften auf; die Eigenschaften des TM-Werkstoffs liegen irgendwo zwischen denen des QT- und dem N-Werkstoffs. Es sei allerdings nachdrücklich darauf hingewiesen, dass die chemische Analyse des Ausgangsmaterials und das vom Stahlproduzenten verwendete Herstellungsverfahren in dieser Hinsicht entscheidende Faktoren sind. Es ist daher möglich, dass das entsprechende Ausgangsmaterial in der Praxis anders reagiert als aufgrund der Ergebnisse dieses Berichts zu erwarten wäre.

2 INTRODUCTION TO THE RESEARCH PROGRAMME

In the past decades, the greater part of the high integrity steel constructions have been designed and built in steel grades equivalent to BS 4360 Gr 50. Developments in steelmaking have led to a more uniform steel quality, with a low level of impurities and interstitials, and improved fracture toughness at subzero temperatures.

Together with the use of modern, low hydrogen/high toughness welding consumables (both manual metal arc welding, gas metal arc welding and submerged arc welding) and knowledge, gained from several extensive research programmes, this leads to a situation in which relatively few problems are encountered in practice when welding Gr 50 materials.

Although on one hand the application of these materials clearly offers benefits, the relatively low yield strength on the other hand leads to the use of relatively thick materials. This means that for constructions in which the wall thickness is not determined by the required stiffness, a substantial reduction in wall thickness can be achieved when applying higher yield strength steels. This reduction in wall thickness reduces weight, welding time and the amount of welding consumables. The reduction in weight can be very beneficial, e.g. in the case of cranes, transport equipment and all constructions that have to be lifted, transported and placed as a whole. In addition, forming operations can be performed more easily on thinner sections.

The steels that can be considered to be competitive for specific applications with the grade 50 material, have a yield strength of approx 460 N/mm^2. This strength level can be achieved by three different ways of producing steel, i.e.

- normalizing (+ tempering);
- quenching + tempering, and
- thermo mechanical treatment.

Although all three steel types have comparable tensile properties, differences exist with respect to the fracture toughness properties and the chemical composition. These differences determine for the greater part the weldability of the material, the susceptibility for embrittlement of the HAZ after stress relieve heat treatment, and the mechanical properties after (hot) forming.

In the present research programme, normalized, quenched and tempered, and thermo-mechanically treated steel types have been subjected to an extensive research programme that is divided into the following main parts:

- Weld thermal simulation tests
- Cold cracking susceptibility
- Qualification and stress relieve heat treatment
- Mechanical properties after (hot) forming.

The data obtained in this research programme have been used to calculate for some structures the difference in fabrication cost when applying FeE 460 instead of BS 4360 Gr 50 material.

3 EXPERIMENTAL PROGRAMME

In this research programme, three types of FeE 460 are tested:

- normalized (and tempered)
- quenched and tempered
- thermo-mechanically treated.

  The thermo-mechanically treated steels have been rolled according to a characteristic TM scheme (specific deformations at well defined temperatures), and have cooled in air.

For each type of steel, two plate thicknesses have been selected: 15 and 50 mm.
The chemical analysis and mechanical properties (certificate values) are given in Table 3.1 and 3.2.
For the part of the project in which the properties of the normalized material after a normalizing treatment have been established, a second normalized 50 mm thick steel has been selected. This steel is called X in Table 3.1 and 3.2.

4 WELD THERMAL SIMULATION

4.1 Aim

The aim of this part of the investigation was to get a thorough understanding of the respons of each steel type to different thermal treatments and to select the cooling times and PWHT temperatures for the qualification programme. By applying weld thermal simulation the different steel types could be compared in detail.

4.2 Programme

The program consisted of determination of hardness, microstructure and Charpy-V fracture toughness properties for a number of peak temperatures and cooling times, see also Table 4.1.
Each combination of peak temperature and cooling time has been tested in the as simulated condition and in several PWHT conditions. The PWHT temperatures were the same as used for the selection of the welding consumables (530, 560, 590°C).
The heating and cooling rates during PWHT amounted to 55°C/h, the hold time on the prescribed temperature amounted to one hour.
The weld thermal simulation tests have been performed on the normalized material N (plate thickness 50 mm), the quenched and tempered material QT (plate thickness 50 mm) and the thermomechanically treated material TM (plate thickness 15 mm). The reason for the selection of the 15 mm plate is that although the 50 mm plate has been delivered in the TM condition it is originally meant to be normalized afterwards. Because of delivery time this plate was accepted, but the chemical analysis is not optimised for TM steel. Therefore, the 15 mm plate which has a genuine TM composition, was selected for the fabrication of the weld thermal simulation specimens.
For the two 50 mm materials (N and QT) the specimens have been taken from the position 2 mm below plate surface. For the 15 mm material (T) the specimens were taken from the position mid-thickness. In all cases transverse specimens have been used.

4.3 Results

4.3.1 Hardness

The results of the hardness measurements in the as delivered condition and after weld thermal simulation at 1350 and 1050°C with and without a post weld heat treatment at 530, 560 or 590°C are given in Figure 4.1 - 4.8.

From Figure 4.1 it appears that after a peak temperature of 1350°C material N gives higher hardness values than the TM material. For a cooling time of 7 sec. the hardness level of the QT material lies in between the hardness level of material N and TM and exceeds the HV = 350 limit.

At higher cooling times the hardness decrease in the QT material is rather pronounced, which results for cooling times Δt (800-500) greater than 20 sec. in hardness values of the QT and TM material being about the same.

For a peak temperature of 1050°C the hardness level of material N is higher than for the material TM and QT. The hardness of the TM and QT material are comparable, see also Figure 4.2.

The higher hardness level of material N with respect to material TM can be ascribed to the higher carbon level and higher carbon equivalent of the N material.

The rather high hardness levels of material QT at Tp = 1350°C and Δt = 7 or 12 sec, cannot be explained. The carbon level and carbon equivalent of this material is even somewhat lower than of the TM material. It might be that the higher Cu and Ni content is responsible for this phenomenon.

Although neither the N nor the TM or QT material have reached their maximum hardness level at a cooling time Δt(800-500) of 7 seconds it can be stated that hardness levels are moderate. Hardness levels below 300 HV10 respectively 350 HV10, in the as simulated (= as welded) condition are for all three materials well within the possibilities. Although the TM material is somewhat better in this respect.

Figure 4.3 - 4.8 show that a post weld heat treatment at 530°C always leads to a decline in hardness (one exception in material QT after Tp = 1350°C, Δt(800-500) = 50 seconds, where the hardness after PWHT is about the same).

For the peak temperature of 1050°C (see Figure 4.4, 4.6 and 4.8) and a PWHT at 560°C or 590°C the hardness levels of material N and TM are slightly higher compared with the values after PWHT at 530°C. For the QT material the values after a PWHT at 560 and 590°C are about the same as they were at 530°C.

For the material simulated at 1350°C (see also Figure 4.3, 4.5 and 4.7) the hardness increase after PWHT at 560 or 590°C (compared with PWHT at 530°C) is even somewhat stronger and also in material QT the hardness can be somewhat higher compared with a PWHT at 530°C.
In five cases (N-1350°C-50 sec., N-1050°C-50 sec, TM-1350°C-50 sec., TM-1050°C-12 sec. and QT-1350°C-50 sec.) the hardness of the 560°C or 590°C PWHT even exceeds the value of the as simulated condition.

4.3.2 Charpy-V fracture energies

Full Charpy-V fracture curves are given in:
Figure 4.9-4.37 for the normalised material (N), Figure 4.38-4.66 for the thermal mechanically treated material (TM), and Figure 4.67-4.94 for the quenched and tempered material (QT).
From the transition curves, given in these figures, the transition temperatures at which the average fracture energy equals 40 Joules (TT40) have been derived. These TT40 temperatures are given in Table 4.2 and the Figures 4.95-4.105.

Both for the N, TM and QT material the fracture energies of the specimens simulated at a peak temperature of 1050°C exceed the values of the specimens simulated at a peak temperature of 1350°C.
The behaviour of the QT material after a simulation treatment at 1050°C is more or less comparable to the behaviour of the TM material: low TT40 temperatures in the as simulated condition which increase with cooling time $\Delta t(800\text{-}500)$, see also Figure 4.95. Compared to the N material, both the QT and the TM material showed excellent notch toughness properties.

After PWHT, the Charpy-V fracture energies of the QT and TM material improve considerably compared to the as simulated condition. For the N material simulated at 1050°C, the only PWHT that clearly improves the TT40 is 530°C. PWHT at 560°C does not clearly influence the toughness behaviour, whereas 590°C leads to less favourable values, see Figure 4.96, 4.97 and 4.98.

For the more critical 1350°C peak temperature it can be seen that in the as simulated condition the TT40 increases with cooling time, this is the case for all three materials, see Figure 4.99. Compared with the N material the TM and QT materials result in quite good Charpy-V notch toughness properties in the as simulated condition. Compared with the TM material, the QT material reached the change in TT40 towards unfavourable values at a relatively short cooling time Δt (800-500), i.e.

20 seconds.
The TM material has in that situation an acceptable TT40 of -25°C.

For all three materials PWHT at 530°C reduces the fracture energies considerably for a cooling time Δt(800-500) of 7 sec., for material QT this has also been found for a cooling time of 12 sec., see Figure 4.100-4.101.
For slower cooling times hardly any influence of the PWHT on the fracture energy of material N and QT has been found. For the TM material, PWHT at 530°C increases the TT40 approximately 15°C for the cooling times 12 and 20 sec., while the TT40 of the material simulated with a cooling time of 50 sec. is hardly influenced.

PWHT, at 560 or 590°C has a dramatic effect on the Charpy-V notch properties of material N and TM. This influence increased when the cooling rate was decreased, see Figure 4.100-4.103. For the QT material the drop in Charpy-V fracture energies after PWHT at 560 and 590°C is less dramatic or negligible compared to both other materials (except for a cooling time of 7 seconds).

For the simulation tests in the so-called intercritical temperature region the Ac1 and Ac3 temperatures were determined. These amounted to 734-866°C for material N, 721-864°C for material QT and 728-875°C for material TM. The simulation tests have been performed at Tp1 = 1350°C and Tp2 = 775°C, with Δt(600-400) = 13.6 and 23.6 sec. respectively. These values for Δt(600-400) correspond with Δt(800-500) values of 12 and 20 sec.
The results of these weld thermally simulation tests in the "intercritical temperature region" can be seen in Table 4.2 and Figure 4.16, 4.18, 4.22-4.24, 4.45-4.47, 4.51-4.53, 4.73-4.75 and 4.79-4.81 and are summarized in Figure 4.104 and 4.105.
Compared with the single simulation tests with Δt(800-500) = 12 sec., the TT40 values of the double simulation tests for material N were about the same. For material TM and QT the TT40 values were 45 resp. 30°C higher.
For the double simulation tests with Δt(600-400) = 22.6 sec. these results were practically the same, the shift of the TT40 of material QT (compared with the single simulation with the same Δt(800-500)) being slightly less.
For the N material only a PWHT at 530°C slightly increased the toughness. PWHT at 560 and 590°C gave lower toughness values than the as simulated condition.
For the TM material a (remarkable) toughness increase take place after a PWHT at 530°C and 560°C. This increase was most pronounced at a cooling time Δt(600-400) of 13.6 seconds. At a PWHT of

590°C the toughness of the TM material was about the same (at Δt(600-400) = 22.6 sec.) or was again decreased (at Δt(600-400) = 13.6 sec.).

The most likely explanation is that the intercritically reheating resulted in the formation of complex carbides including V and Nb. so that after PWHT no precipitates could be formed.
The Charpy-V fracture energies of material QT after double simulation always increased remarkable after PWHT at 530, 560 and 590°C.
After PWHT the TT40 values of the QT material after double simulation were always better than for the other two materials.

4.3.3 Microstructure of the weld thermally simulated specimens

4.3.3.1 Light optical microscopy

The light optical microstructure of the weld thermally simulated conditions are given in Figure 4.106-4.108. For each material, the figures show the microstructure of the specimens simulated at 1350°C, with the cooling times Δt(800-500): 7, 12, 20 and 50 seconds.

The decline in Charpy-V notch toughness properties that has been observed for all materials with increasing cooling time Δt(800-500) corresponds very well with the change into predominantly bainitic microstructures. The difference between the transition temperatures TT40 for the materials TM and QT at a cooling time Δt(800-500) = 20 seconds, can be explained from the relatively coarse, wide spaced bainite that is presenty in the QT material. Although this coarsening of the microstructure is even more significant for the cooling time of 50 seconds, this does not seem to further deteriorate the Charpy-V fracture energies of the QT material.
The microstructures of the 1350°C/12 sec. simulation condition after stress relieve heat treatment at 530°C, 560°C and 590°C are shown in Figures 4.109-4.111. For all materials, a large number of precipitates appear after PWHT.
However, there is no indication from this light optical metallographic examination for the cause of the dramatic drop in Charpy-V fracture energies of the N and TM materials when increasing the PWHT temperature from 530°C to 560°C or 590°C.

4.3.3.2 Scanning Electron Microscopy

Studied are the fracture surfaces of the Charpy-V specimens tested at low temperatures (brittle fracture). This has been done on specimens which were simulated at 1050°C with a cooling rate Δt(800-500) of 7 and 12 seconds and at 1350°C with cooling rates of 7, 12, 20 and 50 seconds, both in the as simulated condition and after post weld heat treatment at 530, 560 and 590°C.
The aim of this part of the investigation was to quantify the fracture behaviour of the materials. The results can be seen in Figure 4.112 and Table 4.3 and can be summarized as follows:

- in the as simulated condition the fracture is always transgranular,
- PWHT does not influence the fracture behaviour of material which has been simulated with a peak temperature of 1050°C; the fracture is always transgranular,
- in material which has been simulated with a peak temperature of 1350°C, PWHT can dramatically change the fracture behaviour (from transgranular to intergranular). The results depend on the cooling rate, Δt(800-500), PWHT temperature, and the base metal used, see also Figure 4.113-4.115,
- at a cooling rate of 7 seconds and, to a lesser extent, 12 seconds the materials are more sensitive for intergranular fracture than at a cooling rate of 20 seconds. However, at a cooling rate of 50 seconds the fracture was always fully transgranular, this was independent of the PWHT and material used,
- the percentage intergranular fracture increased with increasing post weld heat treatment temperatures,
- material QT appeared be more sensitive for intergranular fracture than material TM and N. The latter was somewhat less sensitive than material TM.

It is remarkable that the most sensitive material did not contained V while the least sensitive material contained the highest percentage V (0.15%).

4.3.3.3 Transmission Electron Microscopy

The most likely cause of the change of fracture mode for the materials after PWHT is a change in precipitation structure.
Both thin foils and extraction replicas have therefore been studied in a Transmission Electron Microscope. There is no evidence available that the precipitation structure
is the cause of the change in fracture mode. From the TEM study it did not appear that the grain

boundaries (α or former γ) were more decorated with precipitates for the 590°C PWHT condition compared with the 530°C PWHT condition, see for example Figure 4.116. Even at a proportion of 90% intercristalline fracture (material TM, Tp = 1350°C, Δt(800-500) = 7 sec. PWHT 590°C) the grain boundaries were decorated with precipitates of the same order of magnitude as for the PWHT conditions where the fraction of intergranular fracture was much less.
There was not a continuous string of carbides present, all carbides were isolated. So there was no relation between the quantity of the precipitates on the grain boundaries (strings-no strings) and the fracture behaviour, see Figure 4.117.

ED-spectroscopy has been performed on all three materials (on extraction replicas).
Analysed are the precipitates in the as delivered condition and in the as simulated (1050°C; Δt(800-500) = 12 sec., 1350 °C; Δt(800-500) = 12 and 50 sec.) and simulated + post weld heat treatment condition. The results can be seen in Table 4.4 and Figures 4.118-4.120.
In the as delivered condition and after PWHT the composition of the carbides in material N and QT are about the same. In material N they contained ~ 86% Fe, 12% Mn and 2% V; in material Q ~ 90% Fe and 10% Mn. V is not present. In the as delivered condition and after a PWHT at 530°C the carbides in material TM consisted of ~ 95% Fe, 4.8% Mn and 0.2% V. After a PWHT at 590°C the Mn and V percentage had doubled (Fe 90.7%, Mn 8.8% and V 0.5%).
The Mn and V (when present!) in the carbides of the weld thermally simulated material increases by increasing the post weld heat temperature. This tendency is independent of the peak temperature and cooling rate.
There is no relation between the composition of the carbides and the appearance of intergranular or transgranular fracture. For instance the material without V in the carbides (material QT) is the most sensitive for intergranular fracture, the material with the highest content V (material N) is less sensitive than both material TM and QT, see also Table 4.3 and Figure 4.112.

There is no evidence that the precipitates are the one and only influencing factor for the differences in fracture behaviour after PWHT.

4.3.3.4 Auger Analyses

The investigation has been performed on material N, TM and Q with a PWHT at 590°C after a weld thermal simulation of 1350°C, Δt(800-500) = 7 sec.

Table 4.3 shows that for all 3 the materials that condition gives the most pronounced intergranular fracture. The specimens were broken under high vacuum in the microscope (cold trap with nitrogen) and all specimens showed many intergranular facets.
The analyses have been taken on a surface of 26x15 or 20x30 mm.
The results of the analysis are shown in Figure 4.121-4.123.
On the intergranular facets of the normalized material P, C, Fe, and some Ni was found. After a sputtering time of 2 min. (sputtering depth ~ 90 nm) P had disappeared and only Fe and some C was present. On the intergranular facets of the thermomechanically treated material again P, C and Fe were found. After a sputtering time of 2 minutes P and C almost had disappeared.
The quenched and tempered steel showed the same behaviour as the steels mentioned before, so the intergranular facets contained P, C and Fe. After 2 minutes sputtering P had almost disappeared, C was present but less than at the original fracture surface. In the V containing steels no V could be detected on the intergranular facets,
In the transgranular facets of the three materials no or only minor amounts of P could be detected.

From the results it appears that the toughness behaviour of weld thermally simulated HAZ material after PWHT is influenced by:
- precipitation of carbides,
- phosphor segregation on the former austenite grain boundaries,
- the presence of coarse, well defined former austenite grain boundaries.

The presence of vanadium is considered to be not the decisive factor.

The statements given above mean that probably only the small zone in which coarse former austenite grains are present, next to the fusion line, is sensitive for this kind of toughness degradation after PWHT.
The fact that the QT material, which did not contain any V, showed the most pronouned intergranular fracture, but did not show a very dramatic drop in Charpy-V fracture energies after PWHT at 560 and 590°C can be explained as follows.
The behaviour of the material at low temperature (cleavage/intergranular fracture) is very much influenced by segregation of P to former γ grain boundaries. With increasing test temperature, the fracture mode changes from predomimantly inter- to transgranular.
Then, the level of the fracture energy is strongly influenced by the presence of Vanadium, carbonitrides, which is in accordance with the relatively high values for the QT material.

4.4 Conclusions

- The hardness in the as simulated conditions of the three materials is more or less decreased by a PWHT at 530°C. PWHT at 560 and 590°C mostly gives higher hardness values than PWHT at 530°C and sometimes the hardness even exceeds the hardness values of the as simulated conditions. However, hardness levels below 300 HV10, respectively 350 HV10 are, for all three materials, well within the possibilities. In this respect the TM material has the best behaviour, followed by the QT material and at last the N material.
- After simulation treatments at 1050°C the Charpy-V fracture energies always exceed the energies after simulation at 1350°C. For both the simulation temperatures the toughness values (expressed in TT40) increased with cooling time.
- After simulation at 1050°C the TM and QT material showed a better Charpy-V toughness behaviour than the N-material. For the TM and QT material PWHT at 530, 560, 590°C mostly leads to a increase in fracture toughness, while for the N material only
  PWHT at 530°C gives an increase in toughness (compared with the as simulated conditions).
- Simulation tests at a peak temperature of 1350°C showed that in the as simulated condition the toughness behaviour of the TM and QT material exceeds the behaviour of the N material.
  PWHT at 530, 560 and 590°C mostly remarkable reduces the toughness values. The toughness decrease at 560 and 590°C could be dramatic.
  The drop in Charpy-V toughness by a PWHT treatment is material, cooling time ($\Delta t(800\text{-}500)$ and PWHT temperature dependent.
  The toughness decrease by PWHT was more pronounced at higher cooling times (but at slower cooling times the values in the as simulated condition are much lower!)
  In general the TT40 values of the N material after PWHT were lower than for the TM and QT material (as it was in the as simulated conditions).
- Simulation tests in the so-called intercritically reheated zone (Tp1 = 1350, Tp2 = 775°C) showed for the N material about the same TT40 values as for single simulations with the same cooling time. Material TM and QT however showed at strong toughness decrease, which resulted for both materials in properties comparable with the N material.
  A PWHT treatment at 530°C always improves the impact properties of the intercritical zones (most for TM and QT). PWHT at a temperature of 560 and 590°C improved the toughness of the TM and QT material, while the toughness values of the N material became worse.
- The decline in Charpy-V notch toughness properties with increasing cooling time can be related with the change into predominantly bainitic microstructures, the kinetics of this processes being

material dependent.

- Toughness deterioration after PWHT coincided with a intercrystalline fracture mode. This toughness decrease is probably caused by the presence of P on the former austenite grain sizes and is enhanced when the former austenite grain sizes are well defined ($\Delta t(800\text{-}500)$ is increased).
- The fracture behaviour at temperatures at which transgranular fracture becomes more important than intergranular fracture is determined to a great extent by the presence of Vanadium carbonitrides.

5 COLD CRACKING SUSCEPTIBILITY

5.1 General

The cold cracking susceptibility of the steels has been studied using self restraint Tekken tests. The Tekken test has been chosen, as the results of this test can be translated to practice quite easily. For other tests, e.g. the implant test, this translation is less unambiguous.
A consequense of choosing the Tekken test is that the stresses, that occur after welding the test specimens, in the weld metal and in the heat affected zone are not exactly known.
As these stresses will be comparable with the situation in practice, the transferability of the results into preheat temperatures for practical use was the decisive factor in the choice of the type of cold cracking test.

The choice for the Tekken test implies that cold cracking can take place both in the weld metal and the HAZ. By keeping the welding procedure and the consumables constant (one batch of basic covered electrodes), the varation in the cold cracking susceptibility of the non diluted weld metal is kept to a minimum.
Different behaviour of the test welds can therefore the attributed to a difference in cold cracking susceptibility of the steel, and in case of cold cracks in the weld metal, to dilution of the filler metal with the parent plate.

The following influencing factors have been varied in the programme:
- hydrogen content of the weld metal;
- heat input;
- plate thickness.

5.2 Test conditions

The Tekken test that have been used in this investigation are of the Y-groove type, with the 2 mm slit at an angle of 30° with the plate surface. All test welds are parallel with rolling direction. The dimensions of the test specimens are 150 x 200 mm. The Tekken tests have been welded with one type of basic covered electrode, E9018-G, the same type that was chosen for the qualification programme.

The diameter of this electrode for welding the Tekken tests was 3.25 mm, the welding current amounted to 110-120 A AC.

The hydrogen content of the electrodes amounts to less than 3 ml per 100 gram deposited weld metal. This level of hydrogen is guaranteed by the producer by packing small quantities of electrodes under vacuum conditions in air thight containers.
The hydrogen content of these commercially available vacuum packed electrodes was measured several times, all hydrogen contents (HDM, ISO 3690) being in the range from 2.2-2.9 ml/100 gr. The average value amounted to 2.6 ml/100 gr.

In order to be able to perform the Tekken tests at higher hydrogen contents, electrodes have been exposed in a humidity cabinet at 90% relative humidity, 25°C. By varying the exposure time, different hydrogen contents of the weld metal could be achieved.
However, experiments indicated that the hydrogen content of the weld metal showed considerable variations for a given exposure time. Especially for the level of 5-5.5 ml/100 gr. unacceptable variations (4.1-6.5 ml/100 gr. for one exposure time) were measured.

Previous experiments with the implant test, performed at the TNO Metals Research Institute, indicated a linear relationship between the critical stress (no fracture within 48 hours) and the logarithm of the hydrogen content (HDM). Therefore, another source of E9018-9 electrodes with an increased hydrogen content was considered to be necessary for performing the cold cracking susceptibility with acceptable accuracy.

The variations in the hydrogen content at the level of 10 ml/100 gr. were acceptable. For experimental reasons however, the procedure for reaching this level was changed into immersing the electrodes in destilled water for half a hour, followed by air-drying for another half hour. The hydrogen contents that resulted from this procedure varied between 9.5 and 11.2 ml/100 gr.

For the hydrogen level of 5-5.5 ml/100 gr. the manufacturer of the electrodes produced a batch of electrodes which were baked at several temperatures. The result of these experiment can be seen in Figure 5.1. Based on these results the baking temperature for reaching the desired hydrogen content in the weld metal was set on 410°C.
Measurements (ISO 3690) after the baking procedure confirmed that the hydrogen content amounted 5.1-5.5 ml/100 gr.

5.3 Results and discussion

The results of the Tekken tests are given in Table 5.1 - 5.4.
In these tables, the results are basically presented as a crack/no crack statement. In addition, the average crack length (as a percentage of the bead height) and the crack location are given.

The information from the tables concerning a heat input of 11 kJ/cm is visually presented in Figures 5.2 - 5.4. In these figures, where the percentage crack length is given as a function of the pre-heat temperature, the susceptibility of the different base metals for cold cracking can be compared better.

5.3.1 Tekken tests, HI = 11 kJ/cm

5.3.1.1 15 mm plate thickness

For the 15 mm plates both the TM and the QT material can be welded without pre-heating up to a hydrogen level of 5 ml/100 gr. deposited weld metal. The N material on the other hand, requires a pre-heat temperature of 35 and 80°C, for hydrogen contents that amount to < 3 and 5 ml/100 gr. The crack location at these hydrogen levels in the N material is always the same: initiation at the position fusion line, at the point where the 30° slit of the former Y bevel hits the weld metal. Short cracks preferably run in the HAZ, parallel to the fusion line, whereas longer cracks initiate in the HAZ, and propagate in the weld metal.

For the hydrogen level of 100 ml/100 gr, the N material has a rather narrow temperature regime, in which the percentage crack length drops from approx. 100% to approx. 0%.
The level of preheating that is required for crack-free welds amounts to 80°C. For the TM material, and especially for the QT material, the influence of pre-heat temperature or the percentage crack length is less compared to the N material. The TM material reaches 0% crack length at 95°C, slightly higher than for the N material. At 20°C, 100% crack length has been measured.

The fact that the hydrogen content at the level of 10 ml/100 gr varies between 9.5 and 11.2 ml/100 gr. should be taken into account before conclusions about the cold crack susceptibility of both the N and the TM material are drawn.
For the QT material there is no doubt at all; it is the least crack susceptible material of the 3 materials tested: although a pre-heat temperature of 65°C is needed for crack-free welds, the crack

length at 20°C only amounts to 10%.

The general tendency is that for this rather high hydrogen level, the cracks initiate in the HAZ, and propagate in the weld metal. For the low alloyed QT and TM steels, all weld metal cracking is observed as well.

5.3.1.2 50 mm plate thickness

For the 50 mm plates, generally speaking, the required pre-heat temperature for hydrogen contents of 5 ml/100 gr. and above are higher than for the 15 mm plates. Increased restraint, and cooling rate (reduced $\Delta t(800\text{-}500)$) can be considered to be the cause of this effect.

For the normalized material, the required pre-heat temperatures for the hydrogen levels 5 and 10 ml/100 gr. have increased approx. 20°C compared with the situation for the 15 mm plate. For a hydrogen content less than 3 ml/100 gr, the effect of the increased cooling rate and restraint did not result in a higher pre-heat temperature.
For a hydrogen level of 10 ml/100 gr. the required pre-heat temperatures for both the QT and the TM material are the same as for the N material: approx. 100-110°C. This phenomenon is in accordance with the fact that at this hydrogen level, most cracks are situated in the weld metal.

With decreasing hydrogen content, there appears a difference in the crack position between the N and both the QT and TM material. Whereas at a hydrogen level of 5 ml/100 gr. in the TM or QT material cracks occur both in the HAZ and in the weld metal, cracks in the N material always initiate in the HAZ. The pre-heat temperature for the QT and TM steels is approx. 20°C less than for the N material.

At a hydrogen level of 3 ml/100 gr. all materials require the same pre-heat temperature as has been measured for the 15 mm plates: 35°C for the N material and 20°C for both the TM and the QT material.
As no tests have been performed at temperatures below 20°C, no statement can be given on the lowest temperature at which the QT and TM steels can be welded without cold cracking.

5.3.1.3 Discussion

From the experiments, the conclusion can be drawn that for all materials and conditions that showed cold cracking at ambient temperature, there was a difference in cracking susceptibility between a hydrogen content of 10 and 5 ml/100 gr. This is in accordance with what one would expect, based on e.g. BS 5135. A further reduction of the hydrogen content, to a level < 3 ml/100 gr. has an even greater influence on the required pre-heat temperature. From the results presented in this document, it appears that in a number of cases the decrease in hydrogen content from 5 to 3 ml/100 gr. results in a greater drop in pre-heat temperature than was measured for a reduction of the hydrogen content from 10 to 5 ml/100 gr.

The measured pre-heat temperatures have been correlated with the values predicted by BS 5135 (Table 5.5).
Direct calculation of the pre-heat temperatures of the QT and the TM steels was not possible, as BS 5135 does not give data for carbon equivalents less than 0.40.
On the other hand it was possible to calculate the maximum carbon equivalent that could be welded with 11 kJ/cm, and the relevant hydrogen contents and combined thicknesses.

As can be seen from the data in Table 5.5 the correlation between the measured and the predicted values is not that well.
For the QT and the TM material, the predictions are in a number of situations unsafe. This is a known fact; BS 5135 has been developed for medium or low restraint welding situations, whereas the Tekken test clearly is a very high restraint situation. In addition, BS 5135 is not suitable for modern steels, with a low carbon content and carbon equivalent.

For the N material, the prediction for the thick plates are rather conservative, whereas the predictions for the thin materials are always unsafe. Presumably, the effect of restraint has been overestimated in BS.

5.3.2 HI = 17 kJ

Only a limited number of Tekken tests have been welded with heat input of 17 kJ/cm.
Comparing the results of both heat inputs with each other, it can be seen that for the 15 mm materials, the TM en QT steel can be welded without pre-heating even at a hydrogen level of 10

ml/100 gr. Only the TM material had a little crack (5%) at the condition 5 H_{DM}, 20°C. For the N material, no real effect could be discerned.

The results for 50 mm plate thickness do not show a clear difference between both heat inputs.

5.4 Conclusions

From the experiments performed in this programme, the following conclusions can be drawn:

- For experiments in which different hydrogen contents of the weld metal are required, one should use "green electrodes", directly from the production line, and use special baking procedures.

- The required pre-heat temperature generally increases with increasing hydrogen content of the weld metal and plate thickness.

- For a hydrogen content of 3 ml/100 gr. and a heat input of 11 kJ/cm, both the 15 and 50 mm thick TM and QT steels can be welded without preheating.

- The increase of the hydrogen content to 5 ml/100 gr. reduces this "cold welding" to the 15 mm TM and QT material.

- The general trend is that both the TM and the QT material are not susceptible to cold cracking, the QT material being slightly preferable.
  The N material is sensitive to cold cracking, even at very low hydrogen content, and should be pre-heated in all cases.

- With increasing hydrogen content, the cold cracks run preferably in the weld metal. For the N material, initiation preferable takes place in the HAZ. For both other materials, all weld metal cracks have been found as well.

- An increase of the heat input to 17 kJ/cm leads for the 15 mm plates to a decrease of pre-heat temperature (especially QT and TM, H_{DM}=10 ml/100 gr).
  For the 50 mm plates, the effect is less.
- Prediction of pre-heat temperatures by means of BS 5135 leads to unsafe situations for both QT

and TM materials, and for the thin N material.

Restraint intensity, and the low carbon equivalent (QT and TM) are considered to be the cause of this deviation.

The effect of plate thickness is in this programme less than predicted by BS 5135.

According to the results of this programme, the currently used classification of hydrogen levels is not adequate anymore.
It is suggested that a new classification (extreme low hydrogen content) is installed for hydrogen content less than 3 ml/100 gr.

6 PROCEDURE QUALIFICATION

6.1 General

For all base materials, both the 15 and 50 mm plates have been welded with two levels of applied heat input.
For the thin plates, the submerged arc welding process (SAW) has been used for the high heat input (HI = 23 kJ/cm) whereas the shielded metal arc welding process (SMAW, welding with stick-electrodes) has been used for the low heat input (HI = 12 kJ/cm).
For the thick plates, both the low and the high level of applied heat input (20 vs 35 kJ/cm) has been achieved by means of submerged arc welding.
For the SMAW process, an E9018-G electrode has been applied.
For the SAW process a DIN S3Ni1 wire combined with a FBF155AC10MHP5 flux.

According to the wishes of the former F1-committee, the programme has been extended quite extensively: apart from the welds that were foreseen in the programme, the 50 mm plates have been welded using straight bevels. These bevels have been used in order to get a fusion line as straight as possible, which is important for CTOD testing.

The test welds have all been welded according to very strict welding procedures, in order to exclude an effect of a variation in the welding parameters. The applied welding procedures are given in Appendix 1.
In this appendix, examples of macro's of the 1/2V, I and both K type bevels are given. All other macro's being comparable.

All test welds have been ultrasonically tested before the specimens for mechanical testing were machined. No unacceptable defects were reported apart from one "lack of fusion" at the end of one of the SAW plates.
The mechanical test programme that has been performed is given in Table 6.1.

6.2 Results and discussion

6.2.1 Tensile tests and bend tests

The results of the tensile tests and the side bend tests are given in Table 6.2..
It is shown that all results are acceptable; all tensile tests fractured in the base material, and no cracks with unacceptable length appeared in the side bend tests. The cracks that have been reported, were located in the SMAW weld metal. The SAW welds showed no cracks in the side bend specimens.

6.2.2 Charpy-V tests, 15 mm plate

For all conditions Charpy-V tests have been performed at -40°C. In addition, to some extent, specimens have been tested at -20°C and -60°C.
The results of the Charpy-V tests are given in Table 6.3-6.8.
An overview of the results of the Charpy-V tests at -40°C for all materials, thicknesses and procedures is given in Table 6.26-6.29.

6.2.2.1 SMAW process

The results of the SMAW welds in the 15 mm plates are given in Table 6.3-6.5. From the results of the Charpy-V tests it appears that the fracture energies of the weld metal at -40°C do not give rise to any questions. Values of 80 J and above, both for the as welded and the PWHT conditions, meet any requirement to be set.
In the HAZ, for the materials TM and QT the lowest values are measured at the position fusion line, the overall values of the QT materials being superior to the values of the TM steel.
For the TM material, PWHT at 530°C seems to improve fracture energy at the position fusion line, where as an increase of the PWHT temperature tends to result in less favourable fracture energies at all positions in the HAZ. The extent to which the fracture energies decrease, is far less than what has been measured in the simulation programme.
For the QT material, no influence of PWHT could be discerned.

The N material behaves different to both other materials: the least favorable fracture energies (at -40°C) are measured at the position: fusion line + 5 mm. This can be explained from the poor Charpy-V properties of the base material. PWHT has an adverse effect on the Charpy-V properties at

all positions in the HAZ.

6.2.2.2 SAW welds

The results of the Charpy-V tests are given in Table 6.6-6.8. From these results it appears that the fracture toughness of the weld metal is poor. Fracture energies in the as welded condition vary from 29 to 10 J at -40°C. These values are caused by an improper choice of the welding wire. For two run submerged arc welding, a S2Mo with a wire flux that slightly increased the manganese level would have been the proper choice. In addition it must be noted that the heat input that was applied was rather high. This was done on purpose, in order to get an idea of the mechanical properties of the HAZ well beyond the range of cooling times $\Delta t(800\text{-}500)$ that is applied in practice. For the applied plate thickness, two run SAW welding can be performed successfully at approx. 15 kJ/cm, which of course has its influence upon HAZ properties.

There is a marked difference in the effect of PWHT on the fracture energy of the weld metal between the QT material and both V-micro-alloyed steels. Whereas the weld in the QT material improves with increasing PWHT temperature, the values in both the TM and the TM material decrease.
The dilution with the parent plate, and the corresponding V-levels in the weld metal must be the cause of this phenomenon.

The high heat input, and the absence of a large proportion of transformed regions, led for the N and the TM material to fracture energies in the HAZ that are as a whole less good than for the SMAW welds. For the QT material, no such effect could be discerned. Apparently the influence of both factors mentioned above on the fracture toughness energies is limited for this type of material.

For both the V-micro-alloyed steels, the properties at the position fusion line are poor. These properties improve with increasing distance from the fusion line, for the TM material more than for the N material.
PWHT at 530°C leads for the N material to a further deterioration of the fracture energies at the position fusion line. An increase of the PWHT temperature to 560°C results in fracture energies below 30 J in the entire HAZ.
For the TM material, PWHT at 530°C improves the properties at the position fusion line, just as for the SMAW welds. PWHT at 560°C deteriorates the fusion line properties, where as the fracture energies at greater distances from the fusion line remain quite good.

For the QT material, no influence of PWHT temperature on HAZ fracture toughness properties could be discerned.

6.2.3 Charpy-V tests, 50 mm plates

The measured Charpy-V values for each of the materials the PWHT conditions and the applied heat inputs are given in Table 6.9-6.25.
An overview of the results of the Charpy-V tests at -40°C for all materials, thicknesses and procedures is given in Table 6.26-6.29.

In the as welded condition, the fracture energies at -40°C of the weld metal in each of the base materials are well above the requirements, the lowest values being measured in the root of the high heat input weld in the normalized material.
In almost all cases, the fracture energies decrease with increasing heat input.
Only for the N-material, the properties in the root of the weld are clearly less than in the cap of the weld. Dilution should be the main effect, as in both other steels this phenomenon does not occur.

The HAZ in the 50 mm QT material behaves the same way as in the 15 mm QT material: good fracture toughness properties at -40°C all over the HAZ for both heat inputs. The fracture energies improve with increasing distance from the fusion line.
No systematic influence of the PWHT on the fracture energies in the HAZ could be seen.

For the normalized material the measured Charpy-V values are poor compared to the values of the QT material.
The fracture energies in the HAZ of the N material decrease with increasing heat inputs and with increasing PWHT temperature.
There is an indication that for the root position, just like for the 15 mm plate, poor properties can be measured at the position fusion line + 5 mm where as the corresponding values much closer to the fusion line are better. The fact that at the cap position this phenomenon does not occur could indicate that segregation, and the corresponding mid-thickness properties of the base material, play an important role.

For the TM material, low fracture energies are measured in the HAZ in the as welded condition both in the cap and the root area, and both for the low and the high heat input. Although the Charpy-V tests of the low heat input weld, Post Weld Heat Treated at 560°C have not been tested, it seems that PWHT generally improves the fracture energies in the HAZ.

6.2.4 Discussion

For low temperature applications, the Charpy-V results indicate that the QT material is superior to both other materials. PWHT does not deteriorate the properties in the HAZ, neither for the 15 mm nor for the 50 mm plate thickness.
Based on the results of the Charpy-V test, application of the two run SAW technique is possible, but PWHT preferably at approx. 560°C, is required, as it improves the fracture energy of the S3Ni1 weld metal.
No information is available about the mechanical properties of a two run SAW weld using a S2Mo wire, but based on information outside this project, this type of welding wire should be preferred. However, it is suggested that for this type of welding wire high PWHT temperatures are to be considered with caution.

For application at increased operating temperatures, the TM steel is considered to be a better choice than the normalized steel. This statement is based on the fracture energies in both the coarse grained HAZ and the base material.

The question whether PWHT should be applied depends on the applied temperature and the steel type. For N material, no PWHT should be advised. If the certifying authorities insist on PWHT, than a temperature as low as possible in the PWHT temperature range should be chosen.
The TM material can be Post Weld Heat Treated at 530°C, the properties improve at several locations. PWHT at 560°C is not advisory.

6.2.5 CTOD tests

6.2.5.1 15 mm plates

The CTOD properties of the 15 mm SMAW and SAW weldments are given in Table 6.30 and 6.31. For the SMAW weldments, in the as welded condition, the CTOD properties improve from N to TM

to QT material (0.10 -> 0.17 -> 0.30 mm).
After PWHT at 530/560°C, the N material shows poor CTOD properties. For the TM material, PWHT at 530°C improves CTOD properties.
An increase in PWHT temperature till 560°C slightly reduces the values compared to 530°C, but they remain quite good.
For the QT material PWHT improves the CTOD properties and no effect of PWHT temperatures could be discerned.

Based on this result, and the results of the Charpy-V testing, for the SAW weldments only PWHT at 530°C has been performed.
In the as welded condition, all materials have poor CTOD properties (0.05-0.08 mm). After PWHT at 530°C the ranking is as might be expected based on the results as described before.
For the N material the values remain the same, where as for the TM and the QT materials the values improve. The QT material responds even more favorable than the TM material.

6.2.5.2 50 mm plates

The results of the CTOD tests of the 50 mm K and I type bevels are given in Table 6.31 and 6.32.
Although in a later stage in the project it was decided to perform CTOD tests on specially prepared weldments with straight bevels, the K bevels have been CTOD tested as well.
The results of these CTOD tests show that in the as welded condition, the QT material behaves superior to the N and the TM material.
For the N and QT material increasing the heat input reduces the minimum CTOD values (N: 0,09 -> 0.04 mm, QT: 1.84 -> 0.77 mm). For the TM material no effect has been observed.
The weld metal has been tested as well, both in the as welded and the PWHT (530°C and 560°C) condition.
All measured values are good, without a clear influence of heat input or PWHT temperature.

The results of the straight bevel weldments with a high heat input confirm the statements given above for the 15 mm SMAW weldments.
The N material has poor properties, and does not respond to PWHT.
For the TM material and the QT material, PWHT at 530°C has no influence on the CTOD values PWHT at 560°C leads to a drop in CTOD values for the TM material, the QT material responding less strong.

For the low heat input (20 kJ/cm) welds, some problems have arisen with the positioning of the fatigue crack.
It appeared that in some cases, either the weld metal or the HAZ at a distance of more than 0.5 mm from the fusion line was tested.

Still, it appears that the QT material has the best CTOD properties, especially when PWHT is to be applied.
For the TM material, PWHT at 530°C tends to be beneficial, where as 560°C seems to be to high a PWHT temperature.

For the N material no clear influence of PWHT on the CTOD values has been established, the values being rather poor in all cases.
Only for material N a clear influence of heat input was established: high heat inputs clearly lead to a drastic drop in CTOD values.

6.3 Conclusions

Based on the results which are obtained in this part of the programme, the following conclusions can be drawn:

* tensile and bend properties.
- the tensile and bend properties of all welds (tested in the as welded condition only) are acceptable,

* Charpy-V properties, weld metal
- PWHT decreases the fracture energies of the two run SAW weld metal for the N and TM materials. The QT material shows the opposite effect: at 560°C the best Charpy-V values are obtained,
- PWHT of the SAW welds in 50 mm thick QT and TM materials has hardly an effect on the fracture energy of the weld metals. For the N material, at the root position, PWHT decreases the fracture energy,

* Charpy-V properties, HAZ
- the N material has the least favorable Charpy-V values of all three materials.
  In a number of situations, the least favorable fracture energies are measured at the position fusion

line +5 mm, which can be related to the properties of the base material,

- PWHT is considered to be not advisable for the N materials. If it is required that PWHT is performed, the lowest temperature (approx. 530°C) and the shortest hold time possible within the specifications should be used,
- the properties of the TM material are generally in between the properties of the QT and the N material,
- for the TM material the high heat input two run SAW technique is not advisable. If it has to be performed, PWHT at 530°C improves the properties at the position fusion line, but deteriorates the properties of the weld metal obtained with a S3Ni1 wire,
- the QT steel has good Charpy-V properties at all positions in the HAZ, for all welding procedures, for all conditions.

  PWHT does not change fracture properties to a great extent. The worst values are generally measured at the position fusion line,
- PWHT at 530°C of the SMAW weld and both SAW welds in the 50 mm plate is considered to be beneficial.

* CTOD properties

- generally speaking, the CTOD properties support the statements given for the Charpy-V results,
- for the weld metal in the 50 mm K type welds, very good CTOD properties have been measured, hardly influenced by the applied heat input and PWHT temperatures (up till 560°C),
- for the 15 mm SMAW weldments in the as welded condition, the CTOD properties improve from N to TM to QT material. PWHT improves the CTOD properties of the QT material, when as for the N material no influence could be discerned.

  Based on the CTOD results, the optimum condition for the TM material is PWHT at 530°C.
- both for the 15 mm and the 50 mm SAW weldments basically the same conclusions regarding the CTOD properties can be drawn as for the SMAW welds.

7 MECHANICAL PROPERTIES AFTER FORMING OPERATIONS

7.1 Introduction

It is a well known fact that after forming operations (deformation), the mechanical properties can show a degradation.
In this part of the investigation it has been established to what extent the mechanical properties are influenced by forming operations of the base material.

For normalized steels, forming of e.g. a thick walled tube can be performed at ambient temperature. However, if the deformation in the outer layer of the material amounts to more than 5 %, a normalizing treatment is required afterwards.
Instead of this separate normalizing treatment, the forming operation as a whole can be performed at the normalizing temperature. The additional benefit of this procedure is that the forces required for rolling the tube are reduced considerably.

For Quenched and Tempered and Thermo-mechanically rolled steels however, this hot forming procedure is not possible, as the mechanical properties are only guaranteed for annealing temperatures below the stress relieve temperature (approx. 600°C).

In the present research programme, hot and cold forming operations have been studied separately.

7.2 Forming operations below the Ac1 temperature

7.2.1 Experiments

For this part of the investigation, all three materials have been given 2.5 - 10% deformation by means of rolling. These deformations have all been achieved in one pass of the rolling mill, the temperatures at which the material entered the rolling mill amounted to 20°C, 560°C, 590°C and 620°C. Due to the contact with the cold rolling equipment, the temperature drop during rolling at elevated temperatures amounted to approx. 70°C.

All specimens have been rolled parallel to the final rolling direction of the plate, the percentage deformation being controlled by thickness measurements.

For every condition the following properties have been determined:

- Yield and tensile strength, elongation, all measured on rectangular specimens (full plate thickness), machined parallel to rolling direction (= longitudinal).
- Charpy-V impact properties at 3 temperatures, measured on longitudinal specimens, taken from the mid-thickness position.
- Vickers hardness (HV1).

For imitating strain ageing, part of the material that had been rolled at 20°C, has been given an ageing treatment (0.5 h at 250°C).

7.2.2 Results and discussion

7.2.2.1 Tensile properties

The results of the tensile tests after deformation at 2.5, 5 and 10% at temperatures of 20, 560, 590 and 620°C are given in Table 7.1 and Figure 7.1-7.6.

For all materials the tensile and yield strength increase with deformation. Generally speaking, for a fixed level of deformation the yield and tensile strength decrease with increasing rolling temperature.

Looking at the tensile strength that is prescribed in DIN 17102, it appears that for certain conditions (low rolling temperatures and high deformation percentages) the tensile strength is higher than the maximum allowable value of 730 N/mm^2.
For the N material, 5 and 10% deformation at 20°C leads to this situation, for the TM material the occurrence of this phenomenon is reduced to 10% deformation at 20°C.
Due to the relatively low values of the base material, the QT material never exceeds the DIN 17102 limit for the tensile strength. However, it must be taken into account that the QT material is not supplied under DIN 17102. It is therefore not to be concluded that the QT material never exceeds its guaranteed limits.

The Re/Rm ratio increases with percentage deformation and decreases with increasing rolling temperature. Although in DIN 17102 no maximum value for the Re/Rm ratio is given, a value of 0.90 is accepted as a maximum in practice. This value corresponds with the maximum value that is given in DIN 17172 for TMCP line pipe steels.
Below values of 0.90, it is considered that steels subjected to deformation have enough capacity to

spread this deformation over a wider distance or area.
Especially for TM steels all measured Re/Rm values after rolling at ambient and elevated temperatures are out of limit. Both for the N and QT material values over 0.90 are generally restricted to deformation at 20°C.

Ageing (0.5 h at 250°C) leads for the TM material to a drastic increase in Re, Rm and Re/Rm values. For the QT material this effect is less and for the N material even a decrease in Re and Rm values have been observed.

7.2.2.2 Charpy-V fracture properties

The results of the Charpy-V tests are given in Table 7.1 and Figure 7.7-7.15.
Both for the N and the TM material deformation leads to a decrease in fracture energy. The shift of the transition curve towards less favourable temperatures amounts to approx. +30-40°C for both materials. There does not seem to be a clear relationship between either the percentage deformation and the drop in fracture energy (compared with the base material) or the fracture properties and the rolling temperature.

For the QT material down to a test temperature of -60°C, practically no effect of deformation on Charpy-V notch toughness properties has been observed. At temperatures of -80°C and below, low fracture energies have been measured both in the as delivered condition and after deformation.

7.2.2.3 Hardness

The results of the hardness measurements are given in Table 7.1.
For normalized material all rolling procedures lead to an increased hardness value. The increase in hardness depends on the actual deformation and rolling temperature and amounts to approx. 25-50 HV1.
For the TM material the measured hardness values after deformation are more or less the same as for the N material, but due to a higher hardness in the base material, the increase in hardness is less.
For the QT material the increase in hardness due to rolling is limited to max. approx. 15 HV1 (even for 20°C, 10%). After strain ageing, the hardness values increase another 30 points.
This strong increase in hardness after strain-ageing has not been observed for both other materials.

7.2.3 Conclusions

From the experiments performed in this programme, the folowing results can be drawn:

- Rolling at 20°C with deformation percentages between 2.5-10% can greatly affect the tensile properties of all three materials. The Re/Rm ratio, Rm and elongation values can be changed in such a way that the materials do not meet the requirements as mentioned in DIN 17102. This can happen already after 2.5 deformation. All three materials have their own characteristic behaviour but they all are very sensitive for an increasing Re/Rm ratio.
- Strain ageing of cold deformed material can cause an extra increase of the Re and and Re/Rm ratio (material TM and QT).
- After cold forming the Charpy-V toughness decreased, but the TT40 temperature is always $\leq$ -50°C. Material N, however, is sensitive to strain ageing which causes an increase of the TT40 temperature to 0°C.
- After rolling at 560, 590 and 620°C the Rm and elongation values are always within the specifications. The Re/Rm ratio of the TM materials, however, was always higher than specified.
- Rolling at elevated temperatures (560, 590, 620°C) has a negative effect on the Charpy-V properties of material N and TM. The Charpy-V toughness of the QT material is hardly affected by rolling at these temperatures.
- In general the QT and TM materials are more resistant to rolling cycles between 20 and 620°C than the N material.
- It cannot be guaranteed that after deformation grades up to 5% the FeE 460 material always meets the requirements as mentioned in DIN 17102 (Re/Rm ratio, elongation). In this respect rolling cycles at higher temperatures (560, 590, 620°C) are to be preferred.

7.3 Forming operations at elevated temperatures

7.3.1 General

At the TNO Institute of Production and Logistics Research, it has been experienced that the influencing factor in the hot forming operations is the thermal cycle. Experiments showed that, looking at the mechanical properties, hardly any difference existed between specimens which were hot formed, and specimens which were only given the thermal cycle that corresponded to the hot forming operation.

Based on this experience, the hot forming operations have been replaced by carefully controlled normalizing treatments. These normalizing treatments have been performed in a vacuum furnace.

The experiments have been performed on 2 base materials: material N and X in Table 3.1 and 3.2. The complete programme is listed in Table 7.2.
The main variables concerning the normalizing treatment were the temperature (920°C and 960°C), and the heating and cooling rate (60, 120, 250 and 500°C/h).
From the normalized specimens both the microstructure and the tensile, Charpy-V and CTOD properties have been determined. The orientation of all specimens was with the length perpendicular to the rolling direction of the base material.

7.3.2 Results and discussion

7.3.2.1 Ferrite grain size

Table 7.3 and Figure 7.16-7.17 show the influence of normalizing on the ferrite grainsize.
For both material N and X it appears that after normalizing the ferrite grain size ($d^{-1/2}$) is decreased. Material N showed an influence of the normalizing temperature. Material X seems to be more resistant to grain growth than material N, but for both materials the grain size decrease with decreasing cooling/heating rate.

7.3.2.2 Tensile properties

The tensile properties of both materials are given in Table 7.4 and Figure 7.18-7.19.
It appears that for material X, the yield strength of the base material only just meets the requirements.
After a normalizing treatment, the yield strength decreased for both materials, except for material X, at a heating/cooling rate of 500°C/h. For both materials, an increase in the heating/cooling rate leads to a decrease in the drop in yield strength compared to the base material in the as delivered condition.
For material N an increase of the temperature from 920 to 960°C led to a further decrease in yield strength, for material X no such effect could be discerned.
This decline in yield strength is caused by the grain growth that has been mentioned in 7.3.2. For both materials the effect of $d^{-1/2}$ on the yield strength is given in Figure 7.20.

After normalizing the yield strength generally speaking did not meet the requirements. Only for extreme high heating/cooling rates combined with a low normalizing temperature the yield strength will be acceptable.
For both materials the yield strength decreases linearly with ferrite grain size ($d^{-1/2}$). The minimum yield strength of both materials is reached at a ferrite grain size of approx. 10.5, see Figure 7.20.

7.3.2.3 Charpy-V properties

The results of the Charpy-V tests are given in Table 7.5-7.6 and Figure 7.21-7.27.
Just as has been seen for the tensile properties, the Charpy-V notch toughness properties degrade after normalizing.
However, it appears from the results that there is a great influence of the base material. Material N shows a clear shift of the transition curve for almost every normalizing condition that was tested (only for 920°C, 500°C/h the notch toughness properties are the same as for the base material). For material X on the other hand, the shift is limited.
The influence of the normalizing temperature is material dependent: just like for the tensile properties is material N much more sensitive to increased normalizing temperatures than material X.

7.3.2.4 CTOD properties

The results of the CTOD tests (at -10°C) are given in Table 7.7.
For material N, a normalizing temperature of 960°C leads to CTOD values less than 0.21 mm, even for a heating/cooling rate of 500°C/h.
Reducing the temperature to 920°C results in better CTOD values, but even then a heating/cooling rate of at least 250°C/h is required for getting near acceptable results.

For material X the same influence of temperature on the CTOD properties can be seen from the results. The measured CTOD values however, are for material X far better than for material N.
All values for a normalizing temperature of 920°C are at least equal to 0.33 mm. Although this is not a very favourable value, it is well in excess of the requirements to be set to the welded construction.
For a normalizing temperature of 960°C, the measured values are less favourable.

For both materials, the CTOD properties at -10°C have been plotted versus ferrite grain size in Figure 7.28-7.29. It appears that there is a more or less linear relationship between both parameters. From both figures it appears that in order to prevent to low CTOD properties to occur, one cannot allow a drop in ferrite grain size ($d^{-1/2}$) of more than 2.5 compared to the base material.
In addition a minimum value of $d^{-1/2}$ of 9 is recommended, but this depends on the material.
The fact that the properties (CTOD, Charpy-V and tensile) depend to such extent on the material that is actually tested is in accordance with the results of previously performed research at our institute. One of the main reasons for a material to respond to a normalizing treatment as it does, is the amount, the composition and the (size)distribution of the V, Nb and Ti carbides, nitrides and carbo-nitrides.

7.3.3 Conclusions

From the experiments performed in this programme, the following results can be drawn:

- Both the microstructure, the yield strength, the Charpy-V properties and the CTOD properties are influenced by normalizing treatment.
- Renewed normalizing of FeE 460 can easily result in mechanical properties which do not meet the minimum requirements as mentioned in DIN 17102.
- For the best mechanical properties after normalizing it is important to use a low normalizing temperature (preferably 920°C), and to heat and cool as fast as possible
- There is a great influence of the material to be normalized on the properties to be achieved.

From previous research there are strong indications that the carbo-nitrides of V, Nb and Ti play an important role by controlling the austenite (and hence the ferrite) grain size.

8 CALCULATION

The last part of this research programme consisted of the redesign of two types of constructions: a bridge and 3 pressure vessels.
These construction were originally designed in FeE355, and for this project, the fabricators/designers agreed to redesign the constructions in FeE460. The requirements for the FeE460 constructions had not been changed compared to the original requirements.

8.1 Pressure vessels

8.1.1 General information

The manufacturer has redesigned three pressure vessels with original (FeE355) wall-thicknesses ranging from 25 - 89 mm. The general data concerning these vessels are given in Appendix 2. All vessels operate at a temperature of 100°C or above.

All calculations are performed according to the Rules of "Dienst voor het Stoomwezen", the Dutch certifying authority for boilers and pressure vessels.
According to the Rules, one must use the minimum value of 0,67*Re and 0,44*Rm for the allowable stress in the construction.
If the vessel is to be Post Weld Heat Treated afterwards, the value of 0,44*Rm can be increased to 0,5*Rm.

For WSte 355 and 460 according to DIN 17102, the Re and Rm value as a function of wall thickness and temperature are given in Appendix 3.
In addition, the curves for the determination of the allowable stresses are presented in this appendix.

The effect of temperature on the Re and Rm values is illustrated by the fact that at the operating temperatures the allowable stresses are determined by Re in 4 out of 6 cases (3x WSte 355, 1x Wste 460).

Vessel 1	:	WSte 355 :	0,67Re < 0,5	Rm
		Wste 460 :	0,67Re > 0,44	Rm
Vessel 2	:	WSte 355 :	0,67Re < 0,5	Rm
		Wste 460 :	0,67Re < 0,5	Rm
Vessel 3	:	WSte 355 :	0,67Re < 0,44	Rm
		WSte 460 :	0,67Re > 0,44	Rm

If the vessels would have had an operating temperature of 20°C, Re would have been decisive in 2 out of 5 cases (all WSte 355; for vessel 2 manufactured in WSteE460, the values of 0,67*Re and 0,5*Rm are equal.

At 20°C, these data support the opinion that for the usage in pressure vessels, the "Rules" of "Dienst voor het Stoomwezen" are such that for high yield strength steels, one can not fully use the increase in yield strength compared to e.g. FeE 355.

This is due to the fact that for high yield strength steels the Re/Rm ratio increases. For WStE 355 and 460 this is shown in Appendix for operating temperatures ranging from 20 to 200°C. Apparently the Re(T)/Rm(T) for WStE 460 is less influenced by temperature compared to WStE 355. As the Rm(T) value is not influenced by temperature up till 200°C, this is caused by the fact that for WStE 460, the Re is less influenced by temperature compared to WStE 355.
(See Appendix 4)
The consequence of the above is visible in the allowable stresses presented for the vessels at the actual operating temperature: at operating temperatures above 100°C for WStE 355 the Re value is always the limiting factor.
For WSte 460 this is the case for operating temperature above 150°C (except for 150°C operating temperature, thickness less than 35 mm).

8.1.2 Results

For all three vessels, the weight and the production cost have been calculated.
It was assumed that the price of the steels would be Dfl. 1.25 (FeE 355) resp. Dfl. 1.38 (FeE 460). These values are used by the fabricator for making quotations. The pre-heat level is considered to be the same for FeE 355 and FeE 460.

The results of the calculations of weight and cost are given in Table 8.1.
It appears that for thin walled structures, the type of steel has hardly any influence on the price of the vessel.

For thick walled vessels both the reduction in weight and the reduction in fabrication time lead to considerable saivings.
For the vessel in question (vessel 2) a 29% reduction in weight leads to savings of Dfl. 85.000 on the base material, and Dfl 96.500 on the fabrication cost, resulting in a 23% saving on the total of the fabrication cost.
For vessels which have to be post weld heat trated when constructed in FeE 355, a considerable saving can be achieved when the dimensions are such that when constructed in FeE 460 no PWHT should be applied.
For vessel 1, the wall thicknes is reduced from 38 to 31 mm, thus resulting (according to "Dienst voor het Stoomwezen) in the avoidance of PWHT for FeE 460. On the other hand, the allowable stresses are determined by 0,67*Re if PWHT is applied, and by 0,44*Rm if not (see Appendix 3, Figure A.3.3 B); thus resulting in lower allowable stresses.
Still the reduction in weight amounts to 21.000 kg (=17%), which leads to savings of Dfl. 15.000 on base material and Dfl. 37.500 on fabrication cost. In addition, Dfl. 24.000 is saved on PWHT. This leads to an overall saving of 12%.

8.2 Bridge

For applications in which stability is an important design criterium, the use of high strength steel is considered to be less interesting.
In order to check this point 'Rijkswaterstaat Directie Bruggen', the responsible organization for the design of bridges in the Netherlands, has calculated the effect of application of FeE 460 instead of FeE 355.
A short report concerning the results of these calculations is given in Appendix 5.

The main conclusion that can be drawn from the calculations is that application of FeE 460 does not lead to savings for the constructional parts that were investigated.
As described in Appendix 5, this is partly due to the fact that the design rules require application of FeE 460 in the webb as well. This leads to increased material cost, which compensated the savings due to a reduction of the lower flange thickness.

The additional savings that can be achieved in the case of pressure vessels (the fabrication costs) do not occur in the present construction.
This is mainly due to the fact that only fillet welds have been applied with a throat thickness that is determined by the thickness of the webb.
The thickness of the webb is determined by buckling etc. rather than strength, and can therefore not be reduced, not even in the case FeE 460 material is used.
This leads to a situation in which the welding costs etc. are hardly influenced by the use of FeE 460.

8.3 Conclusions

The figures that have been presented in the previous chapter clearly indicate that:

- the use of FeE 460 can save a considerable amount of money for specific products,
- the highest savings can be achieved for thick walled pressure vessels (up to 23%),
- for situation in which pure strength is the determining factor, the use of FeE 460 is beneficial,
- for structures in which stability and fatigue play an important role, the use of FeE 460 will lead to smaller, if any, savings.

Fig. 4.25: Matériau N, Tp = 1350°C, Δt (800-500) = 50 sec.
□: comme simulé; *: +PWHT (1h530°C)

Fig. 4.26: □: comme simulé; *: +PWHT (1h560°C)

Fig. 4.27: □: comme simulé; *: +PWHT (1h590°C)

Fig. 4.28: Matériau N, Tp = 1050°C, Δt (800-500) = 7 sec.
□: comme simulé

Fig. 4.29: Matériau N, Tp = 1050°C, Δt (800-500) = 12 sec.
□: comme simulé; *: +PWHT (1h530°C)

Fig. 4.30: □: comme simulé; *: +PWHT (1h560°C)

Fig. 4.31: □: comme simulé; *: +PWHT (1h590°C)

Fig. 4.32: Matériau N, Tp = 1050°C, Δt (800-500) = 20 sec.
□: comme simulé; *: +PWHT (1h530°C)

Fig. 4.33: □: comme simulé; *: +PWHT (1h560°C)

Fig. 4.34: □: comme simulé; *: +PWHT (1h590°C)

Fig. 4.35: Matériau N, Tp = 1050°C, Δt (800-500) = 50 sec.
□: comme simulé; *: +PWHT (1h530°C)

Fig. 4.36: □: comme simulé; *: +PWHT (1h560°C)

Fig. 4.37: □: comme simulé; *: +PWHT (1h590°C)

Fig. 4.38-4.66: = Fig. 4.9 - 4.37 matériau TM

Fig. 4.67-4.94: = Fig. 4.10 - 4.37, matériau QT

Fig. 4.95: Le TT40 des trois matériaux ayant subi une simulation à 1050°C comme fonction du cycle refroidissement Δt (800-500)

Fig. 4.96: Les températures TT40 des trois matériaux ayant subi une simulation (à Tp=1050°C et Δt (800-500) = 12 sec.) dans l'état comme simulé et après PWHT

Fig. 4.97: Tp = 1050° C et Δt (800-500) = 20 sec.

Fig. 4.98: Tp= 1050°C etΔt (800-500) = 50 sec.

Fig. 4.99: Le TT40 des trois matériaux ayant subi une simulation à 1350°C comme fonction du cycle de refroidissement Δt (800-500)

Fig. 4.100: Les températures TT40 des trois matériaux ayant subi une simulation (à Tp=1350°C et Δt (800-500) = 7 sec.) dans l'état comme simulé et après PWHT

Fig. 4.101: Tp = 1350°C et Δt (800-500) = 12 sec.

Fig. 4.102: Tp = 1350°C et Δt (800-500) = 20 sec.

Fig. 4.103: Tp = 1350°C et Δt (800-500) = 50 sec.

Fig. 4.104: Tp_1 = 1350°C, Tp_2 = 775°C et Δt (600-400) = 13.6 sec.

Fig. 4.105: Tp_1 = 1350°C, Tp_2 = 775°C et Δt (600-400) = 22.6 sec.

Fig. 4.106: Microstructure des spécimens ayant subi une simulation de matériau N.
a: Δt (800-500) = 7 sec. b: Δt (800-500) = 12 sec.
c: Δt (800-500) = 20 sec. c: Δt (800-500) = 50 sec.
M = x500

Fig. 4.107: Matériau TM

Fig. 4.108: Matériau QT

Fig. 4.109: Microstructure des spécimens ayant subi une simulation de matériau N.
Les états ayant subi une simulation: 1350°C/12 sec.
a: comme simulé b: + 1h 530°C
c: +1h 560°C d: + 1h 590°C
a: M =x500 b-d: M = x1000

Fig. 4.110: Materiau TM

Fig. 4.111: Materiau QT

Fig. 4.112: Le fraction de la rupture intergranulaire du matériau ayant subi une simulation (Tp = 1350°) et les matériaux ayant subi une simulation + PWHT, pour temps réfroidissement différent

Fig. 4.113: Photos effectués au microscope électronique des surfaces de rupture des spécimens Charpy-V rompus friables de matériau N.
Les états simulé: 1350°C/12 sec.
a: comme simulé b: + 1h 530°C
c, d: +1h 590°C

Fig. 4.114: Materiau TM

Fig. 4.115: Materiau QT

Fig. 4.116: Photos effectués au microscope à transmission des productions d'extraction et films minces de matériau TM, l'etat simulé: 1350°C/12 sec.
a: reproduction,+1h 530°C b: reproduction, + 1h 590°C
c: film mince, +1h 530°C d: film mince, + 1h 590°C
a, b: M = x2000 c: M = x6000 d: M = x4000

Fig. 4.117: Micrographs de film mince des limites grains austénitiques anciens dans matériau TM.
Les états simulés: 1350°C/7 sec. PWHT: 590°C,
90% Rupture intergranulair, a: x50.000 b: x60.000

Fig. 4.118: La composition chémique des carbures limites grains dans matériau N dans l'état de

Fig. 7.10-7.12: Fig. 7.7-7.9 Matériau TM

Fig. 7.13-7.15: Fig. 7.7-7.9 Matériau QT

Fig. 7.16 La taille des grains de ferrite du matériau N comme fonction du cycle thermique

Fig. 7.17 La taille des grains de ferrite du matériau X comme fonction du cycle thermique

Fig. 7.18 La limite de résistance du matériau N comme fonction du cycle thermique

Fig. 7.19 La limite de résistance du matériau X comme fonction du cycle thermique

Fig. 7.20 La limite de résistance des matériaux N et X comme fonction de la taille du grain ferritique

Fig. 7.21 Les courbes de transition au cours du test Charpy-V du matériau N après austénitisation à 920°C à une vitesse de chauffe et de refroidissement de 60 et 120°C/h

Fig. 7.22 Austénitisation à 920°C à une vitesse de chauffe et de refroidissement de 250 et 500°C/h

Fig. 7.23 Austénitisation à 960°C à une vitesse de chauffe et de refroidissement de 60 et 120°C/h

Fig. 7.24 Vitesse de chauffe et de refroidissement = 250 et 500°C/h

Fig. 7.25 Les courbes de transsition au cours du test Charpy-V du matériau X après austénitisation à 920°C à une vitesse de chauffre et de refroidissement de 60 et 120°C/h

Fig. 7.26 Vitesse de chauffe et de refroidissement = 250 et 500°C/h

Fig. 7.27 Austénitisation à 960°C à une vitesse de chauffre et de refroidissement de 60 et 500°C/h

Fig. 7.28 Valeurs CTOD du matériau N à - 10°C comme fonction de la taille du grain ferritique

Fig. 7.29 Valeurs CTOD du matériau X à - 10°C comme fonction de la taille du grain ferritique

Fig. A1: Examples de macrostructure des soudures d'essai:

a = SAAP, N, 15mm b = SAS, TR, 15mm

c = SAS, N, 50mm, 22kJ/cm d = SAS, TR, 50mm, 35kJ/cm

Tableau 6.11: PWHT à 560°C

Tableau 6.12: Résultats du test Charpy-V du matériau N, 50 mm, SAS, adduction de chaleur = 35 kJ/cm, soudé

Tableau 6.13: PWHT à 530°C

Tableau 6.14: PWHT à 560°C

Tableau 6.15-6.16: = tableau 6.9-6.10: Matériau TM

Tableau 6.17-6.19: = tableau 6.12-6.14: Matériau TM

Tableau 6.20-6.25 = tableau 6.9-6.14: Matériau QT

Tableau 6.26: Aperçu de l'énergie de rupture moyenne Charpy-V à 40°C pour les soudures SAAP sur matériau de 15 mm d'épaisseur

Tableau 6.27: Aperçu de l'énergie de rupture moyenne Charpy-V à 40°C pour les soudures SAS sur matériau de 15 mm d'épaisseur

Tableau 6.28: Aperçu de l'énergie de rupture moyenne Charpy-V à 40°C pour les soudures SAS (22kJ/cm) sur matériau de 50 mm d'épaisseur

Tableau 6.29: Aperçu de l'énergie de rupture moyenne Charpy-V à 40°C pour les soudures SAS (35kJ/cm) sur matériau de 50 mm d'épaisseur

Tableau 6.30: Propriétés CTOD des soudures SAAP de 15 mm d'épaisseur.
Température d'essai: -10°C
Emplacement du point de soudure: Ligne de fusion
Spécimen: Bx2B

Tableau 6.31: Propriétés CTOD des soudures SAS de 15 mm d'épaisseur.
Température d'essai: -10°C
Emplacement du point de soudure: 50% HAZ - 50%WM
Spécimen: Bx2B

Tableau 6.32: Propriétés CTOD des soudures K de 50 mm d'épaisseur.
Température d'essai: -10°C
Emplacement du point de soudure: Ligne de fusion
Spécimen: Bx2B

Tableau 6.33: Propriétés CTOD des soudures d'angles droits de 50 mm d'épaisseur.
Température d'essai: -10°C
Emplacement du point de soudure: Ligne de fusion
Spécimen: Bx2B

Abb. 4.1: Härtegrade der Probestücke als Funktion des Abkühlungszykluses.
Tp = 1350°C

Abb. 4.2: Tp = 1050°C

Abb. 4.3: Härtegrade der Probestücke als Funktion des Spannungsarmglühtemperaturs.
Werkstoff N, Tp = 1350°C

Abb. 4.4: Werkstoff N, Tp = 1050°C

Abb. 4.5: Werkstoff TM, Tp = 1350°C

Abb. 4.6: Werkstoff TM, Tp = 1050°C

Abb. 4.7: Werkstoff QT, Tp = 1350°C

Abb. 4.8: Werkstoff QT, Tp = 1050°C

Abb. 4.9: Charpy-V-Bruchenergie des N-Werkstoffs im Lieferzustand.

Abb. 4.10: Charpy-V-Bruchenergie der simulierte Werkstoffe.
Werkstoff N, Tp = 1350°C, Δt (800-500) = 7 Sek.
□: wie simuliert, * : + Spannungsarmglühen (1 Std. 530°C).

Abb. 4.11: □: wie simuliert, * : + Spannungsarmglühen (1 Std. 560°C).

Abb. 4.12: □: wie simuliert, * : + Spannungsarmglühen (1 Std. 590°C).

Abb. 4.13: Werkstoff N, Tp = 1350°C, Δt (800-500) = 12 Sek.
□: wie simuliert, * : + Spannungsarmglühen (1 Std. 530°C).

Abb. 4.14: □: wie simuliert, * : + Spannungsarmglühen (1 Std. 560°C).

Abb. 4.15: □: wie simuliert, * : + Spannungsarmglühen (1 Std. 590°C).

Abb. 4.16: Werkstoff N, Tp = 1350°C + 775°C, Δt (600-400) = 13,6 Sek.
□: wie simuliert, * : + Spannungsarmglühen (1 Std. 530°C).

Abb. 4.17: □: wie simuliert, * : + Spannungsarmglühen (1 Std. 560°C).

Abb. 4.18: □: wie simuliert, * : + Spannungsarmglühen (1 Std. 590°C).

Abb. 4.19: Werkstoff N, Tp = 1350°C, Δt (800-500) = 20 Sek.
□: wie simuliert, * : + Spannungsarmglühen (1 Std. 530°C).

Abb. 4.20: □: wie simuliert, * : + Spannungsarmglühen (1 Std. 560°C).

Abb. 4.21: □: wie simuliert, * : + Spannungsarmglühen (1 Std. 590°C).

Abb. 4.22: Werkstoff N, Tp = 1350°C + 775°C, Δt (600-400) = 22,6 Sek.
□: wie simuliert, * : + Spannungsarmglühen (1 Std. 530°C).

Abb. 4.23: □: wie simuliert, * : + Spannungsarmglühen (1 Std. 560°C).

Abb. 4.24: □: wie simuliert, * : + Spannungsarmglühen (1 Std. 590°C).

Abb. 4.25: Werkstoff N, Tp = 1350°C, Δt (800-500) = 50 Sek.
': wie simuliert, * : + Spannungsarmglühen (1 Std. 530°C).

Abb. 4.26: □: wie simuliert, * : + Spannungsarmglühen (1 Std. 560°C).

Abb. 4.27: □: wie simuliert, * : + Spannungsarmglühen (1 Std. 590°C).

Abb. 4.28: Werkstoff N, Tp = 1050°C, Δt (800-500) = 7 Sek.
□: wie simuliert

Abb. 4.29: Werkstoff N, Tp = 1050°C, Δt (800-500) = 12 Sek.
□: wie simuliert, * : + Spannungsarmglühen (1 Std. 530°C).

Abb. 4.30: □: wie simuliert, * : + Spannungsarmglühen (1 Std. 560°C).

Abb. 4.31: □: wie simuliert, * : + Spannungsarmglühen (1 Std. 590°C).

Abb. 4.32: Werkstoff N, Tp = 1050°C, Δt (800-500) = 20 Sek.
□: wie simuliert, * : + Spannungsarmglühen (1 Std. 530°C).

Abb. 4.33: □: wie simuliert, * : + Spannungsarmglühen (1 Std. 560°C).

Abb. 4.34: □: wie simuliert, * : + Spannungsarmglühen (1 Std. 590°C).

Abb. 4.35: Werkstoff N, Tp = 1050°C, Δt (800-500) = 50 Sek.
□: wie simuliert, * : + Spannungsarmglühen (1 Std. 530°C).

Abb. 4.36: □: wie simuliert, * : + Spannungsarmglühen (1 Std. 560°C).

Abb. 4.37: □: wie simuliert, * : + Spannungsarmglühen (1 Std. 590°C).

Abb. 4.38-4.66 = Abb. 4.9-4.37, Werkstoff TM

Abb. 4.67-4.94 = Abb. 4.10-4.37, Werkstoff QT

Abb. 4.95: Die TT40 Temperatur der drei bei 1050°C simulierte Werkstoffe als Funktion des Abkülungszykluses Δt (800-500).

Abb. 4.96: Die TT40 Temperature der drei simulierte Werkstoffe (bei Tp = 1050°C und Δt (800-500) = 12 Sek.), wie simuliert und nach Spannungsarmglühen.

Abb. 4.97: Tp = 1050°C und Δt (800-500) = 20 Sek.

Abb. 4.98: Tp = 1050°C und Δt (800-500) = 50 Sek.

Abb. 4.99: Die TT40 Temperatur der drei bei 1350°C simulierte Werkstoffe als Funktion des Abkülungszykluses Δt (800-500).

Abb. 4.100: Die TT40 Temperature der drei simulierte Werkstoffe (bei Tp = 1350°C und Δt (800-500) = 7 Sek.), wie simuliert und nach Spannungsarmglühen.

Abb. 4.101: Tp = 1350°C und Δt (800-500) = 12 Sek.

Abb. 4.102: Tp = 1350°C und Δt (800-500) = 20 Sek.

Abb. 4.103: Tp = 1350°C und Δt (800-500) = 50 Sek.

Abb. 4.104: Tp = 1350°C + 775°C und Δt (800-500) = 13,6 Sek.

Abb. 4.105: Tp = 1350°C + 775°C und Δt (800-500) = 22,6 Sek.

Abb. 4.106: Mikrostruktur der simulierte Probestücke des N-Werkstoffs
a: Δt (800-500) = 7 Sek. b: Δt (800-500) = 12 Sek.
c: Δt (800-500) = 20 Sek. d: Δt (800-500) = 50 Sek.
V = x500

Abb. 4.107: Werkstoff: TM

Abb. 4.108: Werkstoff: QT

Abb. 4.109: Mikrostruktur der simulierte Probestücke des N-Werkstoffs
Simulationsverhältnis : 1350°C/12 Sek.
a: wie simuliert b: +1 Std. 530°C
c: +1 Std. 560°C d: +1 Std. 590°C
a: V = x500 b-d: V = x1000

Abb. 4.110: Werkstoff: TM

Abb. 4.111: Werkstoff: QT

Abb. 4.112: Das Teil intergranularer Bruch des simuliertes Werkstoffs (Tp = 1350°C) und des simuliertes und vorgewärmtes Werkstoffs, für verschiedene Abkühlungsrate.

Abb. 4.113: Rasterelektronenmikroskopische Abbildung der Bruchoberfläche von spröde gebrochene Charpy-V-Probestücke des N-Werkstoffs.
Simulationsverhältnis : 1350°C/12 Sek.
a: wie simuliert b: +1 Std. 530°C
c, d: +1 Std. 590°C

Abb. 4.114: Werkstoff: TM.

Abb. 4.115: Werkstoff: QT.

Abb. 4.116: Transmission-Elektronenmikroskopische Abbildung des Extraktionsreplikas und Folie des TM-Werkstoffs, Simulationsverhältnis: 1350°C/12 Sek.
a: Replika, +1 Std. 530°C b: Replika, +1 Std. 590°C
c: Folie, +1 Std. 530°C d: Folie, +1 Std. 590°C
a, b: V = x2000 c: V = x6000 d: V = x4000

Abb. 4.117: Folie-Mikrographs auf frühere austenitischen Korngrenzen im TM-Werkstoff.
Simulationsverhältnis : 1350°C/ 7 Sek.,
Spannungsarmglühen: 590°C, 90% intergranulare Bruch.
a: x50.000 b: x60.000

Abb. 4.118: Die chemische Zusammenstellung der Korngrenzen des N-Werkstoffs im Lieferzustand, nach einer thermischen Schweisssimulation und nach Spannungsarmglühen.

Abb. 4.119: Werkstoff: TM.

Abb. 4.120: Werkstoff: QT.

Abb. 4.121: Auger Analyse der Korngrenze des N-Werkstoffs.
Verhältnis : 1350°C/7 Sek., Spannungsarmglühen: 590°C.
(a) Mikrograph der Korngrenze
(b) Analyse der gebrochene Oberfläche

Abb. 4.122: Auger Analyse der Korngrenze des TM-Werkstoffs.
Verhältnis : 1350°C/7 Sek., Spannungsarmglühen: 590°C.
(a) Mikrograph der Korngrenze
(b) Analyse der gebrochene Oberfläche
(c) Analyse nach 2 Min. Kathodenzerstäubung

Abb. 4.123: Werkstoff: QT.

Abb. 5.1: Einfluss der Einbrenntemperatur von E9018-G Stabelektroden auf den diffusionsfähigen Wasserstoffgehalt gemäss ISO 3690.

Abb. 5.2: Risslänge in den Prüfstücken des Tekken-Tests als Funktion der Vorwärmtemperatur. Werkstoff N.
a = 15 mm Blechdicke;
b = 50 mm Blechdicke.

Abb. 5.3: Werkstoff TM.

Abb. 5.4: Werkstoff TM.

Abb. 7.1: Ergebnisse der Zugversuche mit bei 20°C (a) und 560°C (b) gewalztem N-Werkstoff.

Abb. 7.2: Werkstoff N, gewalzt bei 590°C (a) und 620°C (b).

Abb. 7.3: Werkstoff TM gewalzt bei 20°C (a) und 560°C (b).

Abb. 7.4: Werkstoff TM gewalzt bei 590°C (a) und 620°C (b).

Abb. 7.5: Werkstoff QT gewalzt bei 20°C (a) und 560°C (b).

Abb. 7.6: Werkstoff Qt gewalzt bei 590°C (a) und 620°C (b).

Abb. 7.7: Ergebnisse der Kerbschlagbiegeprobe beim N-Werkstoff, bei 20°C gewalzt (a) und nach Reckalterung (b).

Abb. 7.8: Werkstoff N, gewalzt bei 560°C (a) und 590°C (b).

Abb. 7.9: Werkstoff N, gewalzt bei 620°C.

Abb. 7.10-7.12 = Abb. 7.7-7.9, Werkstoff TM.

Abb. 7.13-7.15 = Abb. 7.7-7.9, Werkstoff QT.

Abb. 7.16: Die Ferritkorngrösse des N-Werkstoffs als Funktion des Erhitzungszyklus.

Abb. 7.17: Die Ferritkorngrösse des X-Werkstoffs als Funktion des Erhitzungszyklus.

Abb. 7.18: Die Streckgrenze des N-Werkstoffs als Funktion des Erhitzungzykluses.

Abb. 7.19: Die Streckgrenze des X-Werkstoffs als Funktion des Erhitzungzykluses.

Abb. 7.20: Die Streckgrenze des N- und X-Werkstoffs als Funktion der Ferritkorngrösse.

Abb. 7.21: Charpy-V-Temperaturkurven des N-Werkstoffs nach der Austenitisierung bei 920°C mit einer Erhitzungs- und Abkühlungsrate von 60°C und 120°C/Std.

Abb. 7.22: Erhitzungs- und Abkühlungsrate = 250°C und 500°C/Std.

Abb. 7.23: Austenitisierung bei 960°C mit einer Erhitzungs- und Abkühlungsrate von 60°C und 120°C/Std.

Abb. 7.24: Erhitzungs- und Abkühlungsrate = 250°C und 500°C/Std.

Abb. 7.25: Charpy-V-Temperaturkurven des X-Werkstoffs nach der Austenitisierung bei 920°C mit einer Erhitzungs- und Abkühlungsrate von 60°C und 120°C/Std.

Abb. 7.26: Erhitzungs- und Abkühlungsrate = 250°C und 500°C/Std.

Abb. 7.27: Austenitisierung bei 960°C mit einer Erhitzungs- und Abkühlungsrate von 60°C und 500°C/Std.

Abb. 7.28: CTOD-Werte des N-Werkstoffs bei -10°C als Funktion der Ferritkorngrösse.

Abb. 7.29: CTOD-Werte des X-Werkstoffs bei -10°C als Funktion der Ferritkorngrösse.

Abb. A1: Beispiele für die Makrostrukturen der Schweissproben:
a = Lichtbogenschweissen mit Stabelektroden, N, 15 mm
b = UP-Schweissen, QT, 15 mm
c = UP-Schweissen, N, 50 mm, 22 kJ/cm
d = UP-Schweissen, QT, 50 mm, 35 kJ/cm.

Tabelle 6.12 : Wärmeeinbring = 35 kJ/cm, Zustand: wie geschweisst.

Tabelle 6.13 : Zustand: Spannungsgeglüht 530°C.

Tabelle 6.14 : Zustand: Spannungsgeglüht 560°C.

Tabelle 6.15-6.16 = Tabelle 6.9-6.10, Werkstoff: TM.

Tabelle 6.17-6.19 = Tabelle 6.12-6.14, Werkstoff: TM.

Tabelle 6.20-6.25 = Tabelle 6.9-6.14, Werkstoff: QT.

Tabelle 6.26 : Übersicht über die mittlere Charpy-V-Bruchenergie bei -40°C für die Schweissproben beim Lichtbogenschweissen mit Stabelelektroden im 15 mm dickem Blech.

Tabelle 6.27 : Übersicht über die mittlere Charpy-V-Bruchenergie bei -40°C für die Schweissproben beim UP-Schweissen im 15 mm dickem Blech.

Tabelle 6.28 : Übersicht über die mittlere Charpy-V-Bruchenergie bei -40°C für die Schweissproben beim UP-Schweissen (22 kJ/cm) im 50 mm dickem Blech.

Tabelle 6.29 : Übersicht über die mittlere Charpy-V-Bruchenergie bei -40°C für die Schweissproben beim UP-Schweissen (35 kJ/cm) im 50 mm dickem Blech.

Tabelle 6.30 : CTOD-Eigenschaften der 15 mm dicken Schweissproben beim Lichtbogenschweissen mit Stabelelektroden.

Versuchstemperatur : -10°C

Lage der Einkerbung : Schmelzlinie

Probestücktyp : Bx2B

Tabelle 6.31 : CTOD-Eigenschaften der 15 mm dicken Schweissproben beim UP-Schweissen.

Versuchstemperatur : -10°C

Lage der Einkerbung : 50% HAZ - 50% WM

Probestücktyp : Bx2B

Tabelle 6.32 : CTOD-Eigenschaften der 50 mm dicken Schweissproben bei K-Schweissungen.

Versuchstemperatur : -10°C

Lage der Einkerbung : Schmelzlinie

Probestücktyp : Bx2B

Tabelle 6.33 : CTOD-Eigenschaften der 50 mm dicken rechteckige Schweissproben.

Versuchstemperatur : -10°C

Lage der Einkerbung : Schmelzlinie

Probestücktyp : Bx2B

Table 3.1 : Chemical analysis of the applied steel plates (certificate values)

Steel type	Thickness (mm)	Chemical analyses in weight %														
		C	Mn	Si	P	S	Cr	Ni	Cu	Al	Nb	V	Ti	Ceq*	Pcm**	N (ppm)
N	15	0.14	1.55	0.44	0.020	0.003	0.05	0.43	0.21	0.033	0.03	0.13	--	0.48	0.27	49
N	50	0.13	1.62	0.45	0.007	0.003	0.02	0.55	0.21	0.034	0.03	0.15	--	0.48	0.26	87
X	50	0.14	1.52	0.14	0.012	0.002	0.04	0.53	0.05	0.033	--	0.16	0.002	0.47	0.25	
QT	15	0.106	1.27	0.409	0.009	0.001		0.139	0.237	0.036	0.002	--	--	0.34	0.20	55
QT	50	0.0905	1.361	0.319	0.010	0.001		0.315	0.232	0.025	0.016	--	--	0.35	0.19	72
TM	15.7	0.10	1.58	0.31	0.014	0.002		0.028	0.016	0.035	0.032	0.06	0.002	0.38	0.20	53
TM	50.8	0.10	1.51	0.43	0.011	0.001		0.42	0.22	0.039	0.017	0.002	0.010	0.39	0.21	33

* Ceq $= \% C + \frac{Mn}{6} + \frac{Cr+Mo+V}{5} + \frac{Ni+Cu}{15}$

** Pcm(%) $= \% C + \frac{Si}{30} + \frac{Mn+Cu+Cr}{20} + \frac{Ni}{60} + \frac{Mo}{15} + \frac{V}{10} + 5B$

Table 3.2 : Mechanical Properties of the applied steel plates (certificate values)

Steel Type	Thickness (mm)	Tensile properties			Charpy-V properties (-40 °C)				
		Re N/mm²	Rm N/mm²	A5 %	Position	1	2	3	Av
N	15	525	640	27	surface	124	126	30	93
		538	649	25	surface	70	120	78	89
N	50	468	598	28	1/4 t	26	76	23	42
		467	599	23	1/4 t	31	76	75	61
X	50	446	603	25	1/4 t	98*	51*	76*	75*
		454	606	25	1/4 t	81*	56*	71*	69*
TM	15.7	567	646	23	1/2 t	132	113	131	125
TM	50.8	442	534	30	t - 2	217	243	228	229
					1/2 t	194	200	208	201
QT	15	455	574	20	1/2 t	236	234	246	239
		451	569	21	1/2 t	264	244	252	253
QT	50	448	556	27	1/2 t	174	188	176	179
		434	538	26	1/2 t	182	204	184	190

* test results at -50 °C

Table 4.1 ***Parameters of the weld thermal simulation tests on the normalise quenched and tempered and thermo mechanically treated steel***

Thermal Cycle number	Peak temperature		Cooling time Δt (800-500) (sec)	Cooling time Δt (600-400) (sec)	
	Tp1	Tp2		Δt1	Δt2
1	1350°C		7		
2	1350°C		12		
3	1350°C		20		
4	1350°C		50		
5	1050°C		7		
6	1050°C		12		
7	1050°C		20		
8	1050°C		50		
9	775°C			13.6	
10	775°C			22.6	
11	1350°C	775°C		13.6	13.6
12	1350°C	775°C		22.6	22.6

Table 4.2 ***Transition temperatures for the weld thermally simulated specimens***

Material	Peak temperature (°C)		Cooling time Δt (800-500) (sec)	Transition temperature TT40			
	Tp1	Tp2		as simulated (°C)	+1h 530°C	+1h 560°C	+1h 590°C
N	as delivered		-	-65	-	-	-
	1350	-	7	-45	35J at+60	20J at+60	15J at +60
	1350	-	12	0	0	20J at+60	16J at +60
	1350	775	13.6	0	-25	+20	+35
	1350	-	20	+15	+20	30J at+60	16J at +60
	1350	775	22.6	+10	+10	+20	+45
	1350	-	50	30J at +20	+40	30J at+60	16J at +60
	1050	-	7	-50			
	1050	-	12	-10	-40	-10	35J at 0
	1050	-	20	-20	70J at -40	-10	-10
	1050	-	50	-20	50J at -40	-30	- 5
TM	as delivered		-	<-100	-	-	-
	1350	-	7	-50	0	+60	+60
	1350	-	12	-45	-30	10J at+20	12J at +20
	1350	775	13.6	0	-50	-60	-10
	1350	-	20	-25	- 5	30J at+20	25J at +20
	1350	775	22.6	+25	0	-10	-10
	1350	-	50	+10	+ 5	30J at+20	+20
	1050	-	7	-100			
	1050	-	12	-100	120Jat-100	60J at-100	<-40
	1050	-	20	-85	150Jat- 80	165J at-80	170J at -70
	1050	-	50	-70	180Jat- 80	155J at-80	<-40

Table 4.3 Results of the SEM investigation on the fracture behaviour of weld thermal simulated and post weld heat treated (PWHT) material

Condition			Percentage of intergranular fracture		
Peak temp. °C	Cooling time Δt (800-500) sec.	PWHT °C	N	TM	QT
1050	7	-	0	0	0
	7	530	0	0	0
	7	560	0	0	0
	7	590	0	0	0
1050	12	-	0	0	0
	12	530	0	0	0
	12	560	0	0	0
	12	590	0	0	0
1350	7	-	0	0	0
	7	530	20	65	75
	7	560	40	75	90
	7	590	70	90	95
1350	12	-	0	0	0
	12	530	0	15	50
	12	560	50	60	90
	12	590	75	70	95
1350	20	-	0	0	0
	20	530	0	15	5
	20	560	30	10	10
	20	590	65	15	15
1350	50	-	0	0	0
	50	530	0	0	0
	50	560	0	0	0
	50	590	0	0	0

Table 4.4 Chemical composition (Fe, Mn, V) of the grain boundary precipitates analysed on extraction replicas with ED-spectroscopy (TEM investigation)

Condition			Fe, Mn and V in wt % in material								
Peak temp.	Cooling time Δt800-500	PWHT	N			TM			O		
			Fe	Mn	V	Fe	Mn	V	Fe	Mn	V
°C	sec.	°C									
as delivered		-	86.2	11.5	2.3	95	4.8	0.2	89.6	10.4	np
		530	85.5	12.3	2.2	94.8	4.9	0.3	89.5	10.5	np
		590	85.6	12.2	2.2	90.7	8.8	0.5	90	10.0	np
1050	12	530	94.3	5.2	0.5	95.9	4.1	np	na	na	na
	12	560	90.6	7.8	1.6	94.7	5.0	0.3	na	na	na
	12	590	85.7	12.5	1.8	89.6	9.9	0.5	na	na	na
1350	12	530	95.0	4.5	0.5	96.5	3.5	np	97.1	2.9	np
	12	560	94.0	4.9	1.1	95.0	4.1	0.4	na	na	na
	12	590	89.1	9.5	1.4	90.3	8.8	0.9	94.5	5.5	np
1350	50	530	97.5	2.5	np	97.7	2.3	np	97.8	2.2	np
	50	590	92.1	6.8	1.1	93.8	5.8	0.4	95.1	4.9	np

np = not present (< 0.2%)

na = not analysed

Table 5.1 : ***Results of the Tekken tests; HI = 11 kJ/cm, t = 15 mm, - = cracked; + = not cracked***

Material	Pre-heat temp. (°C)	HDM < 3			HDM = 5			HDM = 10		
		Crack/ no crack	Crack-length	Crack-locat.*	Crack/ no crack	Crack-length	Crack-locat.*	Crack/ no crack	Crack-length	Crack-locat.*
N	20	- -	40 35	3 2						
	35	+ + +								
	50	+			-	80	2	-	100	2
	65				- +	20	3			
	80				+ + +			-	Q	2
	95							+ +		
	110							+		
								+		
TM	20	+ + +			+ + +			-	100	1
	35									
	50				+ +			- -	10 70	1 2
	65									
	80							+ -	15	
	95							+ +		
	110							+		
QT	20	+ + +			+ + +			-	10	3
	35									
	50				+			-	10	1
	65									
	80							+ +		
	95							+		
	110									

* 1 = all weld metal crack;
* 2 = crack initiated HAZ, and propagated in weld;
* 3 = all HAZ cracks

Table 5.2 *: Results of the Tekken tests; HI = 11 kJ/cm, t = 50 mm*
- = cracked; + = not cracked

Material	Pre-heat temp. (°C)	HDM < 3			HDM = 5			HDM = 10		
		Crack/ no crack	Crack-length	Crack-* locat.	Crack/ no crack	Crack-length	Crack-* locat.	Crack/ no crack	Crack-length	Crack-* locat.
N	20	- -	80 15	2 3						
	35	+ + +								
	50	+						-	100	2
	65				- -	30 90	2 2	-	100	1
	80				+ - +	15	3	-	100	2
	95				+ + +			+ -	40	2
	110							+ +		
TM	20	+ + +			-	100	1			
	35				-	75				
	50				- -	80 60	2 1	-	100	1
	65				+ + +			-	100	1
	80				+			-	100	1
	95							- -	75 30	2 1
	110							+ +		
QT	20	+ + +								
	35				-	100	2			
	50				- -	60 10	1 3	-	100	1
	65				+ + +			-	100	2
	80							-	100	1
	95							-	20	1
	110							+ +		

* 1 = all weld metal crack;
* 2 = crack initiated HAZ, and propagated in weld;
* 3 = all HAZ cracks

Table 5.3 *: Results of the Tekken tests; HI = 17 kJ/cm, t = 15 mm*
- = cracked; + = not cracked

Material	Pre-heat temp. (°C)	HDM < 3			HDM = 5			HDM = 10		
		Crack/ no crack	Crack-length	Crack-* locat.	Crack/ no crack	Crack-length	Crack-* locat.	Crack/ no crack	Crack-length	Crack-locat.
N	20	+ +			+ +			-	100	2
	35									
	50				+			-	40	3
	65									
	80				+			+		
	95									
	110									
TM	20	+ +			- +	5		+ +		
	35				+ +					
	50									
	65									
	80									
	95									
	110									
QT	20	+ +			+ +			+ +		
	35									
	50									
	65									
	80									
	95									
	110									

* 1 = all weld metal crack;
* 2 = crack initiated HAZ, and propagated in weld;
* 3 = all HAZ cracks

Table 5.4 : ***Results of the Tekken tests; HI = 17 kJ/cm, t = 50 mm***
- = cracked; + = not cracked

Material	Pre-heat temp. (°C)	HDM < 3			HDM = 5			HDM = 10		
		Crack/ no crack	Crack-length	Crack-* locat.	Crack/ no crack	Crack-length	Crack-* locat.	Crack/ no crack	Crack-length	Crack-locat.
N	20	-	10	3				-	100	2
	35	+								
	50	+								
	65				-	10	2	-	100	1
	80				+			+		
	95									
	110									
TM	20	+								
	35							-	100	1
	50				-	20	2			
	65				+			-	90	1
	80							+		
	95									
	110									
QT	20	+								
	35							-	100	1
	50				-	5	2			
	65				+			-	90	1
	80							-	90	1
	95							+		
	110									

* 1 = all weld metal crack;
* 2 = crack initiated HAZ, and propagated in weld;
* 3 = all HAZ cracks

Table 5.5 : ***Comparison of the pre-heat temperatures measured in this research programme, and predicted according to BS 5135***

		HDM < 3		HDM = 5		HDM = 10	
		Tekken tests	BS 5135	Tekken tests	BS 5135	Tekken tests	BS 5135
N	15 mm	35°C	0°C	70°C	0°C	80	15°C
	50 mm	35°C	105°C	85°C	105°C	105	150°C
TM	15 mm	20*	0	20*	0°C	95	0
	50 mm	20*	0	65	0°C	105	0
QT	15 mm	20*	0	20*	0°C	60	0
	50 mm	20*	0	60	0°C	110	0

* 20°C is the lowest temperature at which Tekken tests have been performed.
It is therefore possible that lower ambient temperatures are acceptable.

Table 6.1 : ***Mechanical test programme, performed for all three materials***

Thickness (mm)	Welding process	Bevel	HI (kJ/cm)	Condition	Tensile test	Side bend test	Charpy-V test	CTOD test
15	SMAW	1/2V	12	AW	x	x	x	x
				PWHT 530°C			x	x
				PWHT 560°C			x	x
15	SAW	I	25	AW	x	x	x	x
				PWHT 530°C			x	x
				PWHT 560°C			x	
50	SAW	K	20	AW	x	x	x	x
				PWHT 530°C			x	
				PWHT 560°C			x	
50	SAW	K	35	AW	x	x	x	x
				PWHT 530°C			x	
				PWHT 560°C			x	
50	SAW	straigt	20	AW				x
				PWHT 530°C				x
				PWHT 560°C				x
50	SAW	straigt	35	AW				x
				PWHT 530°C				x
				PWHT 560°C				x

Table 6.2 : ***Results of the tensile tests and side bend test (D=3d)***

Material	Thickness /bevel	Welding process	Tensile tests		Side bend tests	
			Rm (N/mm^2)	Location of fracture	Crack length (mm)	
N	15, 1/2V	SMAW	655-670	parent plate	-	<1.5
TM	15, 1/2V	SMAW	665-670	parent plate	<1.0	<0.5
QT	15, 1/2V	SMAW	610-605	parent plate	<1.0	<1.5
N	15, I	SAW	670-665	parent plate	-	-
TM	15, I	SAW	655-650	parent plate	-	-
QT	15, I	SAW	565-570	parent plate	-	-
N	50, K	SAW, 20kJ	635-641	parent plate	-	-
TM	50, K	SAW, 20kJ	577-572	parent plate	-	-
QT	50, K	SAW, 20kJ	565-567	parent plate	-	-
N	50, K	SAW, 35kJ	632-636	parent plate	-	-
TM	50, K	SAW, 35kJ	583-606	parent plate	-	-
QT	50, K	SAW, 35kJ	555-550	parent plate	-	-

Table 6.3 : ***Charpy-V test results material N, 15 mm, SMAW***

Code N	Welded joint 1/2V																Welding process SMAW
Condition	Location*)	Charpy Impact Values Temperature															
		0°C				-20°C				-40°C				-60°C			
		1	2	3	AV	1	2	3	AV	1	2	3	AV	1	2	3	AV
As welded	W									96	94	68	86				
	F					177	195	54	142	70	138	56	88	42	74	110	75
	F2					114	152	138	135	78	141	106	107				
	F5									38	108	53	66	45	46	36	42
PWHT	W									72	53	120	82				
1/2h 530°C	F					136	72	77	95	28	57	79	55	32	32	39	34
	F2									69	82	72	74	52	39	67	53
	F5									46	55	42	48				
PWHT	W									84	103	103	96				
1/2h 560°C	F					21	7	77	35	69	15	70	51	8	26	10	15
	F2									49	48	16	38	34	33	16	23
	F5									12	47	35	31				

*) W = Weld metal
F = Fusion line
F2 = Fusion line + 2 mm
F5 = Fusion line + 5 mm

Table 6.4 : ***Charpy-V test results material TM, 15 mm, SMAW***

Code TM	Welded joint 1/2																Welding process SMAW
Condition	Location*)	Charpy Impact Values Temperature															
		0°C				-20°C				-40°C				-60°C			
		1	2	3	AV	1	2	3	AV	1	2	3	AV	1	2	3	AV
As welded	W									70	120	122	104				
	F					61	51	143	85	28	11	66	35	34	58	43	45
	F2					205	186	130	174	188	160	104	151				
	F5									100	100	118	106	88	96	87	90
1/2h 530°	W									77	94	108	93				
	F					60	90	46	99	160	52	112	108	11	90	101	67
	F2					196	156	52	168	121	141	128	130				
	F5									148	108	116	124	108	84	124	105
1/2h 560°	W									118	70	99	96				
	F					72	99	68	113	14	52	134	67	164	48	57	90
	F2									83	95	116	98	59	68	60	62
	F5									106	96	106	103				

*) W = Weld metal
F = Fusion line
F2 = Fusion line + 2 mm
F5 = Fusion line + 5 mm

Table 6.5 **: *Charpy-V test results material QT, 15 mm, SMAW***

Code QT		Welded joint 1/2V												Welding process SMAW			
Condition	Location*)	Charpy Impact Values Temperature															
		0°C				-20°C				-40°C				-60°C			
		1	2	3	AV	1	2	3	AV	1	2	3	AV	1	2	3	AV
As welded	W									128	114	137	126				
	F					159	263	200	207	103	165	146	138				
	F2					254	242	260	252	159	230	268	219				
	F5									280	288	214	261				
PWHT	W									92	76	148	105				
1/2h 530°C	F					101	141	66	136	143	88	80	104	18	31	58	36
	F2									255	245	258	253				
	F5									252	252	248	251	261	250	216	242
PWHT	W									126	137	117	127				
1/2h 560°C	F					299	54	38	230	130	94	234	153	104	126	192	141
	F2									262	278	283	274	262	276	288	275
	F5									300	286	220	269				

*) W = Weld metal
F = Fusion line
F2 = Fusion line + 2 mm
F5 = Fusion line + 5 mm

Table 6.6 **: *Charpy-V test results material N, 15 mm, SAW***

Code NO		Welded joint I												Welding process SAW			
Condition	Location*)	Charpy Impact Values Temperature															
		0°C				-20°C				-40°C				-60°C			
		1	2	3	AV	1	2	3	AV	1	2	3	AV	1	2	3	AV
As welded	W									21	18	15	18				
	F	42	83	92	72	31	36	74	47	30	32	34	32	11	16	30	19
	F2					29	43	23	32	19	32	20	24				
	F5									73	64	93	77	16	52	54	41
PWHT	W									10	12	20	14				
1/2h 530°C	F	28	24	22	25	14	39	22	25	13	12	12	12				
	F2					109	113	101	108	114	44	39	66				
	F5									42	46	48	45	7	11	5	8
PWHT	W									9	8	6	8				
1/2h 560°C	F	29	11	15	18	14	15	7	12	10	14	9	11				
	F2									5	40	31	25	10	48	9	22
	F5									37	15	38	30				

*) W = Weld metal
F = Fusion line
F2 = Fusion line + 2 mm
F5 = Fusion line + 5 mm

Table 6.7 **: *Charpy-V test results material TM, 15 mm, SAW***

Code TM0		Welded joint I												Welding process SAW			
Condition	Location*)	Charpy Impact Values Temperature															
		0°C				-20°C				-40°C				-60°C			
		1	2	3	AV	1	2	3	AV	1	2	3	AV	1	2	3	AV
As welded	W									29	18	24	24				
	F					88	62	70	73	43	27	30	33	11	16	30	19
	F2					192	187	207	195	186	197	178	187				
	F5									199	160	143	167	125	108	118	117
PWHT	W									25	16	5	15				
1/2h 530°C	F					81	34	53	56	162	34	20	72	114	8	34	52
	F2					189	188	175	127	135	110	163	136	174	80	287	180
	F5									126	101	106	111				
PWHT	W									9	7	10	9				
1/2h 560°C	F					139	166	172	159	24	17	14	18	19	15	17	17
	F2									170	160	123	151	174	80	287	180
	F5									126	101	106	111				

*) W = Weld metal
F = Fusion line
F2 = Fusion line + 2 mm
F5 = Fusion line + 5 mm

Table 6.8 **: *Charpy-V test results material QT, 15 mm, SAW***

Code QTO		Welded joint I												Welding process SAW			
Condition	Location*)	Charpy Impact Values Temperature															
		0°C				-20°C				-40°C				-60°C			
		1	2	3	AV	1	2	3	AV	1	2	3	AV	1	2	3	AV
As welded	W									16	12	10	13				
	F					252	205	195	217	78	182	150	137	37	29	64	34
	F2					252	249	249	250	254	259	258	257				
	F5									145	241	260	215	275	282	266	274
PWHT	W					118	97	100	105	18	19	82	40				
1/2h 530°C	F					164	185		175	171	158	142	157	76	76	39	64
	F2					228	147	224	200	230	235	180	215	194	166	110	157
	F5									201	266	260	242	195	215	161	190
PWHT	W									56	40	102	66				
1/2h 560°C	F					210	255	186	217	168	168	168	168	187	189	140	172
	F2									248	184	169	200	191	183	200	191
	F5									228	288	292	269				

*) W = Weld metal
F = Fusion line
F2 = Fusion line + 2 mm
F5 = Fusion line + 5 mm

Table 6.9 : ***Charpy-V test results material N, 50 mm, SAW, HI = 22kJ/cm, condition as welded***

Code GL		Welded joint K												Welding process SAW			
		Condition: as welded															
Location*)		Charpy Impact Values (J) Temperature															
		0°C				-20°C				-40°C				-60°C			
		1	2	3	AV	1	2	3	AV	1	2	3	AV	1	2	3	AV
CAP	W									155	148	156	153				
	F					190	96	112	133	72	79	110	87	94	36	65	65
	F2									39	50	52	47	33	14	39	29
	F5									76	66	74	72	15	19	35	23
Root	W									93	150	108	117				
	F					232	102	177	170	197	72	173	147	55	76	28	53
	F2									27	106	67	67	22	11	41	25
	F5									19	19	62	33	15	22	24	20

*) W = Weld metal
F = Fusion line
F2 = Fusion line + 2 mm
F5 = Fusion line + 5 mm

Table 6.10 : ***Charpy-V test results material N, 50 mm, SAW, HI = 22kJ/cm, condition PWHT 530°C***

Code GL 1		Welded joint K												Welding process SAW			
		Condition: PWHT 530°C															
Location*)		Charpy Impact Values (J) Temperature															
		0°C				-20°C				-40°C				-60°C			
		1	2	3	AV	1	2	3	AV	1	2	3	AV	1	2	3	AV
CAP	W									147	150	131	143				
	F					130	111	101	114	81	37	73	64	35	25	59	40
	F2									77	106	85	89	129	137	113	126
	F5									29	78	29	45	11	19	19	16
Root	W									100	91	97	96				
	F					118	68	59	82	52	51	51	51	37	13	25	25
	F2									83	45	53	60	26	43	25	31
	F5					59	73	41	58	15	16	25	19				

*) W = Weld metal
F = Fusion line
F2 = Fusion line + 2 mm
F5 = Fusion line + 5 mm

Table 6.11 : ***Charpy-V test results material N, 50 mm, SAW, HI = 22 kJ/cm, condition PWHT 560°C***

Code GL 2		Welded joint K												Welding process SAW			
		Condition: PWHT 560°C															
Location*)		Charpy Impact Values (J) Temperature															
		0°C				-20°C				-40°C				-60°C			
		1	2	3	AV	1	2	3	AV	1	2	3	AV	1	2	3	AV
CAP	W									101	105	123	110				
	F					85	53	40	59	76	50	57	61	18	6	17	14
	F2									71	57	65	64	12	5	9	9
	F5									40	46	48	45	13	35	10	19
Root	W									45	43	55	48				
	F	47	25	23	32	13	16	16	1	14	7	17	13				
	F2					63	48	37	49	37	26	20	28				
	F5					37	29	37	34	15	15	36	22				

*) W = Weld metal
F = Fusion line
F2 = Fusion line + 2 mm
F5 = Fusion line + 5 mm

Table 6.12 : ***Charpy-V test results material N, 50 mm, SAW, HI = 35 kJ/cm, condition as welded***

Code GH		Welded joint K												Welding process SAW			
		Condition: as welded															
Location*)		Charpy Impact Values (J) Temperature															
		0°C				-20°C				-40°C				-60°C			
		1	2	3	AV	1	2	3	AV	1	2	3	AV	1	2	3	AV
CAP	W									98	112	95	102				
	F					31	67	48	49	28	38	63	43	26	34	23	28
	F2									32	56	29	39	16	26	22	21
	F5									54	84	66	68	22	15	32	23
Root	W									64	106	64	78				
	F					140	191	60		40	49	49	46	22	18	15	18
	F2									71	86	195	117	102	29	29	53
	F5									56	10	15	27	12	7	9	9

*) W = Weld metal
F = Fusion line
F2 = Fusion line + 2 mm
F5 = Fusion line + 5 mm

Table 6.13 : ***Charpy-V test results material N, 50 mm, SAW, HI = 35 kJ/cm, condition PWHT 530°C***

Code GH 1		Welded joint K												Welding process SAW			
		Condition: PWHT 530°C															
Location*)		Charpy Impact Values (J)															
		Temperature															
		0°C				-20°C				-40°C				-60°C			
		1	2	3	AV	1	2	3	AV	1	2	3	AV	1	2	3	AV
CAP	W									96	103	83	94				
	F					69	73	24	55	34	29	61	41	29	22	30	27
	F2					26	31	23	27	17	23	23	21				
	F5									83	49	70	67	8	35	55	33
Root	W									99	71	67	79				
	F					41	34	54	4	3	1	1	2	1		1	13
	F2					25	51	51	42	16	28	39	28				
	F5					19	42	26	29	17	20	24	20				

*) W = Weld metal
F = Fusion line
F2 = Fusion line + 2 mm
F5 = Fusion line + 5 mm

Table 6.14 : ***Charpy-V test results material N, 50 mm, SAW, HI = 35 kJ/cm, condition PWHT 560°C***

Code GH2		Welded joint K												Welding process SAW			
PWHT:		560															
Location*)		Charpy Impact Values (J)															
		Temperature															
		0°C				-20°C				-40°C				-60°C			
		1	2	3	AV	1	2	3	AV	1	2	3	AV	1	2	3	AV
CAP	W									146	131	101	126				
	F					--	33	65	49	25	57	56	46	--	49	55	52
	F2									18	10	10	13	15	13	8	12
	F5									94	15	90	66	9	8	39	19
Root	W									51	61	51	54				
	F					74	36	28	46	51	27	27	35	11	25	18	18
	F2					68	89	34	64	22	28	13	21				
	F5					39	51	87	59	31	22	39	31				

*) W = Weld metal
F = Fusion line
F2 = Fusion line + 2 mm
F5 = Fusion line + 5 mm

Table 6.15 : ***Charpy-V test results material TM, 50 mm, SAW, HI = 22 kJ/cm, condition as welded***

Code TL		Welded joint K								Welding process SAW							
		Condition: as welded															
Location*)		Charpy Impact Values (J)															
		Temperature															
		0°C				-20°C				-40°C				-60°C			
		1	2	3	AV	1	2	3	AV	1	2	3	AV	1	2	3	AV
CAP	W									139	135	148	141				
	F					138	188	119	148	115	183	183	160	38	74	44	52
	F2									42	59	63	55	36	21	25	27
	F5									170	103	138	137	35	19	71	42
Root	W									109	153	137	133				
	F					118	138	31	96	57	39	127	74	8	20	21	16
	F2									156	29	104	96	11	52	53	39
	F5									75	63	134	91	20	47	20	29

*) W = Weld metal
F = Fusion line
F2 = Fusion line + 2 mm
F5 = Fusion line + 5 mm

Table 6.16 : ***Charpy-V test results material TM, 50 mm, SAW, HI = 22 kJ/cm, condition PWHT 530°C***

Code TL1		Welded joint K								Welding process SAW							
		Condition: PWHT 530°C															
Location*)		Charpy Impact Values (J)															
		Temperature															
		0°C				-20°C				-40°C				-60°C			
		1	2	3	AV	1	2	3	AV	1	2	3	AV	1	2	33	AV
CAP	W									151	159	135	148				
	F					199	129	207	178	157	109	151	139	203	61	108	124
	F2									192	192	54	146	167	68	159	131
	F5									197	188	193	193	157	155	158	166
Root	W									141	141	137	140				
	F					112	92	150	118	94	48	54	65	15	18	45	26
	F2									164	205	229	199	180	60	96	112
	F5									169	176	159	168	27	117	23	55

*) W = Weld metal
F = Fusion line
F2 = Fusion line + 2 mm
F5 = Fusion line + 5 mm

Table 6.17 : ***Charpy-V test results material TM, 50 mm, SAW, HI = 35 kJ/cm, condition as welded***

Code TH		Welded joint K												Welding process SAW			
		Condition: as welded															
Location*)		Charpy Impact Values (J) Temperature															
		0°C				-20°C				-40°C				-60°C			
		1	2	3	AV	1	2	3	AV	1	2	3	AV	1	2	3	AV
CAP	W									137	116	101	118				
	F					153	54	51	86	38	77	87	67	67	29	27	41
	F2									49	33	81	54	20	37	21	26
	F5									201	192	37	143	16	25	19	20
Root	W									108	139	165	137				
	F					139	191	52	94	81	65	137	94	17	21	15	18
	F2									139	159	257	185	15	17	105	46
	F5									145	47	100	97	58	17	123	66

*) W = Weld metal
F = Fusion line
F2 = Fusion line + 2 mm
F5 = Fusion line + 5 mm

Table 6.18 : ***Charpy-V test results material TM, 50 mm, SAW, HI = 35 kJ/cm, condition PWHT 530°C***

Code TH 1		Welded joint K												Welding process SAW			
		Condition: 530°C															
Location*)		Charpy Impact Values (J) Temperature															
		0°C				-20°C				-40°C				-60°C			
		1	2	3	AV	1	2	3	AV	1	2	3	AV	1	2	3	AV
CAP	W									153	116	141	137				
	F					186	192	189	189	188	135	174	166	11	57	105	58
	F2									208	216	730	241	220	211	156	196
	F5									197	156	205	186	178	157	147	161
Root	W									150	149	144	148				
	F					193	142	235	157	191	174	37	134	12	35	9	19
	F2									198	201	179	193	63	57	153	91
	F5									155	143	119	139	79	58	23	53

*) W = Weld metal
F = Fusion line
F2 = Fusion line + 2 mm
F5 = Fusion line + 5 mm

Table 6.19 : ***Charpy-V test results material TM, 50 mm, SAW, HI = 35 kJ/cm, condition PWHT 560°C***

Code TH 2		Welded joint K												Welding process SAW			
		Condition: PWHT 560°C															
Location*)		Charpy Impact Values (J)															
		Temperature															
		0°C				-20°C				-40°C				-60°C			
		1	2	3	AV	1	2	3	AV	1	2	3	AV	1	2	3	AV
CAP	W									135	127	131	131				
	F					171	135	121	142	146	120	127	131	23	21	33	26
	F2									195	175	185	185	13	141	37	64
	F5									201	173	209	209	155	155	87	126
Root	W									134	145	149	143				
	F					121	129	119	123	168	154	37	120	19	196	11	75
	F2									131	171	181	161	119	97	92	103
	F5									31	129	161	107	123	53	13	63

*) W = Weld metal
F = Fusion line
F2 = Fusion line + 2 mm
F5 = Fusion line + 5 mm

Table 6.20 : ***Charpy-V test results material QT, 50 mm, SAW, HI= 22 kJ/cm, condition as welded***

Code QL		Welded joint K												Welding process SAW			
		Condition: as welded															
Location*)		Charpy Impact Values (J)															
		Temperature															
		0°C				-20°C				-40°C				-60°C			
		1	2	3	AV	1	2	3	AV	1	2	3	AV	1	2	3	AV
CAP	W									169	166	156	164	92	39	24	52
	F					283	177	270	243	194	92	102	129	258	270	288	272
	F2									269	268	284	274	227	272	222	240
	F5									288	276	269	278				
Root	W									75	179	179	144				
	F					109	157	286	184	286	>300	290	>292	227	223	154	201
	F2									190	214	215	206	180	182	47	136
	F5									278	198	217	231	22	182	40	81

*) W = Weld metal
F = Fusion line
F2 = Fusion line + 2 mm
F5 = Fusion line + 5 mm

Table 6.21 : ***Charpy-V test results material QT, 50 mm, SAW, HI = 22 kJ/cm, condition PWHT 530°C***

Code QL1		Welded joint K								Welding process SAW							
		Condition: PWHT 530°C															
Location*)		Charpy Impact Values (J)															
		Temperature															
		0°C				-20°C				-40°C				-60°C			
		1	2	3	AV	1	2	3	AV	1	2	3	AV	1	2	3	AV
CAP	W									169	155	157	160				
	F					189	210	191	197	85	211	229	175	165	221	219	202
	F2									289	297	299	295	287	243	222	251
	F5									295	300	269	288	225	293	295	271
Root	W									152	154	171	159				
	F					122	131	205	153	87	75	61	74	45	65	149	86
	F2									287	268	214	260	213	195	221	210
	F5									198	177	191	189	55	180	162	132

*) W = Weld metal
F = Fusion line
F2 = Fusion line + 2 mm
F5 = Fusion line + 5 mm

Table 6.22 : ***Charpy-V test results material QT, 50 mm, SAW, HI = 22 kJ/cm, condition PWHT 560°C***

Code QL2		Welded joint K								Welding process SAW							
		Condition: PWHT 560°C															
Location*)		Charpy Impact Values (J)															
		Temperature															
		0°C				-20°C				-40°C				-60°C			
		1	2	3	AV	1	2	3	AV	1	2	3	AV	1	2	3	AV
CAP	W									154	157	148	153				
	F					125	195	135	152	172	173	78	141	60	77	145	94
	F2									285	>300	217	267	210	>300	221	241
	F5									280	297	297	291	195	299	296	263
Root	W									11	105	12	112				
	F					47	93	71	70	93	118	57	89	102	46	79	76
	F2									181	299	231	237	23	157	194	125
	F5									196	201	202	200	259	224	149	211

*) W = Weld metal
F = Fusion line
F2 = Fusion line + 2 mm
F5 = Fusion line + 5 mm

Table 6.23 : ***Charpy-V test results material QT, 50 mm, SAW, HI = 35 kJ/cm, condition as welded***

Code QH		Welded joint K												Welding process SAW			
		Condition: as welded															
Location*)		Charpy Impact Values (J)															
		Temperature															
		0°C				-20°C				-40°C				-60°C			
		1	2	3	AV	1	2	3	AV	1	2	3	AV	1	2	3	AV
CAP	W									104	98	78	93				
	F					196	159	194	183	148	60	65	91	34	34	40	36
	F2					162	206	192	187	185	152	50	129				
	F5									244	254	252	250	251	264	244	235
Root	W									88	133	80	100				
	F					186	86	195	156	140	30	270	147	32	256	35	108
	F2					256	256	235	249	160	157	90	136				
	F5									166	83	168	139	188	212	202	201

*) W = Weld metal
F = Fusion line
F2 = Fusion line + 2 mm
F5 = Fusion line + 5 mm

Table 6.24 : ***Charpy-V test results material QT, 50 mm, SAW, HI = 22 kJ/cm, condition PWHT 530°C***

Code QH1		Welded joint K												Welding process SAW			
		Condition: PWHT 530°C															
Location*)		Charpy Impact Values (J)															
		Temperature															
		0°C				-20°C				-40°C				-60°C			
		1	2	3	AV	1	2	3	AV	1	2	3	AV	1	2	3	AV
CAP	W									89	111	109	103				
	F					163	170	171	168	191	163	151	168	113	68	169	117
	F2									203	183	143	176	202	71	36	103
	F5									206	270	194	223	279	288	282	283
Root	W									149	143	150	147				
	F					121	109	181	137	144	96	83	108	39	103	77	73
	F2									77	215	135	142	115	112	36	88
	F5									214	187	247	216	46	102	160	103

*) W = Weld metal
F = Fusion line
F2 = Fusion line + 2 mm
F5 = Fusion line + 5 mm

Table 6.25 : ***Charpy-V test results material QT, 50 mm, SAW, HI = 35 kJ/cm, condition PWHT 560°C***

Code QH2		Welded joint K												Welding process SAW			
		Condition: 560°C															
Location*)		Charpy Impact Values (J)															
		Temperature															
		0°C				-20°C				-40°C				-60°C			
		1	2	3	AV	1	2	3	AV	1	2	3	AV	1	2	3	AV
CAP	W									125	123	106	118				
	F					193	177	173	181	100	87	189	125	151	148	55	118
	F2									199	188	199	195	186	259	183	209
	F5									279	>300	278	286	283	285	215	261
Root	W									135	134	91	120				
	F					249	254	177	227	152	140	213	168	167	21	190	126
	F2									141	269	>300	237	191	207	89	162
	F5									91	271	295	219	195	145	120	153

*) W = Weld metal
F = Fusion line
F2 = Fusion line + 2 mm
F5 = Fusion line + 5 mm

Table 6.26 : ***Overview of the average Charpy-V fracture energie at -40°C for the SMAW weldments in 15 mm thick materials.***

Base material	Condition	Charpy-V fracture energies (J) at -40°C			
		WC	FL	F2	F5
N	AW	86	88	107	66
	PWHT 530°C	82	55	74	48
	PWHT 560°C	96	51	38	31
TM	AW	104	35	151	106
	PWHT 530°C	93	108	130	124
	PWHT 560°C	96	67	98	103
QT	AW	126	138	219	216
	PWHT 530°C	105	104	253	251
	PWHT 560°C	127	153	274	269

Table 6.27 : ***Overview of the average Charpy-V fracture energie at -40°C for the SAW weldments in 15 mm thick materials.***

Base material	Condition	Charpy-V fracture energies (J) at -40°C			
		WC	FL	F2	F5
N	AW	18	32	24	77
	PWHT 530°C	14	12	66	45
	PWHT 560°C	8	11	25	30
TM	AW	24	33	187	167
	PWHT 530°C	15	72	136	111
	PWHT 560°C	9	18	151	111
QT	AW	13	137	257	215
	PWHT 530°C	40	157	215	242
	PWHT 560°C	66	168	200	269

Table 6.28 : ***Overview of the average Charpy-V fracture energie at -40°C for the SAW weldments (22 kJ/cm) in 50 mm thick materials.***

Base material	Condition	Charpy-V fracture energies (J at -40°C)							
		CAP				ROOT			
		WC	FL	F2	F5	WC	FL	F2	F5
N	AW	153	87	47	72	117	147	67	33
	PWHT 530°C	143	64	89	45	96	51	60	19
	PWHT 560°C	110	61	64	45	48	13	28	22
TM	AW	141	160	55	137	133	74	96	91
	PWHT 530°C	148	139	146	193	140	65	199	168
	PWHT 560°C								
QT	AW	164	129	274	278	144	292	206	231
	PWHT 530°C	160	175	295	288	159	74	200	189
	PWHT 560°C	153	141	267	291	112	89	237	200

Table 6.29 : ***Overview of the average Charpy-V fracture energie at -40°C for the SAW weldments (35 kJ/cm) in 50 mm thick materials.***

Base material	Condition	Charpy-V fracture energies (J at -40°C)							
		CAP				ROOT			
		WC	FL	F2	F5	WC	FL	F2	F5
N	AW	102	43	39	68	78	46	117	27
	PWHT 530°C	94	41	21	67	79	20	28	22
	PWHT 560°C	126	46	13	66	54	35	21	31
TM	AW	118	67	54	143	137	94	185	97
	PWHT 530°C	137	166	241	186	148	134	193	139
	PWHT 560°C	131	131	185	209	143	120	161	107
QT	AW	93	91	129	250	100	147	136	139
	PWHT 530°C	103	168	176	223	147	108	142	216
	PWHT 560°C	118	125	195	286	120	168	237	219

Table 6.30 : ***CTOD properties of 15 mm SMAW weldments***
Test temperature: -10°C
Notch location : Fusion line
Specimen type : Bx2B

Base material	Condition	CTOD values (mm)					
N	AW	0.10(δc)	0.17(δc)	0.30(δu)	0.26(δm)	0.17(δc)	0.61(δm)
	530	0.08(δc)	0.60(δc)	0.23(δu)			
	560	0.19(δc)	0.09(δc)	0.28(δu)			
TM	AW	0.67(δu)	0.54(δu)	0.17(δc)	0.38(δm)	0.56(δm)	0.32(δm)
	530	0.79(δm)	0.75(δm)	0.70(δm)			
	560	0.54(δm)	0.61(δm)	0.29(δm)			
QT	AW	1.18(δm)	0.77(δm)	0.30(δu)	0.87(δm)	0.82(δm)	0.33(δm)
	530	1.28(δm)	1.02(δm)	0.83(δm)			
	560	1.16(δm)	1.02(δm)	0.95(δm)			

Table 6.31 : ***CTOD properties of the 15 mm SAW weldments***
Test temperature: -10°C
Notch location : 50% HAZ - 50% WM
Specimen type : Bx2B

Base material	CTOD values (mm)					
	As welded			PWHT 530°C		
N	0.05(δc)	0.07(δc)	0.08(δc)	0.08(δc)	0.07(δc)	0.07(δc)
TM	0.27(δc)	0.50(δm)	0.05(δc)	0.78(δm)	0.89(δm)	0.34(δc)
QT	0.08(δc)	0.13(δc)	0.22(δc)	1.20(δm)	1.37(δm)	1.26(δm)

Table 6.32 : ***CTOD properties of 50 mm K weldments***
Test temperature: -10°C
Notch location : Fusion line
Specimen type : Bx2B

Base material	Condition	CTOD values (mm)					
		HI = 20 kJ/cm			HI = 35 kJ/cm		
N	AW	0.09(δc)	0.36(δc)	-	0.04(δc)	0.05(δc)	0.07(δc)
TM	AW	0.09(δc)	0.14(δc)	0.30(δu)	0.36(δu)	0.10(δc)	0.10(δc)
QT	AW	1.97(δu)	1.97(δm)	1.84(δu)	0.77(δu)	1.95(δm)	1.97(δc)
QT	WM AW	>1.99(δm)	>2.04(δm)	>2.01(δm)	>2.01(δm)	>2.01(δm)	1.38(δu)
QT	WM 530	>1.99(δm)	0.79(δu)	2.09(δm)	1.98(δu)	1.98(δm)	1.97(δm)
QT	WM 560	1.96(δm)	1.93(δm)	1.54(δu)	1.69(δm)	1.20(δu)	0.51(δu)

Table 6.33 : ***CTOD properties of 50 mm straight bevel weldments***
Test temperature: -10°C
Notch location : Fusion line
Specimen type : Bx2B

Base material	Condition	CTOD values (mm)					
		HI = 20 kJ/cm			HI = 35 kJ/cm		
N	AW	0.14(δc)	0.47(δc)	0.41(δc)	0.03(δc)	0.14(δc)	0.05(δc)
	530	1.27(δu)	2.02(δu)	0.20(δu)	0.11(δc)	1.84(δu)	0.03(δc)
	560	0.92(δu)	0.95(δu)	0.06(δc)	0.08(δc)	0.05(δc)	0.02(δc)
TM	AW	>2.00(δm)	0.12(δc)	0.18(δc)	0.45(δc)	0.20(δc)	0.26(δc)
	530	2.03(δm)	1.02(δm)	0.58(δu)	0.25(δc)	0.34(δc)	2.12(δm)
	560	2.05(δm)	1.17(δu)	0.37(δu)	0.10(δc)	0.09(δc)	0.38(δu)
QT	AW	0.36(δc)	>2.04(δm)	0.89(δu)	>2.00(δm)	0.77(δu)	2.29(δu)
	530	2.00(δm)	2.03(δm)	2.00(δm)	2.11(δm)	0.80(δu)	2.04(δm)
	560	1.99(δm)	2.05(δm)	2.10(δm)	0.44(δu)	1.65(δu)	2.05(δm)

Table 7.1: Results of the hardhess measurements and tensile and impact test on normalised, thermo mechanically treated and quenched + tempered Fe460 in the as delivered condition and after rolling at several temperatures and deformation grades.

Material conditons	normalised (15.2 mm)						Thermo mechanically treated (15.7 mm)						quenched and tempered (15.4 mm)					
	Re Mpa	Rm Mpa	Re/Rm	A %	HV1	OT40 °C	Re Mpa	Rm Mpa	Re/Rm	A %	HV1	OT40 °C	Re Mpa	Rm Mpa	Re/Rm	A %	HV1	OT40
DIN 17.102;FeE460	>460	560 730	0.9	17				560 730	0.9 [2] 0.85	17				560 730	0.9	17		
Euronorm 113-72	>460	570 720		17			>460	570 720		17			>460	570 720		17		
as delivered conditon	550	637	0.86	27.9	207±9	≈-75	560	625	0.9	29.5	220±7	<-100	407[1]	545[1]	0.75	26.27	198+13	<-100
2 1/2% at 20°C	580	700	0.83	21.9		≈-50	552	635	0.87	26.4			528	580	0.91	23		<-100
2 1/2% at 20°C + 1/2h/250°C	605	685	0.88	22.1		≈-20	660	680	0.97	21.8			532	585	0.91	19.7		≈- 80
5% at 20°C	702	737	0.95	16.9	250±10	≈-50	630	685	0.92	17.8	242±7	<-100	551	583	0.95	19.3	210+5	<-100
5% at 20°+1/2h/250°C	695	727	0.96	16.4	245±7	≈0	712	712	1.0	18.2	252±6	<-100	590	617	0.96	18.6	243+8	<-100
10% at 20°C	712	757	0.94	13.1	258±11	≈-50	677	715	0.95	14.6	251±9	<-100	567	616	0.92	15.6	213+5	<-100
10% at 20°C+1/2h/250°C	685	737	0.93	14	262±13	≈-50	732	752	0.97	15.1	263±8	<-100	636	655	0.97	13.4	243+8	≈- 90
aged 1hr at 560°C	550	640	0.86	27.2		≈-40	550	615	0.89	29		<-100	455	545	0.83	26		<-100
2 1/2% at 560-480°C	580	670	0.87	23.2		≈-10	620	670	0.93	23.2		<-100	492	570	0.86	22		<-100
5% at 560-480°C	622	697	0.89	21.9	233±6	≈-30	622	667	0.93	23.9	235±4	<-100	505	578	0.87	19.5	221±7	<-100
10% at 560-480°C	657	722	0.91	19.3	244±4	≈-50	667	697	0.96	21.5	244±7	<-100	540	602	0.9	20.8	220±4	<-100
aged 1hr at 590°C	540	645	0.84	27.5		≈-60	555	620	0.9	31.4		<-100	450	545	0.83	22.8		<-100
2 1/2% at 590-520°C	582	680	0.86	25.3		≈-50	592	645	0.92	26.9		<-100	497	585	0.85	22.8		<-100
5% at 590-520°C	587	680	0.86	24.2	232±5	≈-50	588	642	0.92	24.5	233±4	<-100	425	585	0.73	24	204±7	<-100
10% at 590-520°C	632	705	0.9	22.5	237±4	≈-50	605	662	0.91	22.1	245±5	<-100	512	592	0.86	19.8	209±4	<-100
aged 1hr at 620°C	555	650	0.85	27.1		≈-60	550	605	0.91	31.2		<-100	445	545	0.82	23.3		<-100
2 1/2% at 620-550°C	570	667	0.85	24.8	234±5	≈-70	582	635	0.92	27.6		<-100	467	570	0.82	26.3		<-100
5% at 620-550°C	590	682	0.87	23.4	254±7	≈-30	591	650	0.91	25.2	235±8	<-100	474	565	0.84	24.2	198±11	≈-90
10% at 620-550°C	620	702	0.88	21.9		≈-50	600	662	0.91	24.6	232±7	<-100	515	597	0.86	23.1	203±8	<-100

1) average of 4 values.
2) 0.85 when Re = 100 MPa higher than Re minimum (460 MPa)

Table 7.2 : ***Programme concerning the properties of the normalized materials N and X after normalizing***

Steel type		Normalizing treatment				Mechanical properties			Microstructure investigation
N	X	Heating rate (°C/hour)	T max (°C)	Hold time at T max (hr)	Cooling rate (°C/hour)	Charpy-V transition curves	Tensile tests (20°C)	CTOD tests (-10°C)	Ferrite grain size ($d^{-1/2}$)
X	X	as delivered condition				X	X	X	X
X	X	60	920	1	60	X	X	X	X
X	X	120	920	1	120	X	X	X	X
X	X	250	920	1	250	X	X	X	X
X	X	500	920	1	500	X	X	X	X
X	X	60	960	1	60	X	X	X	X
X		120	960	1	120	X	X	X	X
X		250	960	1	250	X	X	X	X
X	X	500	960	1	500	X	X	X	X

Table 7.3 ***Results of the determinations of the ferrite grain sizes of material N and X in the as delivered condition and after normalizing.***

Material	Normalizing treatment			Ferrite grain size $d^{-1/2}$
	Heating and cooling rate (°C/hr)	T max (°C)	Hold time at T max (hr)	($mm^{-1/2}$)
Material N	as delivered condition			11.9
50 mm	60	920	1	8.9
	120	920	1	9.2
	250	920	1	9.7
	500	920	1	11.2
	60	960	1	8.3
	120	960	1	8.3
	250	960	1	8.8
	500	960	1	9.0
Material X	as delivered condition			10.5
50 mm	60	920	1	9.2
	120	920	1	9.5
	250	920	1	10.4
	500	920	1	10.3
	60	960	1	8.9
	500	960	1	10.2

Table 7.4 : ***Results of the tensile tests of material N and X in the as delivered condition and after several normalizing treatments.***

Material	Normalizing treatment			Tensile tests								
	Heating and cooling rate (°C/hr)	T max (°C)	Hold time at T max (hr)	Yield strength (MPa)			Tensile strength (MPa)			Elongation A5 (%)		
				1	2	av.	1	2	av.	1	2	av.
N	as delivered condition			500	500	500	600	615	608	28	27	28
50 mm	60	920	1	398	412	405	584	586	585	26	26	26
	120	920	1	414	395	404	604	601	603	26	26	26
	250	920	1	431	447	439	592	603	598	26	26	26
	500	920	1	434	465	450	605	615	610	25	26	26
	60	960	1	368	382	375	586	581	584	26	26	26
	120	960	1	387	398	393	600	600	600	23	26	25
	250	960	1	400	417	409	605	625	615	22	22	22
	500	960	1	427	415	421	621	608	615	25	24	25
X	as delivered condition			444	438	441	595	595	595	26	25	26
50 mm	60	920	1	388	382	385	560	565	563	26	27	27
	120	920	1	395	395	395	565	565	565	26	26	26
	250	920	1	435	428	432	565	575	570	27	27	27
	500	920	1	437	450	444	600	570	585	28	26	27
	60	960	1	380	380	380	565	560	563	26	26	26
	500	960	1	445	435	440	570	565	568	26	28	27
DIN 17.102	Requirements for StE 460				≥ 440			560-730			17	

Table 7.5 : *Results of the charpy impact tests in the as delivered condition and after normalizing.*

Material	Normalizing treatment			Charpy impact values (J)																												
	Heating and cooling rate (°C/hr)	T max (°C)	Hold time at Tmax	Temperature (°C)																												
				-100			-80			-60			-40			-20			0			+20			+40			+60			+80		
				1	2	av	1	2	av	1	2	av	1	2	av	1	2	av	1	2	av	1	2	av	1	2	av	1	2	av	1	2	av
N	as delivered						21	26	24	26	60	58	91	92	92	122	138	130	146	165	156	168	154	161	216	202	209				230	216	223
50 mm	60	920	1										12	13	13	28	26	27	87	67	77	96	118	107	147	127	137	157	159	158	182	187	185
	120	920	1										12	18	15	20	27	24	85	62	74	96	106	101	126	145	136	146	163	155	185	193	189
	250	920	1										12	14	13	17	47	27	50	75	63	96	112	104	145	159	152	158	166	162	190	184	187
	500	920	1				7	13	10	37	53	45	100	92	96	114	90	102	132	122	127	150	144	147	172	158	165				184	186	185
	60	960	1										6	7	7	10	11	11	13	16	15	91	60	76	98	118	108	151	123	137	183	168	176
	120	960	1										10	9	10	19	11	15	43	26	35	132	76	104	74	117	96	121	127	124	170	172	171
	250	960	1										8	9	9	20	21	21	48	28	38	75	102	89	103	118	111	144	136	140	167	161	164
	500	960	1							3			13	16	15	36	36	36	46	53	50	65	80	73	86	82	84	118	118	118	130	148	139
X	as delivered			21	58	40	98	82	90	92	130	111	105	138	122	145	149	148	152	156	154	188	186	187							196	208	202
50 mm	60	920	1	12	8	10	45	14	30	70	98	84	114	90	102	160	146	153	139	156	148	187	224	206							200	188	194
	120	920	1	9	10	10	45	19	32	82	36	59	110	135	123	150	150	150	156	160	158	158	172	165							192	190	191
	250	920	1	12	10	11	52	56	54	65	72	69	140	136	138	182	168	175	194	157	176	190	196	193							202	186	194
	500	920	1	10	16	13	18	54	36	88	86	87	110	120	115	152	150	151	166	169	168	186	200	193							188	198	193
	60	960	1				9	7	8	56	32	44	84	48	66	110	100	105	82	138	110	159	136	148	164	162	163				186	176	178
	500	960	1	16	10	13	42	50	46	68	52	60	130	120	125	135	144	140	147	170	159	180	188	187							186	190	188

Table 7.6 : ***Transition temperatures (TT40 and TT27) and shift in transition curve for the materials N and X in the as delivered condition and after normalizing***

Material	Normalizing treatment			Transition temperatures		Shift in transition curve
	Heating and cooling rate (°C/hr)	T max (°C)	Hold time at T max (hr)	TT40 Joules (°C)	TT27 Joules (°C)	
N	as delivered			~ - 70	~ - 80	
50 mm	60	920	1	~ - 15	~ - 25	~ + 45°C
	120	920	1	~ - 15	~ - 20	~ + 45°C
	250	920	1	~ - 15	~ - 30	~ + 45°C
	500	920	1	~ - 60	~ - 70	~ + 15°C
	60	960	1	~ + 10	~ + 5	~ + 70°C
	120	960	1	~ 0	~ - 10	~ + 60°C
	250	960	1	~ 0	~ - 15	~ + 60°C
	500	960	1	~ - 10	~ - 25	~ + 70°C
X	as delivered			~ -100	< -100	
50 mm	60	920	1	~ - 70	~ - 80	~ + 15°C
	120	920	1	~ - 70	~ - 85	~ + 15°C
	250	920	1	~ - 85	~ - 90	~ + 15°C
	500	920	1	~ - 80	~ - 90	~ + 15°C
	60	960	1	~ - 60	~ - 65	~ + 35°C
	500	960	1	~ - 80	~ - 90	~ + 20°C

Table 7.7 : ***Results of the CTOD tests on material N and X in the as delivered condition and after reniewed normalizing. Test temperature: -10°C, test specimen: BxB type.***

Material	Normalizing treatment			CTOD values (mm)		
	Heating and cooling rate (°C/hr)	T max (°C)	Hold time at Tmax (hr)	1	2	3
N	as delivered condition			0.68 2)	0.82 2)	0.63 2)
50 mm	60	920	1	0.12 1)	0.11 1)	0.11 1)
	120	920	1	0.10 1)	0.13 1)	0.12 1)
	250	920	1	0.22 1)	0.15 1)	0.17 1)
	500	920	1	0.58 2)	0.51 2)	0.30 1)
	60	960	1	0.06 1)	0.06 1)	0.04 1)
	120	960	1	0.08 1)	0.09 1)	0.07 1)
	250	960	1	0.09 1)	0.10 1)	0.12 1)
	500	960	1	0.15 1)	0.21 1)	0.13 1)
X	as delivered condition			1.23 2)	1.32 2)	--
50 mm	60	920	1	0.33 2)	1.12 2)	0.37 2)
	120	920	1	0.65 2)	0.43 1)	0.70 2)
	250	920	1	0.42 1)	1.01 2)	0.58 1)
	500	920	1	2.26 2)	1.14 2)	1.11 2)
	60	960	1	0.18 1)	0.28 1)	0.41 1)
	500	960	1	1.49 2)	1.04 2)	0.91 2)

1) : δ_c

2) : δ_u

Table 8.1 : ***Effect of the use of FeE 355/FeE 460 on the weight and costs of the vessels 1, 2 and 3 (Appendix 2)***

	Wall thick-ness	Weight (1000 kg)	Cost (1000 Dfl)	Specification of cost reduction (1000 Dfl.) Steel	Fabrication	NDT	PWHT
Vessel 1 355	38	124	640				
460	31	103	561	-15	-37.5	-2.5	-24
Vessel 2 355	89	180	845				
460	61	128	654	-85	-96.5	-8.5	
Vessel 3 355	25	39,5	282				
460	21	34	276	-3	-3		

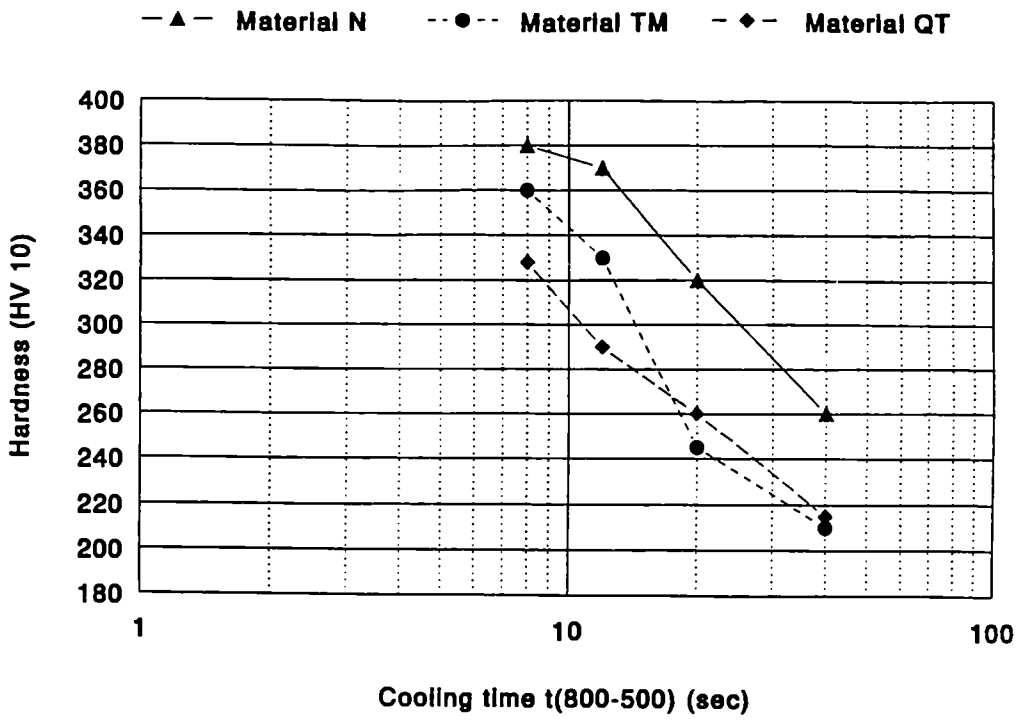

Fig. 4.1 Hardness values of simulated specimens as a function of cooling time
Tp = 1350°C
• = material N, *: material TM, : material QT

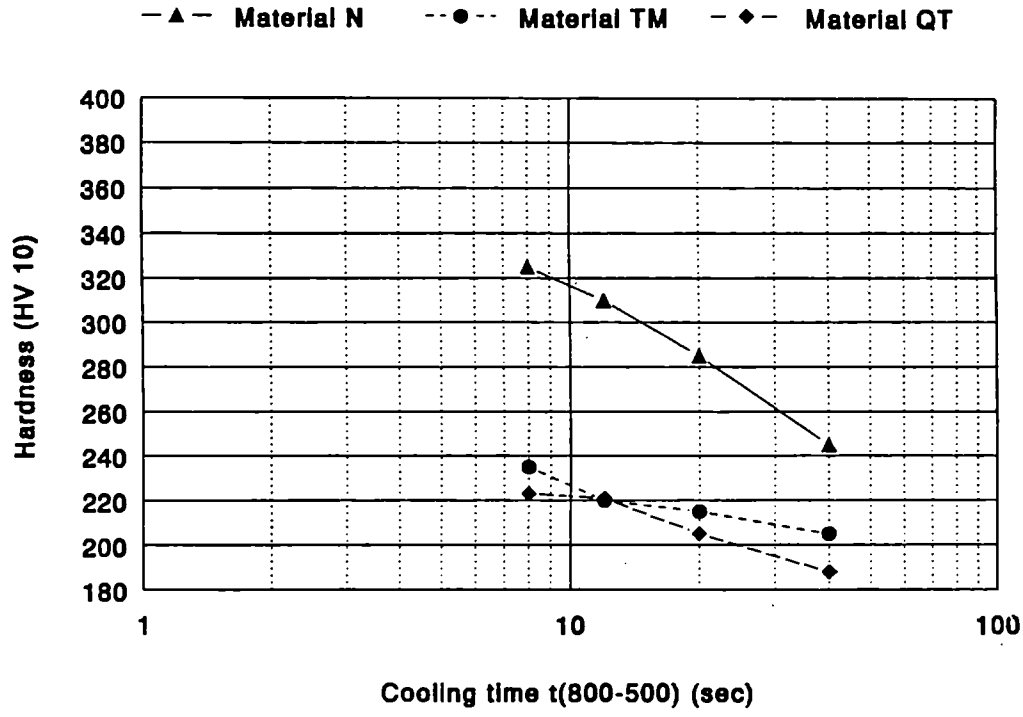

Fig. 4.2 Hardness values of simulated specimens as a function of cooling time.
Tp = 1050°C
• = material N, *: material TM, : material QT

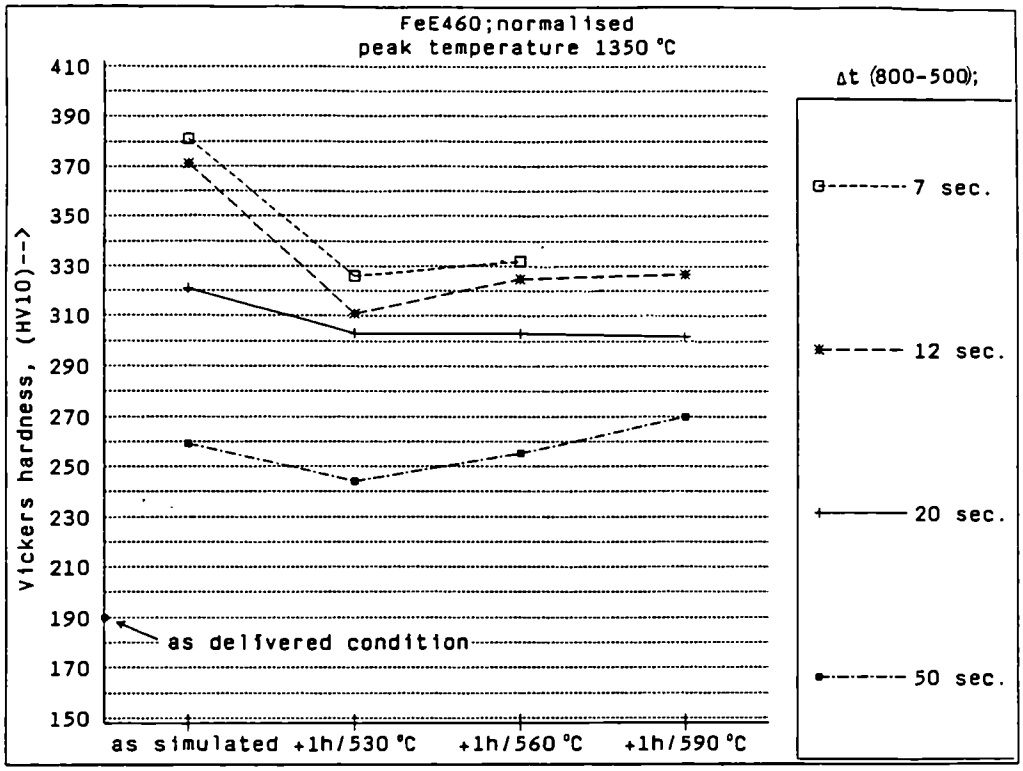

Fig. 4.3 Hardness values of simulated specimens as a function of PWHT temperature.
Material N, Tp = 1350°C

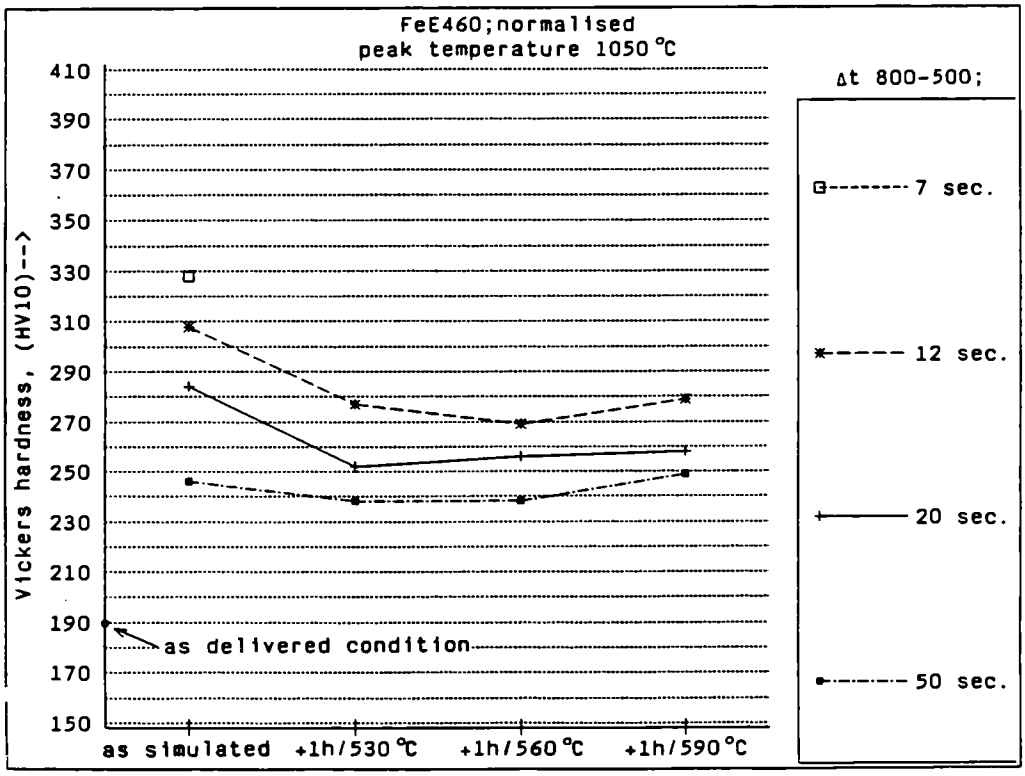

Fig. 4.4 Hardness values of simulated specimens as a function of PWHT temperature.
Material N, Tp = 1050°C

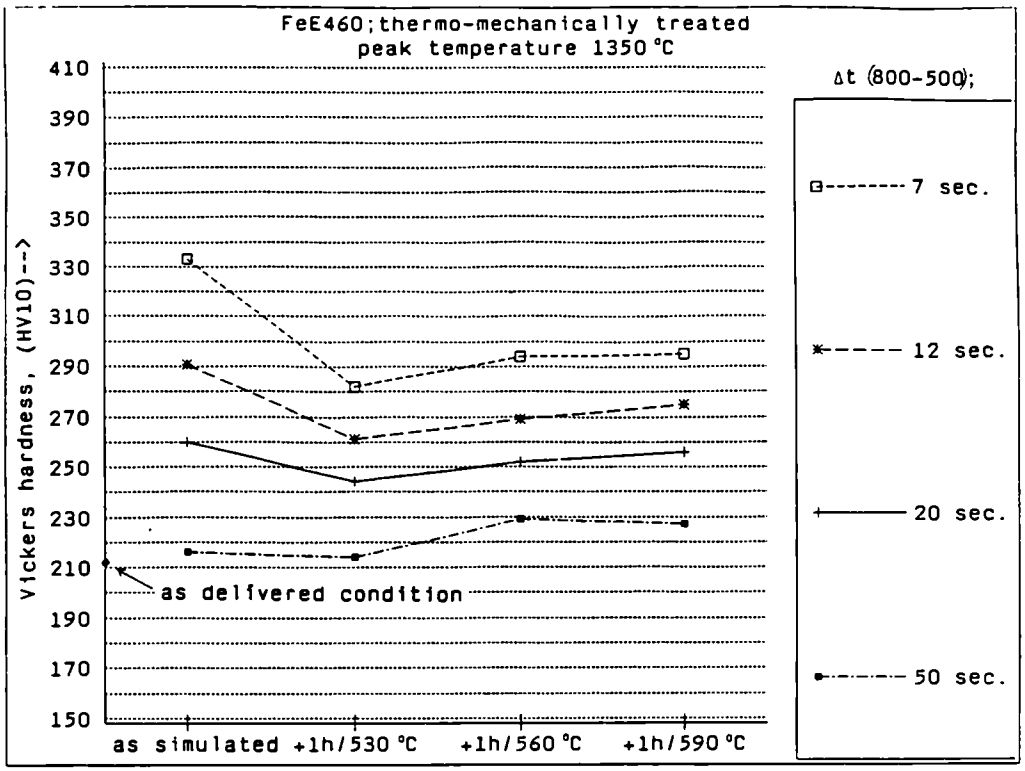

Fig. 4.5 Hardness values of simulated specimens as a function of PWHT temperature.
Material TM, Tp = 1350°C

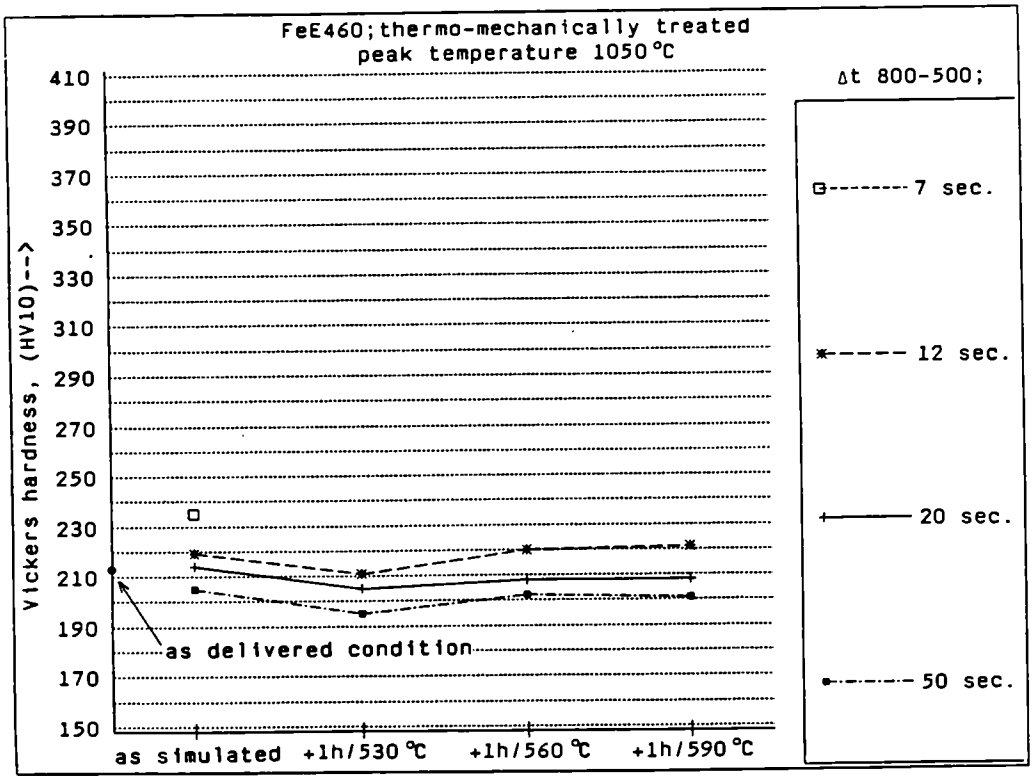

Fig. 4.6 Hardness values of simulated specimens as a function of PWHT temperature.
Material TM, Tp = 1050°C

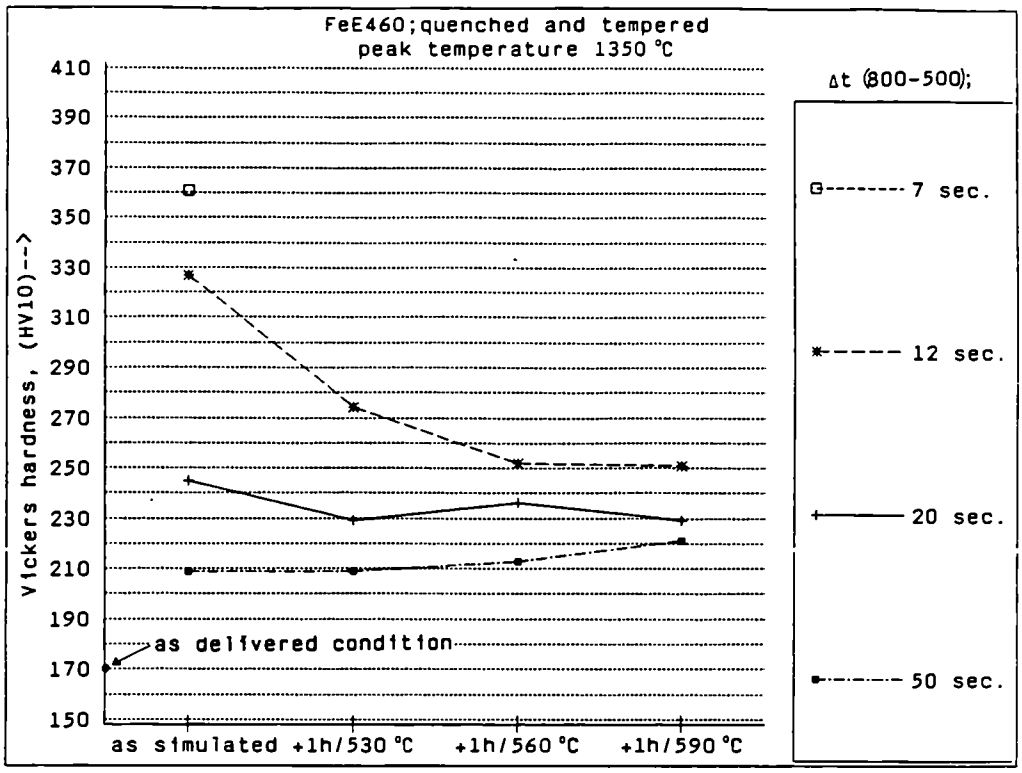

Fig. 4.7 Hardness values of simulated specimens as a function of PWHT temperature.
Material QT, Tp = 1350°C

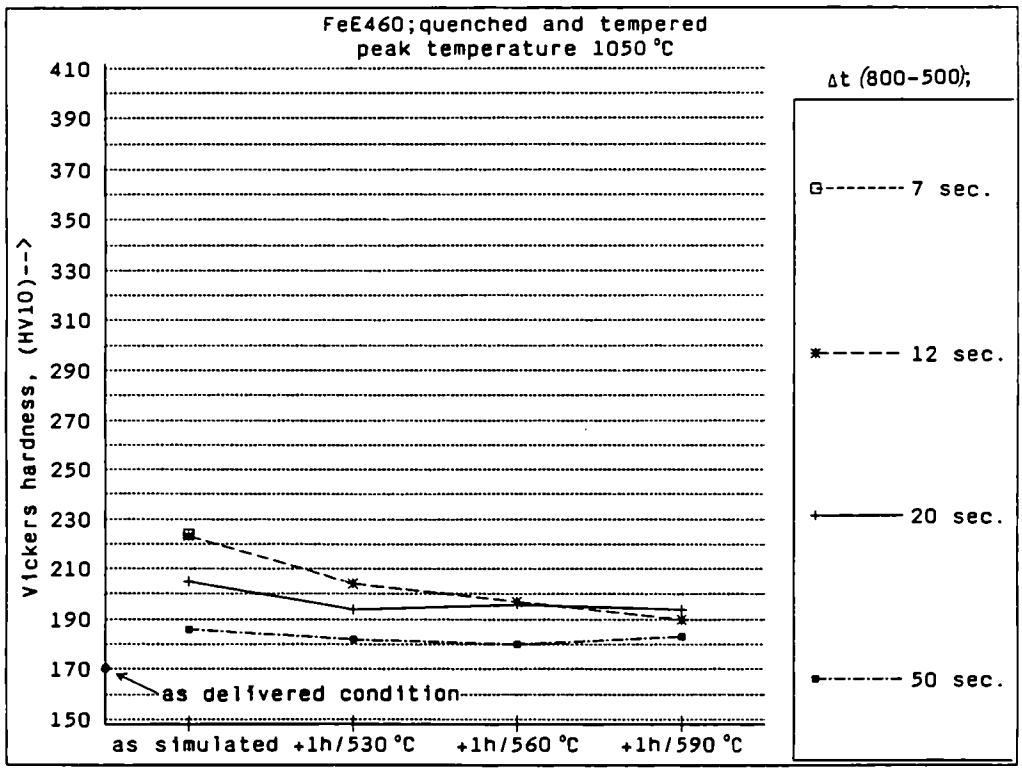

Fig. 4.8 Hardness values of simulated specimens as a function of PWHT temperature.
Material QT, Tp = 1050°C

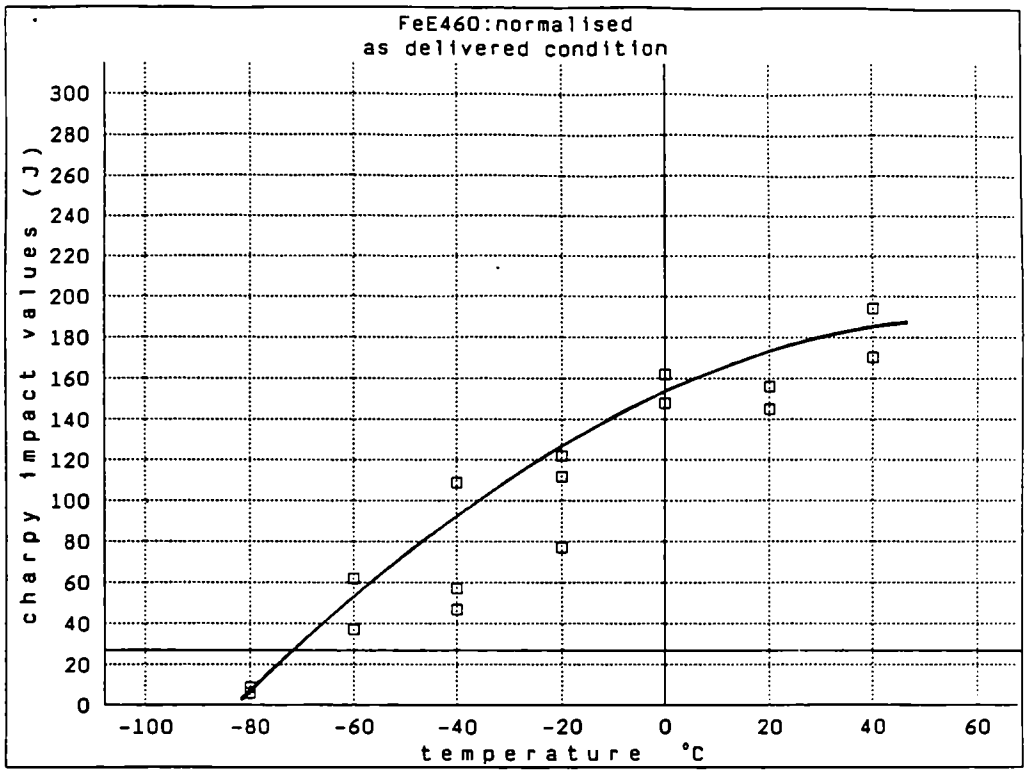

Fig. 4.9 Charpy-V fracture energies of the as delivered condition of material N

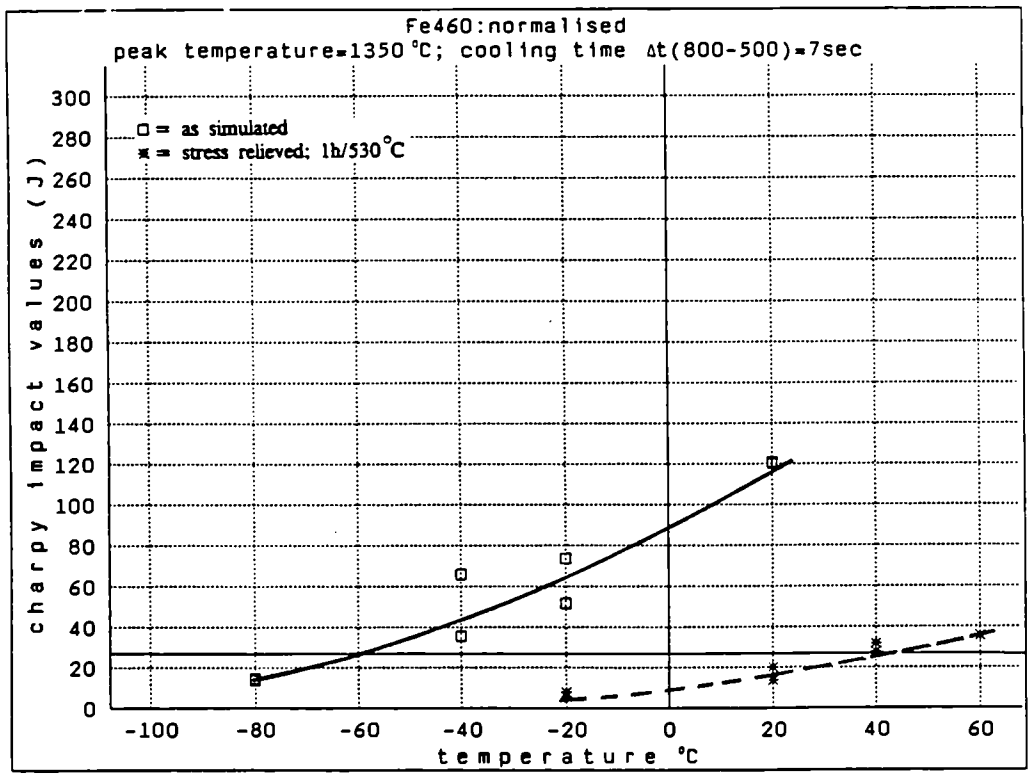

Fig. 4.10 Charpy-V fracture energies of simulated specimens. Material N, Tp = 1350°C, Δt (800-500) = 7 sec. □: as simulated *: + PWHT (1h 530°C)

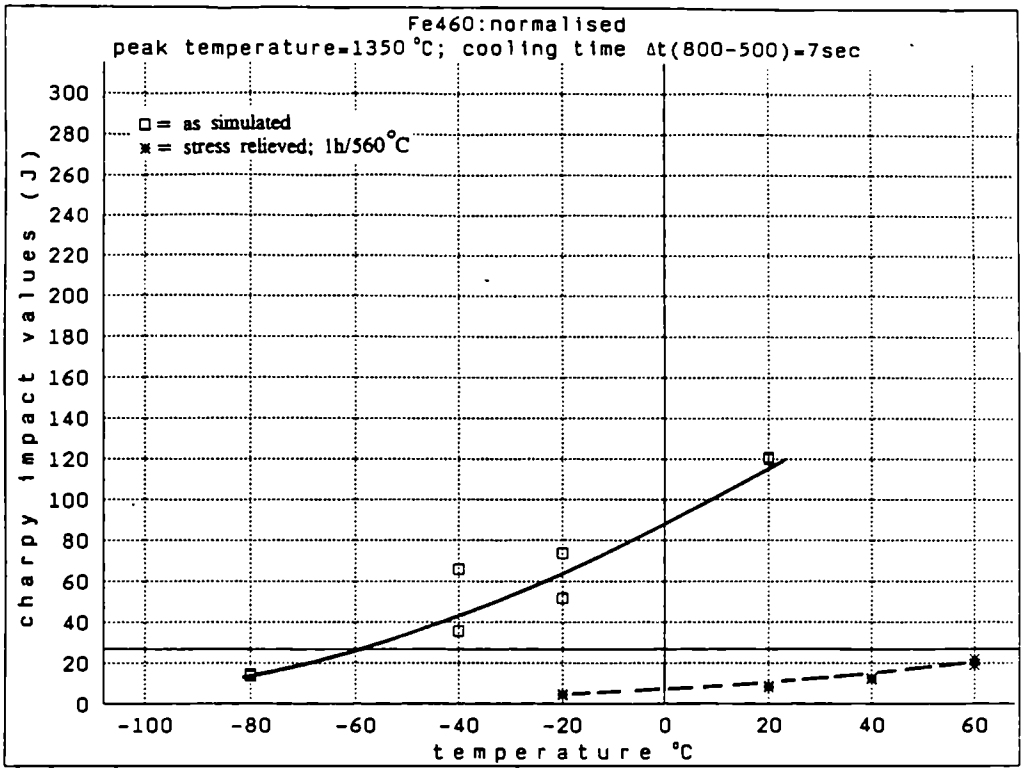

Fig. 4.11 Charpy-V fracture energies of simulated specimens. Material N, Tp = 1350°C, Δt (800-500) = 7 sec. □: as simulated *: + PWHT (1h 560°C)

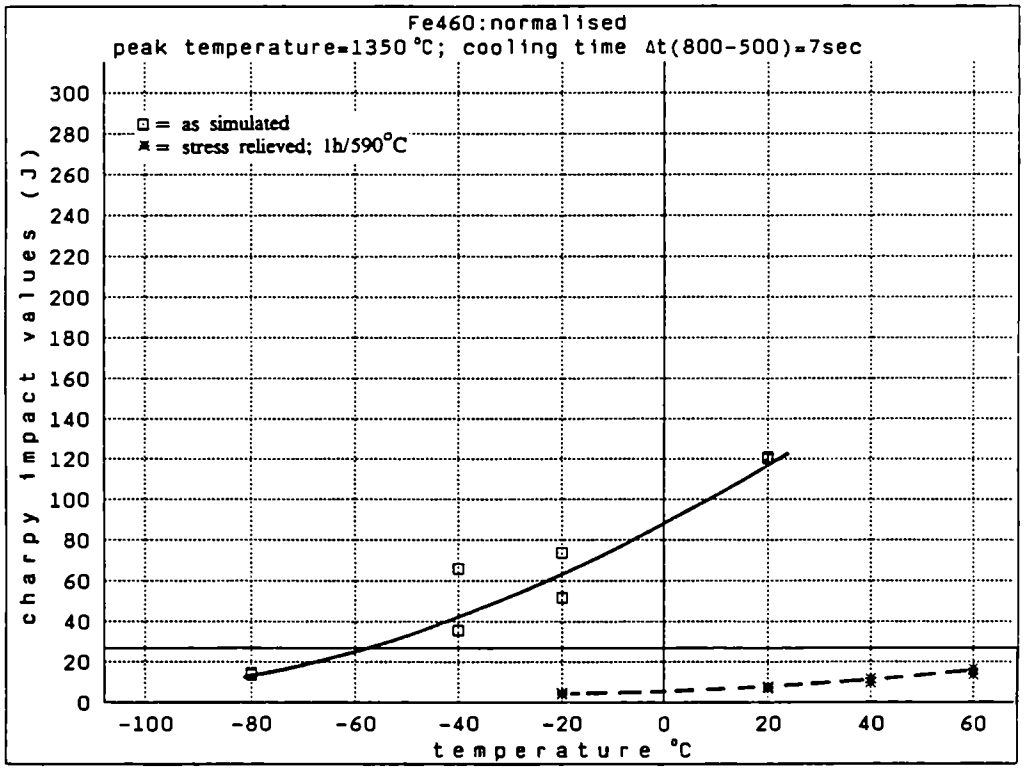

Fig. 4.12 Charpy-V fracture energies of simulated specimens. Material N, Tp = 1350°C, Δt (800-500) = 7 sec. □: as simulated *: + PWHT (1h 590°C)

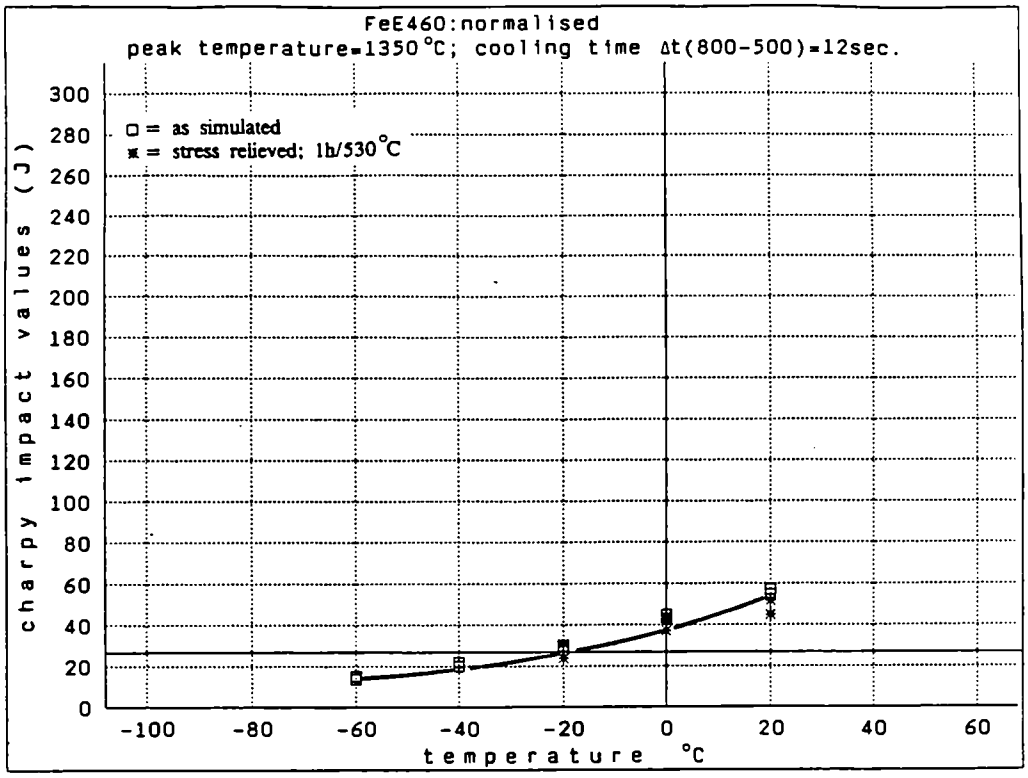

Fig. 4.13 Charpy-V fracture energies of simulated specimens. Material N, Tp = 1350°C, Δt (800-500) = 12 sec. □: as simulated *: + PWHT (1h 530°C)

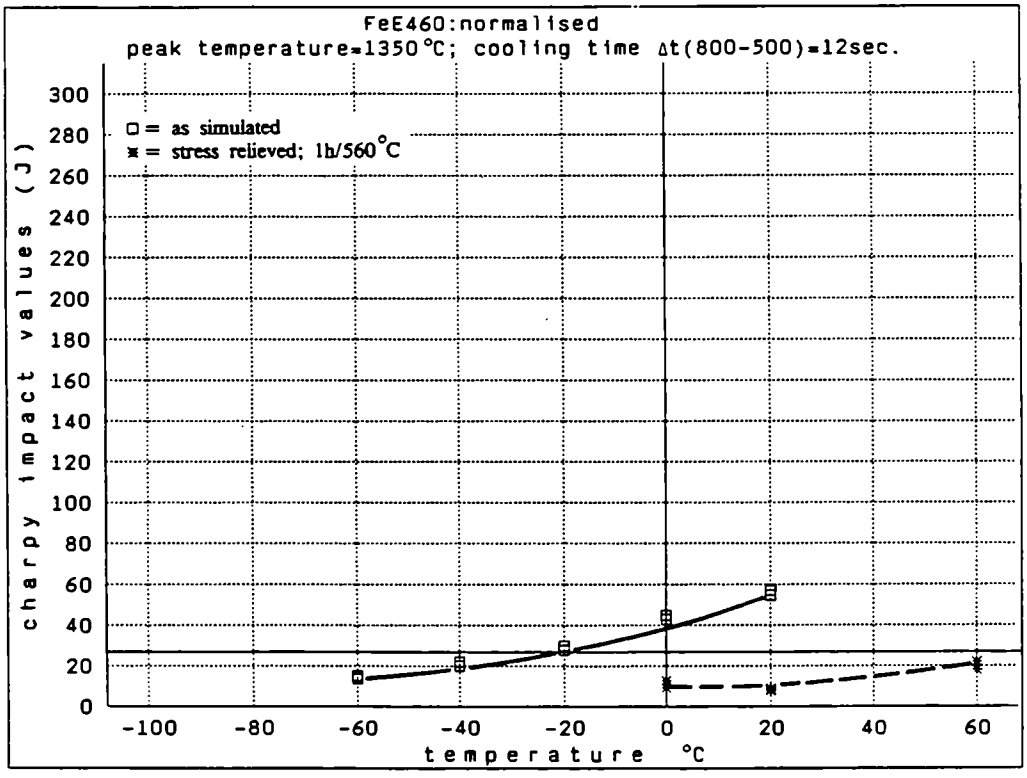

Fig. 4.14 Charpy-V fracture energies of simulated specimens. Material N, Tp = 1350°C, Δt (800-500) = 12 sec. □: as simulated *: + PWHT (1h 560°C)

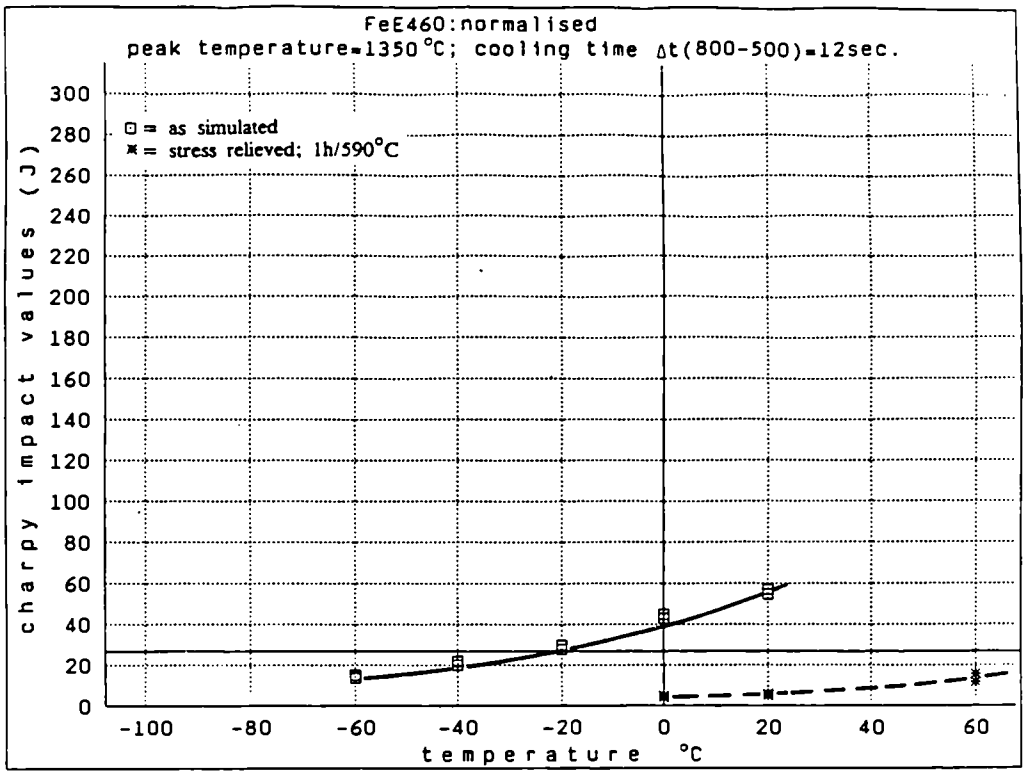

Fig. 4.15 Charpy-V fracture energies of simulated specimens. Material N, Tp = 1350°C, Δt (800-500) = 12 sec. □: as simulated *: + PWHT (1h 590°C)

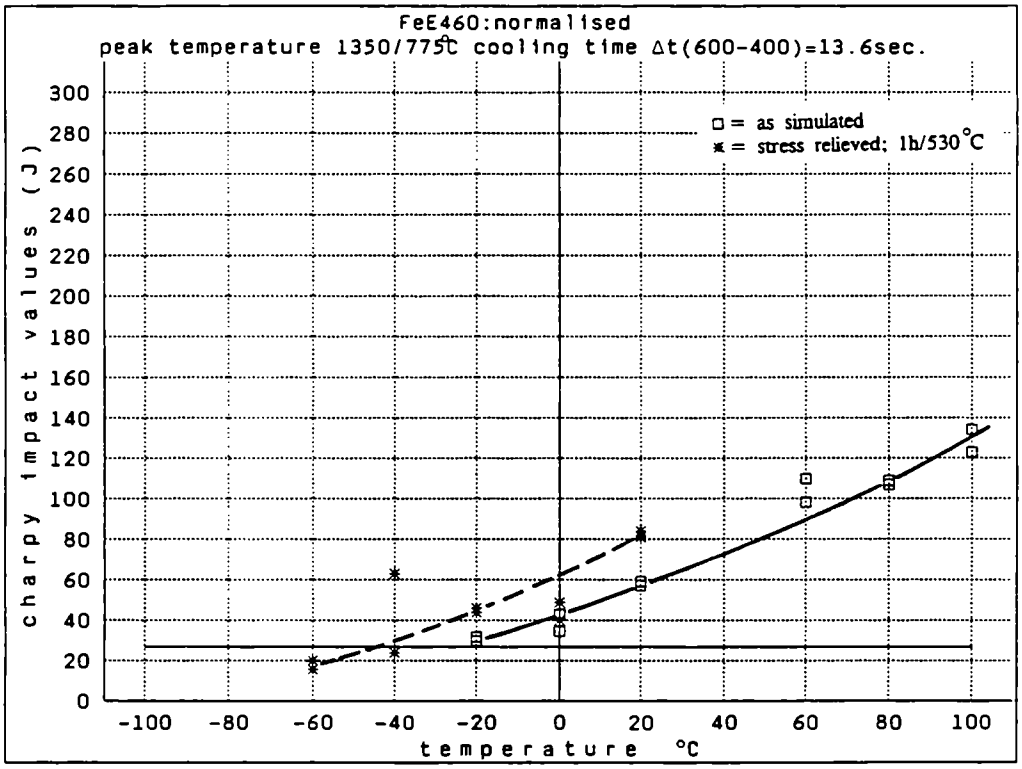

Fig. 4.16 Charpy-V fracture energies of simulated specimens. Material N, Tp = 1350°C + 775°C, Δt (600-400) 13,6 sec. □: as simulated *: + PWHT (1h 530°C)

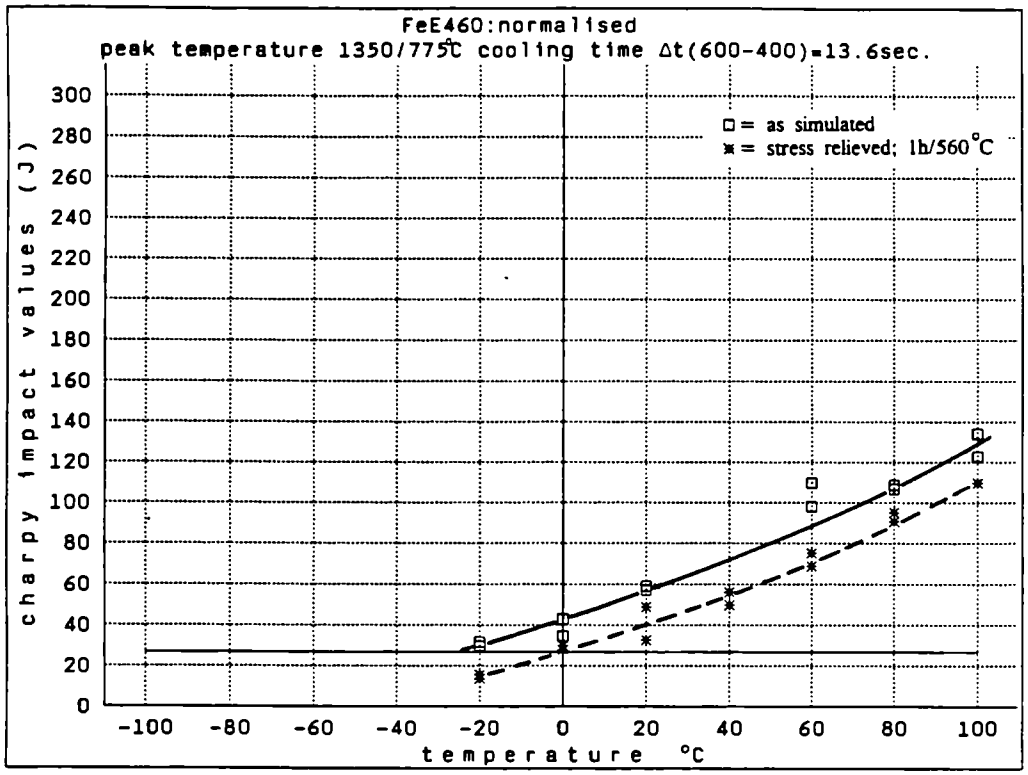

Fig. 4.17 Charpy-V fracture energies of simulated specimens
Material N Tp = 1350°C + 775°C, Δt (600-400) 13.6 sec.
□: as simulated *: + PWHT (1h 560°C)

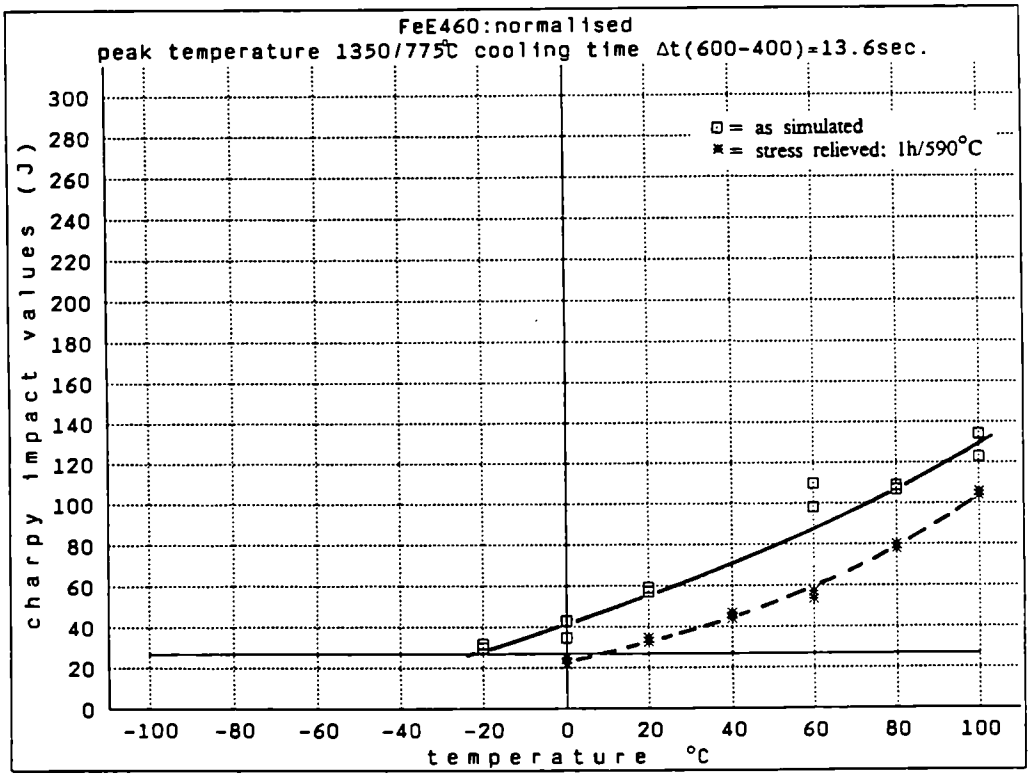

Fig. 4.18 Charpy-V fracture energies of simulated specimens.
Material N, Tp = 1350°C + 775°C, Δt (600-400) 13.6 sec.
□: as simulated *: + PWHT (1h 590°C)

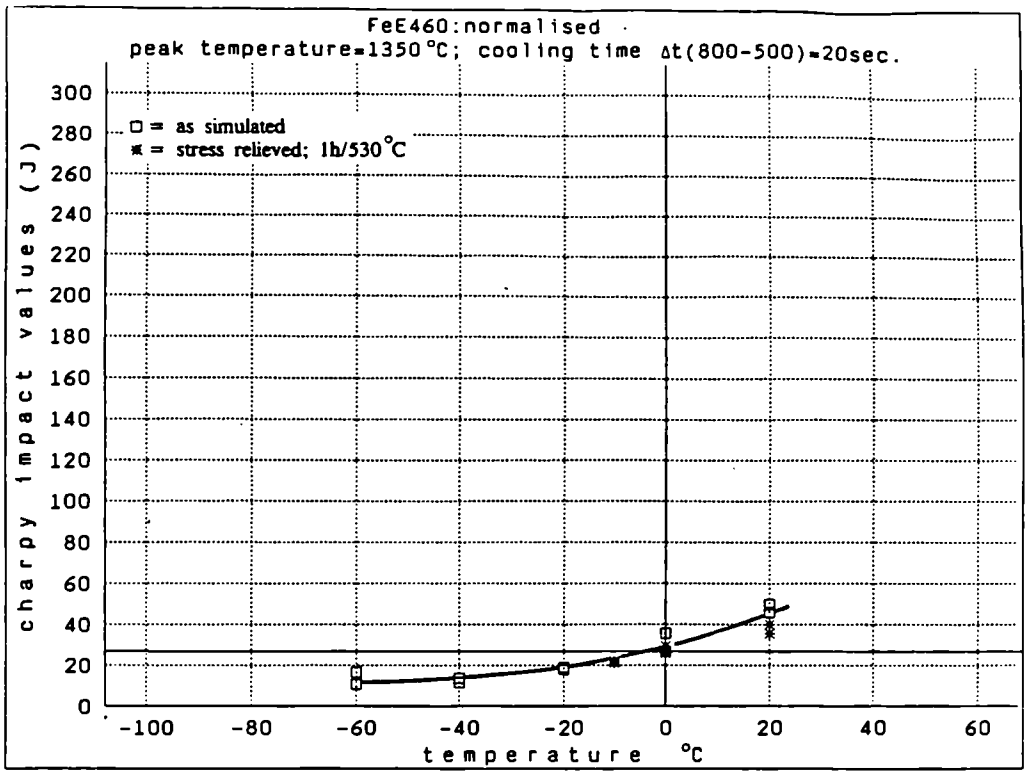

Fig. 4.19 Charpy-V fracture energies of simulated specimens. Material N, Tp = 1350°C, Δt (800-500) 20 sec.
□: as simulated *: + PWHT (1h 530°C)

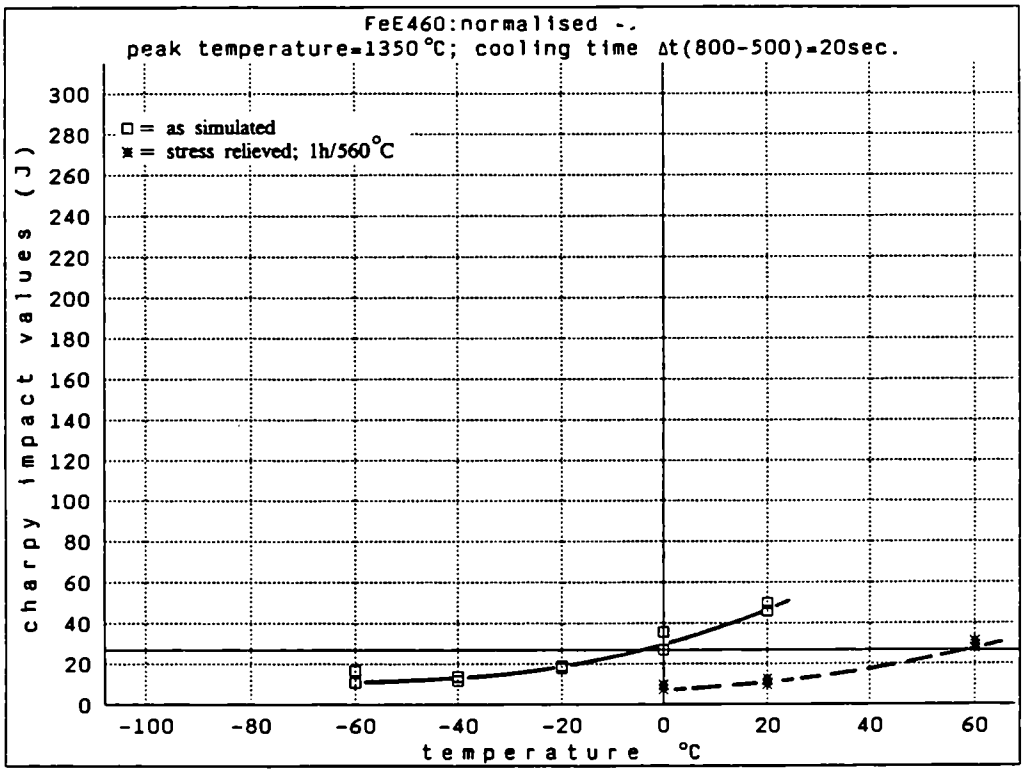

Fig. 4.20 Charpy-V fracture energies of simulatd specimens. Material N, Tp = 1350°C, Δt (800-500) 20 sec.
□: as simulated *: + PWHT (1h 560°C)

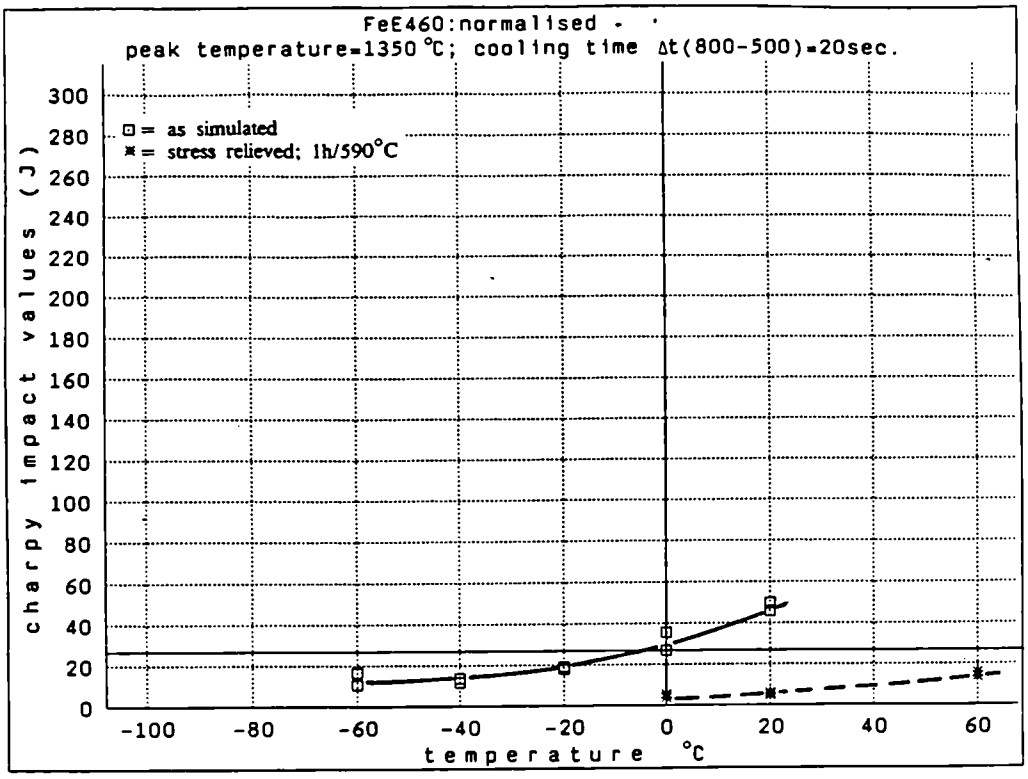

Fig. 4.21 Charpy-V fracture energies of simulated specimens. Material N, Tp = 1350°C, Δt (800-500) 20 sec.

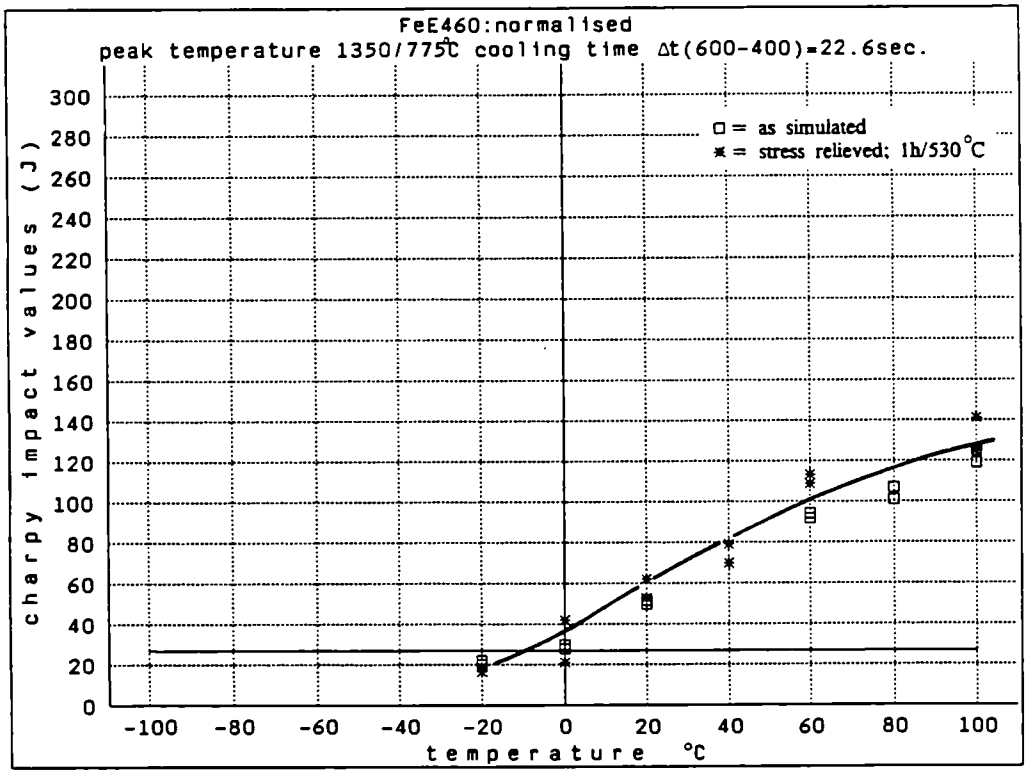

Fig. 4.22 Charpy-V fracture energies of simulated specimens. Material N, Tp = 1350°C + 775°C, Δt (600-400) 22.6 sec. □: as simulated *: + PWHT (1h 530°C)

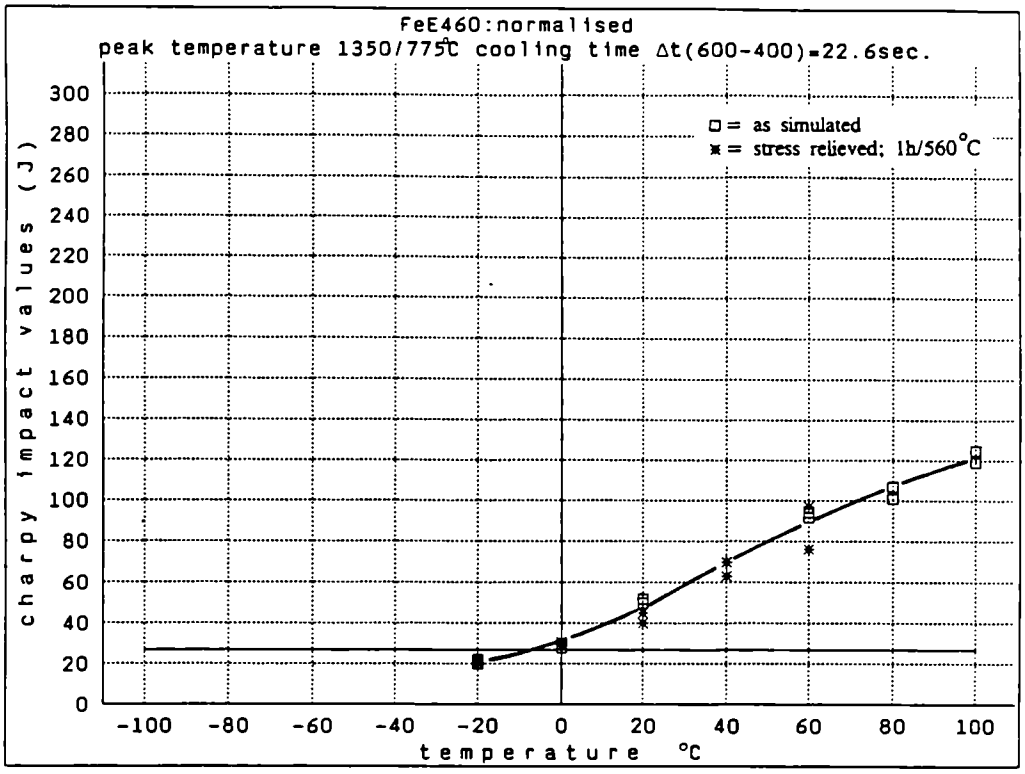

Fig. 4.23 Charpy-V fracture energies of simulated specimens. Material N, Tp = 1350°C + 775°C, Δt (600-400) 22.6 sec. □: as simulated *: + PWHT (1h 560°C)

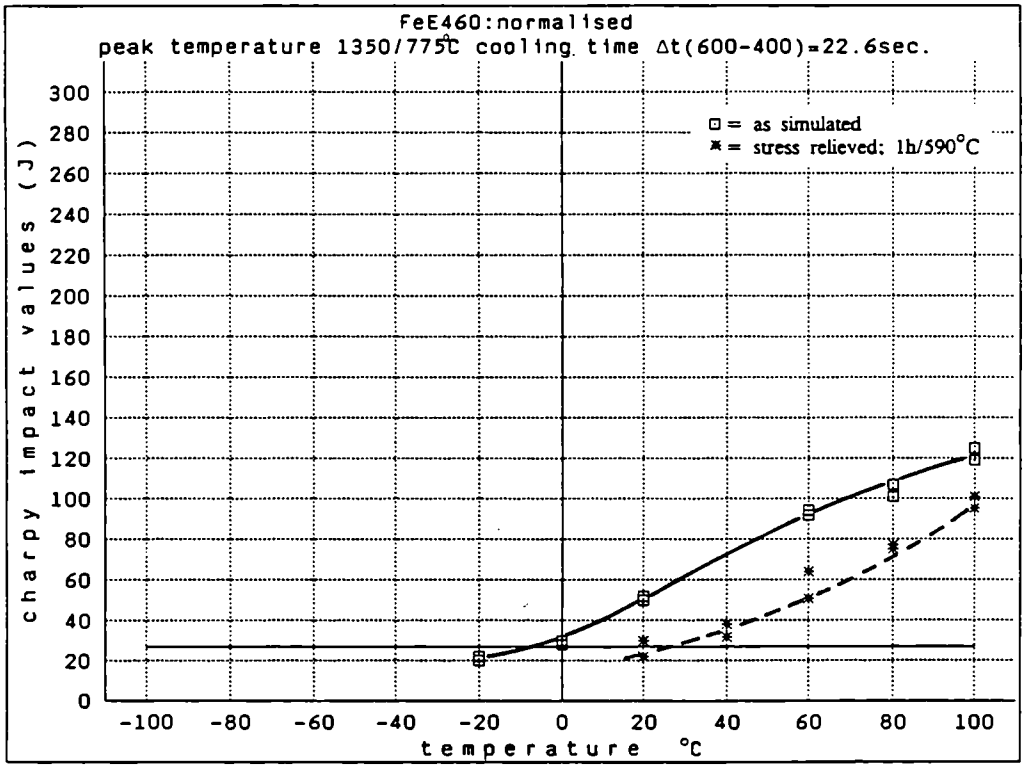

Fig. 4.24 Charpy-V fracture specimens of simulated specimens. Material N, Tp = 1350°C + 775°C, Δt (600-400) 22.6 sec. □: as simulated *: + PWHT (h 590°C)

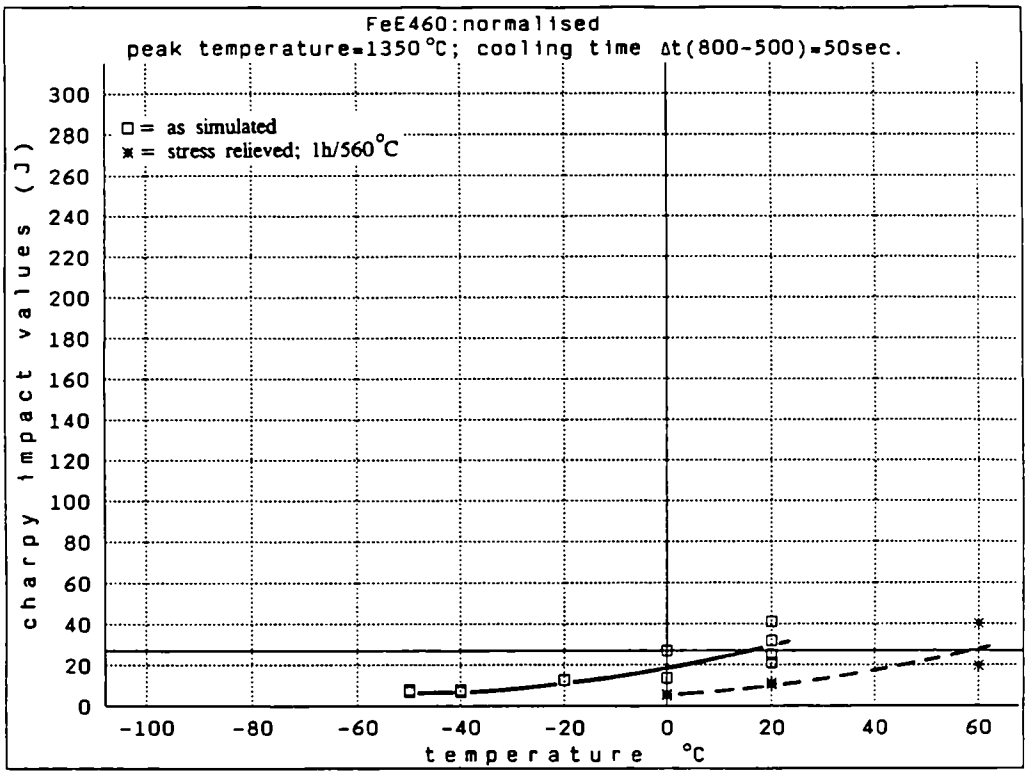

Fig. 4.25 Charpy-V fracture energies of simulated specimens. Material N, Tp = 1350°C, Δt (800-500) 50 sec. □: as simulated *: + PWHT (1h 530°C)

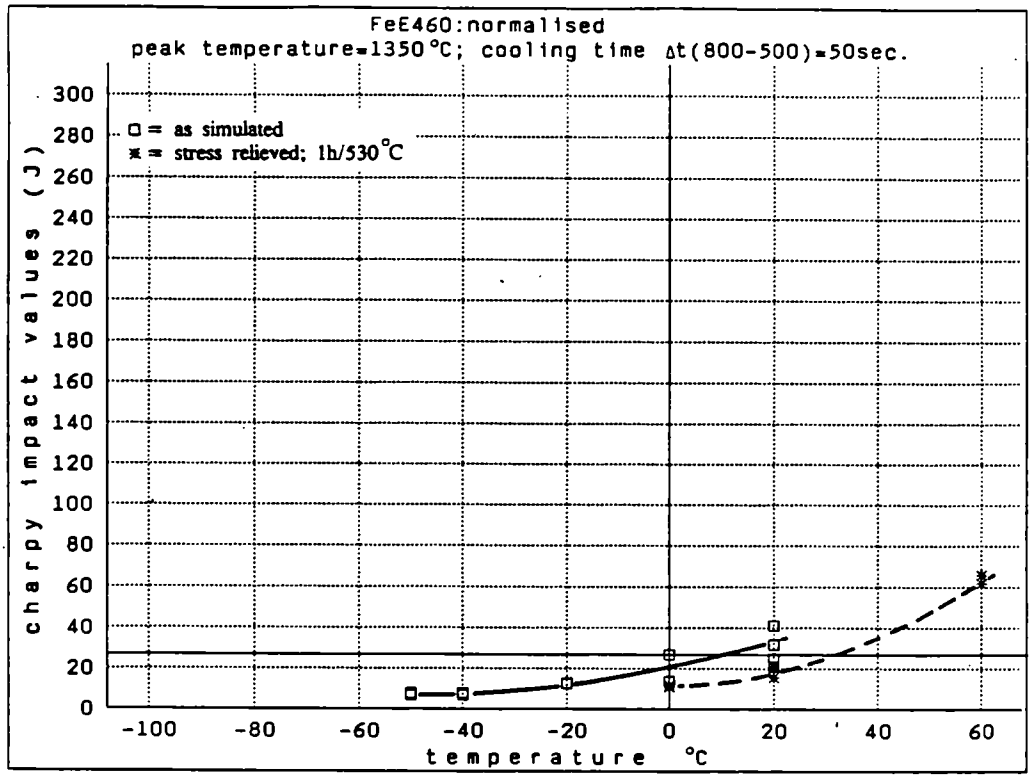

Fig. 4.26 Charpy-V fracture energies of simulated specimens. Material N, Tp = 1350°C, Δt (800-500) 50 sec. □: as simulated *: + PWHT (1h 560°C)

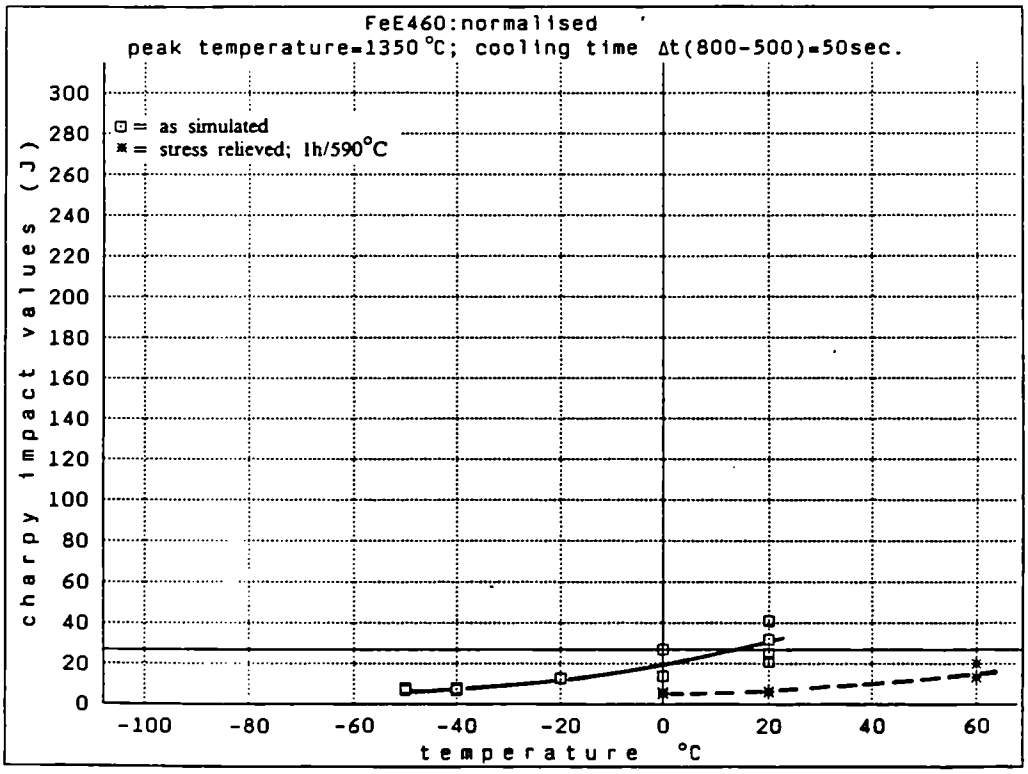

Fig. 4.27 Charpy-V fracture energies of simulated specimens. Material N, Tp = 1350°C, Δt (800-500) 50 sec. □: as simulated *: + PWHT (1h 590°C)

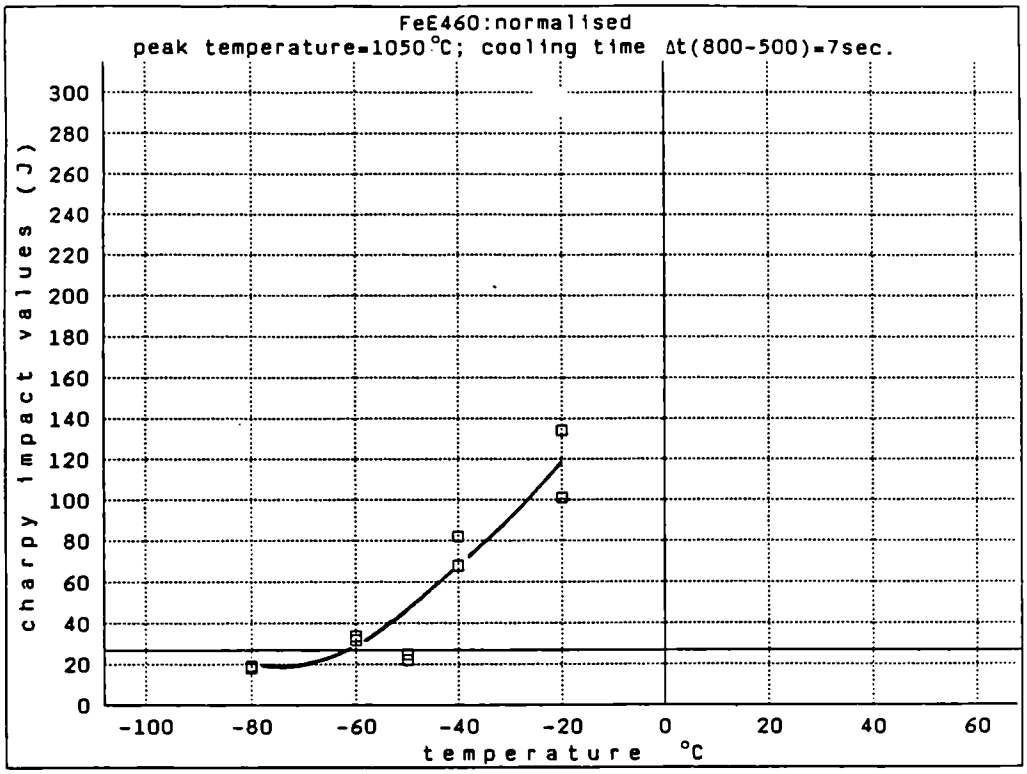

Fig. 4.28 Charpy-V fracture energies of simulated specimens.
Material N, Tp = 1050°C, Δt (800-500) = 7 sec.
□: as simulated

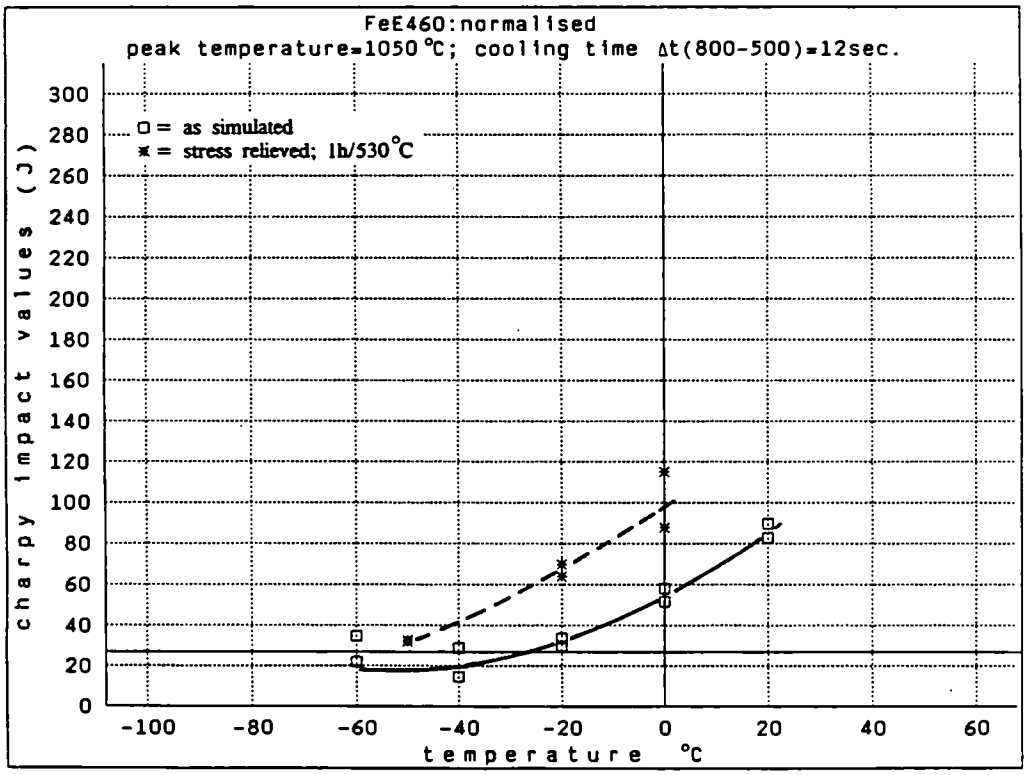

Fig. 4.29 Charpy-V fracture energies of simulated specimens.
Material N, Tp = 1050°C, Δt (800-500) = 12 sec.
□: as simulated *: + PWHT (1h 530°C)

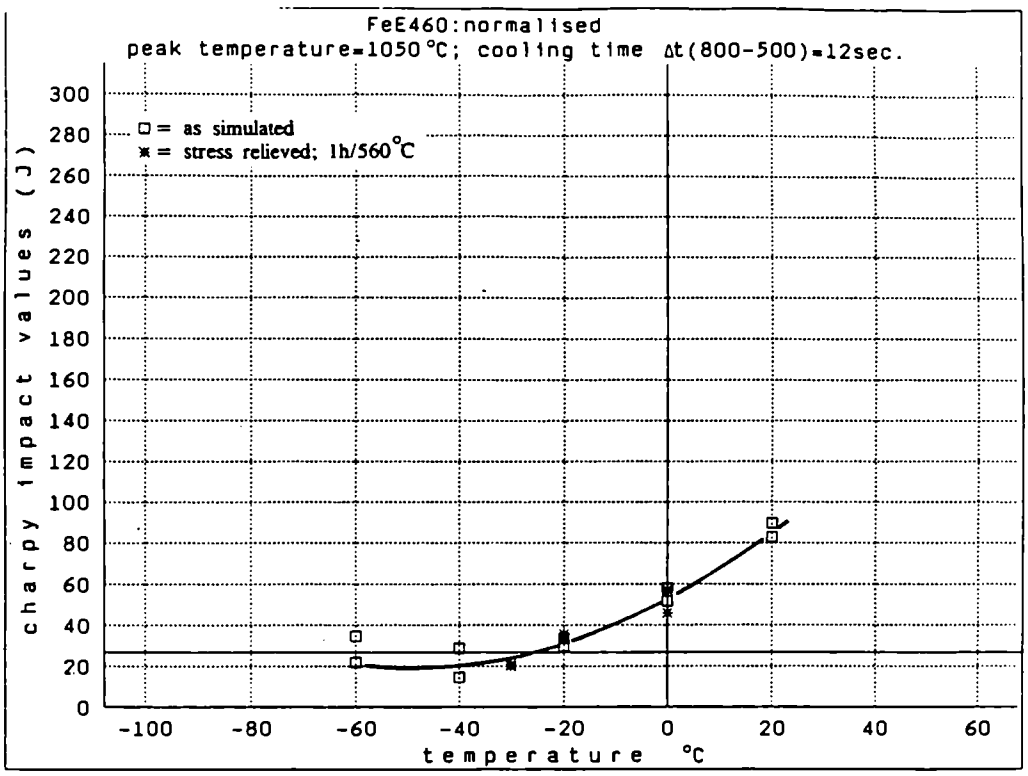

Fig. 4.30 Charpy-V fracture energies of simulated specimens.
Material N, Tp = 1050°C, Δt (800-500) = 12 sec.
□: as simulated *: + PWHT (1h 560°C)

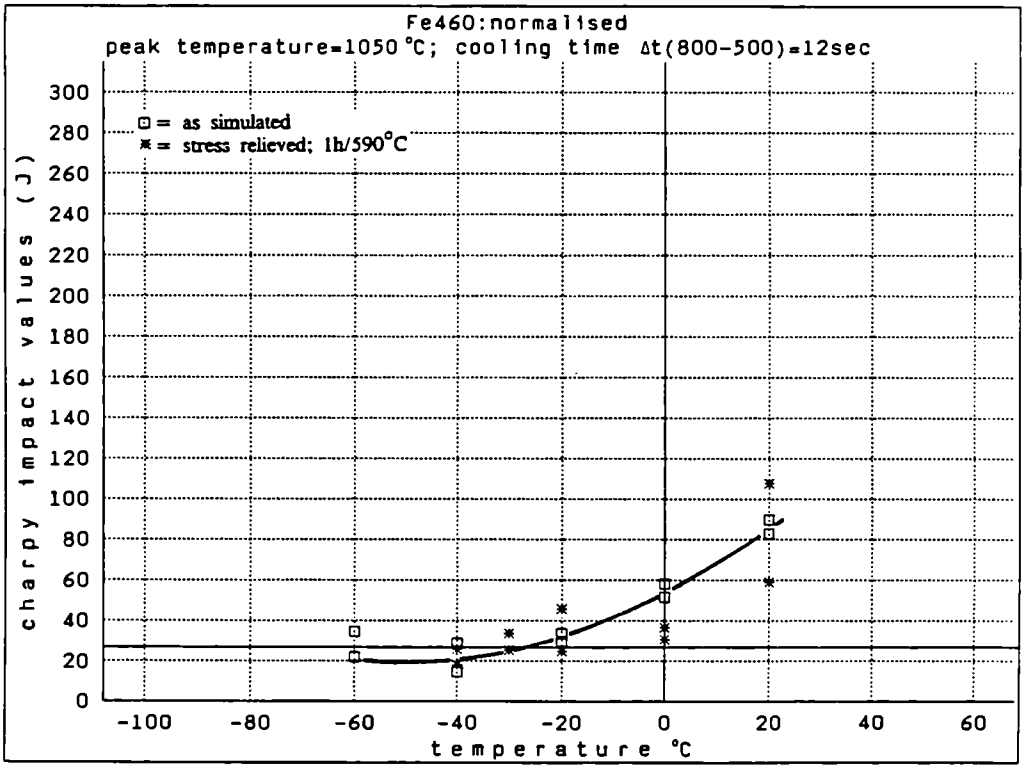

Fig. 4.31 Charpy-V fracture energies of simulated specimens.
Material N, Tp = 1050°C, Δt (00-500) = 12 sec.
□: as simulated *: + PWHT (1h 590°C)

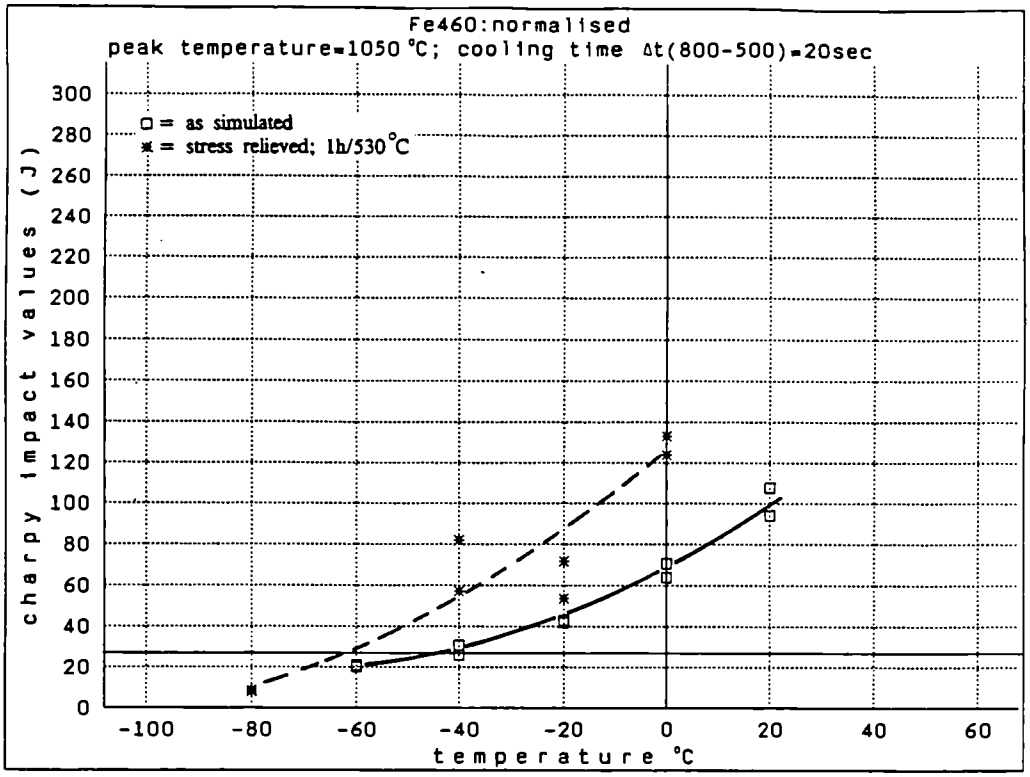

Fig. 4.32 Charpy-V fracture energies of simulated specimens. Material N, Tp = 1050°C, Δt (800-500) 20 sec. □: as simulated *: = PWHT (1h 530°C)

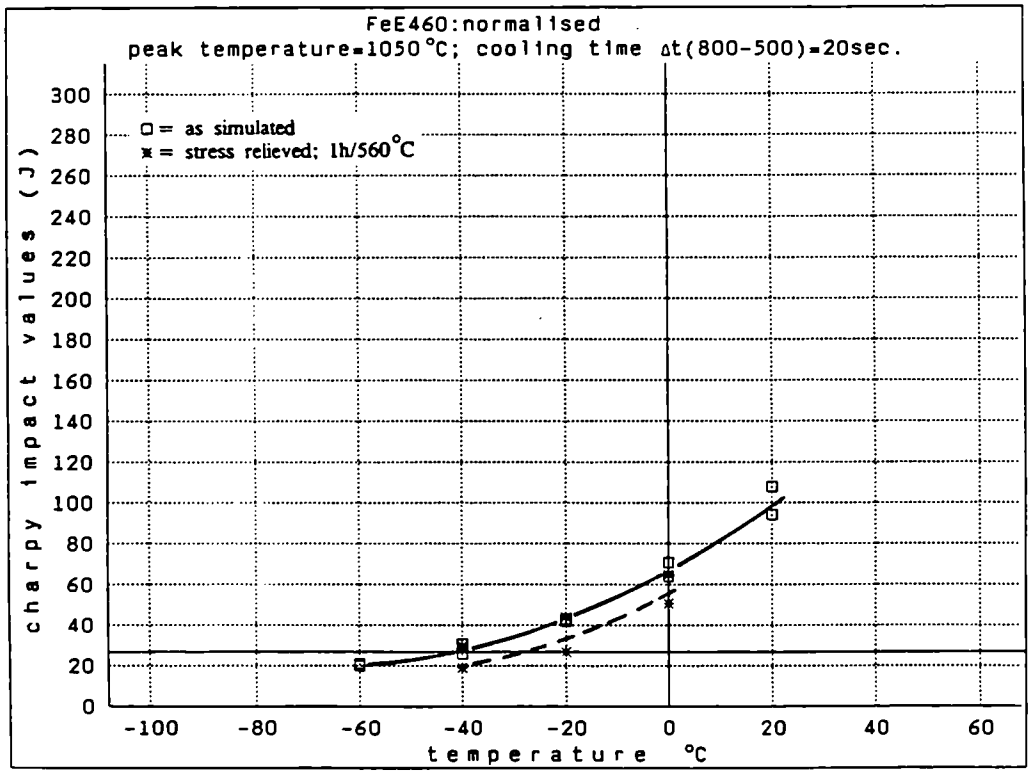

Fig. 4.33 Charpy-V fracture energies of simulated specimens. Material N, Tp = 1050°C, Δt (800-500) 20 sec. □: as simulated *: + PWHT (1h 560°C)

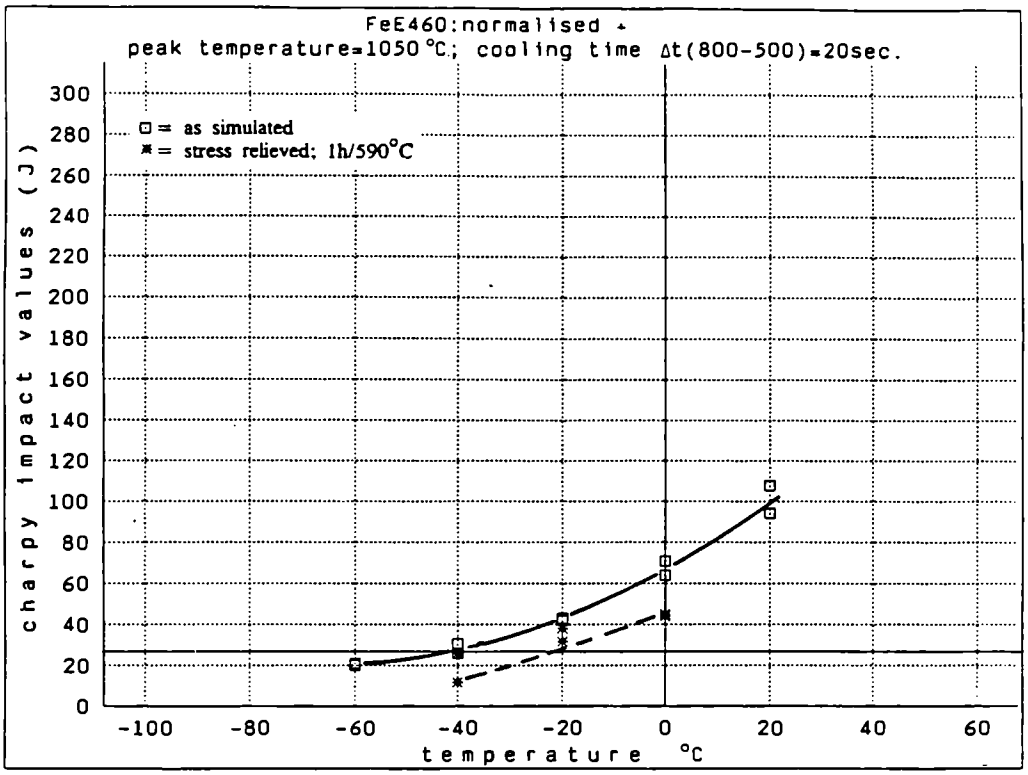

Fig. 4.34 Charpy-V fracture energies of simulated specimens. Material N, Tp = 1050°C, Δt (800-500) 20 sec. □: as simulated *: + PWHT (1h 590°C)

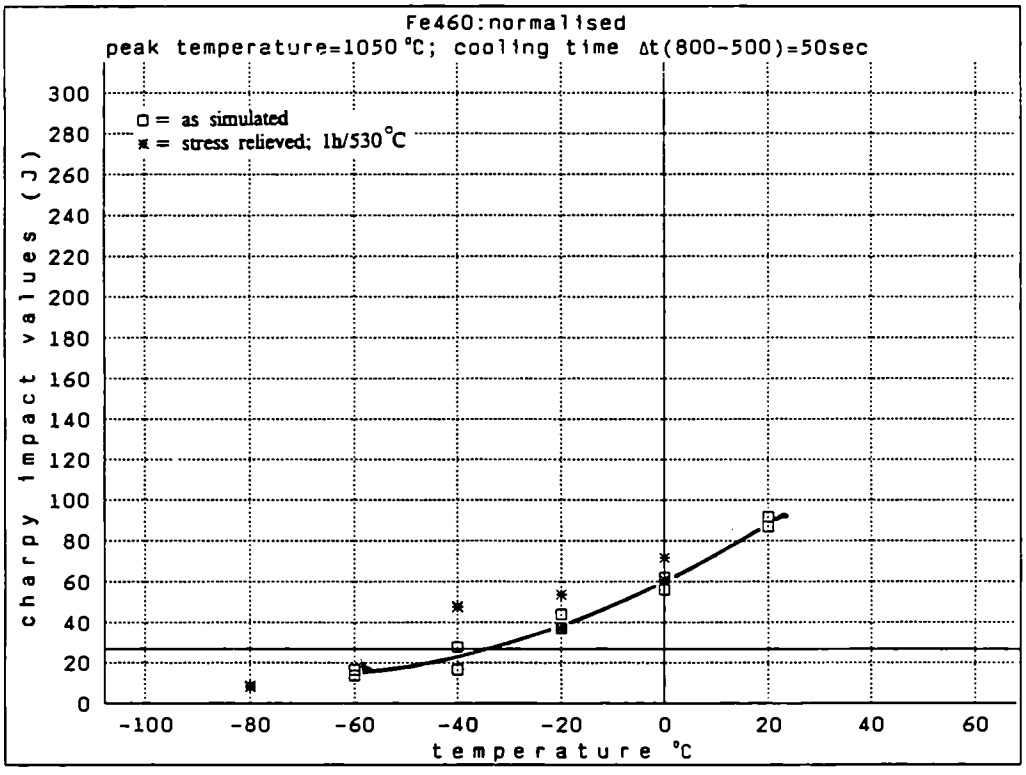

Fig. 4.35 Charpy-V fracture energies of simulated specimens. Material N, Tp = 1050°C, Δt (800-500) 50 sec. □: as simulated *: + PWHT (1H 530°C)

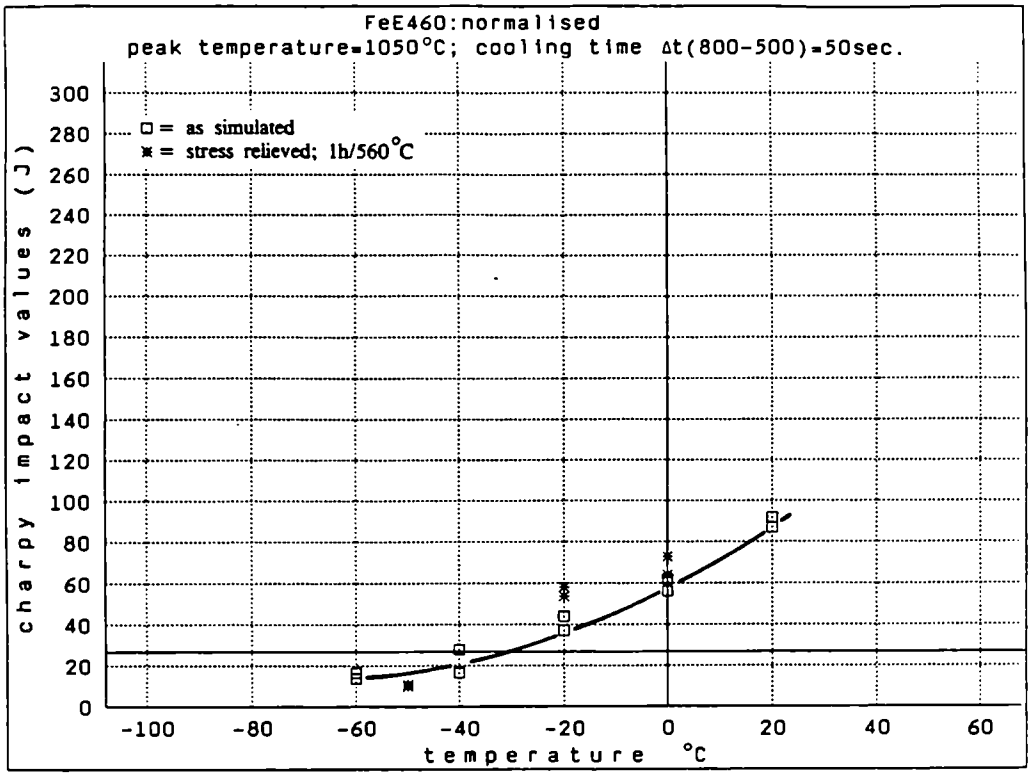

Fig. 4.36 Charpy-V fracture energies of simulated specimens.
Material N, Tp = 1050°C, Δt (800-500) 50 sec.
□: as simulated *: + PWHT (1h 560°C)

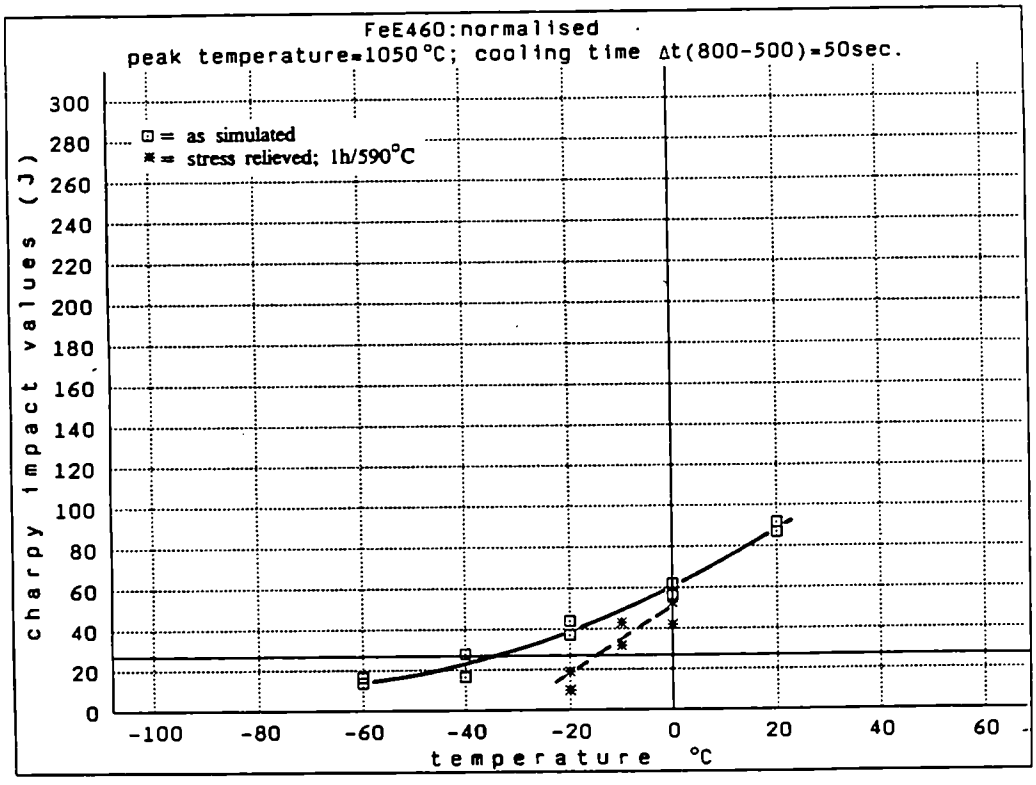

Fig. 4.37 Charpy-V fracture energies of simulated specimens.
Material N, Tp = 1050°C, Δt (800-500) 50 sec.
□: as simulated *: + PWHT (1h 590°C)

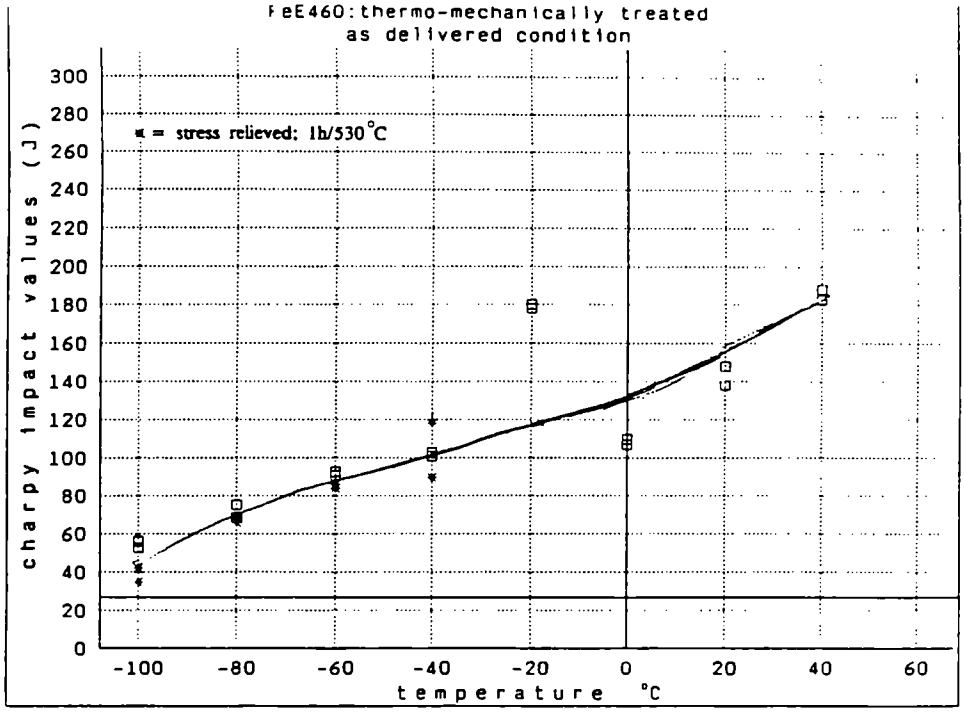

Fig. 4.38 Charpy-V fracture energies of the as delivered condition of material TM

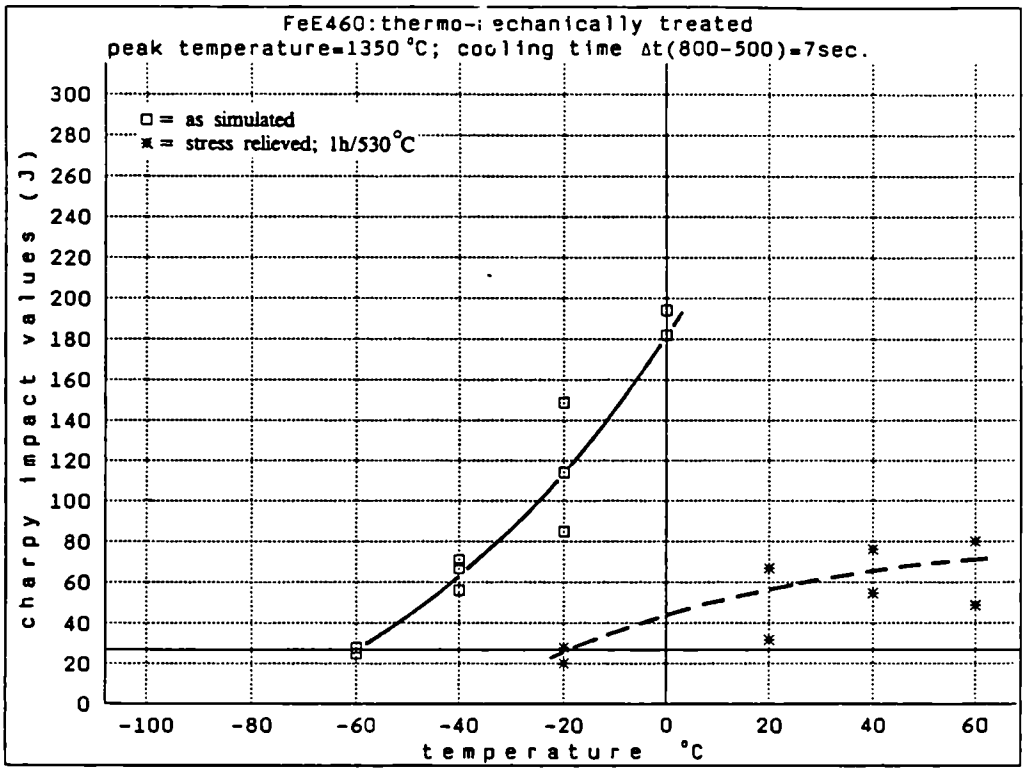

Fig. 4.39 Charpy-V fracture energies of the simulated specimens. Material TM, Tp = 1350°C, Δt (800-500) = 7 sec.
□: as simulated *: + PWHT (1h 530°C)

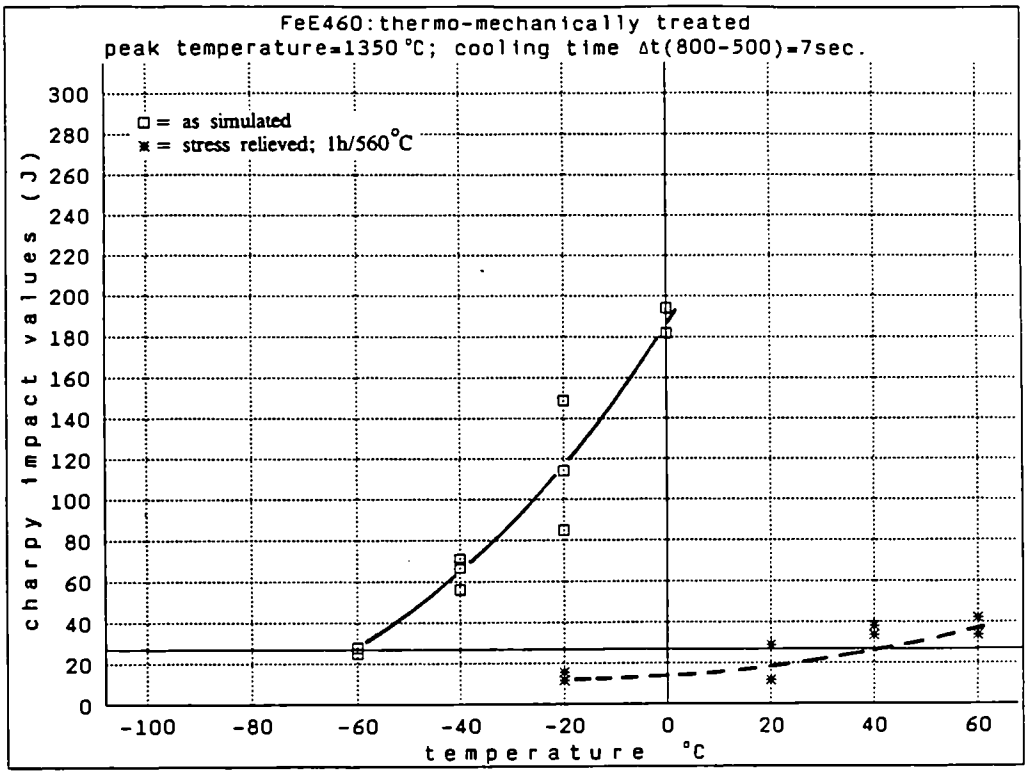

Fig. 4.40 Charpy-V fracture energies of the simulated specimens. Material TM, Tp = 1350°C, Δt (800-500) = 7 sec. □: as simulated *: + PWHT (1h 560°C)

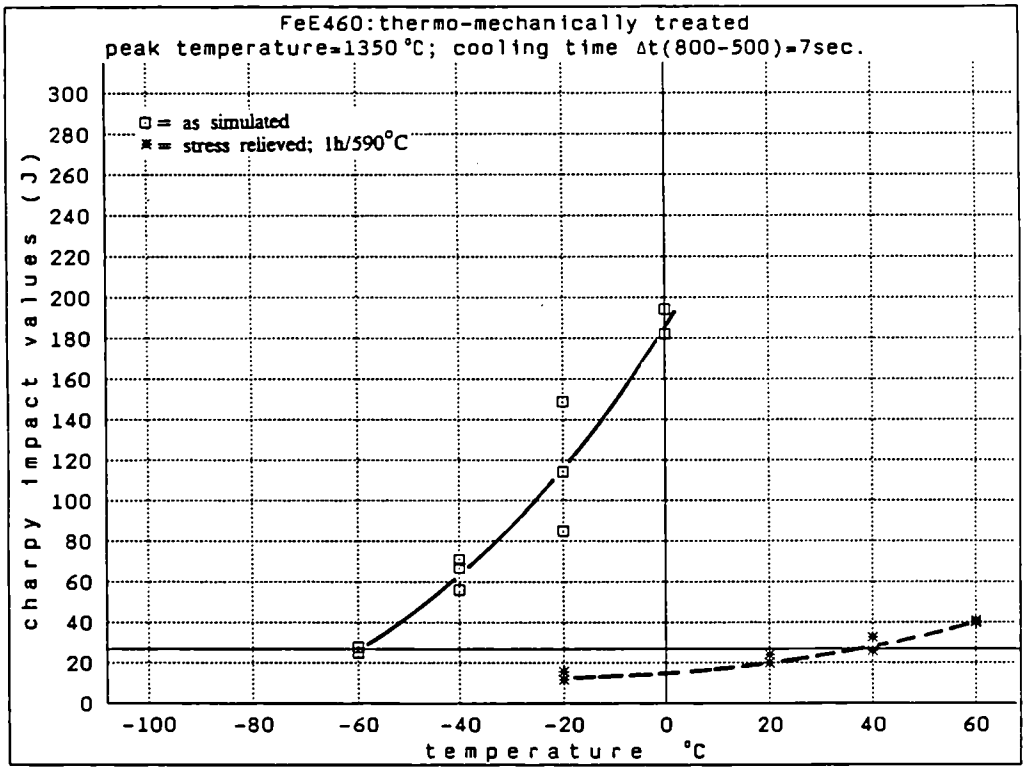

Fig. 4.41 Charpy-V fracture energies of the simulated specimens. Material TM, Tp = 1350°C, Δt (800-500) = 7 sec. □: as simulated *: + PWHT (1h 590°C)

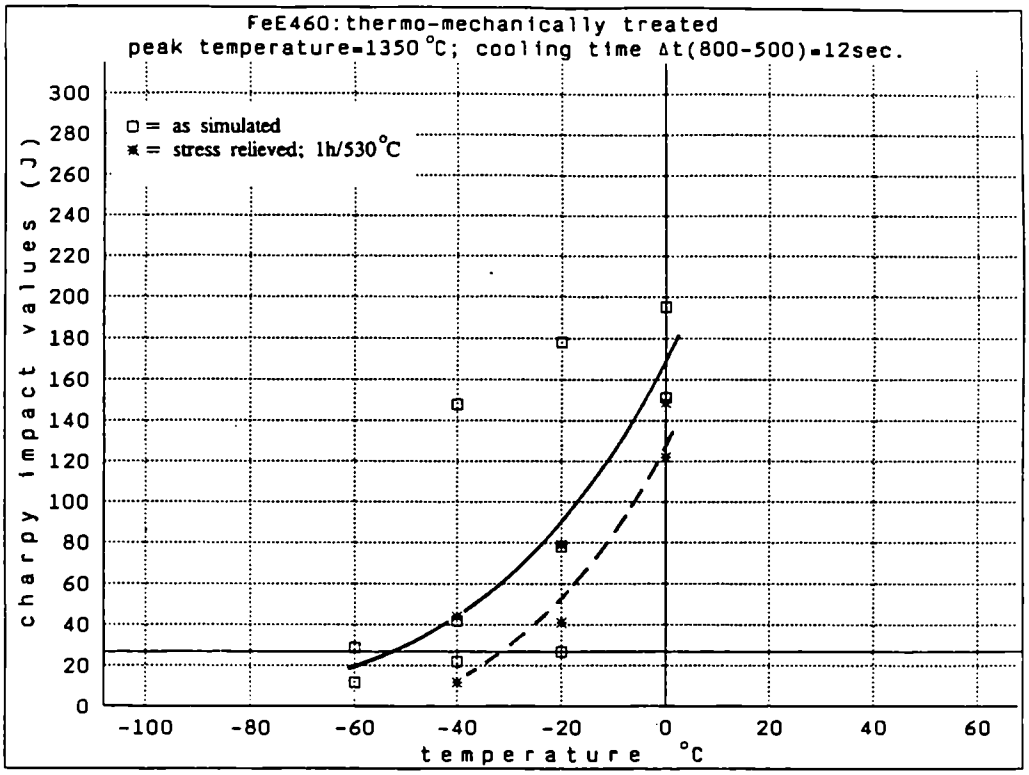

Fig. 4.42 Charpy-V fracture energies of the simulated specimens. Material TM, Tp = 1350°C, Δt (800-500) = 12 sec. □: as simulated *: + PWHT (1h 530°C)

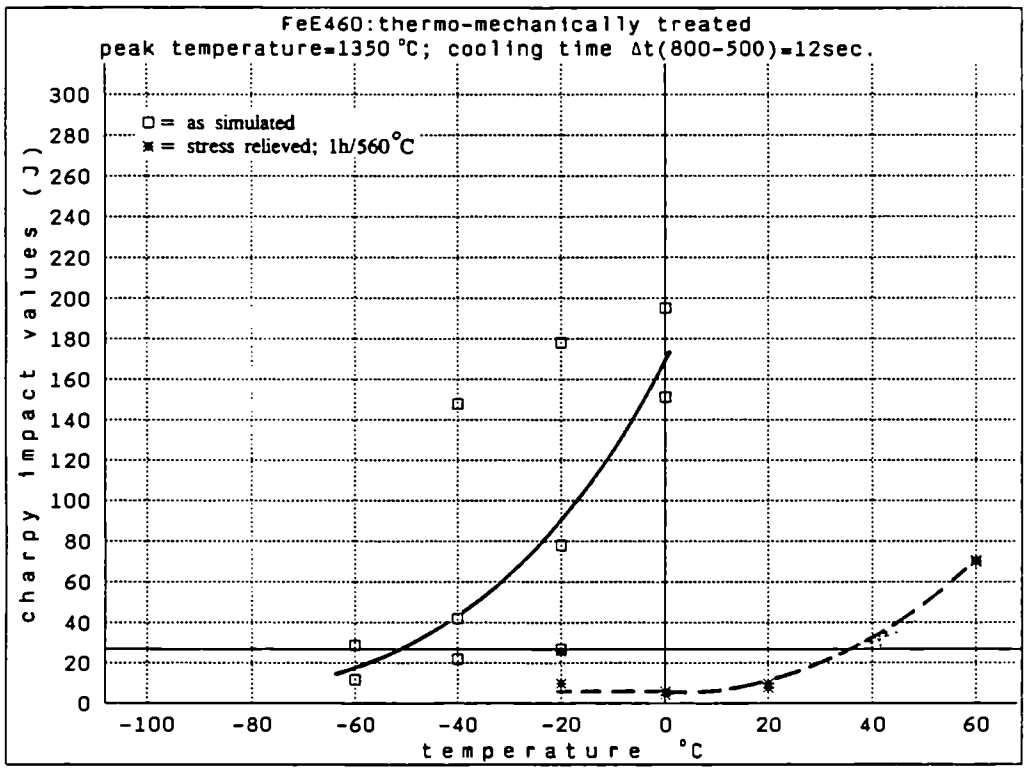

Fig. 4.43 Charpy-V fracture energies of the simulated specimens. Material TM, Tp = 1350°C, Δt (800-500) = 12 sec. □: as simulated *: + PWHT (1h 560°C)

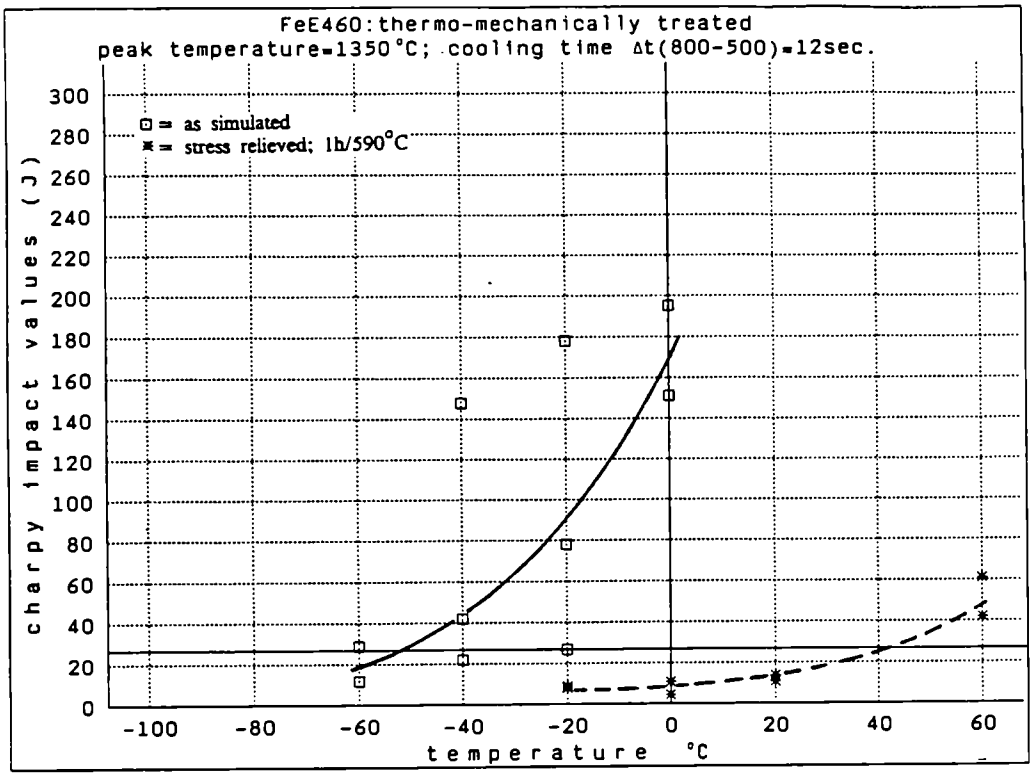

Fig. 4.44 Charpy-V fracture energies of the simulated specimens. Material TM, Tp = 1350°C, Δt (800-500) = 12 sec. □: as simulated *: + PWHT (1h 590°C)

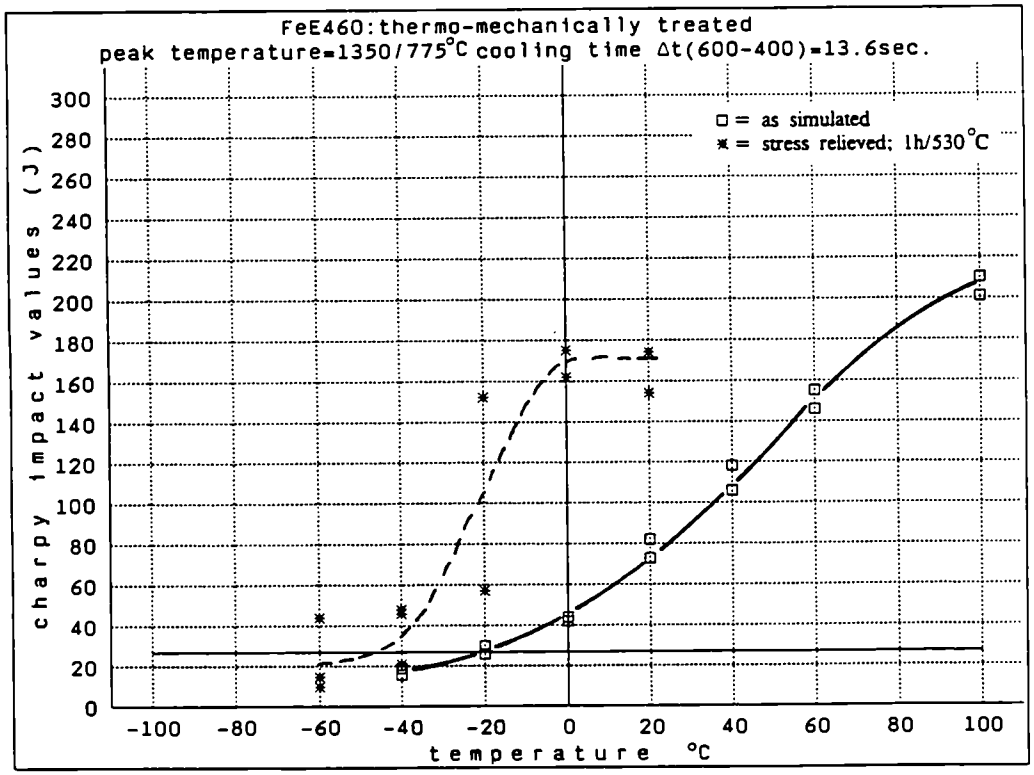

Fig. 4.45 Charpy-V fracture energies of the simulated specimens. Material TM, Tp = 1350°C, Δt (600-400) = 13,6 sec. □: as simulated *: + PWHT (1h 530°C)

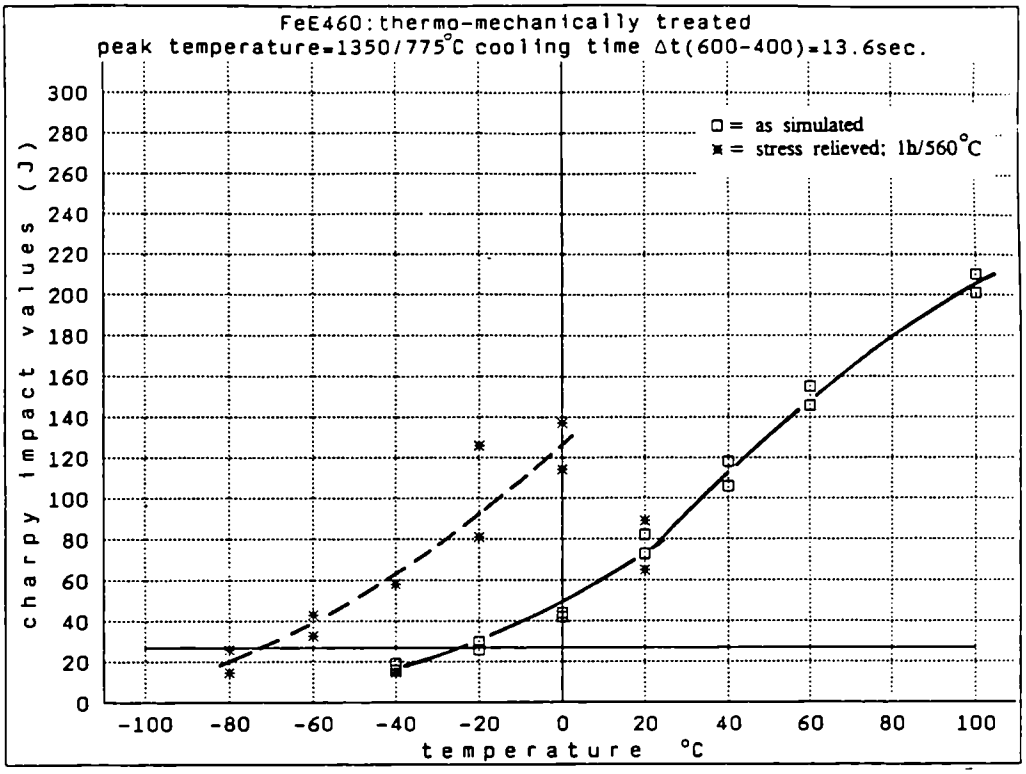

Fig. 4.46 Charpy-V fracture energies of the simulated specimens. Material TM, Tp1 = 1350°C and Tp2 = 775°C, Δt (600-400) 13.6 sec.
□: as simulated *: + PWHT (1h 560°C)

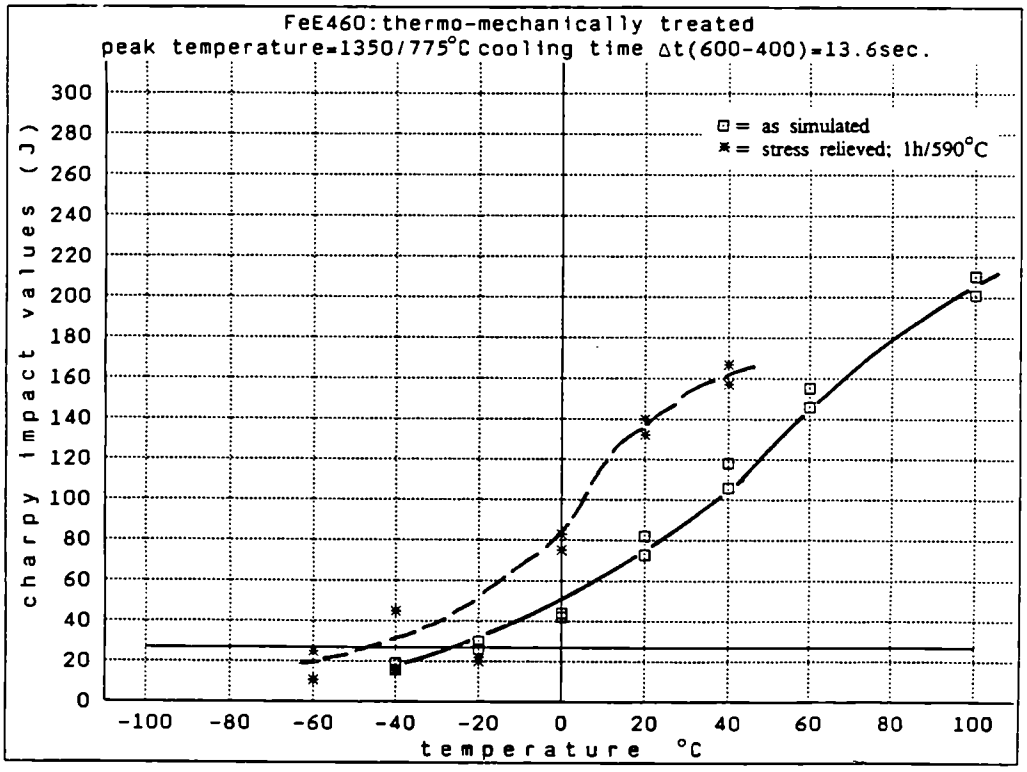

Fig. 4.47 Charpy-V fracture energies of the simulated specimens. Material TM, Tp1 = 1350°C and Tp2 = 775°C, Δt (600-400) 13.6 sec.
□: as simulated *: + PWHT (1h 590°C)

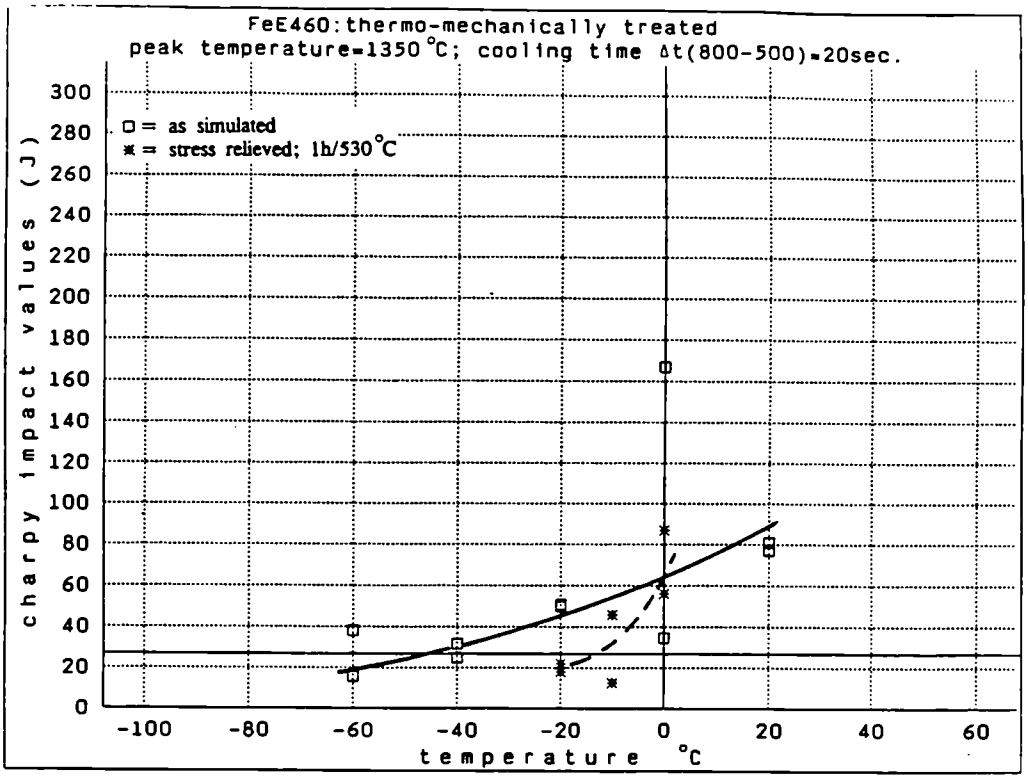

Fig. 4.48 Charpy-V fracture energies of simulated specimens. Material TM, Tp = 1350°C, Δt (800-500) 20 sec. □: as simulated *: + PWHT (1h 530°C)

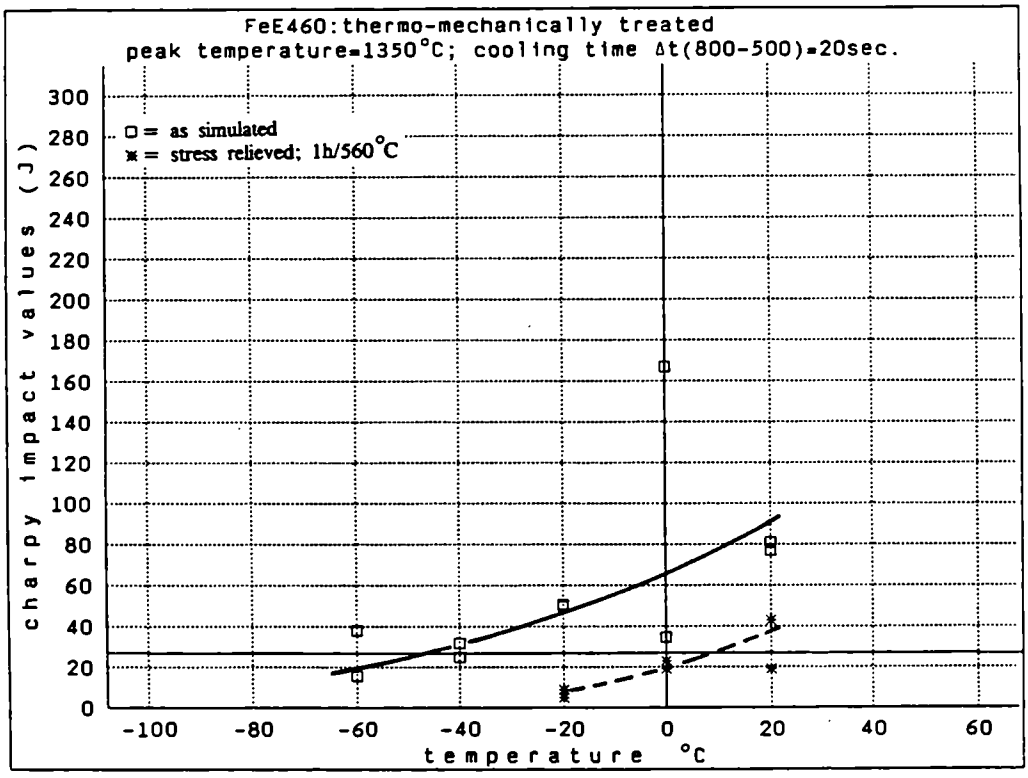

Fig. 4.49 Charpy-V fracture energies of simulated specimens. Material TM, Tp = 1350°C, Δt (800-500) 20 sec. □: as simulated *: + PWHT (1h 560°C)

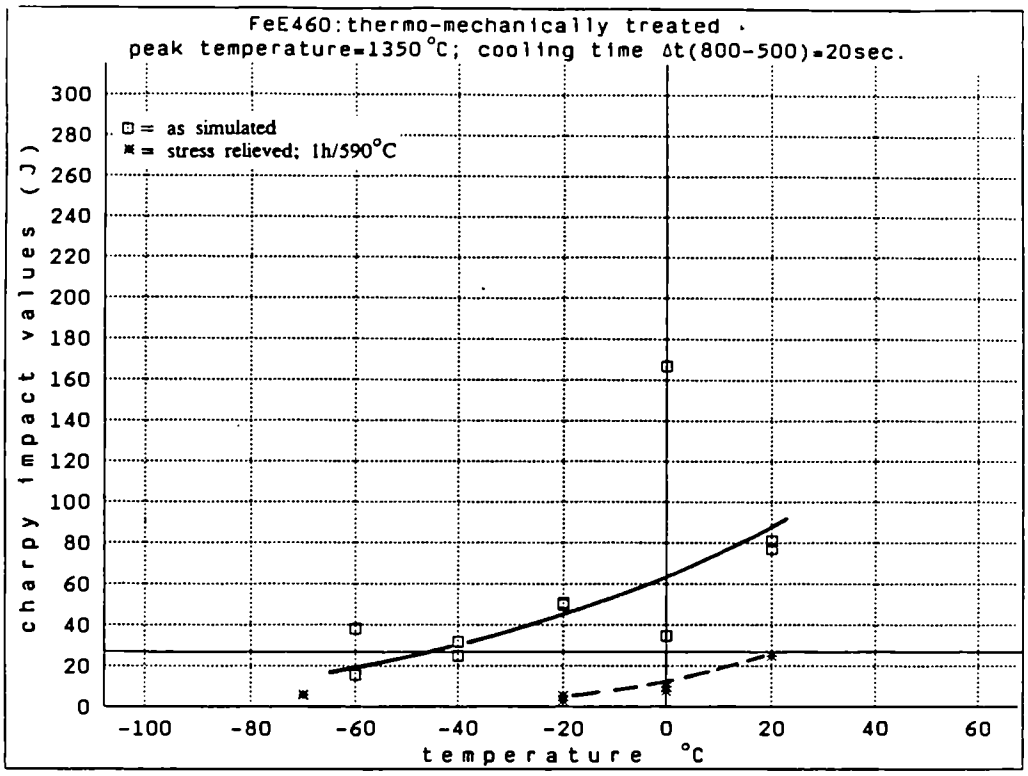

Fig. 4.50 Charpy-V fracture energies of simulated specimens. Material TM, Tp = 1350°C, Δt (800-500) 20 sec. □: as simulated *: + PWHT (1h 590°C)

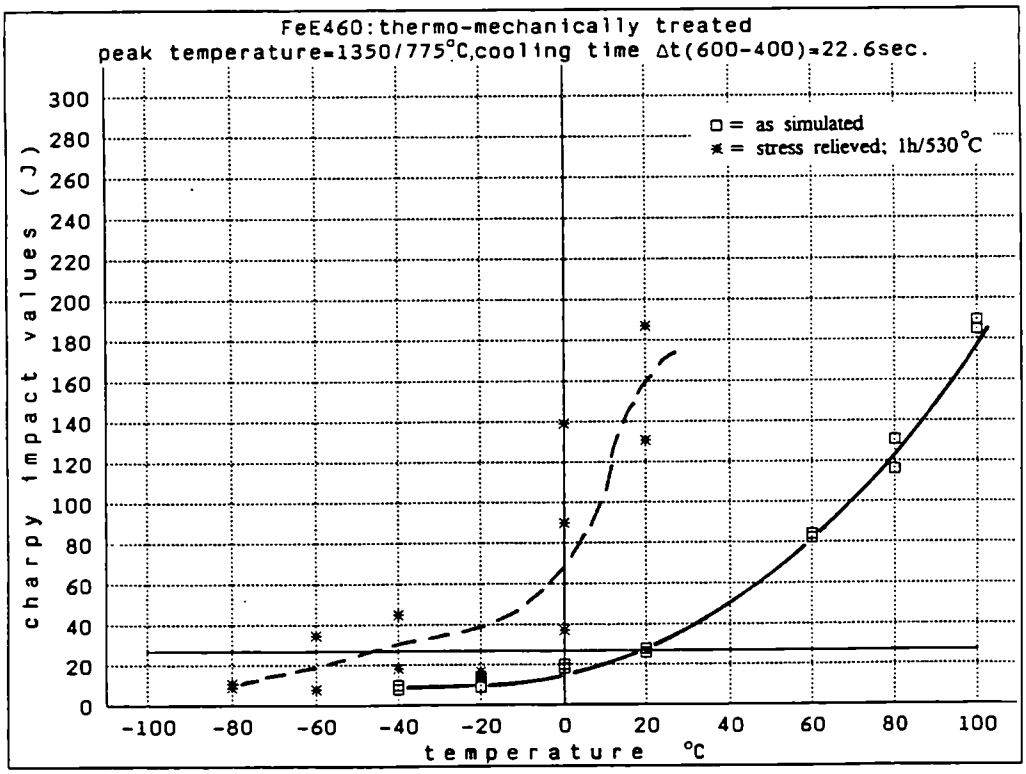

Fig. 4.51 Charpy-V fracture energies of simulated specimens. Material TM, Tp1 = 1350°C and Tp2 = 775°C, Δt (600-400) 22.6 sec. □: as simulated *: + PWHT (1h 530°C)

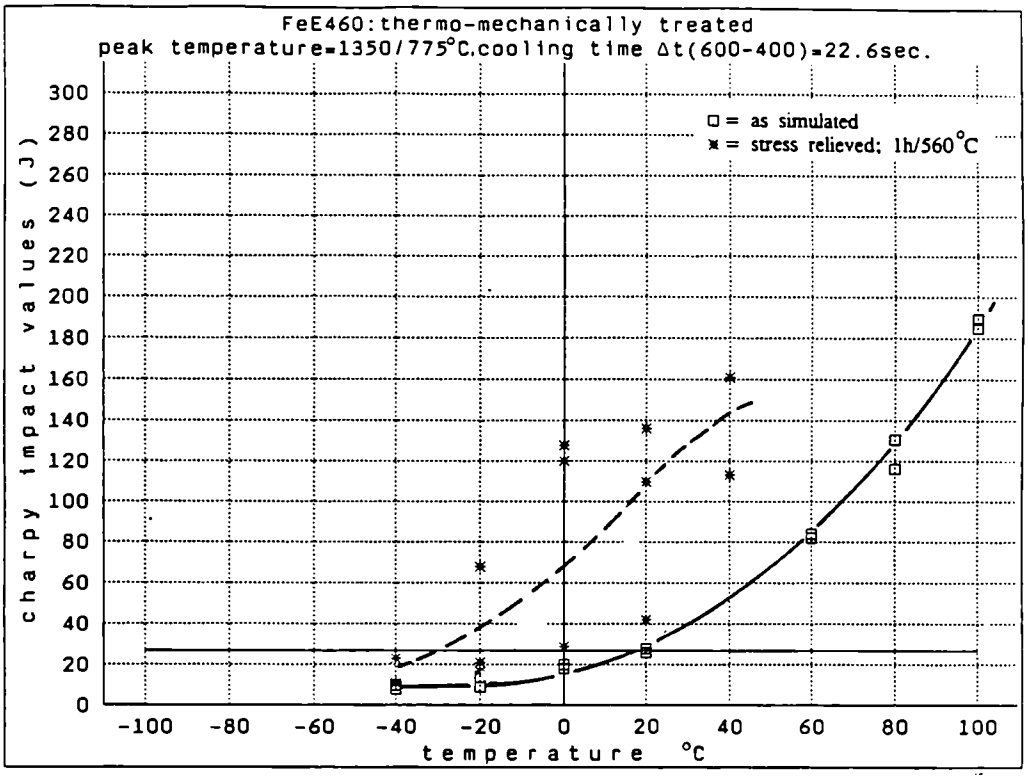

Fig. 4.52 Charpy-V fracture energies of simulated specimens. Material TM, Tp1 = 1350°C and Tp2 = 775°C, Δt (600-400) 22.6 sec.
□: as simulated *: + PWHT (1h 560°C)

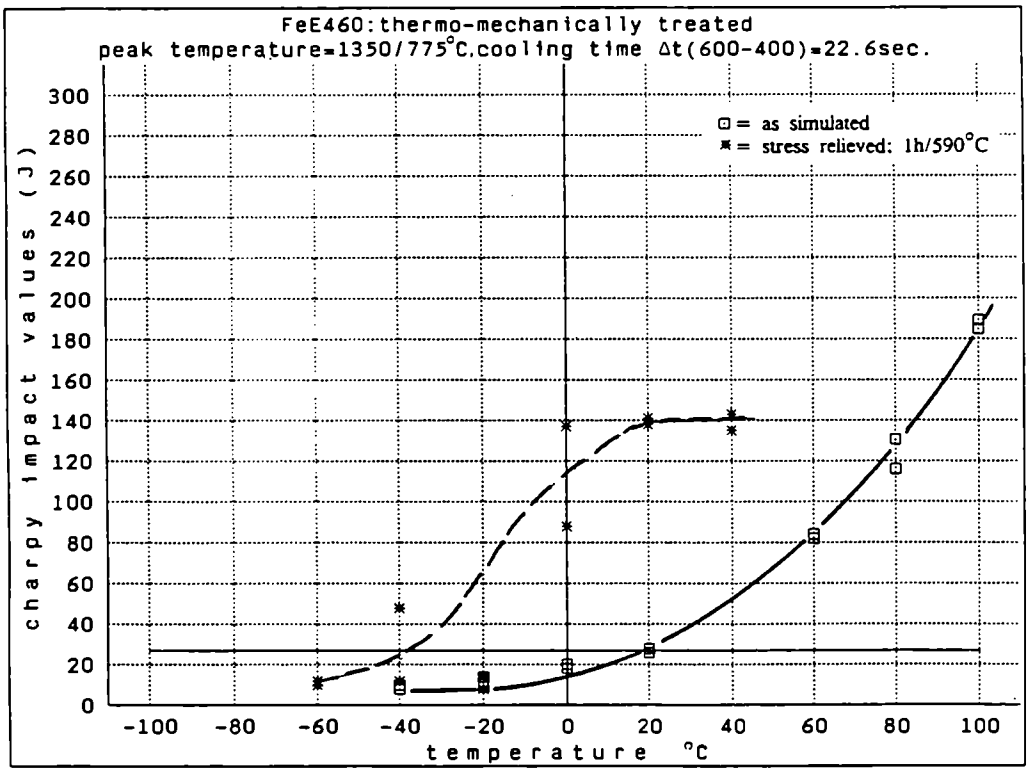

Fig. 4.53 Charpy-V fracture energies of simulated specimens. Material TM, Tp1 = 1350°C and Tp2 = 775°C, Δt (600-400) 22.6 sec.
□: as simulated *: + PWHT (1h 590°C)

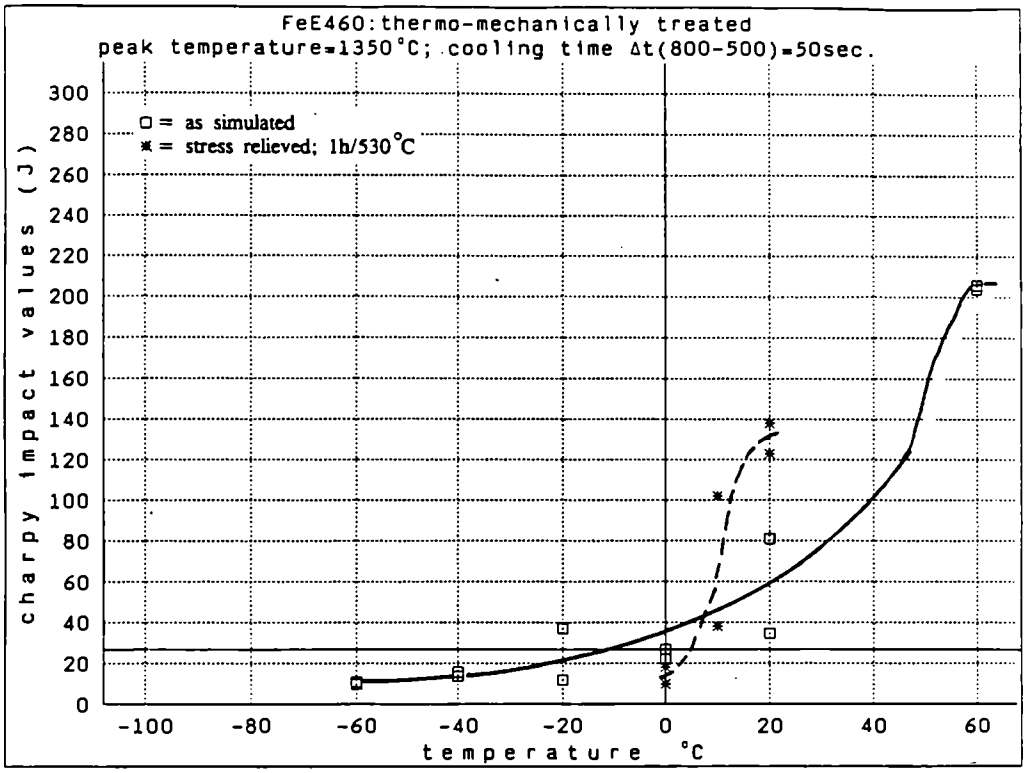

Fig. 4.54 Charpy-V fracture energies of simulated specimens.
Material TM, Tp = 1350°C, Δt (800-500) 50 sec.
□: as simulated *: + PWHT (1h 530°C)

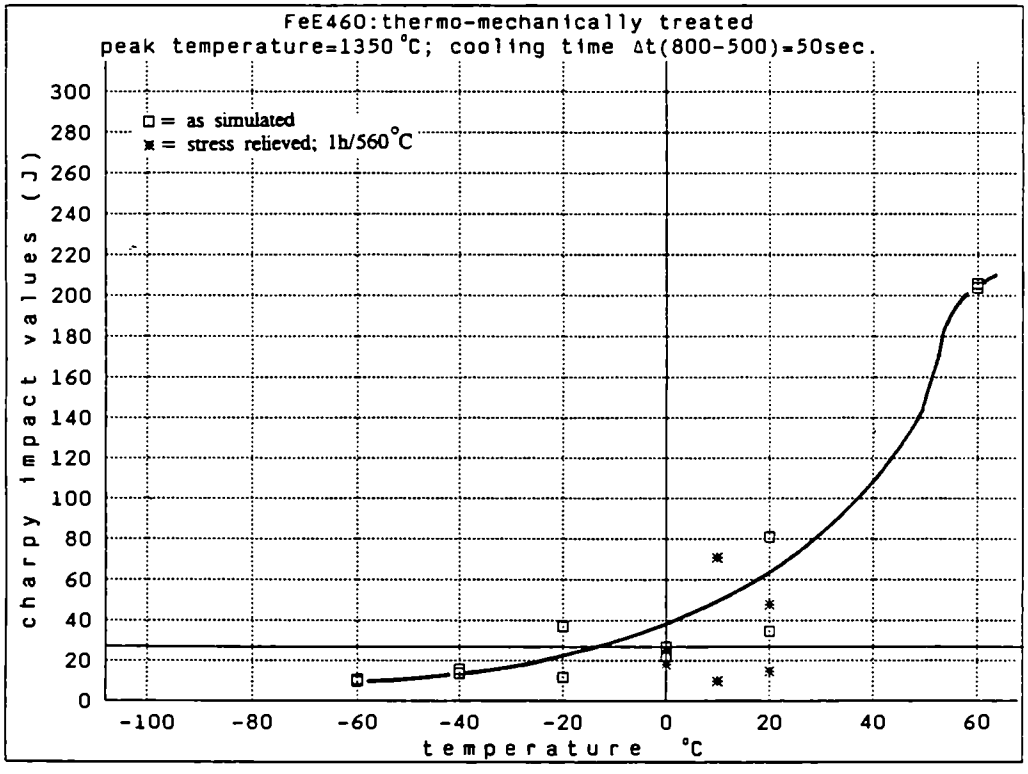

Fig. 4.55 Charpy-V fracture energies of simulated specimens.
Material TM, Tp = 1350°C, Δt (800-500) 50 sec.
□: as simulated *: + PWHT (1h 560°C)

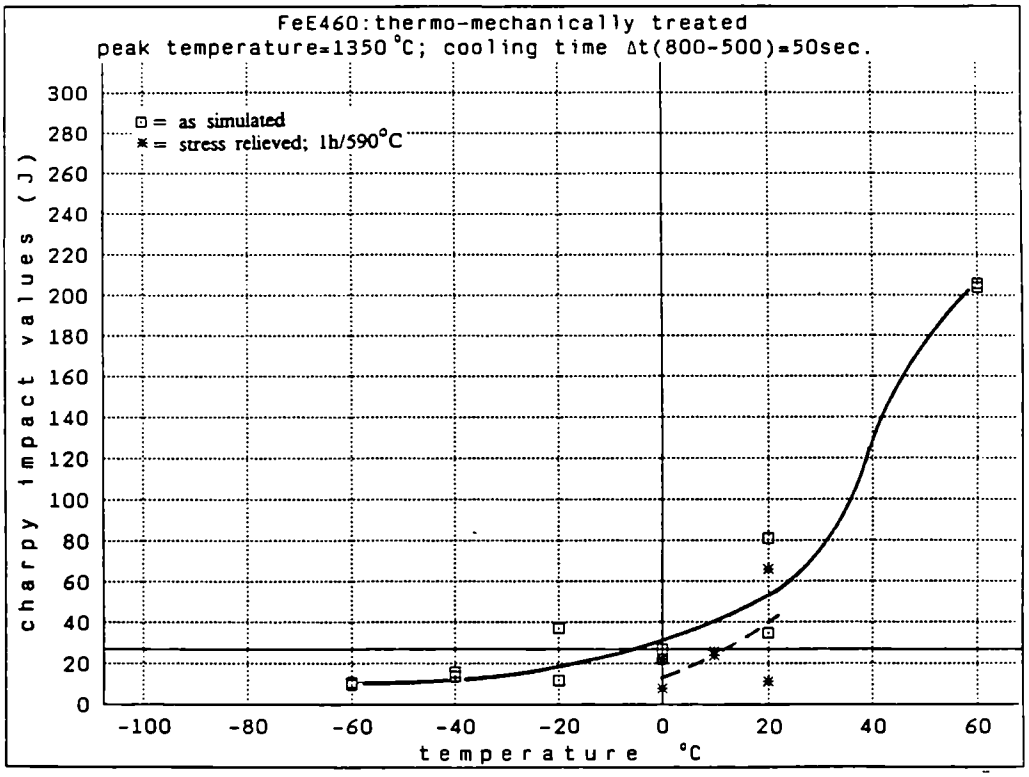

Fig. 4.56 Charpy-V fracture energies of simulated specimens. Material TM, Tp = 1350°C, Δt (800-500) 50 sec. □: as simulated *: + PWHT (1h 590°C)

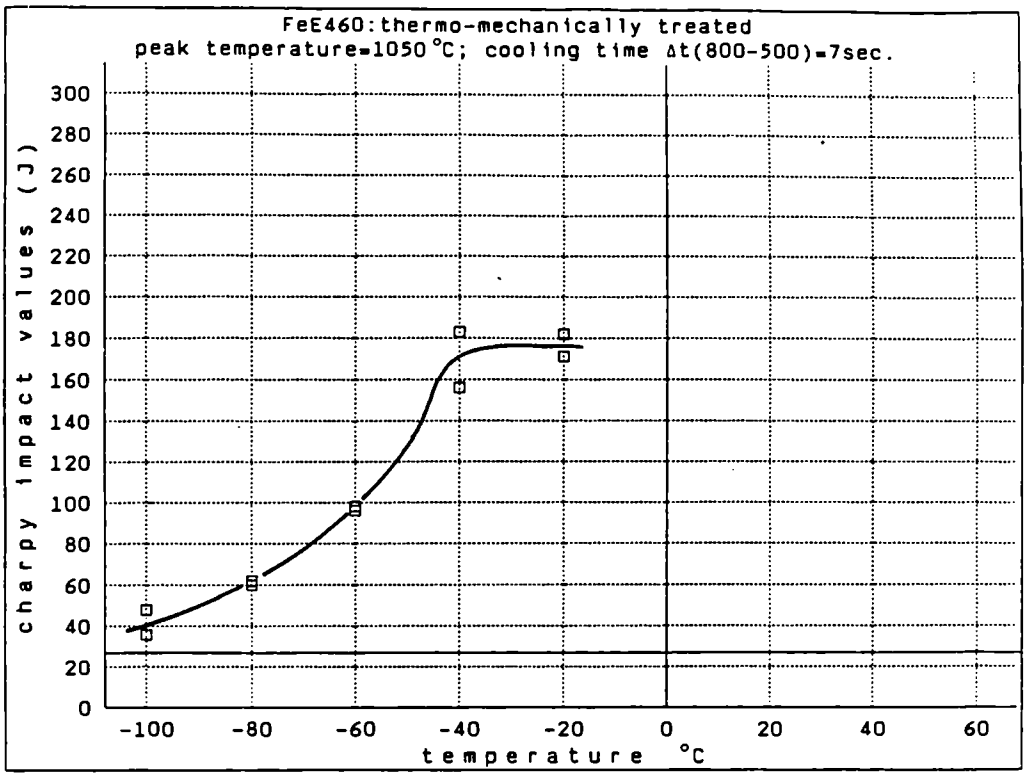

Fig. 4.57 Charpy-V fracture energies of simulated specimens. Material TM, Tp = 1050°C, Δt (800-500) 7 sec. □: as simulated

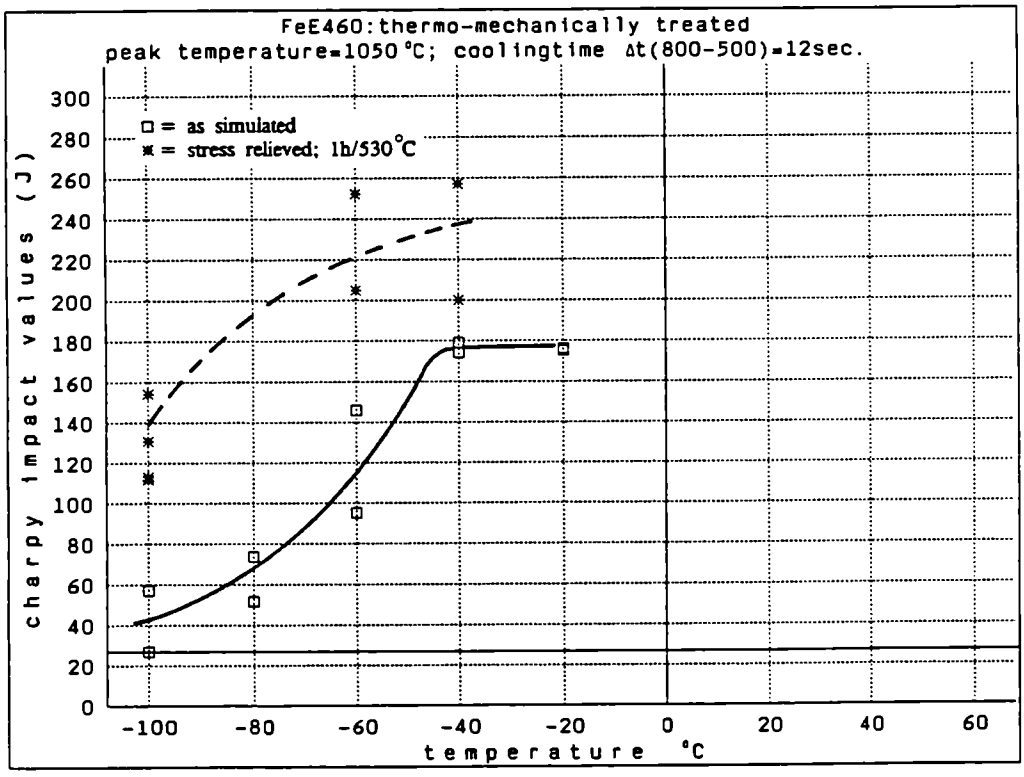

Fig. 4.58 Charpy-V fracture energies of simulated specimens. Material TM, Tp = 1050°C, Δt (800-500) 12 sec. □: as simulated *: + PWHT (1h 530°C)

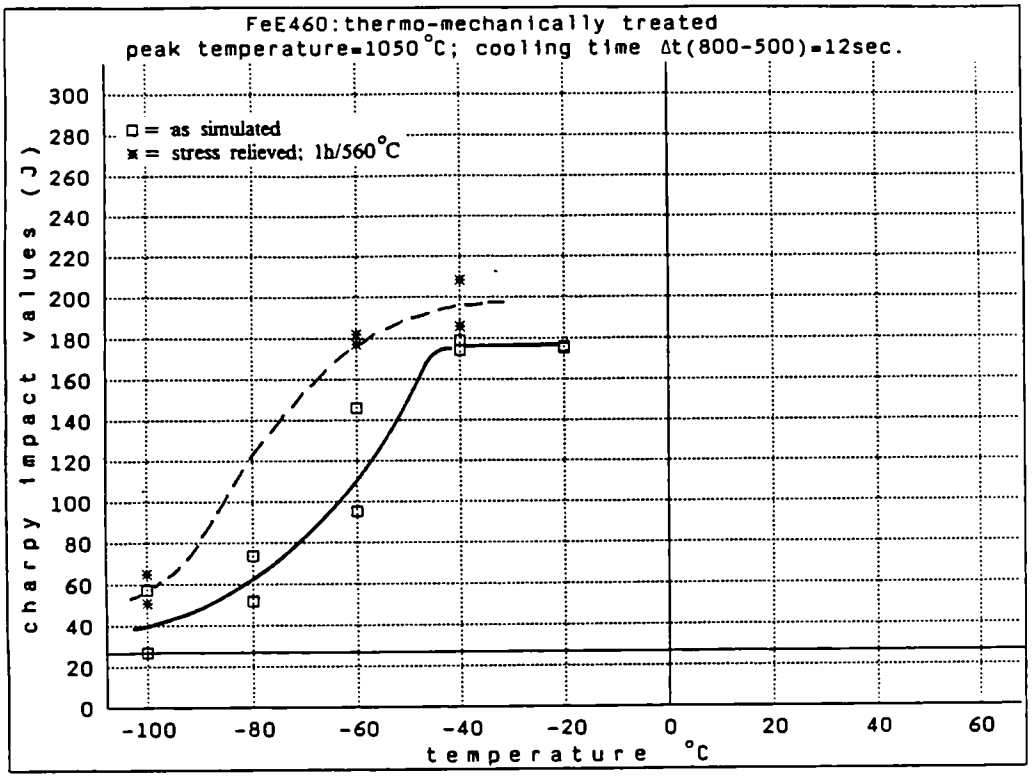

Fig. 4.59 Charpy-V fracture energies of simulated specimens. Material TM, Tp = 1050°C, Δt (800-500) 12 sec. □: as simulated *: + PWHT (1h 560°C)

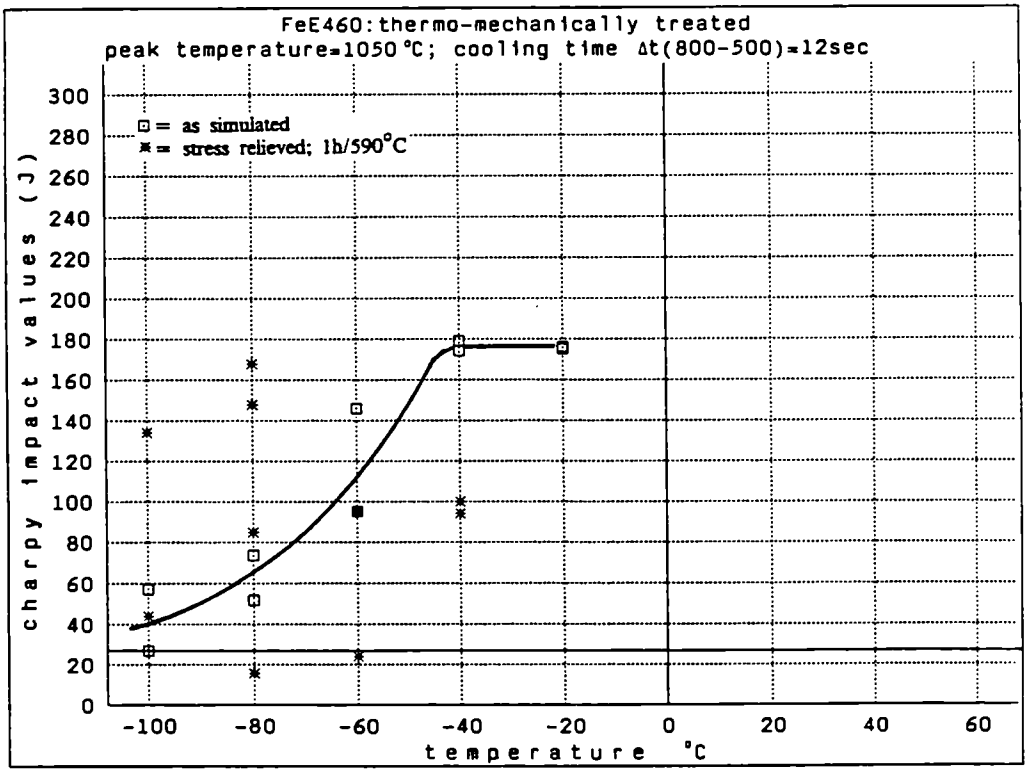

Fig. 4.60 Charpy-V fracture energies of simulated specimens. Material TM, Tp = 1050°C, Δt (800-500) 12 sec. □: as simulated *: + PWHT (1h 590°C)

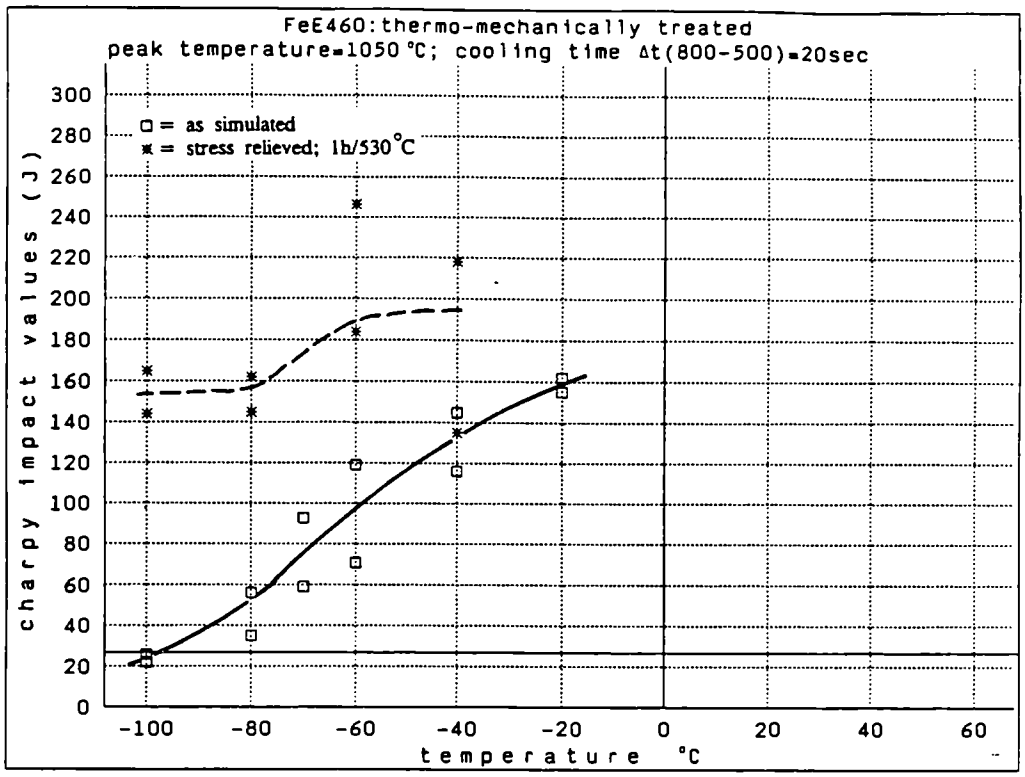

Fig. 4.61 Charpy-V fracture energies of simulated specimens. Material TM, Tp = 1050°C, Δt (800-500) 20 sec. □: as simulated *: + PWHT (1h 530°C)

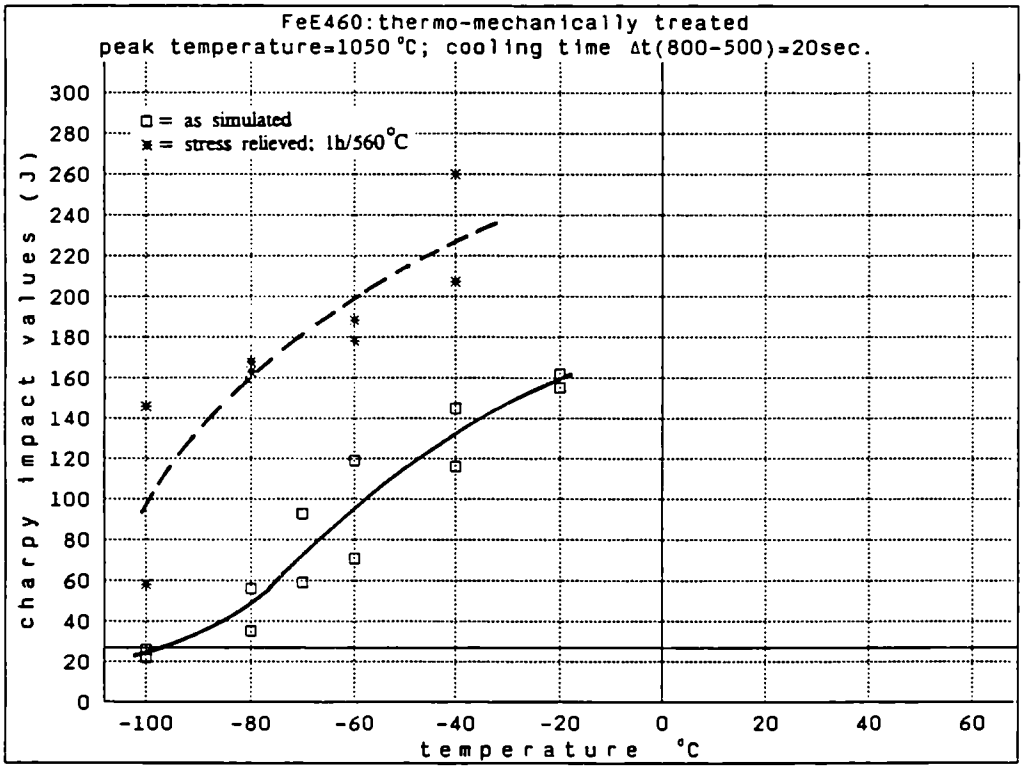

Fig. 4.62 Charpy-V fracture energies of simulated specimens. Material TM, Tp = 1050°C, Δt (800-500) 20 sec. □: as simulated *: + PWHT (1h 560°C)

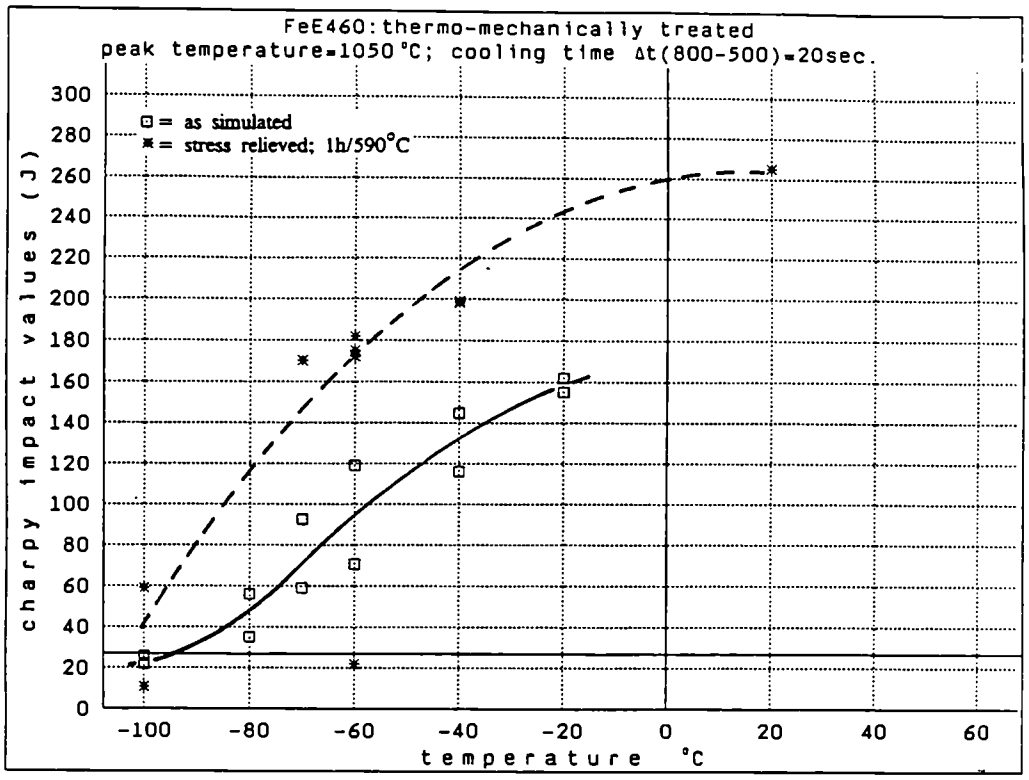

Fig. 4.63 Charpy-V fracture energies of simulated specimens. Material TM, Tp = 1050°C, Δt (800-500) 20 sec. □: as simulated *: + PWHT (1h 590°C)

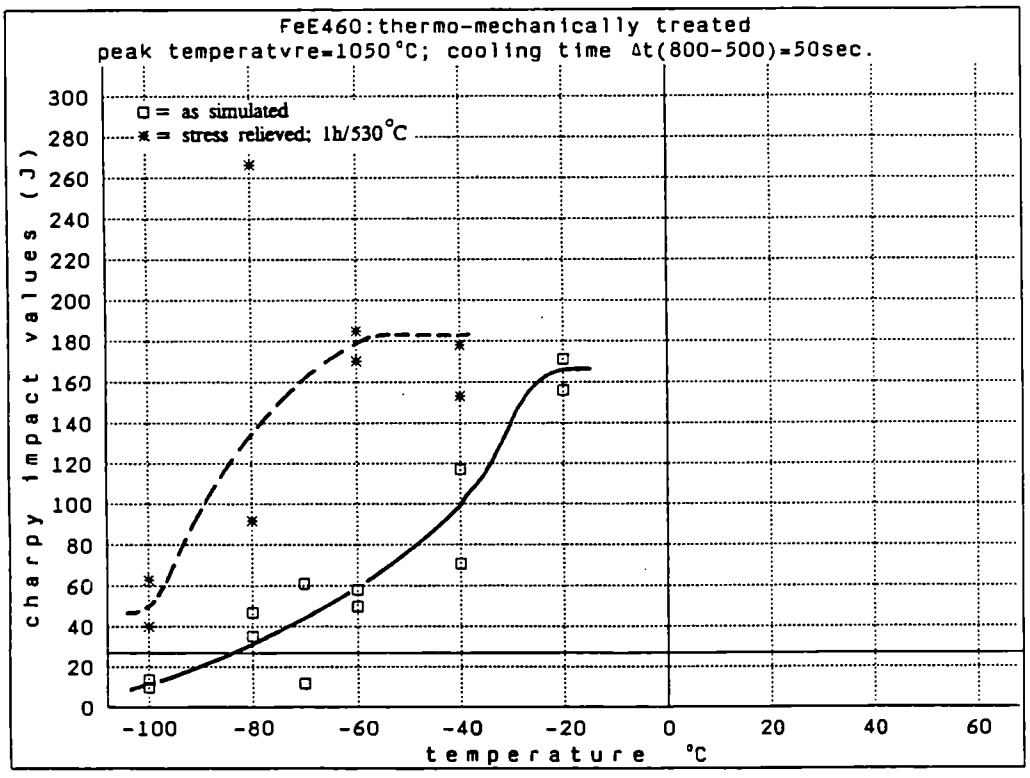

Fig. 4.64 Charpy-V fracture energies of simulated specimens. Material TM, Tp = 1050°C, Δt (800-500) 50 sec. □: as simulated *: + PWHT (1h 530°C)

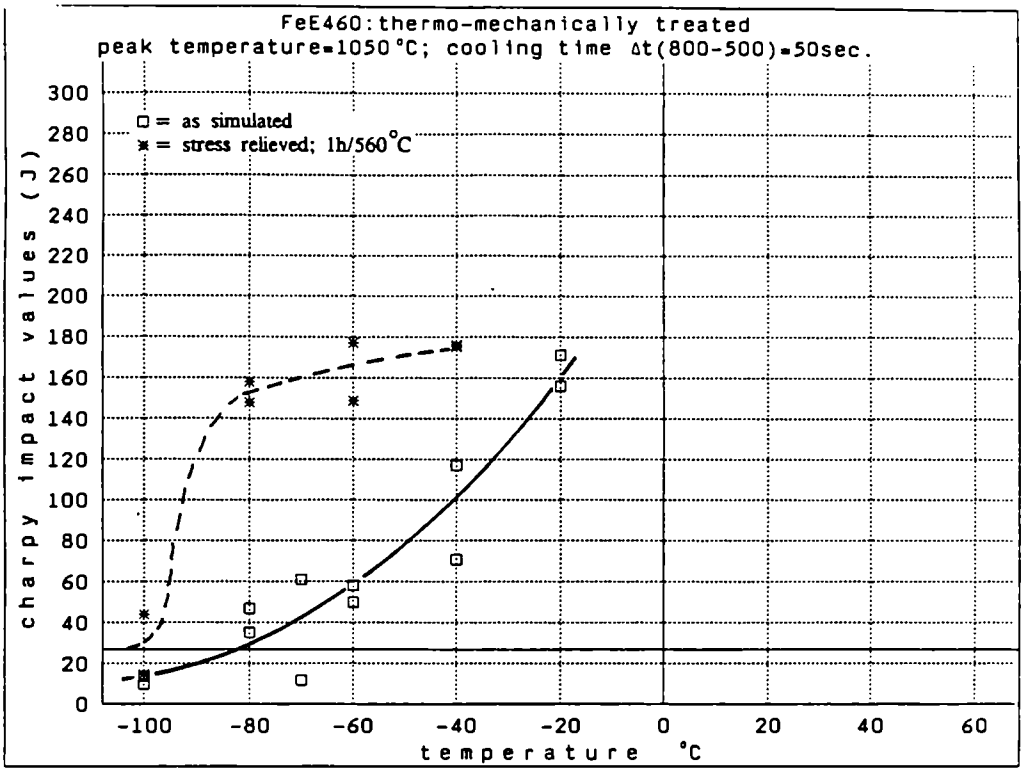

Fig. 4.65 Charpy-V fracture energies of simulated specimens.
Material TM, Tp = 1050°C, Δt (800-500) 50 sec.
□: as simulated *: + PWHT (1h 560°C)

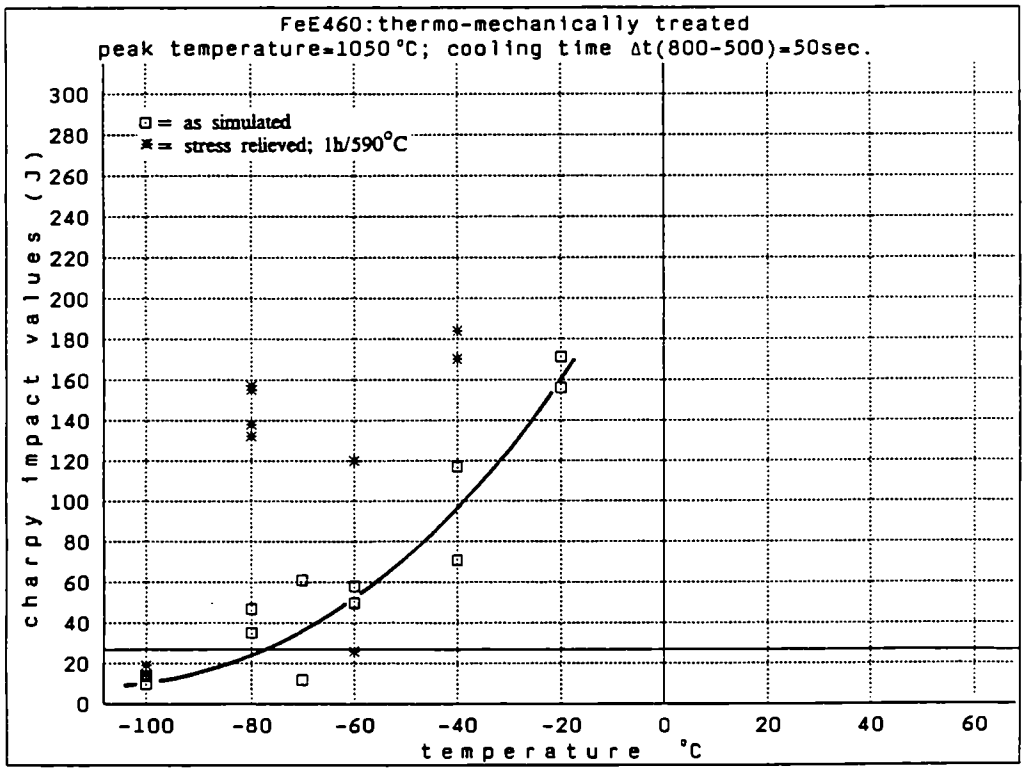

Fig. 4.66 Charpy-V fracture energies of simulated specimens.
Material TM, Tp = 1050°C, Δt (800-500) 50 sec.
□: as simulated *: + PWHT (1h 590°C)

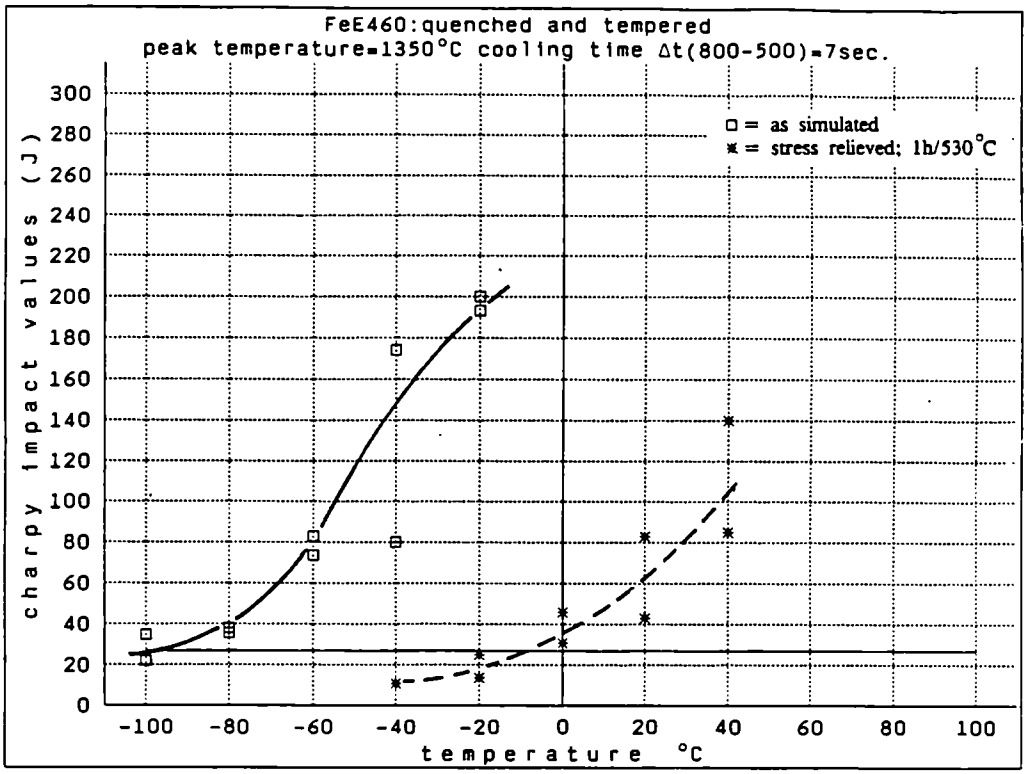

Fig. 4.67 Charpy-V fracture energies of simulated specimens.
Material QT, Tp = 1350°C, Δt (800-500) 7 sec.
□: as simulated *: + PWHT (1h 530°C)

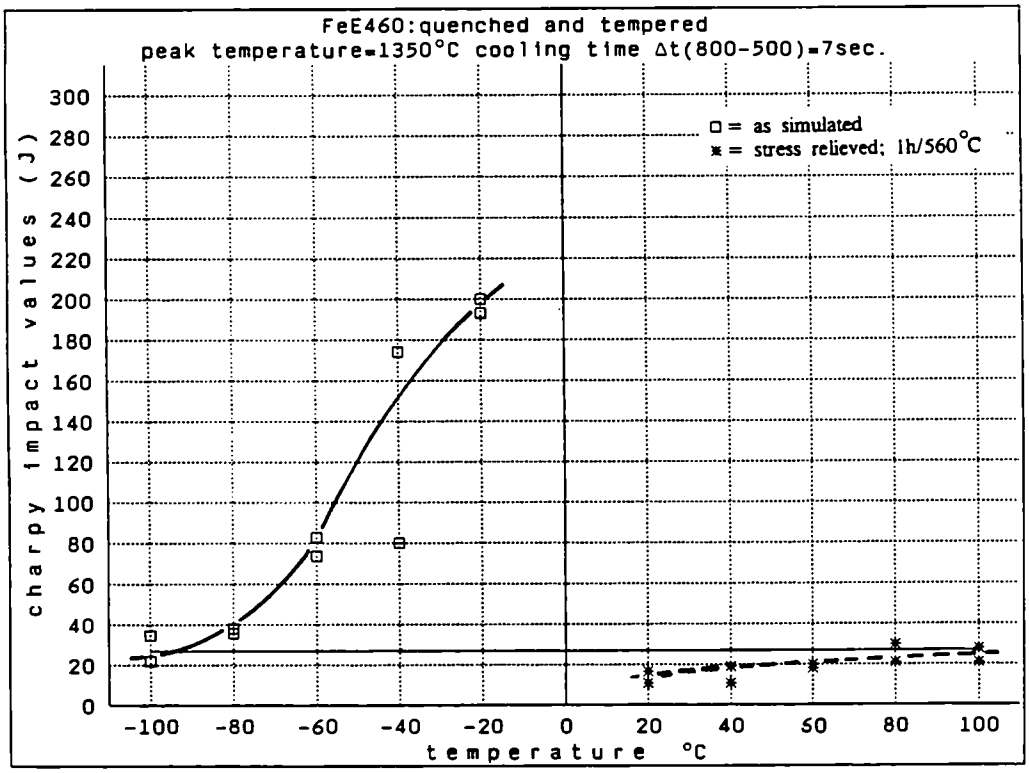

Fig. 4.68 Charpy-V fracture energies of simulated specimens.
Material QT, Tp = 1350°C, Δt (800-500) 7 sec.
□: as simulated *: + PWHT (1h 560°C)

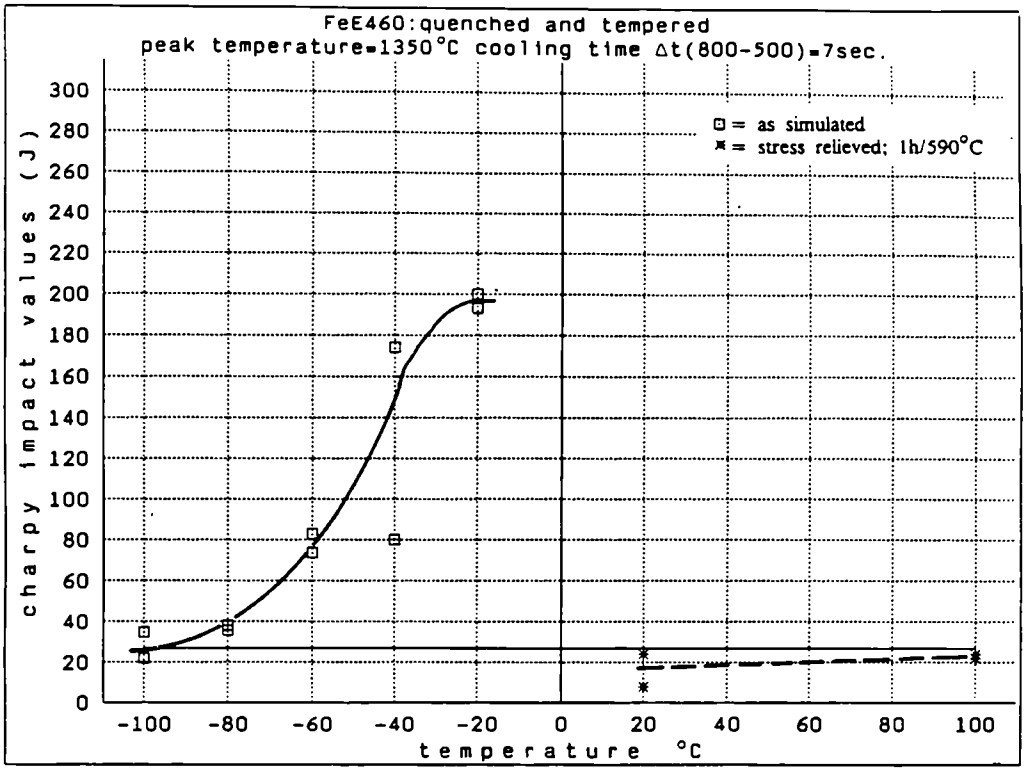

Fig. 4.69 Charpy-V fracture energies of simulated specimens. Material QT, Tp = 1350°C, Δt (800-500) 7 sec. □: as simulated *: + PWHT (1h 590°C)

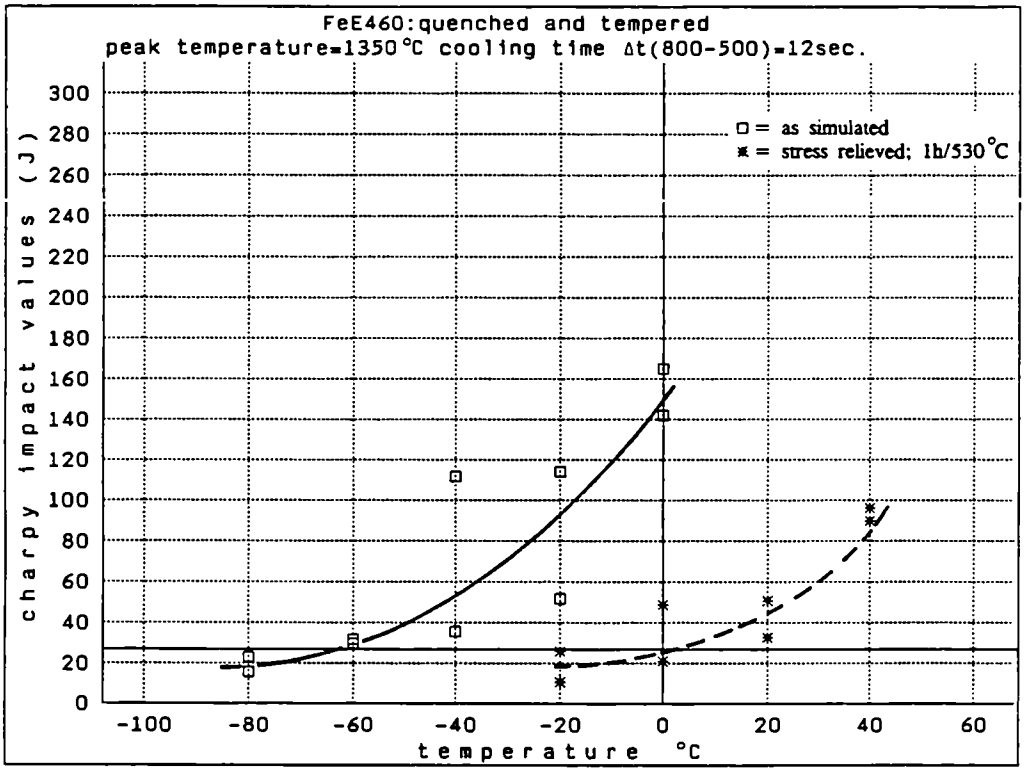

Fig. 4.70 Charpy-V fracture energies of simulated specimens. Material QT, Tp = 1350°C, Δt (800-500) 12 sec. □: as simulated *: + PWHT (1h 530°C)

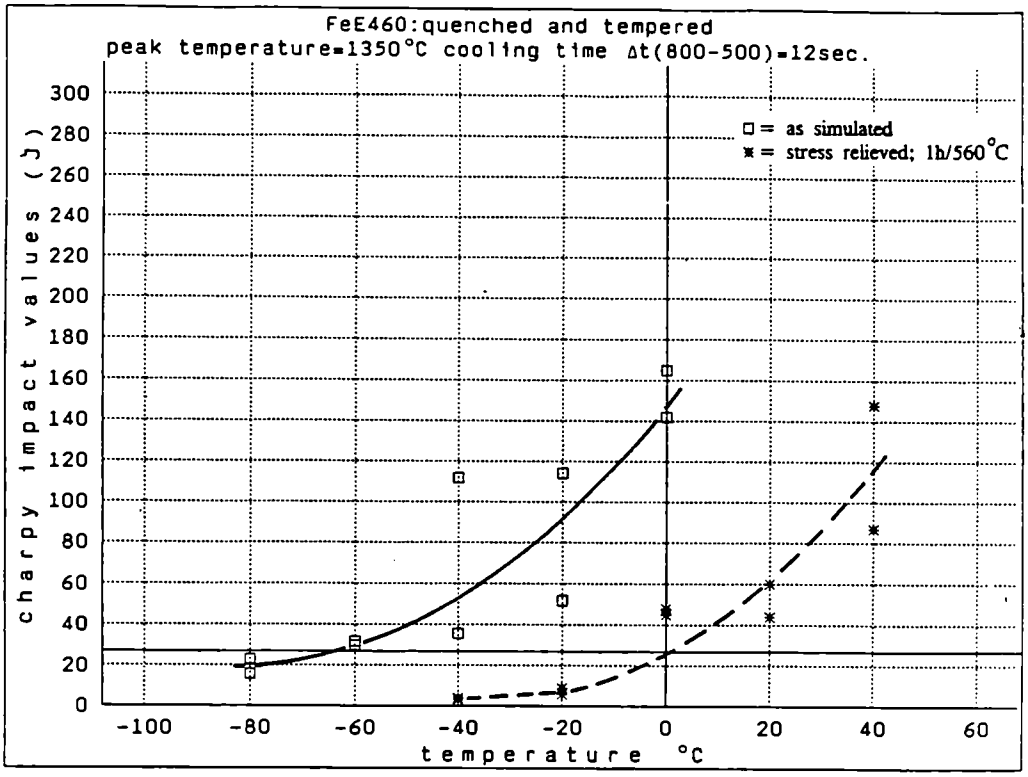

Fig. 4.71 Charpy-V fracture energies of simulated specimens. Material QT, Tp = 1350°C, Δt (800-500) 12 sec. □: as simulated *: + PWHT (1h 560°C)

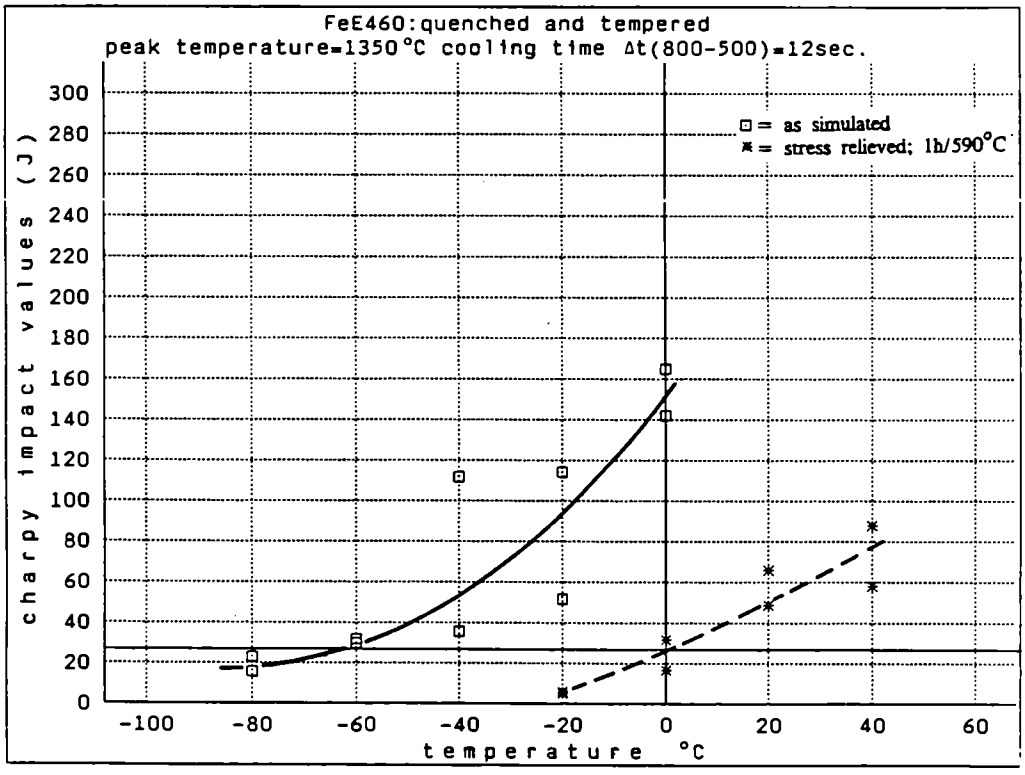

Fig. 4.72 Charpy-V fracture energies of simulated specimens. Material QT, Tp = 1350°C, Δt (800-500) 12 sec. □: as simulated *: + PWHT (1h 590°C)

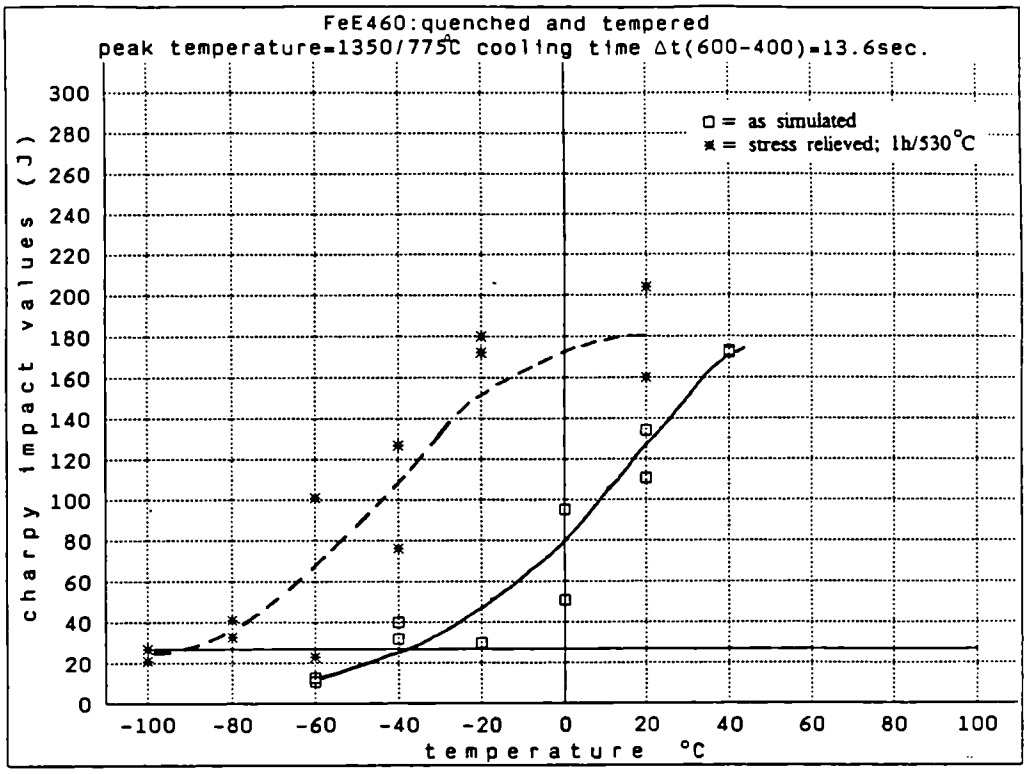

Fig. 4.73 Charpy-V fracture energies of simulated specimens. Material QT, Tp1 = 1350°C and Tp2 = 775°C, Δt (600-400) 13.6 sec.
□: as simulated *: + PWHT (1h 530°C)

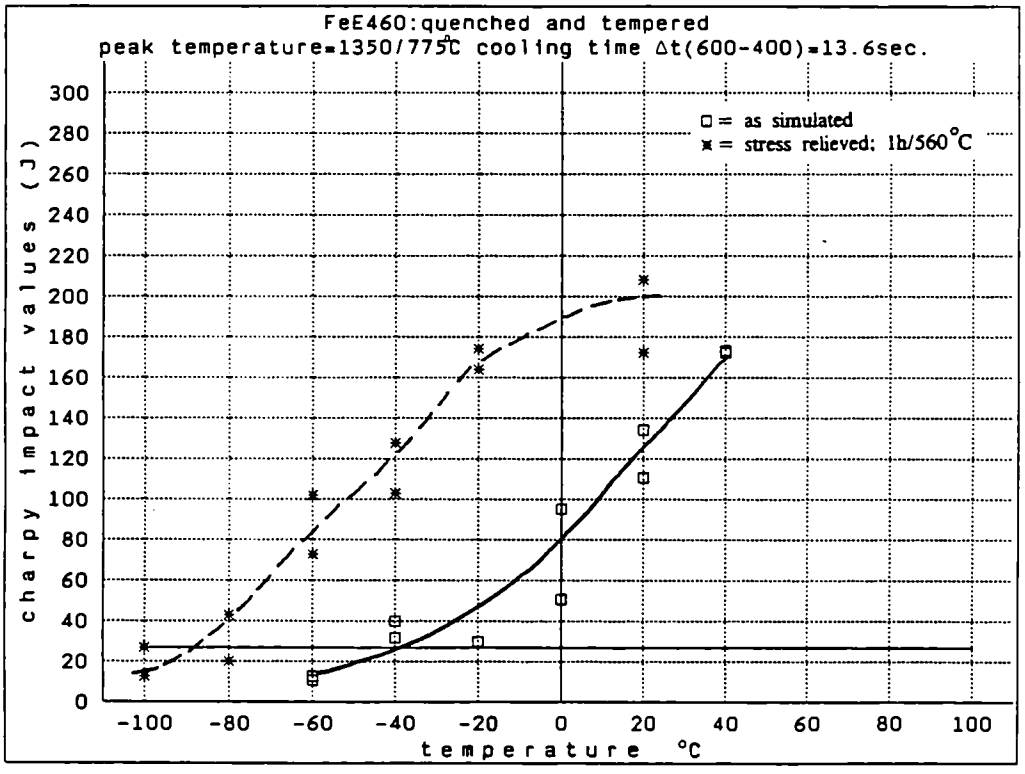

Fig. 4.74 Charpy-V fracture energies of simulated specimens. Material QT, Tp1 = 1350°C and Tp2 = 775°C, Δt (600-400) 13.6 sec.
□: as simulated *: + PWHT (1h 560°C)

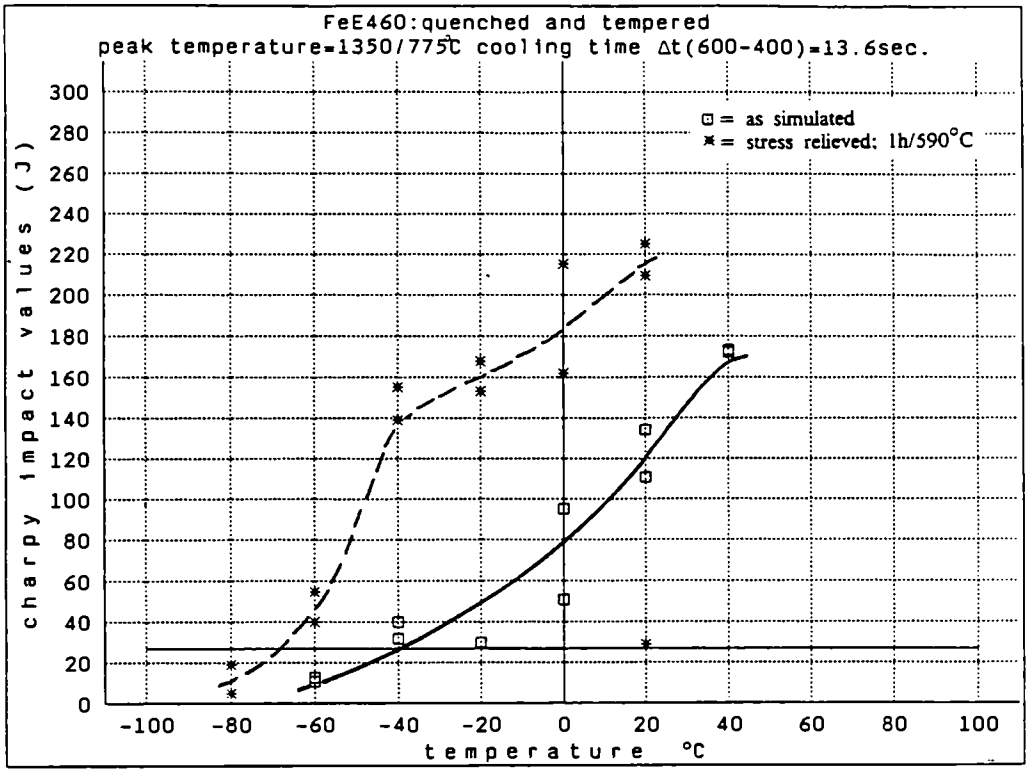

Fig. 4.75 Charpy-V fracture energies of simulated specimens. Material QT, Tp1 = 1350°C and Tp2 = 775°C, Δt (600-400) 13.6 sec.
□: as simulated *: + PWHT (1h 590°C)

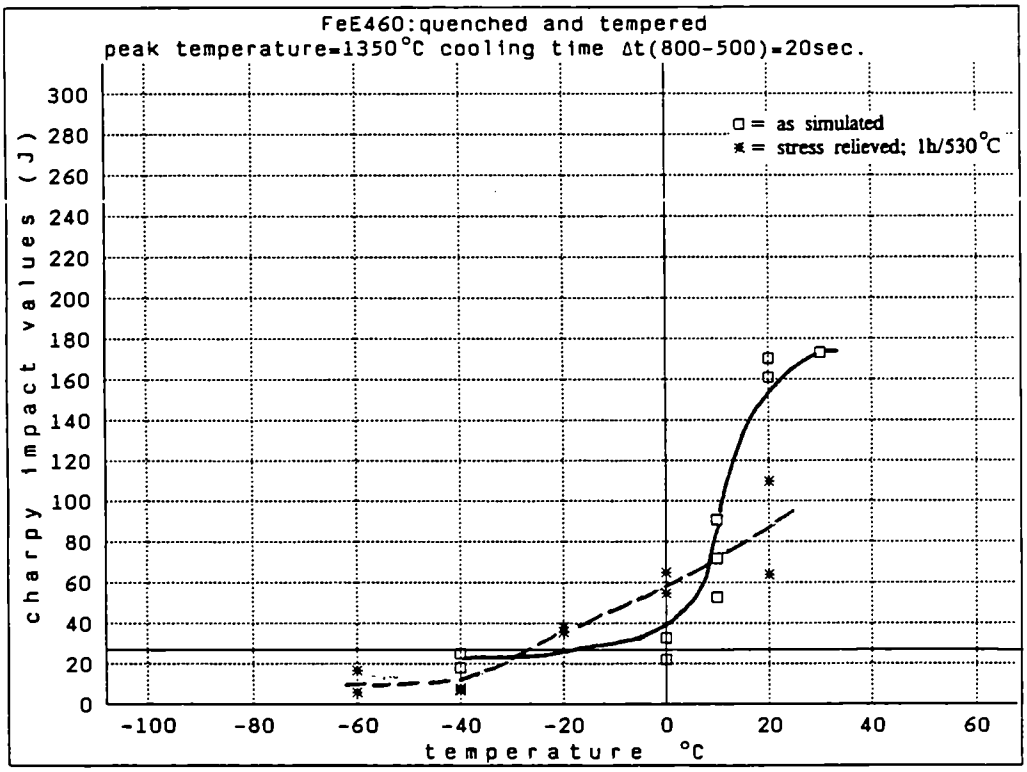

Fig. 4.76 Charpy-V fracture energies of simulated specimens. Material QT, Tp = 1350°C ,Δt (800-500) 20 sec.
□: as simulated *: + PWHT (1h 530°C)

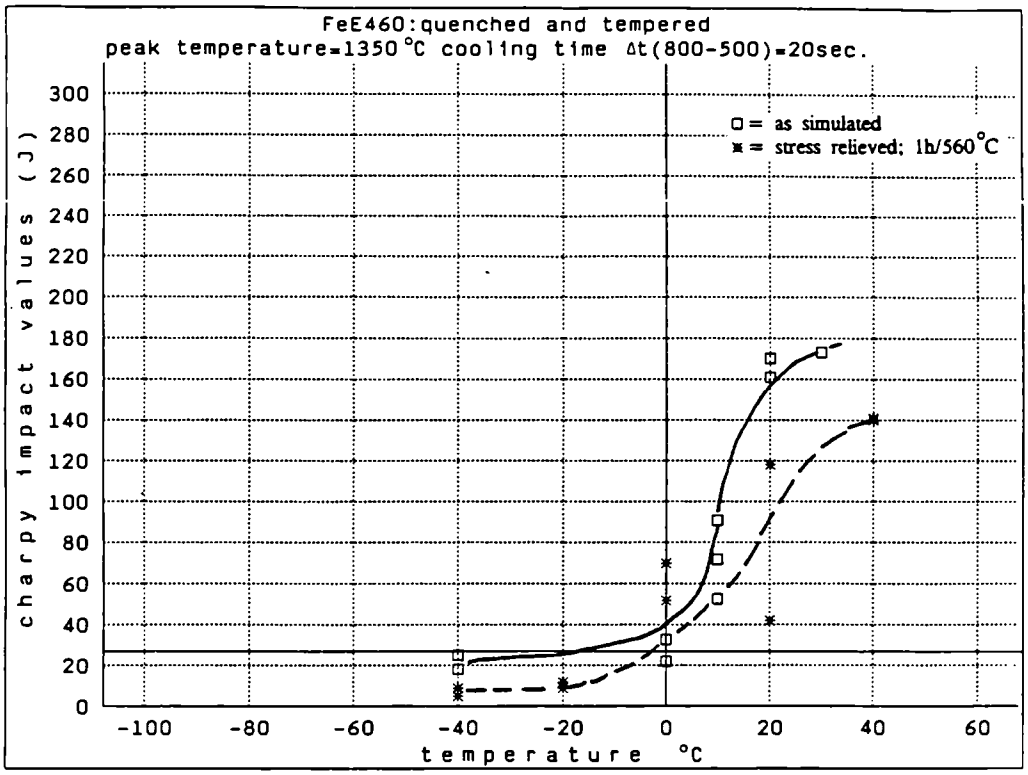

Fig. 4.77 Charpy-V fracture energies of simulated specimens.
Material QT, Tp = 1350°C ,Δt (800-500) 20 sec.
□: as simulated *: + PWHT (1h 560°C)

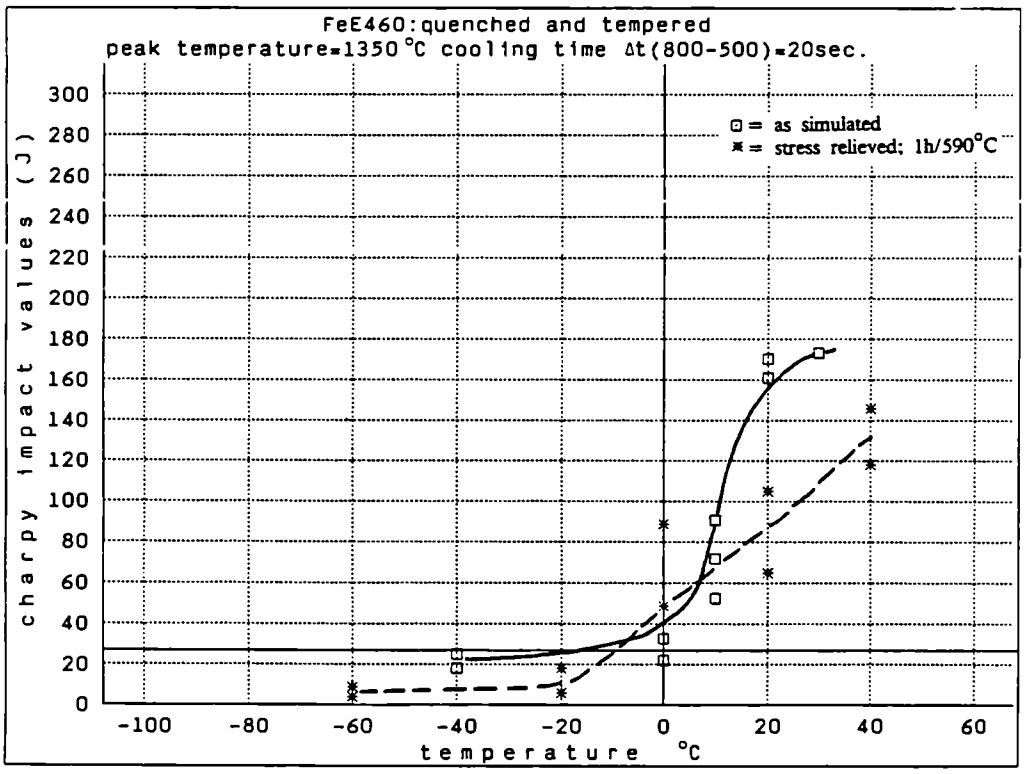

Fig. 4.78 Charpy-V fracture energies of simulated specimens.
Material QT, Tp = 1350°C ,Δt (800-500) 20 sec.
□: as simulated *: + PWHT (1h 590°C)

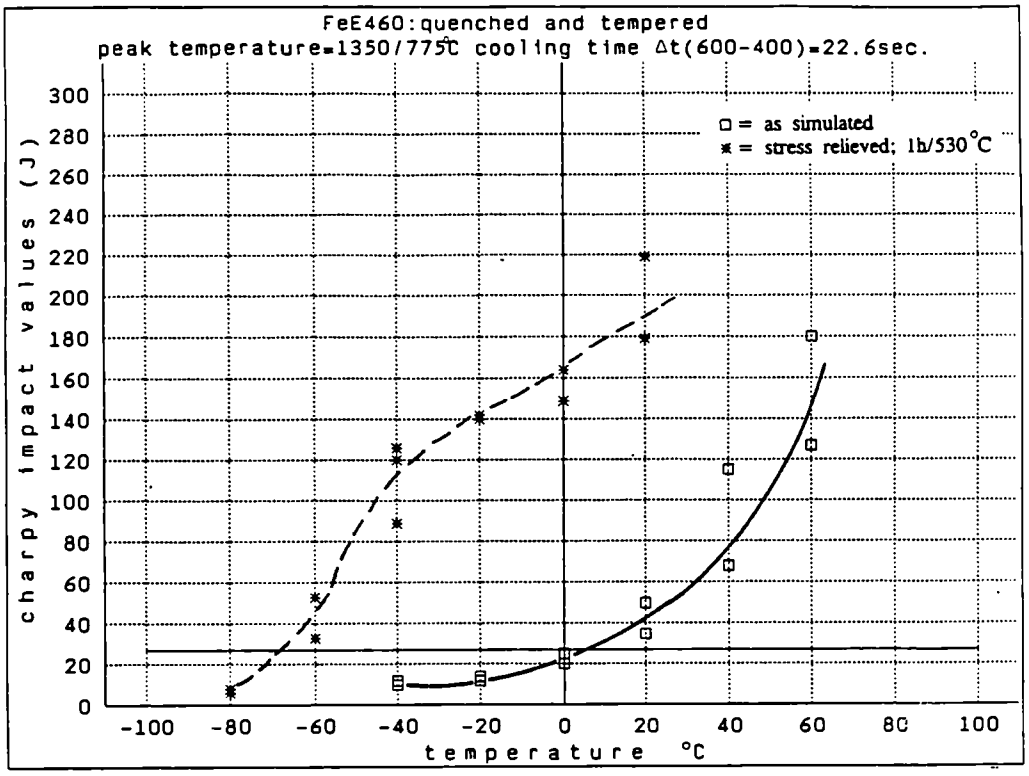

Fig. 4.79 Charpy-V fracture energies of simulated specimens. Material QT, Tp1 = 1350°C and Tp2 = 775°C, Δt (600-400) 22.6 sec.
□: as simulated *: + PWHT (1h 530°C)

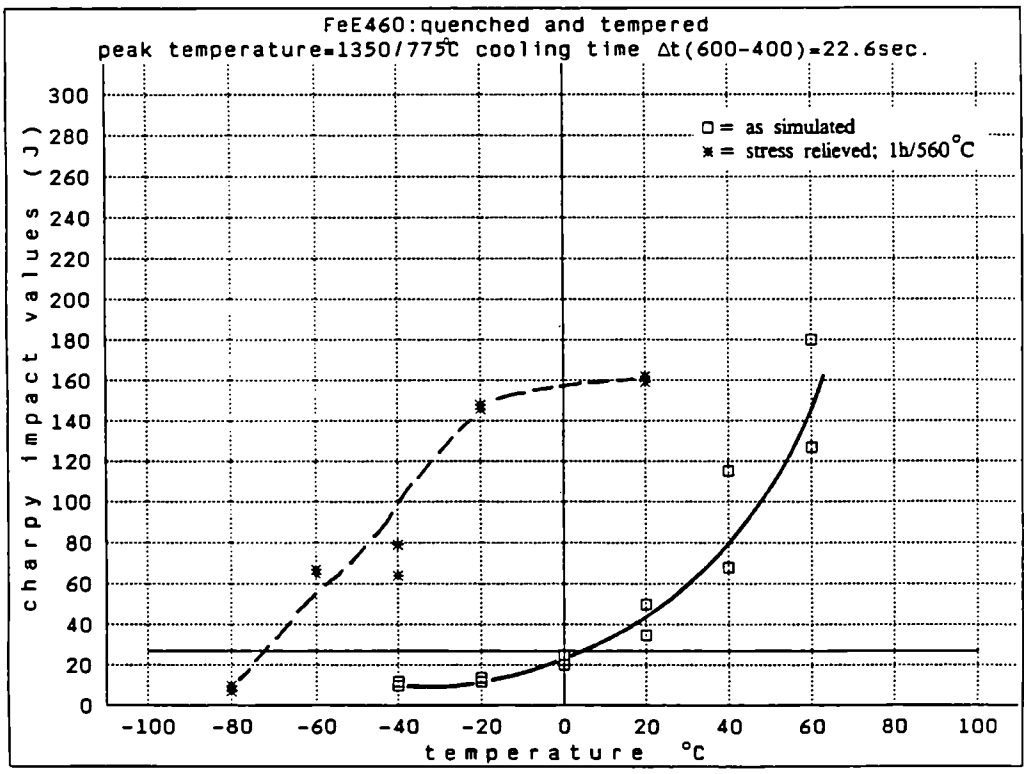

Fig. 4.80 Charpy-V fracture energies of simulated specimens. Material QT, Tp1 = 1350°C and Tp2 = 775°C, Δt (600-400) 22.6 sec.
□: as simulated *: + PWHT (1h 560°C)

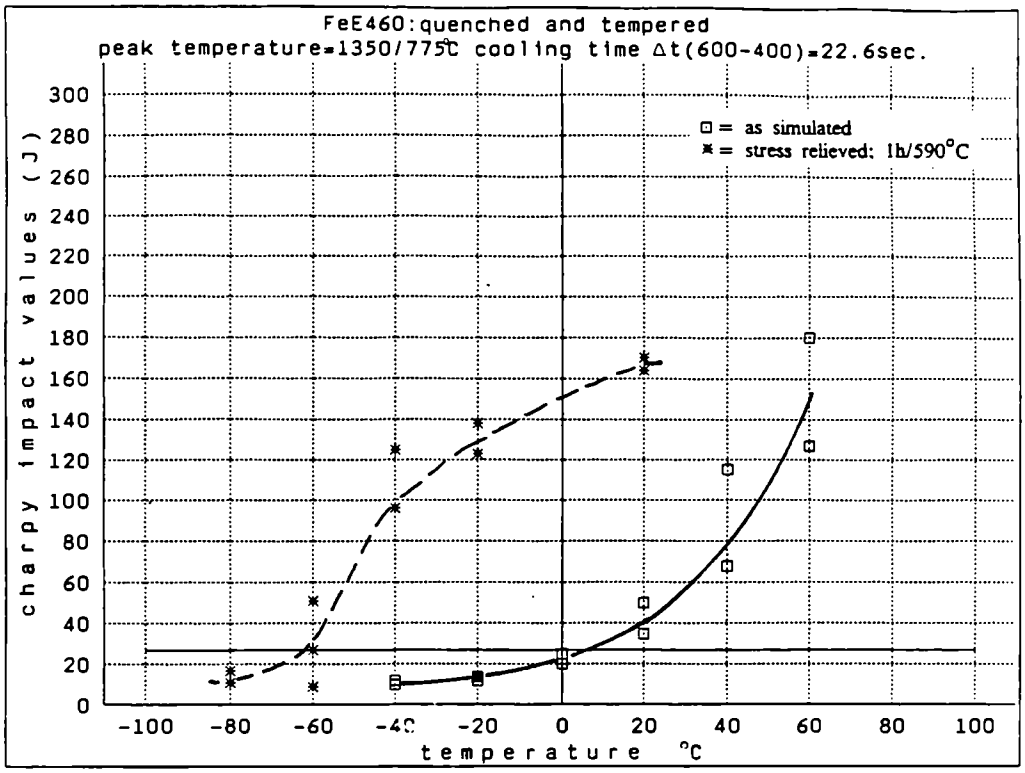

Fig. 4.81 Charpy-V fracture energies of simulated specimens. Material QT, Tp1 = 1350°C and Tp2 = 775°C, Δt (600-400) 22.6 sec.
□: as simulated *: + PWHT (1h 590°C)

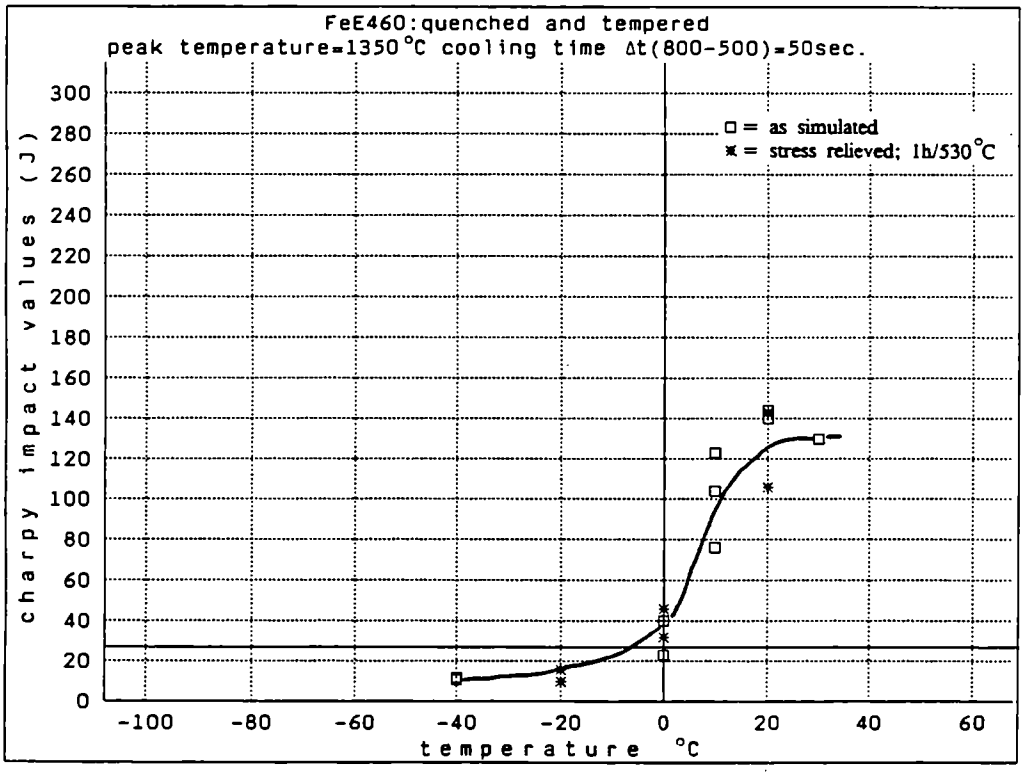

Fig. 4.82 Charpy-V fracture energies of simulated specimens. Material QT, Tp = 1350°C, Δt (800-500) 50 sec.
□: as simulated *: + PWHT (1h 530°C)

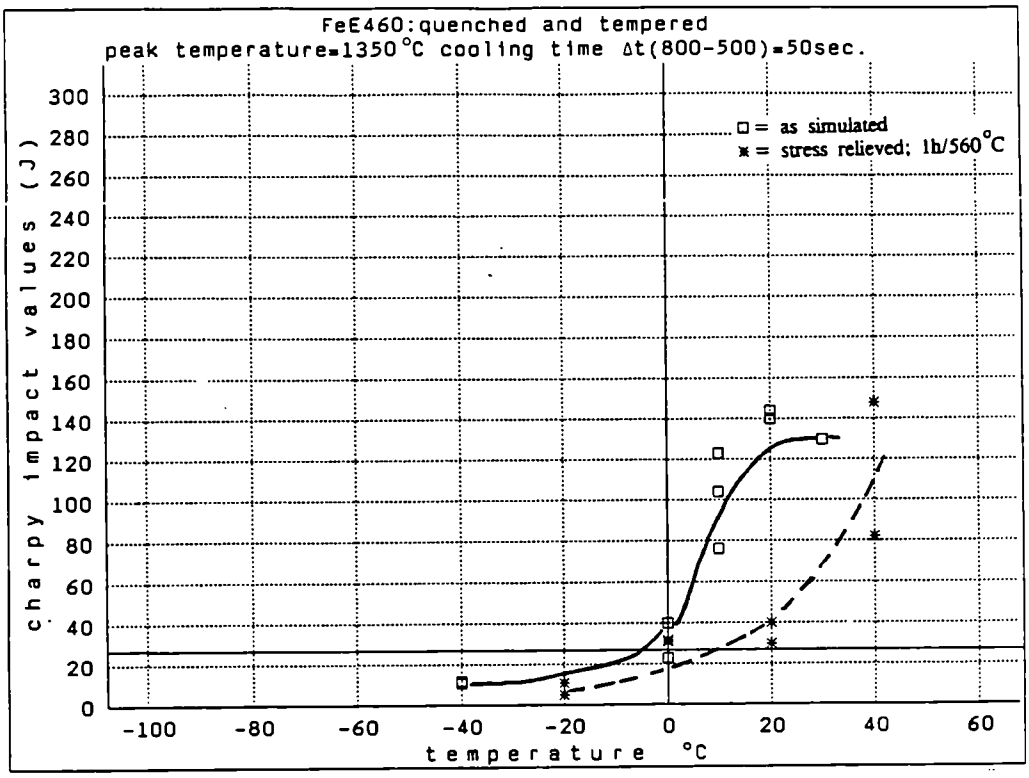

Fig. 4.83 Charpy-V fracture energies of simulated specimens.
Material QT, Tp = 1350°C, Δt (800-500) 50 sec.
□: as simulated *: + PWHT (1h 560°C)

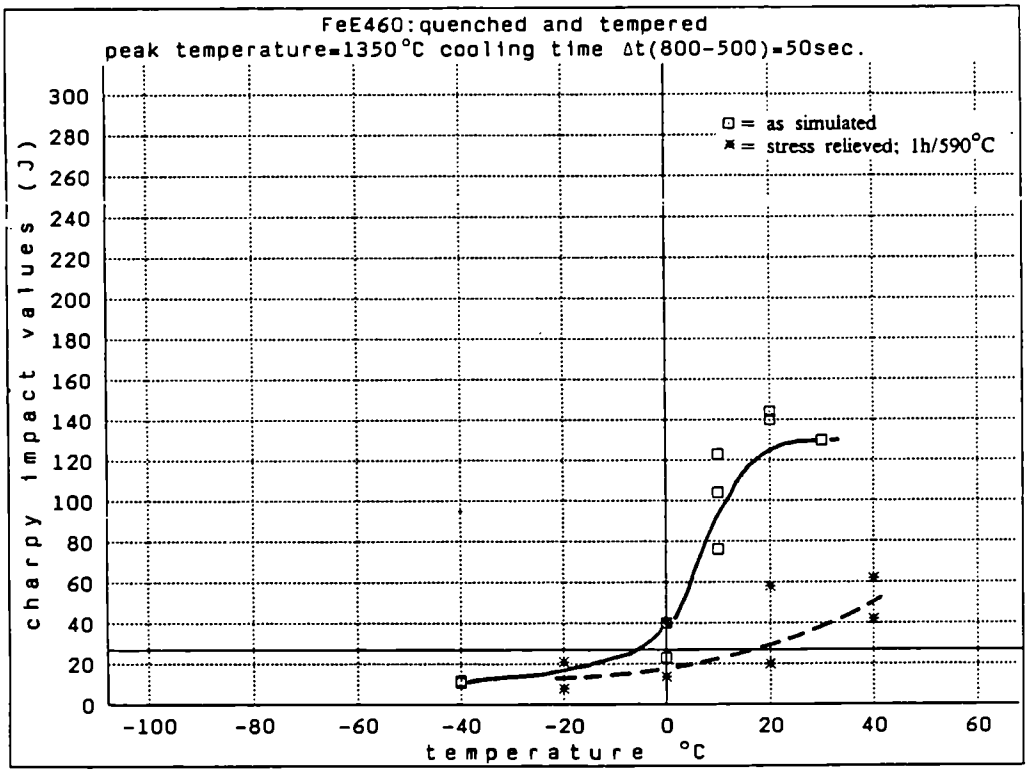

Fig. 4.84 Charpy-V fracture energies of simulated specimens.
Material QT, Tp = 1350°C, Δt (800-500) 50 sec.
□: as simulated *: + PWHT (1h 590°C)

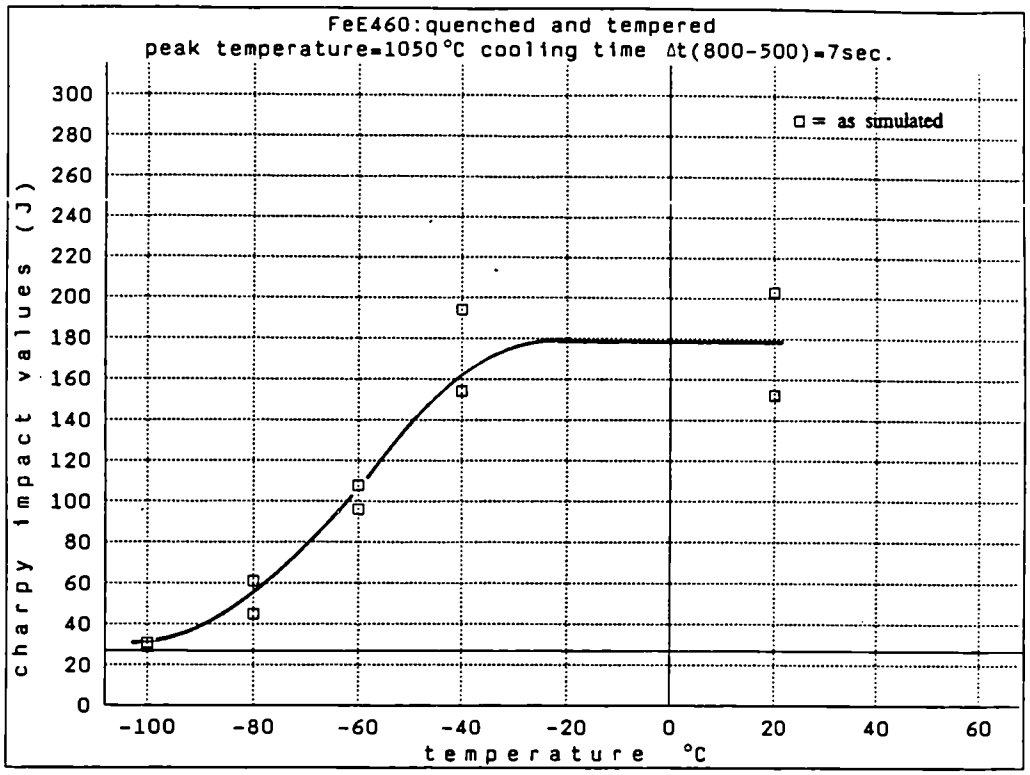

Fig. 4.85 Charpy-V fracture energies of simulated specimens. Material QT, Tp = 1050°C, Δt (800-500) 7 sec. □: as simulated

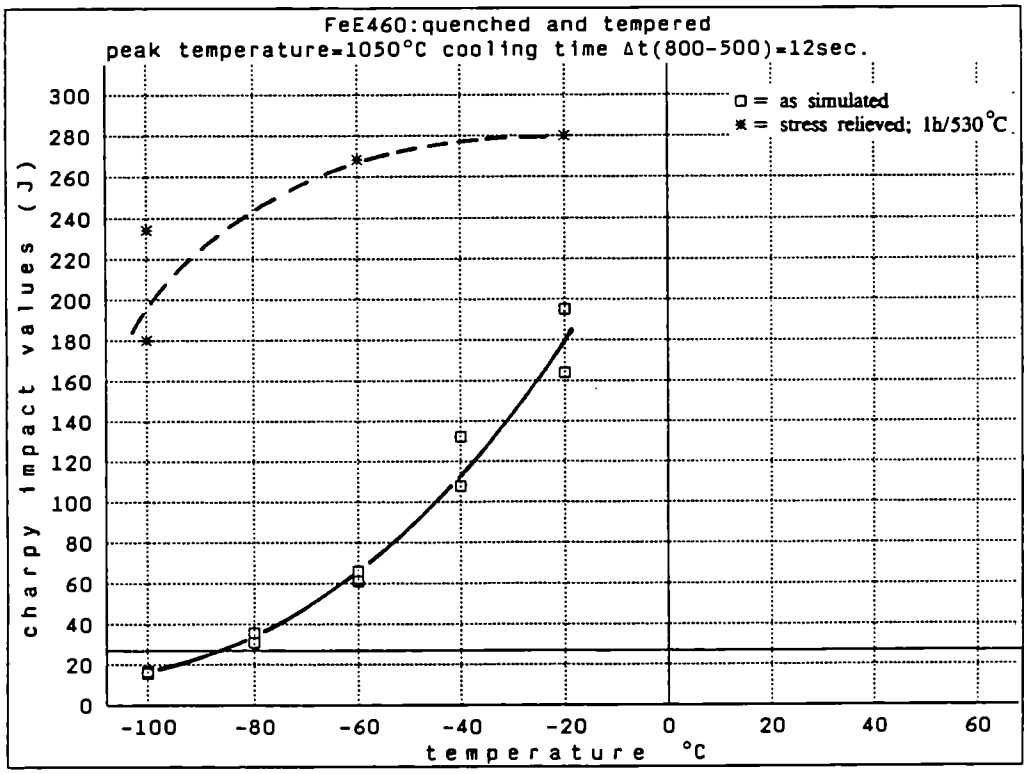

Fig. 4.86 Charpy-V fracture energies of simulated specimens. Material QT, Tp = 1050°C, Δt (800-500) 12 sec. □: as simulated *: + PWHT (1h 530°C)

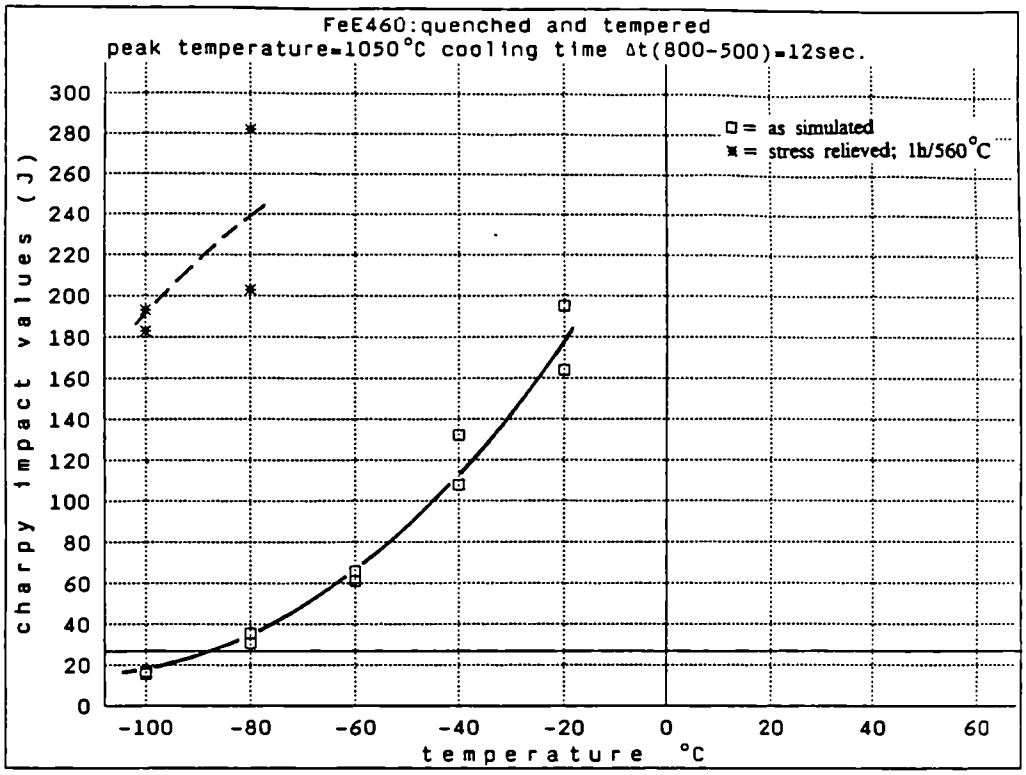

Fig. 4.87 Charpy-V fracture energies of simulated specimens. Material QT, Tp = 1050°C, Δt (800-500) 12 sec. □: as simulated *: + PWHT (1h 560°C)

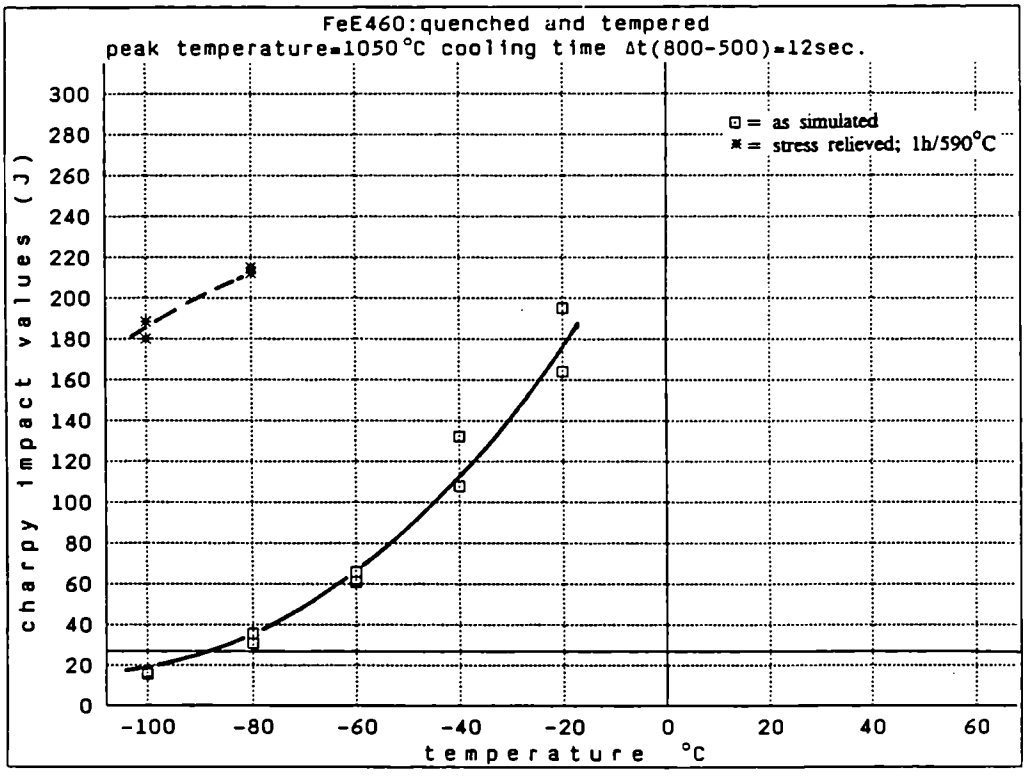

Fig. 4.88 Charpy-V fracture energies of simulated specimens. Material QT, Tp = 1050°C, Δt (800-500) 12 sec. □: as simulated *: + PWHT (1h 590°C)

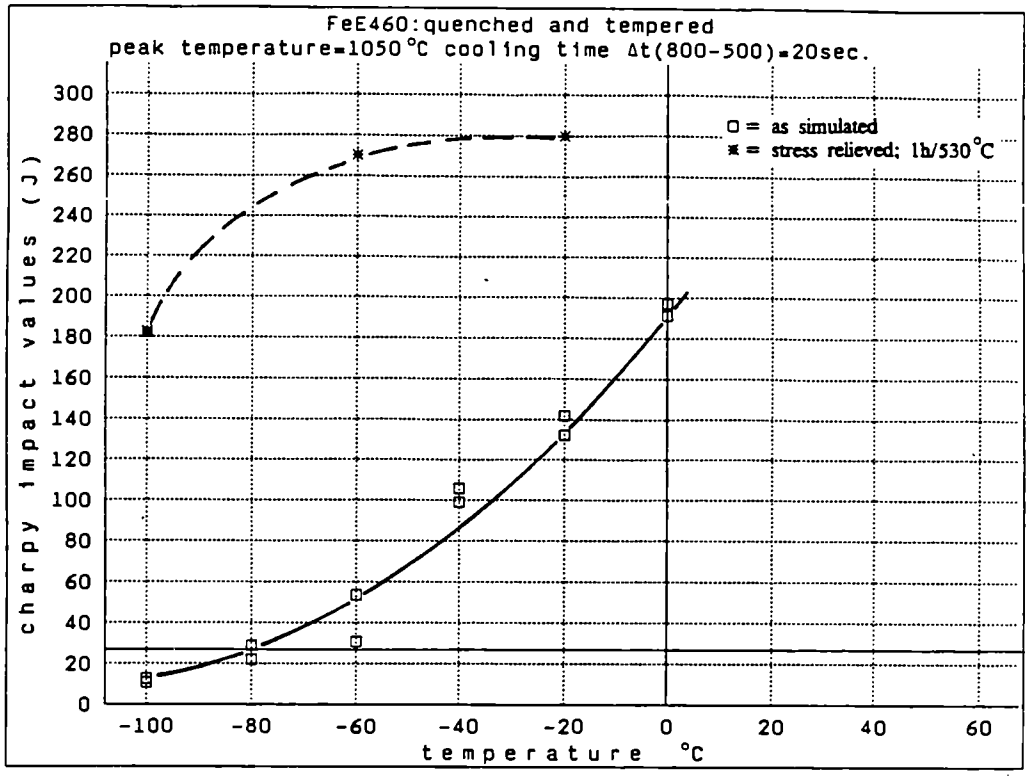

Fig. 4.89 Charpy-V fracture energies of simulated specimens. Material QT, Tp = 1050°C, Δt (800-500) 20 sec. □: as simulated *: + PWHT (1h 530°C)

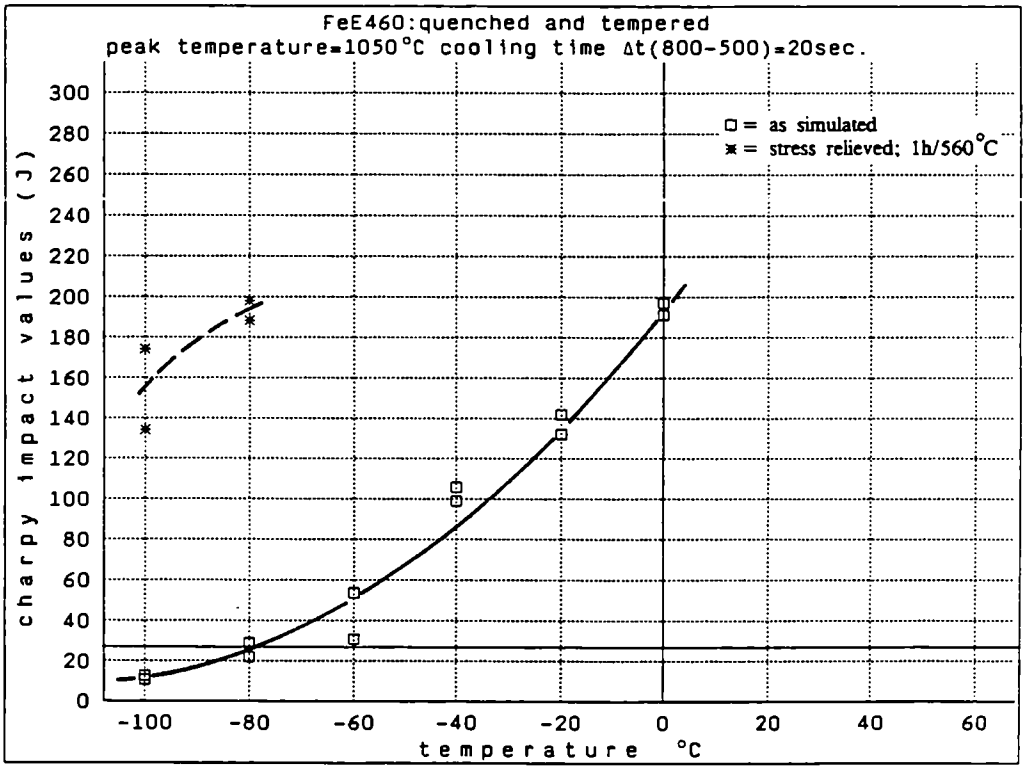

Fig. 4.90 Charpy-V fracture energies of simulated specimens. Material QT, Tp = 1050°C, Δt (800-500) 20 sec. □: as simulated *: + PWHT (1h 560°C)

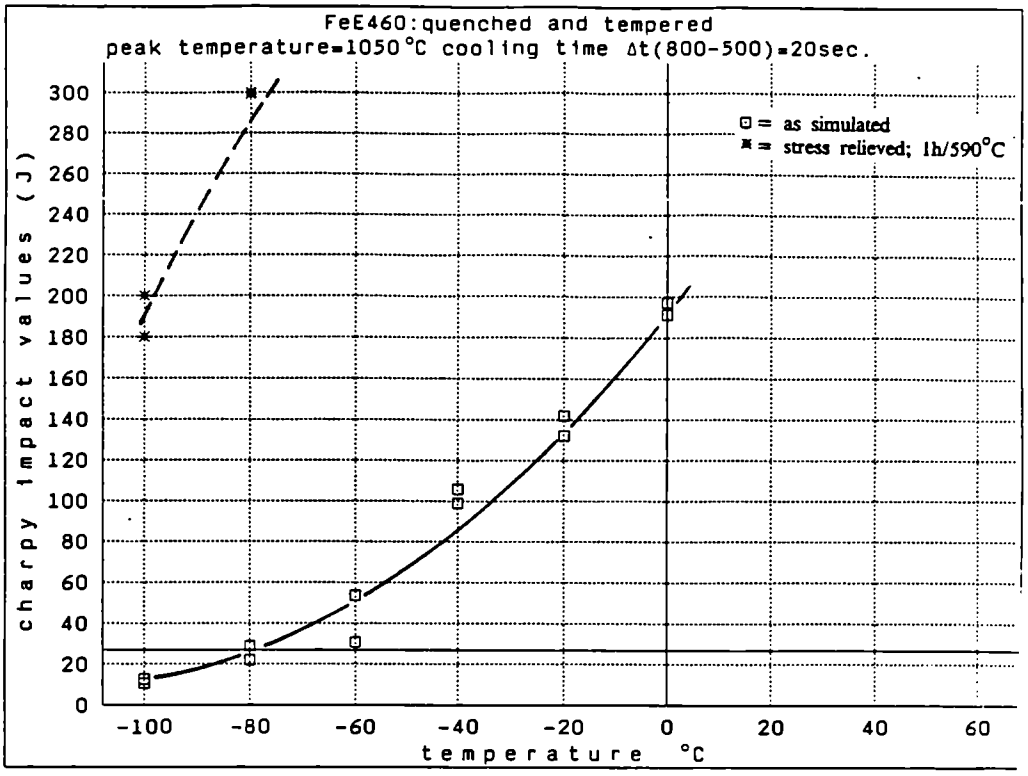

Fig. 4.91 Charpy-V fracture energies of simulated specimens. Material QT, Tp = 1050°C, Δt (800-500) 20 sec. □: as simulated *: + PWHT (1h 590°C)

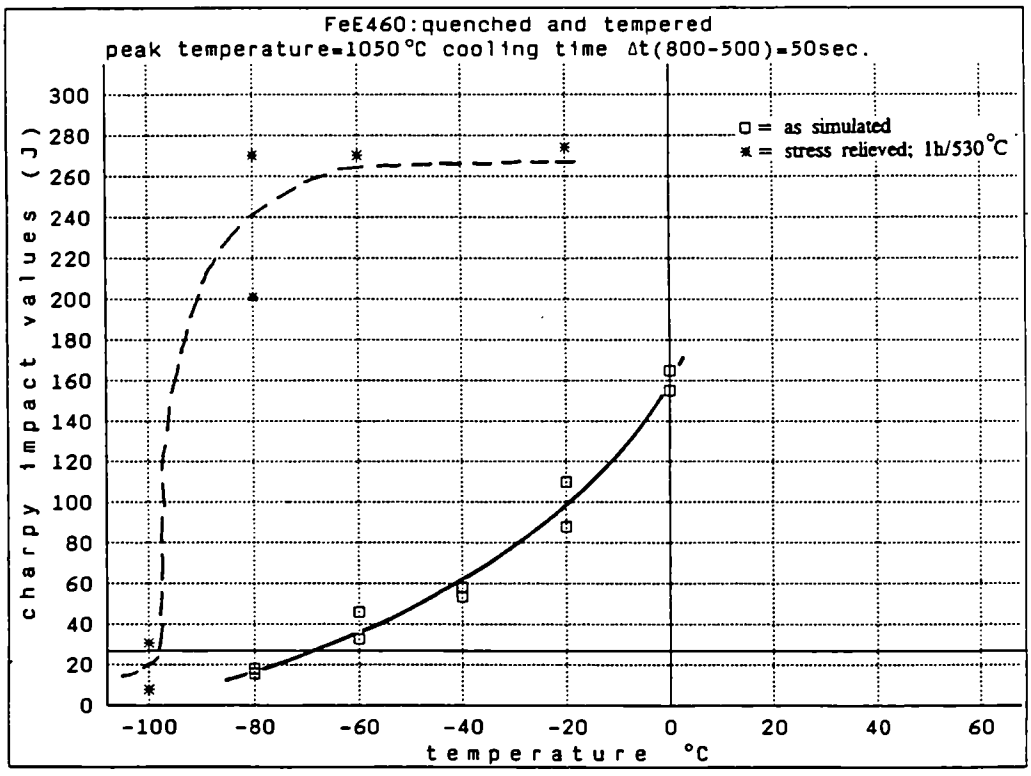

Fig. 4.92 Charpy-V fracture energies of simulated specimens. Material QT, Tp = 1050°C, Δt (800-500) 50 sec. □: as simulated *: + PWHT (1h 530°C)

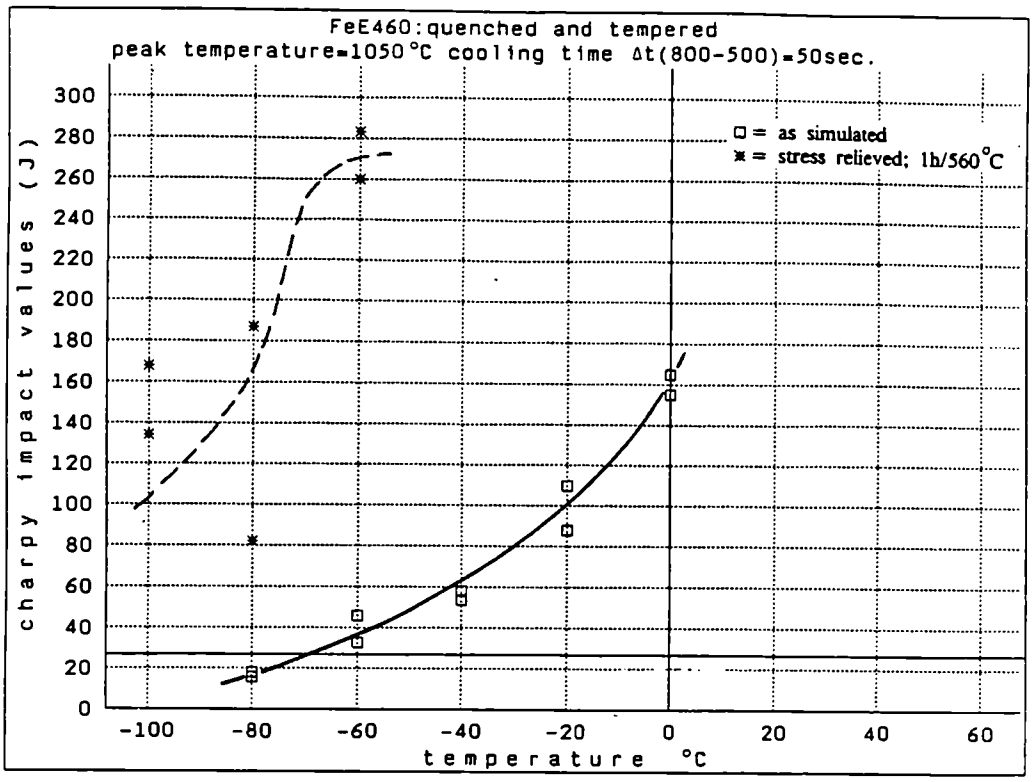

Fig. 4.93 Charpy-V fracture energies of simulated specimens.
Material QT, Tp = 1050°C, Δt (800-500) 50 sec.
□: as simulated *: + PWHT (1h 560°C)

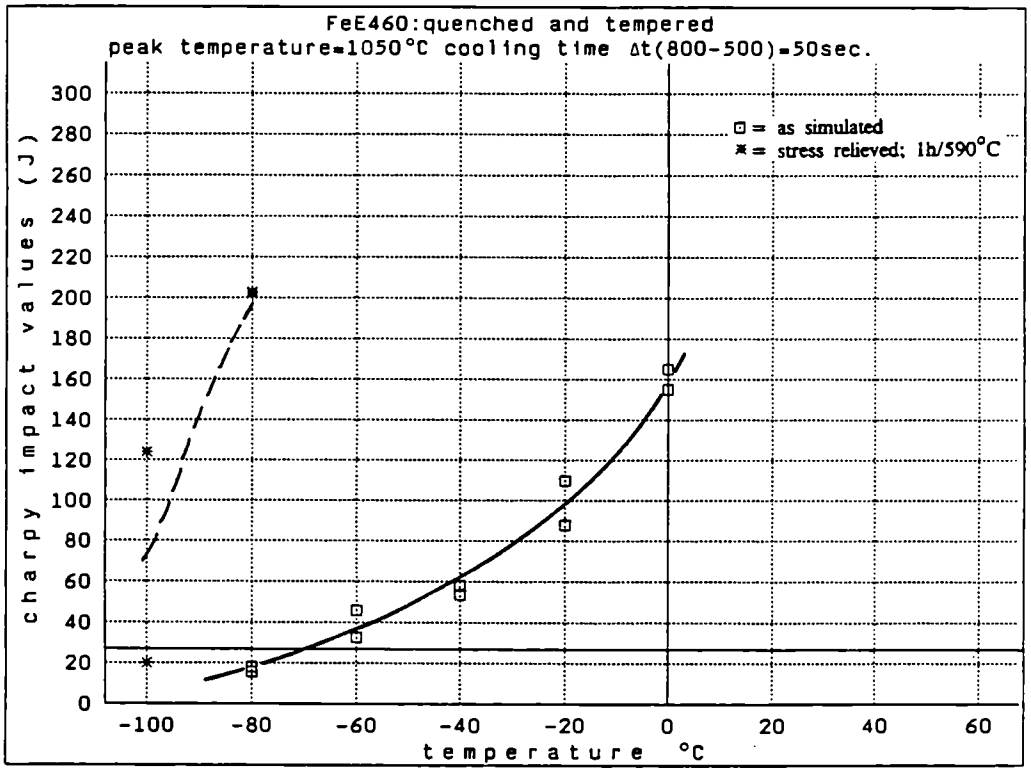

Fig. 4.94 Charpy-V fracture energies of simulated specimens.
Material QT, Tp = 1050°C, Δt (800-500) 50 sec.
□: as simulated *: + PWHT (1h 590°C)

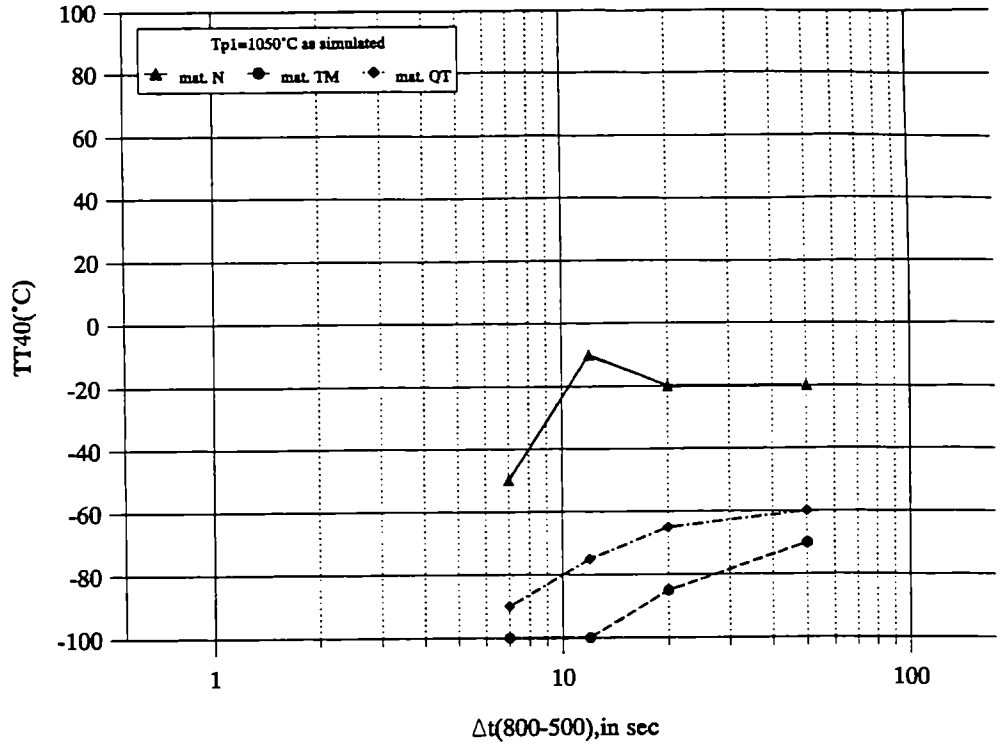

Fig. 4.95 The TT40 of the three at 1050°C simulated materials as a function of the cooling rate Δt (800-500)

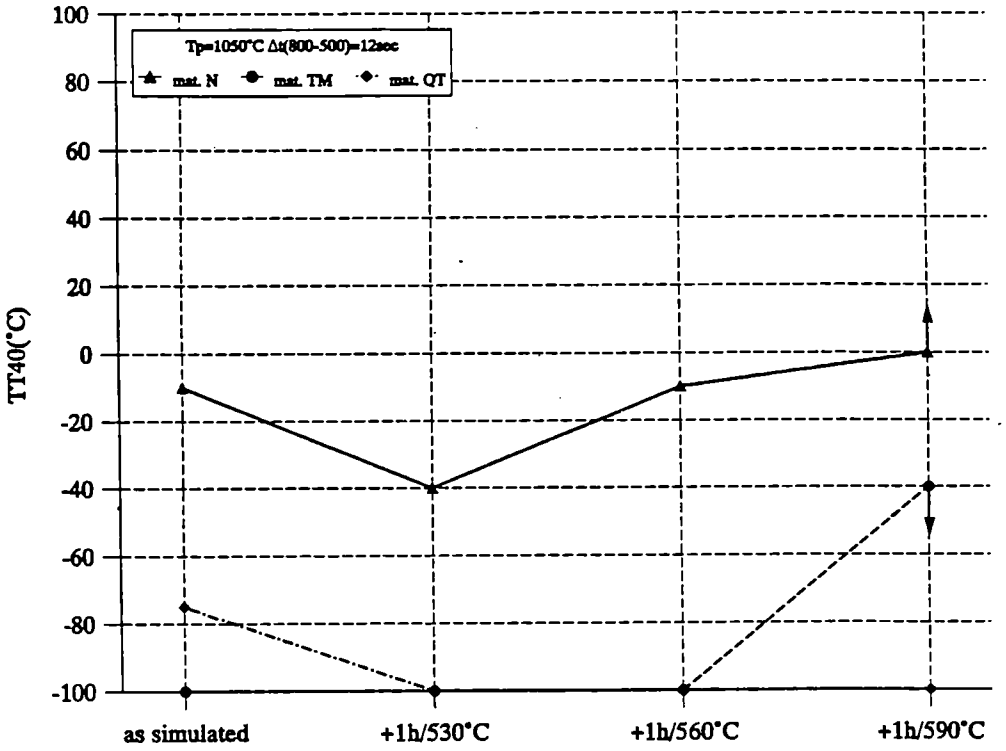

Fig. 4.96 The TT40 temperatures of the three simulated materials (at Tp1 = 1050°C and Δt (800-500) = 12 sec.)in the as simulated condition and after PWHT

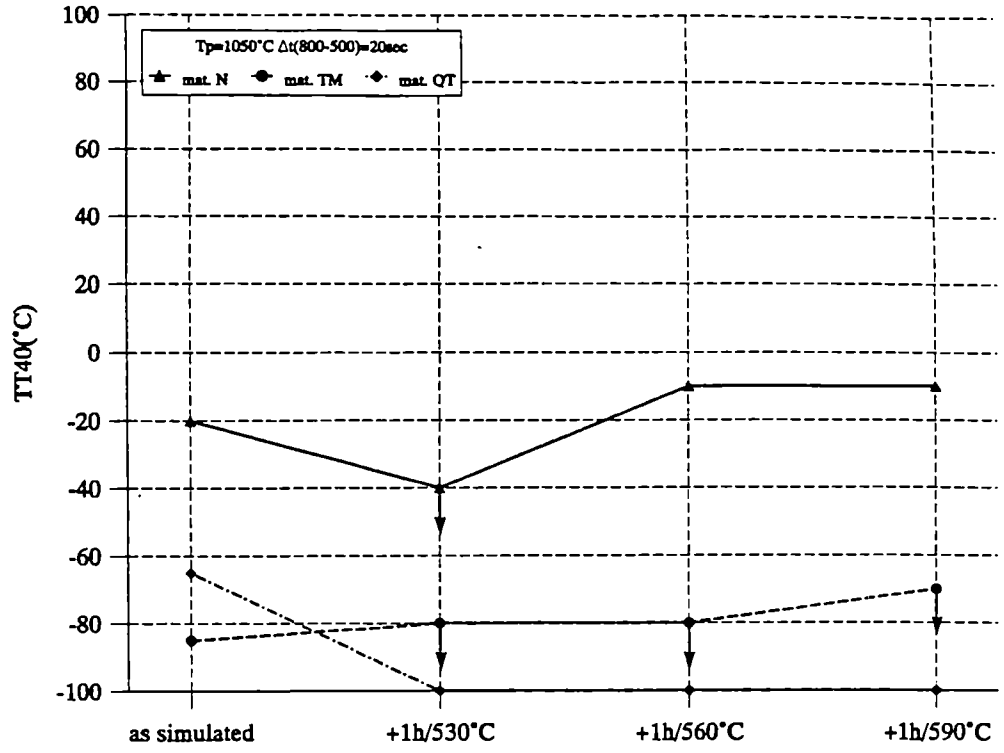

Fig. 4.97 The TT40 temperatures of the three simulated materials (at Tp1 = 1050°C and Δt (800-500) = 20 sec.) in the as simulated condition and after PWHT

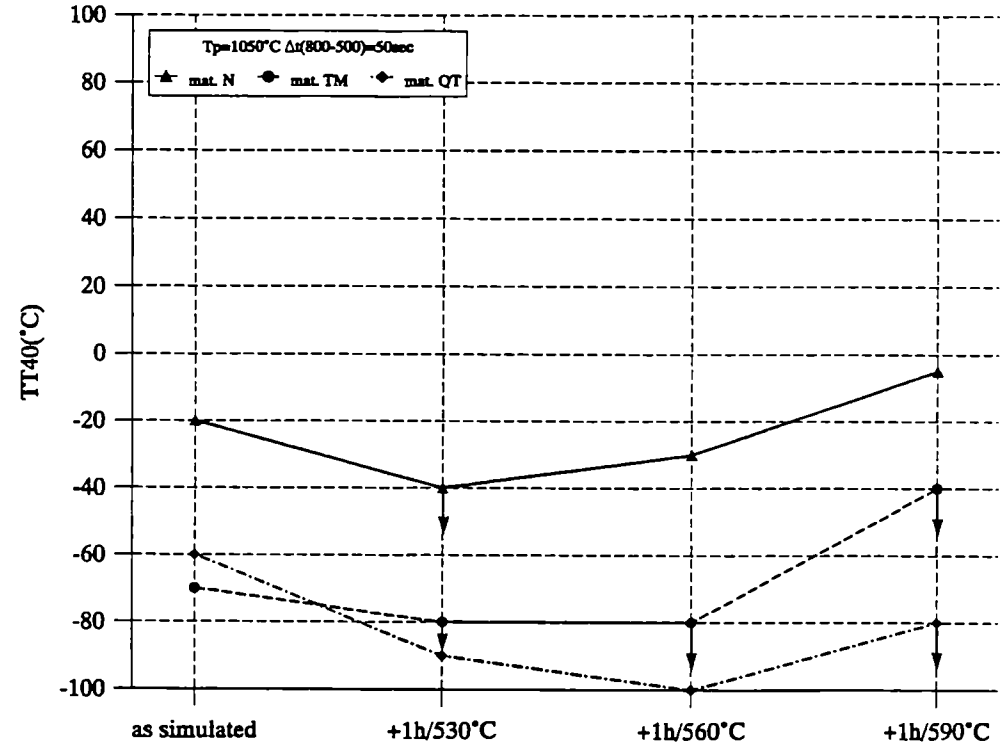

Fig. 4.98 The TT40 temperatures of the three simulated materials (at Tp1 = 1050°C and Δt (800-500) = 50 sec.) in the as simulated condition and after PWHT

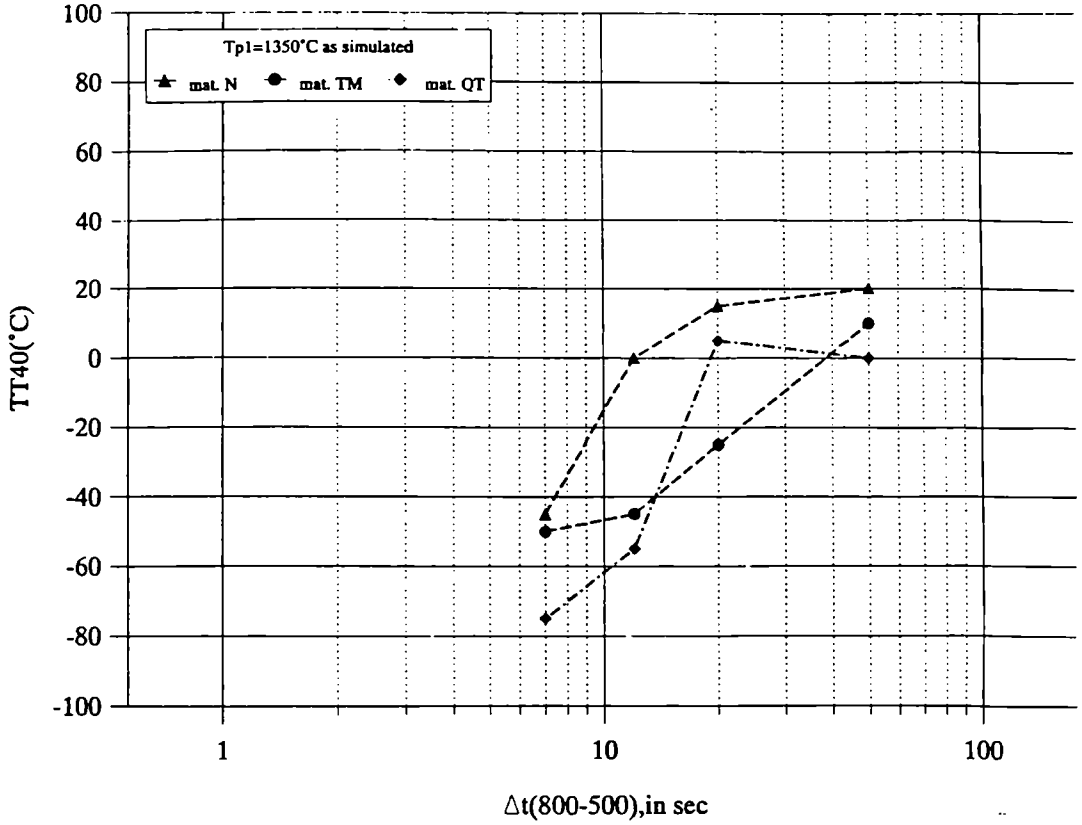

Fig. 4.99 The TT40 temperatures of the three at 1350°C simulated materials as a function of the cooling rate Δt (800-500)

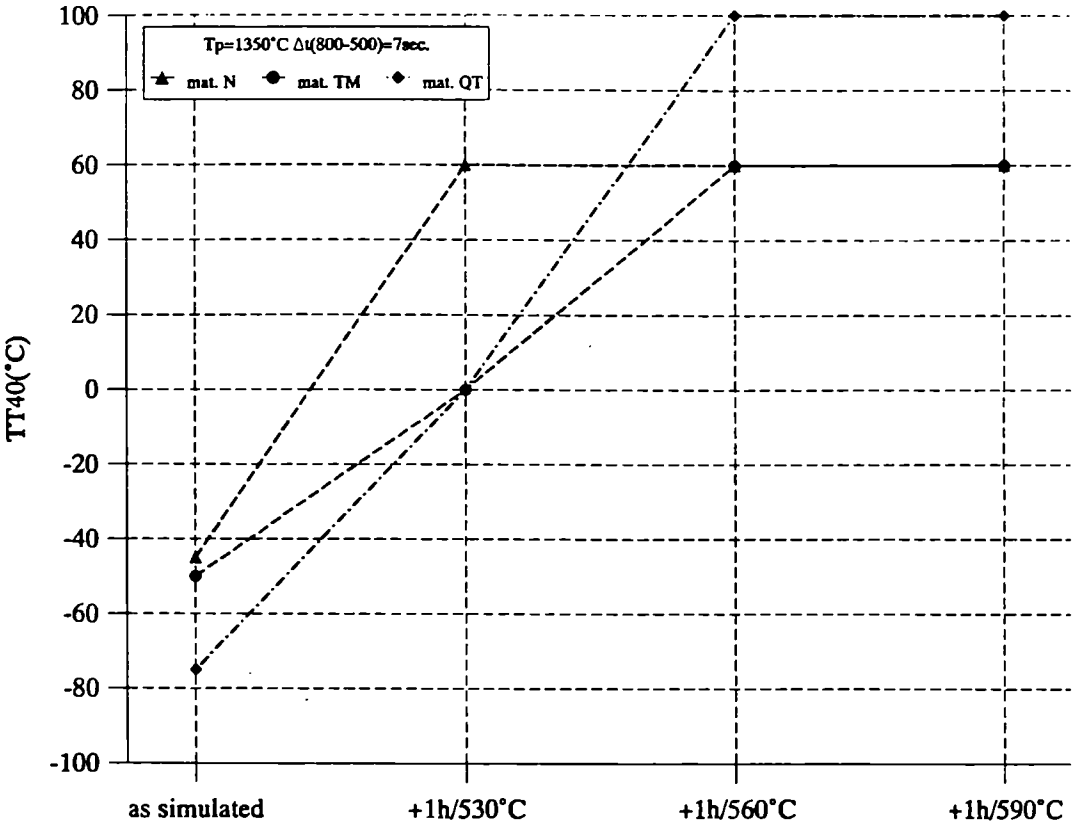

Fig. 4.100 The TT40 temperatures of the three at 1350°C simulated materials (at Tp1 = 1350°C and Δt (800-500) = 7 sec.) in the as simulated condition and after PWHT

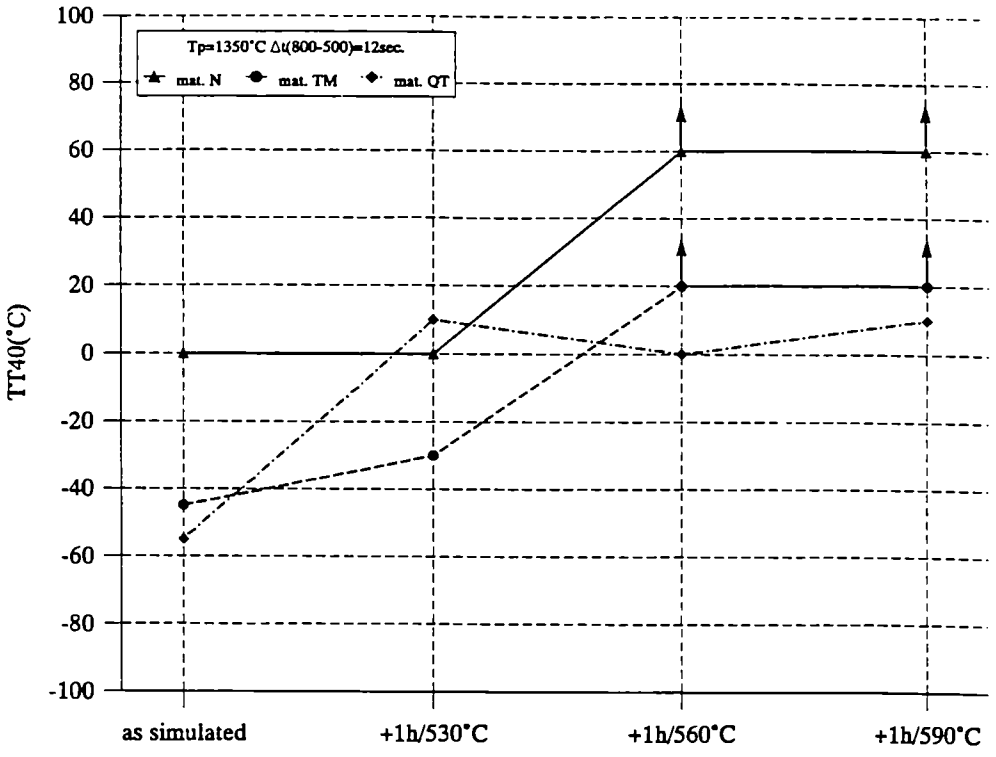

Fig. 4.101 The TT40 temperatures of the three simulated materials (at Tp1 = 1350°C and Δt (800-500) = 12 sec.) in the as simulated condition and after PWHT

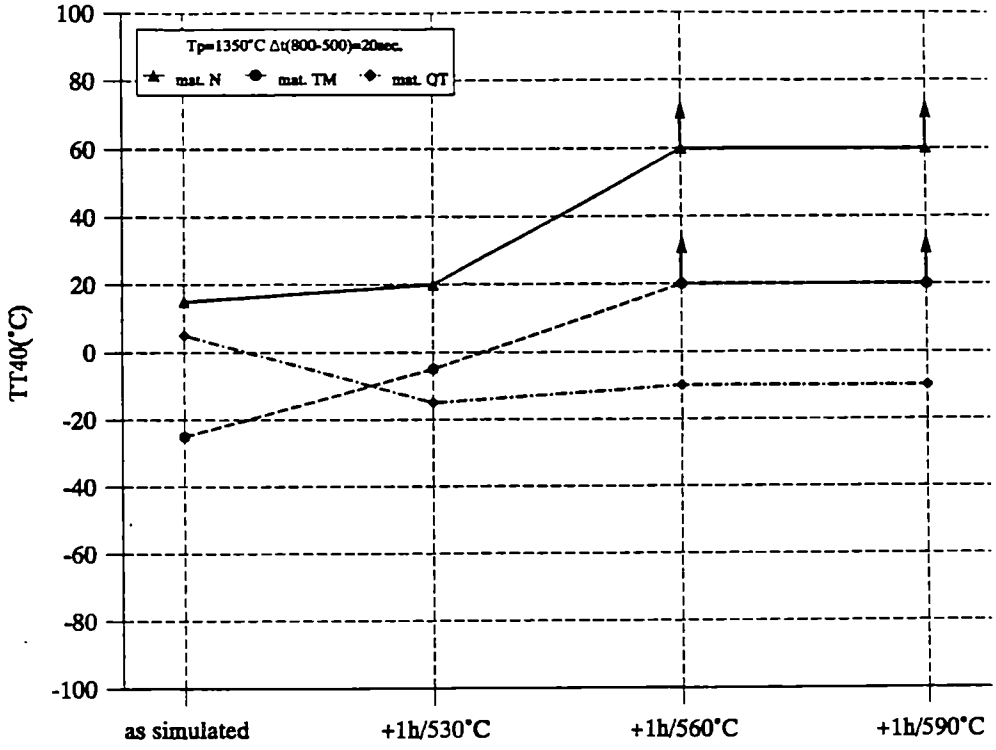

Fig. 4.102 The TT40 temperatures of the three simulated materials (at Tp1 = 1350°C and Δt (800-500) = 20 sec.) in the as simulated condition and after PWHT

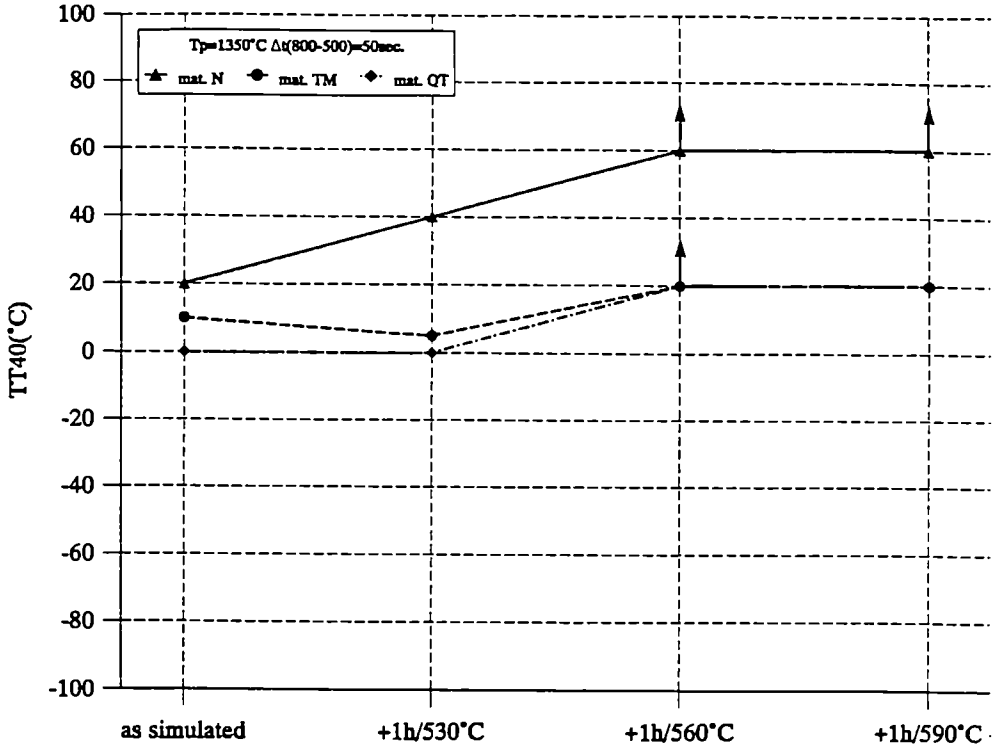

Fig. 4.103 The TT40 temperatures of the three simulated materials (at Tp1 = 1350°C and Δt (800-500) = 50 sec.) in the as simulated condition and after PWHT

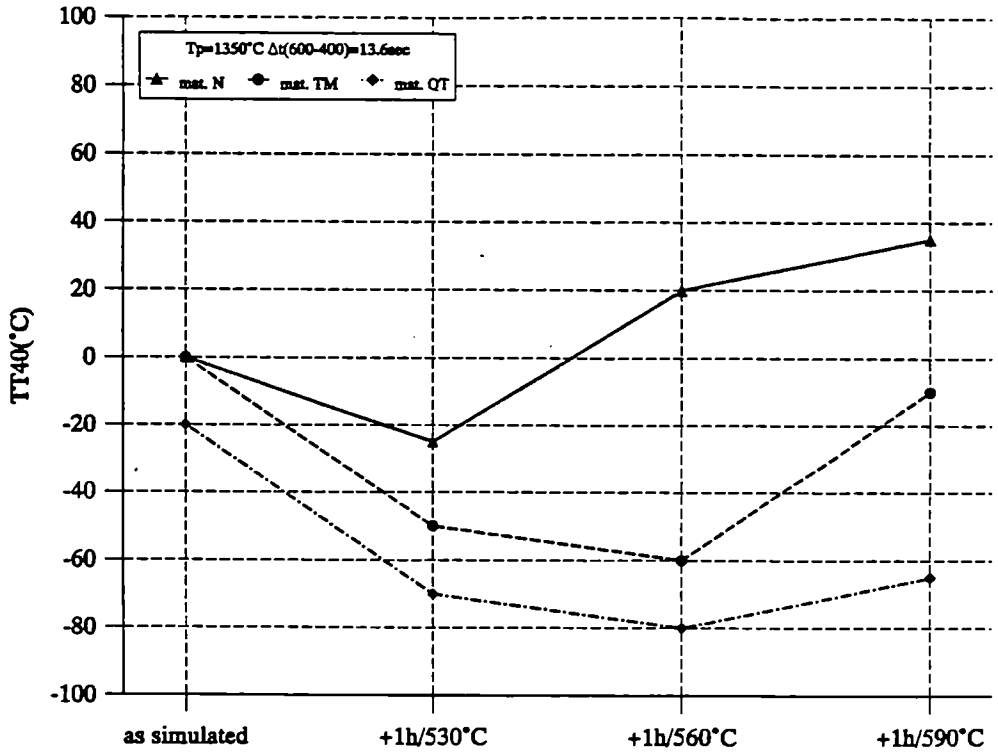

Fig. 4.104 The TT40 temperatures of the three simulated materials (with Tp1 = 1350°C Tp2 = 775°C and Δt (800-500) = 13.6 sec.) in the as simulated condition and after PWHT

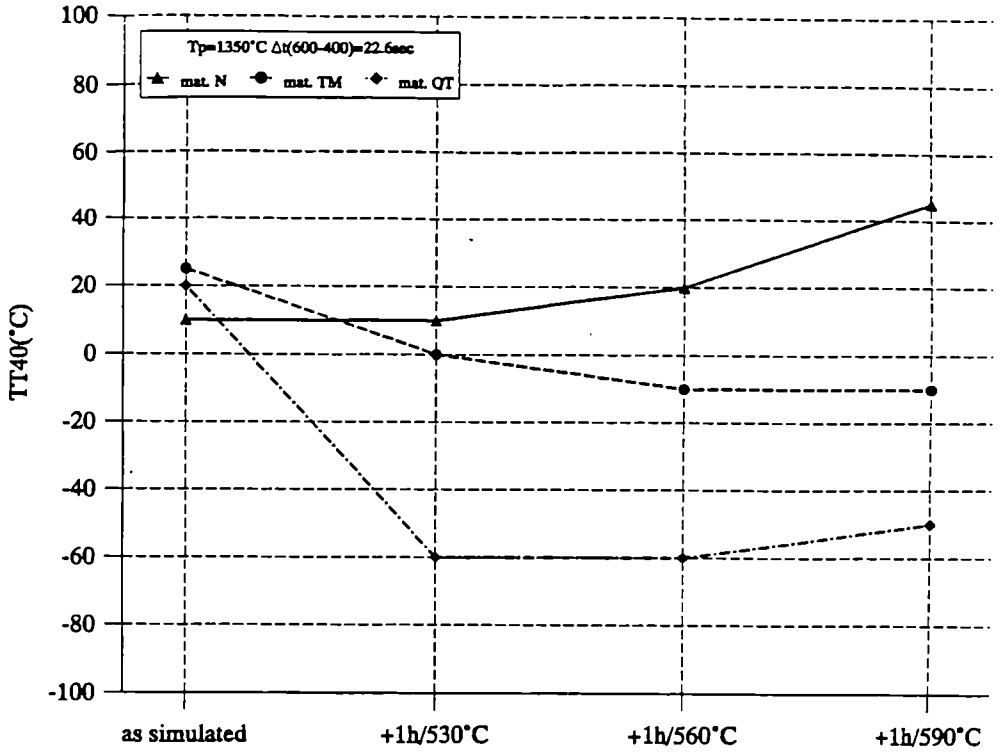

Fig. 4.105 The TT40 temperatures of the three simulated materials (with Tp1 = 1350°C Tp2 = 775°C and Δt (800-500) = 22.6 sec.) in the as simulated condition and after PWHT

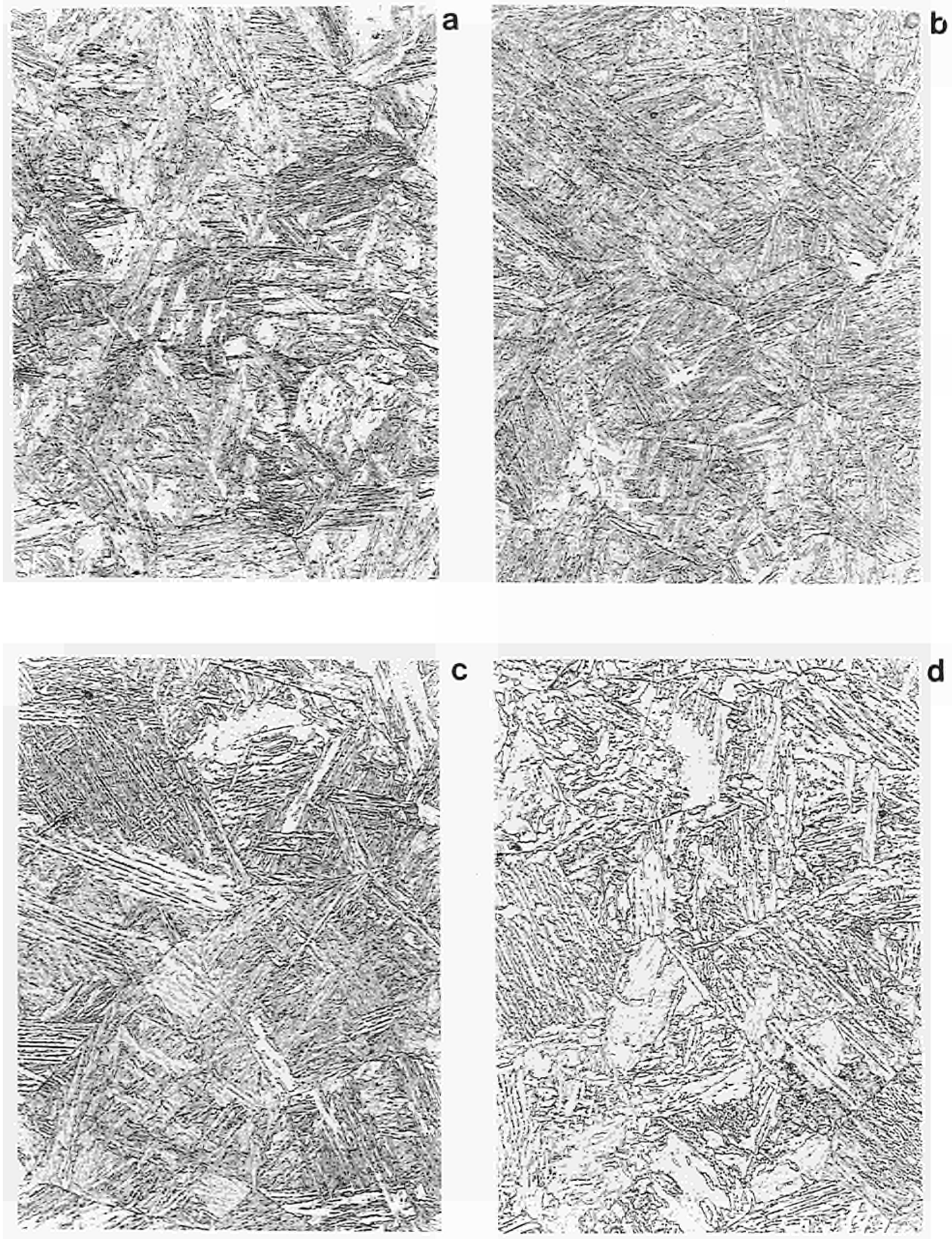

Fig. 4.106 Microstructure of simulated specimens of material N
a: Δt(800-500) = 7 sec. b: Δt(800-500) = 12 sec.
c: Δt(800-500) = 20 sec. d: Δt(800-500) = 50 sec.
M=x500

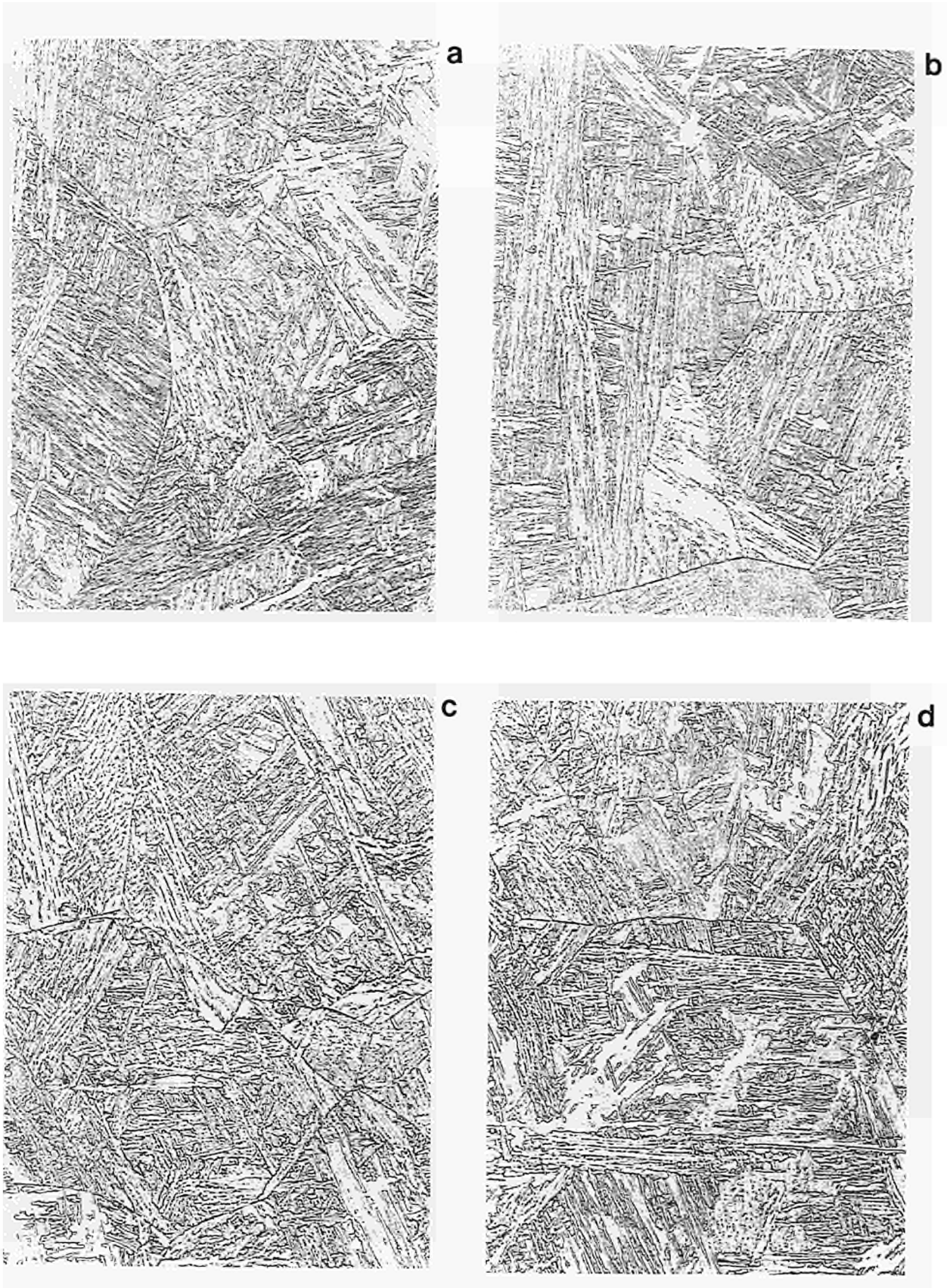

Fig. 4.107 Microstructure of simulated specimens of material TM
a: $\Delta t(800-500)$ = 7 sec. b: $\Delta t(800-500)$ = 12 sec.
c: $\Delta t(800-500)$ = 20 sec. d: $\Delta t(800-500)$ = 50 sec.
M=x500

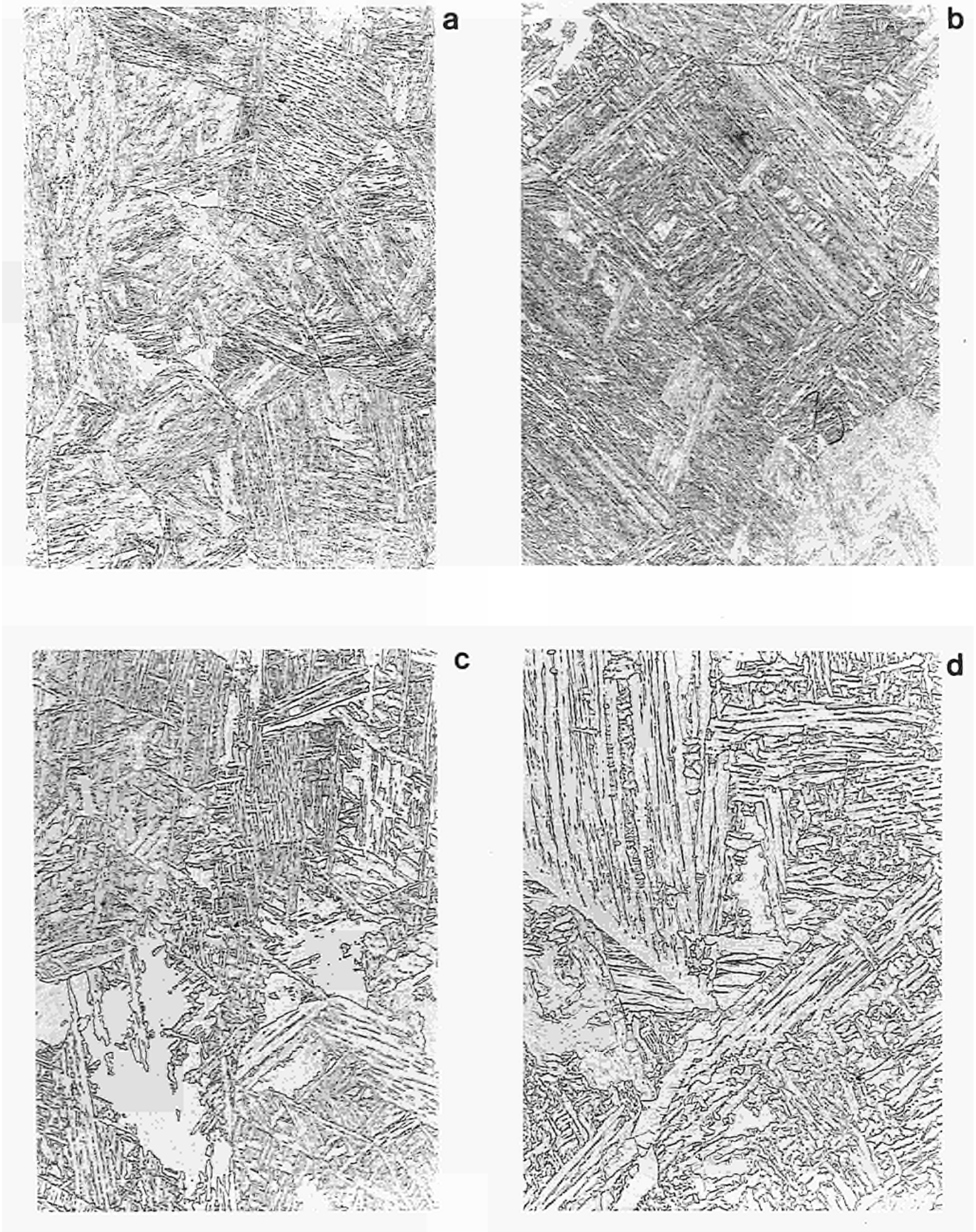

Fig. 4.108 Microstructure of simulated specimens of material QT
a: $\Delta t(800\text{-}500)$ = 7 sec. b: $\Delta t(800\text{-}500)$ = 12 sec.
c: $\Delta t(800\text{-}500)$ = 20 sec. d: $\Delta t(800\text{-}500)$ = 50 sec.
M=x500

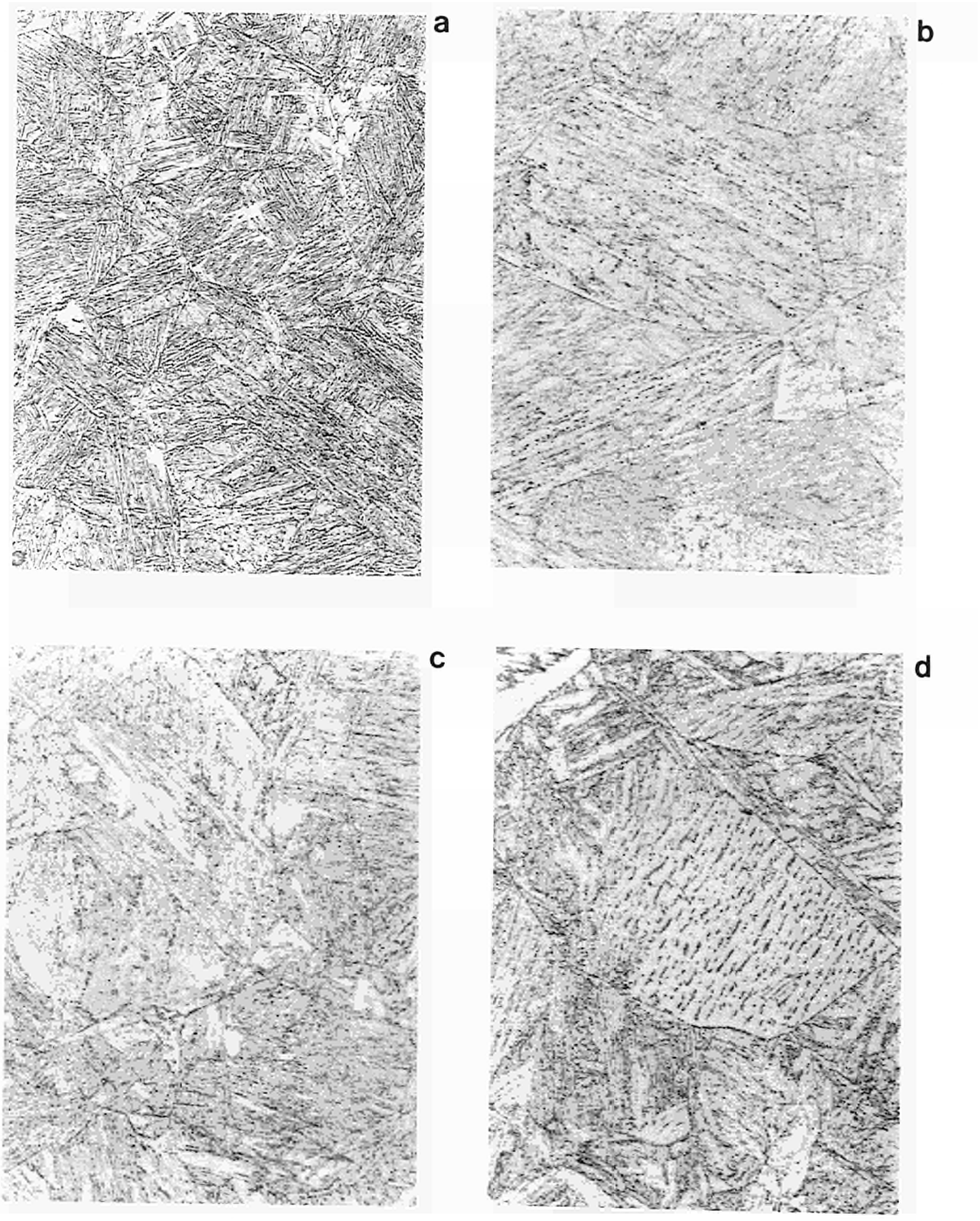

Fig. 4.109 Microstructure of simulated specimens of material N
Simulation conditions: 1350°C/12 sec.
a: as simulated
b: +1h 530°C
c: + 1h 560°C
d: +1h 590°C
a: M=x500
b-d: M=x1000

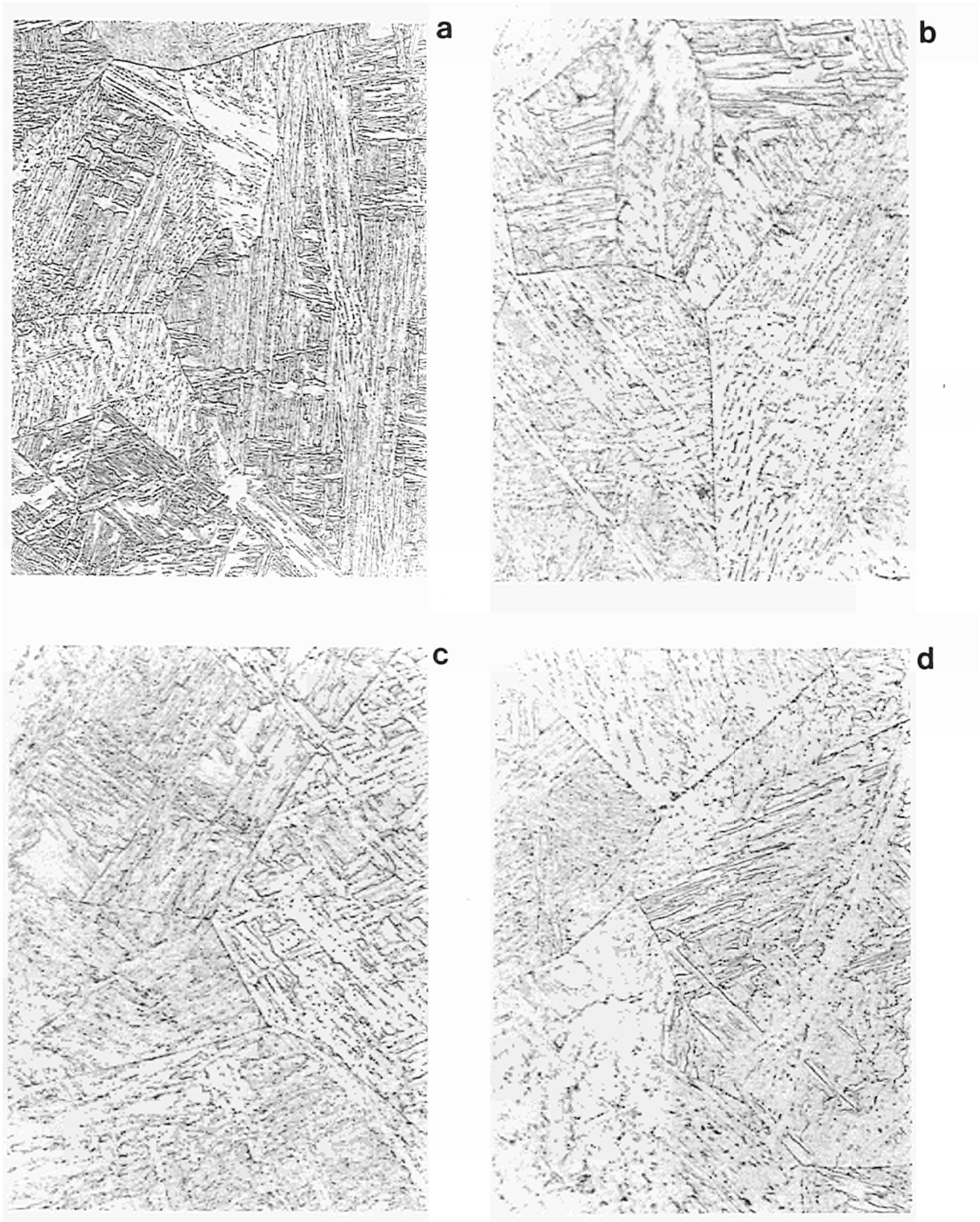

Fig. 4.110 Microstructure of simulated specimens of material TM
Simulation conditions: 1350°C/12 sec.
a: as simulated b: +1h 530°C
c: + 1h 560°C d: +1h 590°C
a: M=x500 b-d: M=x1000

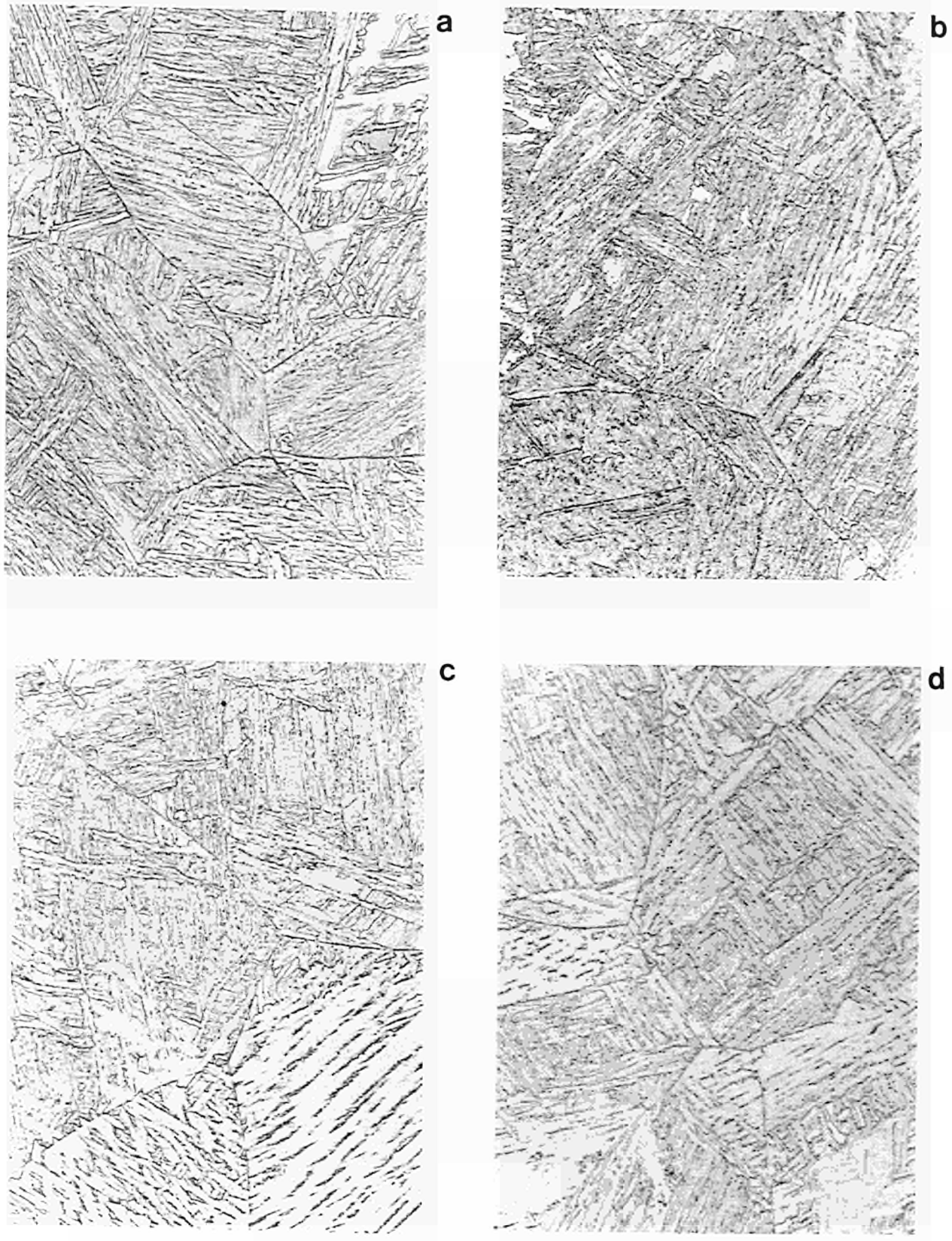

Fig. 4.111 Microstructure of simulated specimens of material QT
Simulation conditions: 1350°C/12 sec.
a: as simulated b: +1h 530°C
c: + 1h 560°C d: +1h 590°C
M=x1000

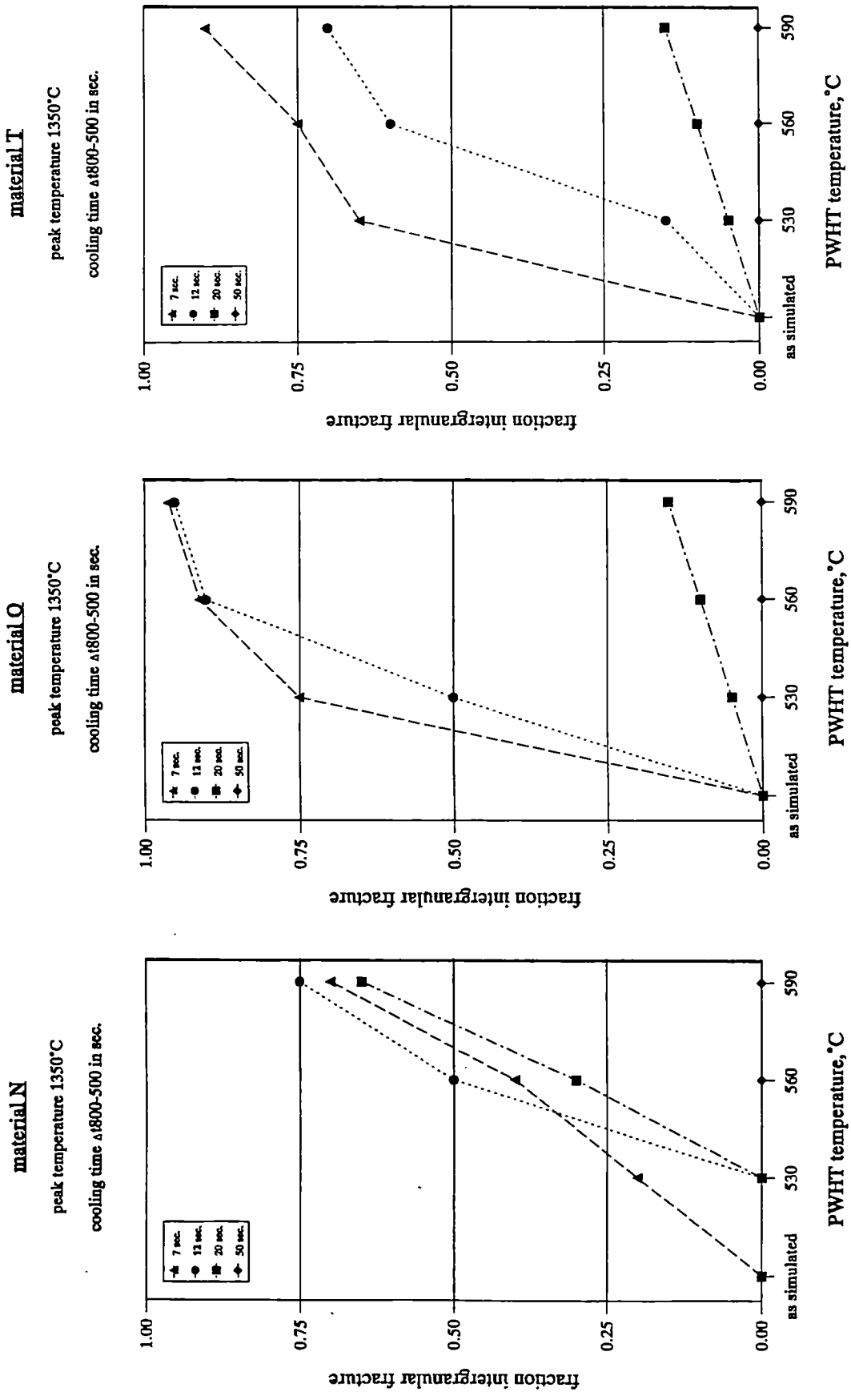

Fig. 4.112 The fraction intergranular fracture of the as simulated material (Tp = 1350°C) and the simulated + PWHT material, for different cooling times

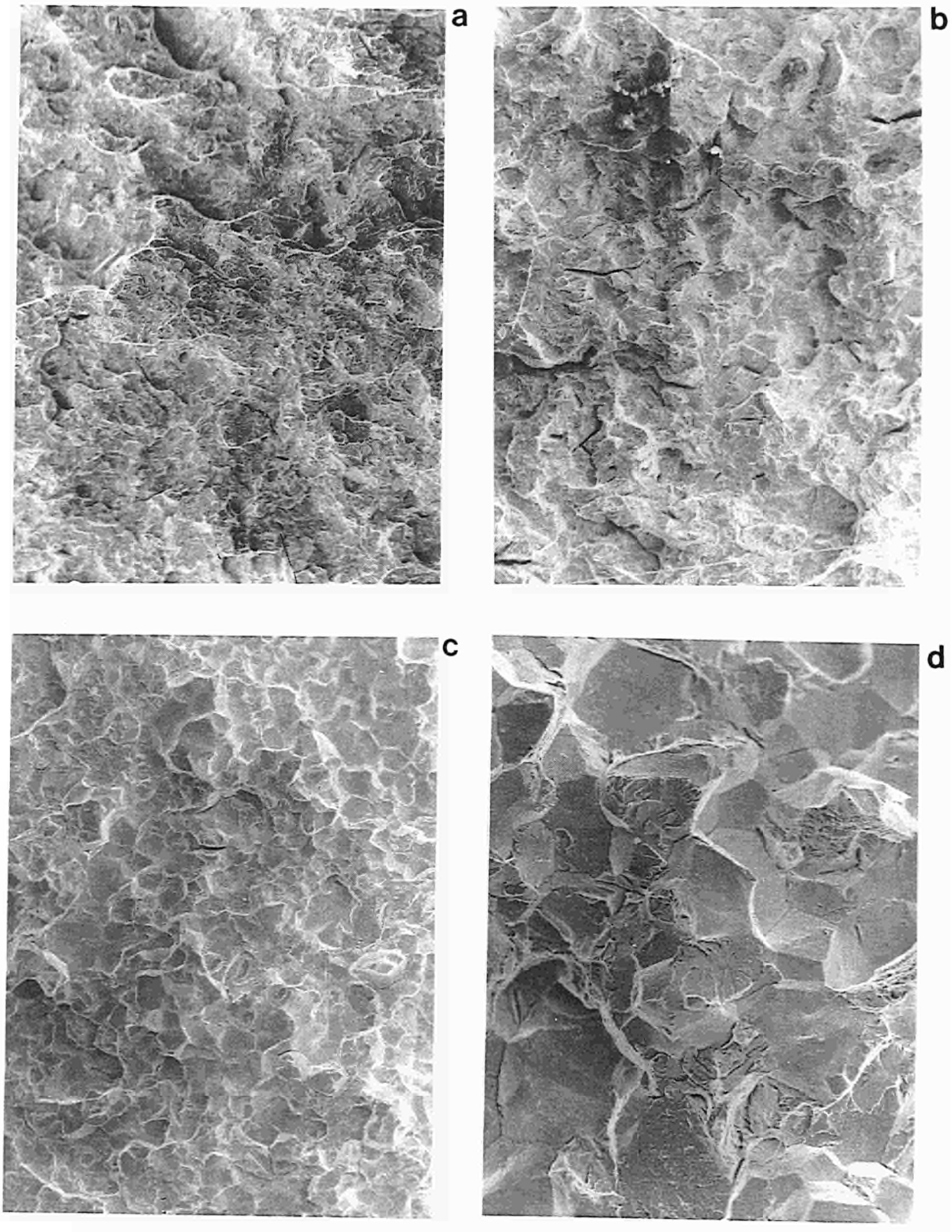

Fig. 4.113 SEM pictures of fracture surfaces of brittle broken Charpy-V specimens of material N
Simulation conditions: 1350°C/12 sec.
a: as simulated b: +1h 530°C
c,d: +1h 590°C

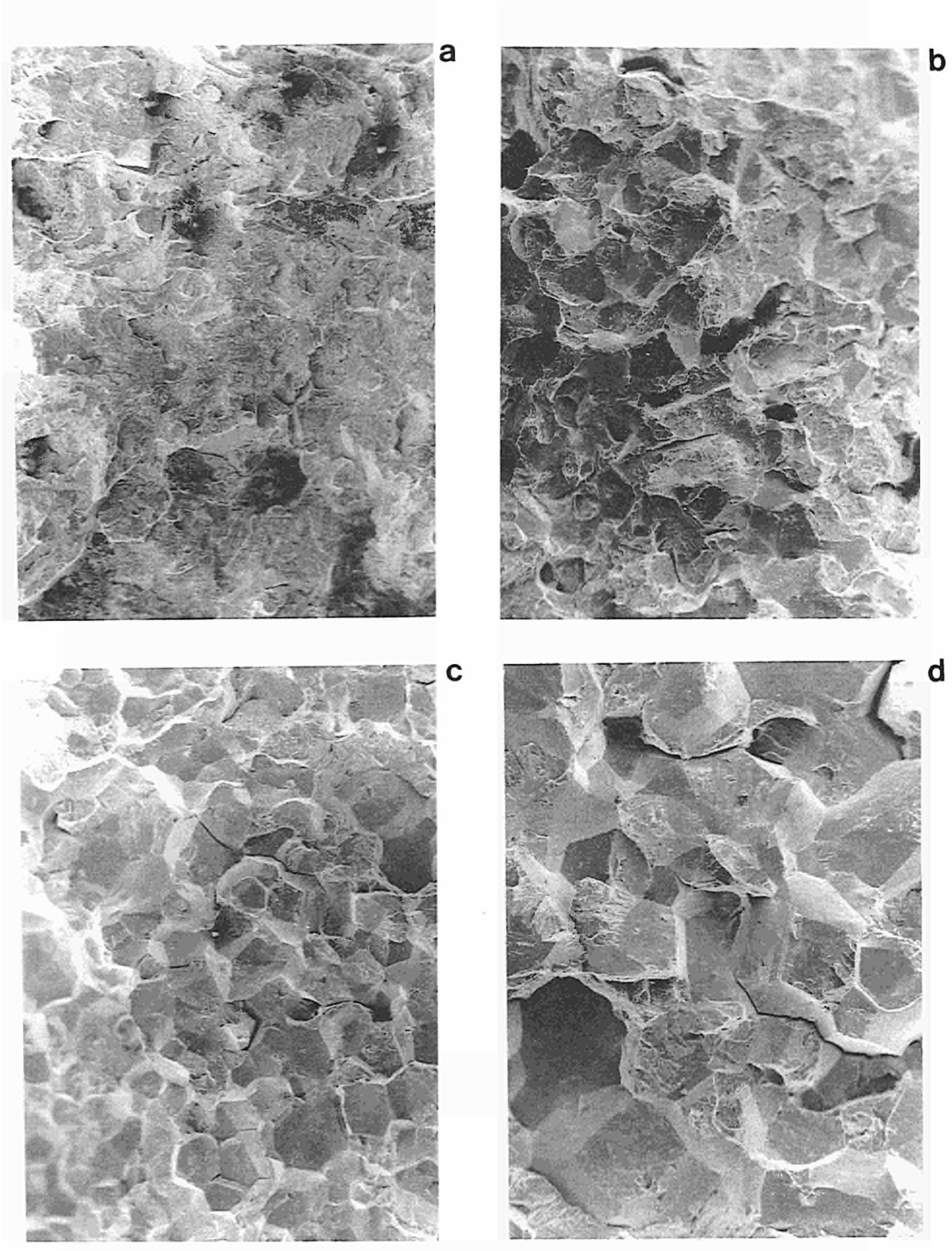

Fig. 4.114 SEM pictures of fracture surfaces of brittle broken Charpy-V specimens of material TM
Simulation conditions: 1350°C/12 sec.
a: as simulated b: +1h 530°C
c: +1h 560°C d: +1h 590°C

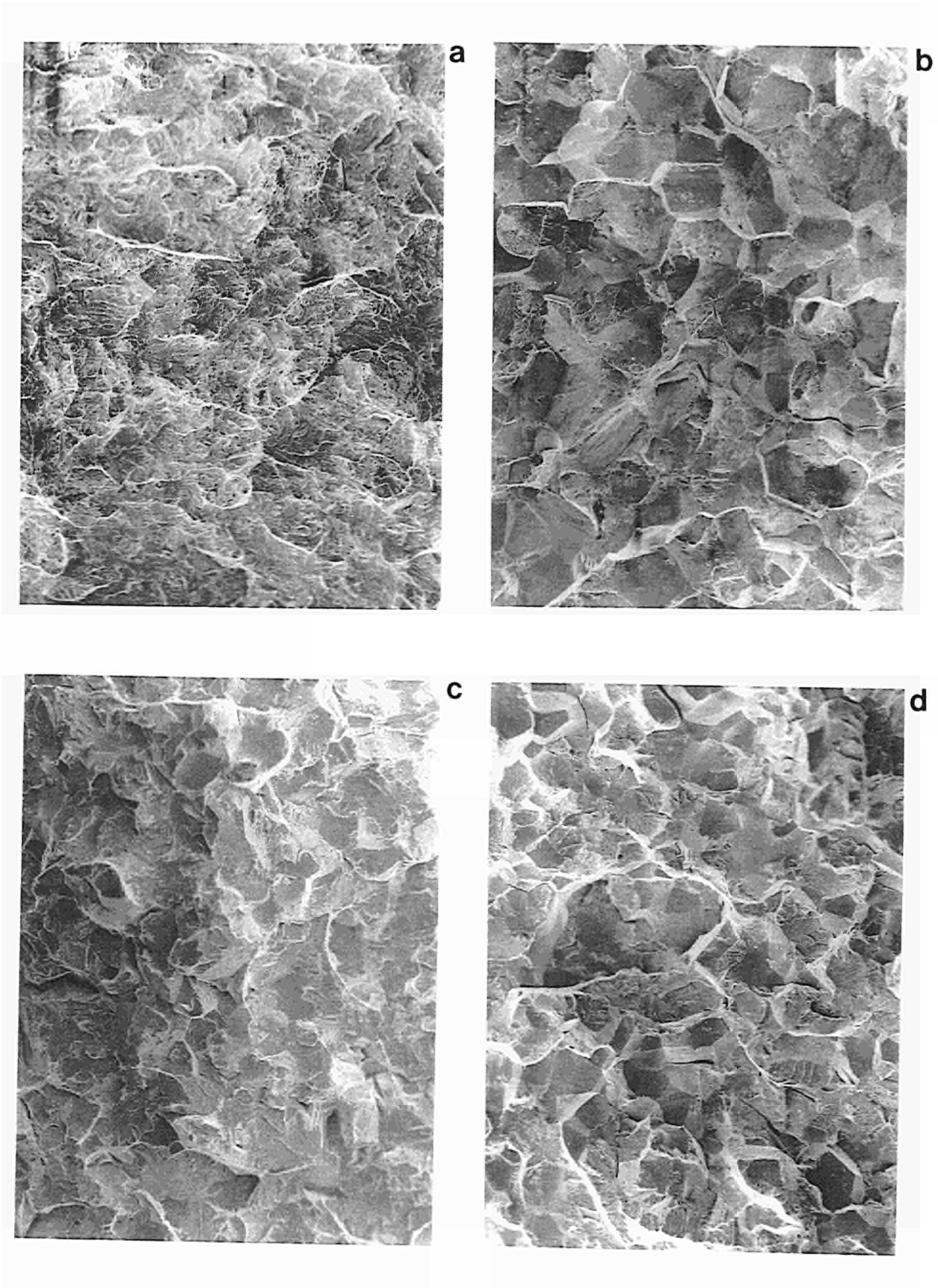

Fig. 4.115 SEM pictures of fracture surfaces of brittle broken Charpy-V specimens of material QT
Simulation conditions: 1350°C/12 sec.
a: as simulated b: +1h 530°C
c, +1h 560°C d: +1h 590°C

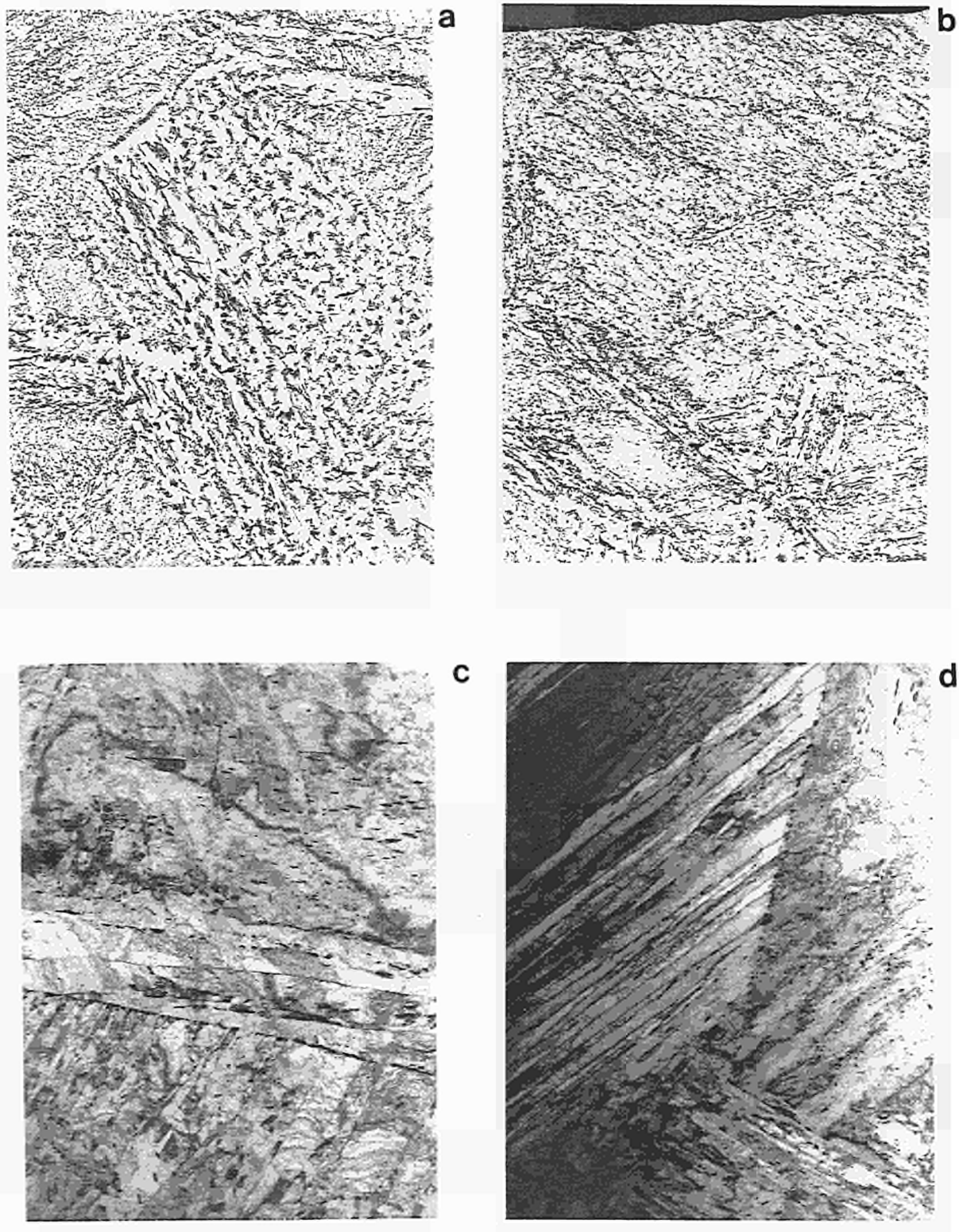

Fig. 4.116 TEM pictures of extraction replica's and thin foils of material TM, simulation condition: 1350°C/12 sec.
a: replica, +1h 530°C b: replica, +1h 590°C
c: thin foil, +1h 530°C d: thin foil, +1h 590°C
a,b: M=x2000 c: M=x6000 d: M=x4000

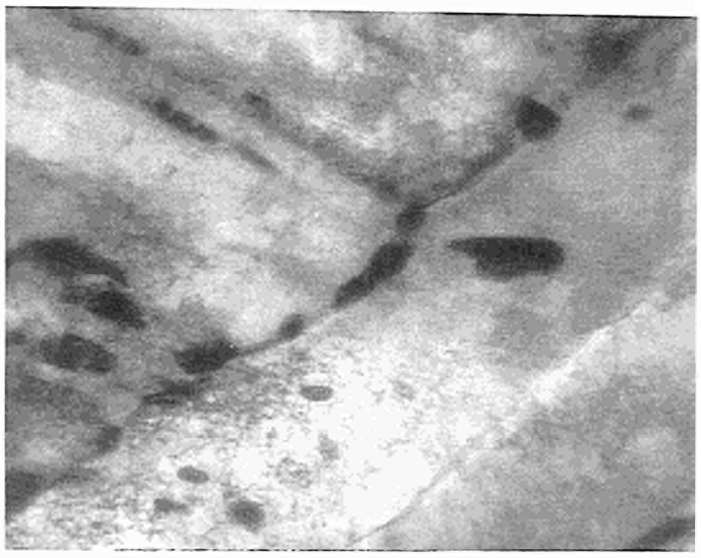

Fig. 4.117 Thin foil micrographs of former austenite grain boundaries in material TM.
Simulation conditions: 1350°/7 sec, PWHT: 590°C, 90% intergranular fracture, a: x50.000 b: x 60.000

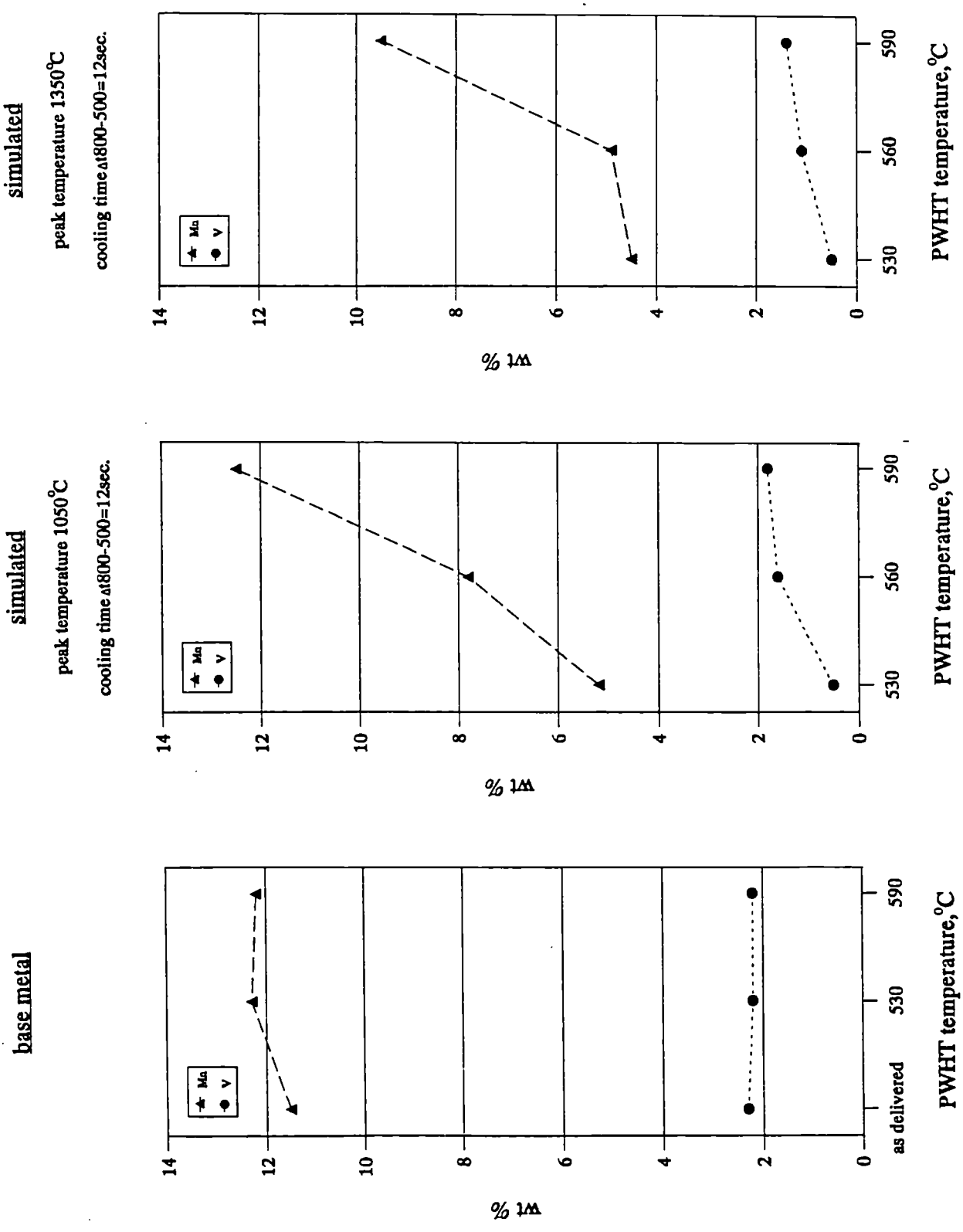

Fig. 4.118 The chemical composition of the grain boundary carbides in material N in the as delivered condition, after weld thermal simulation and after PWHT

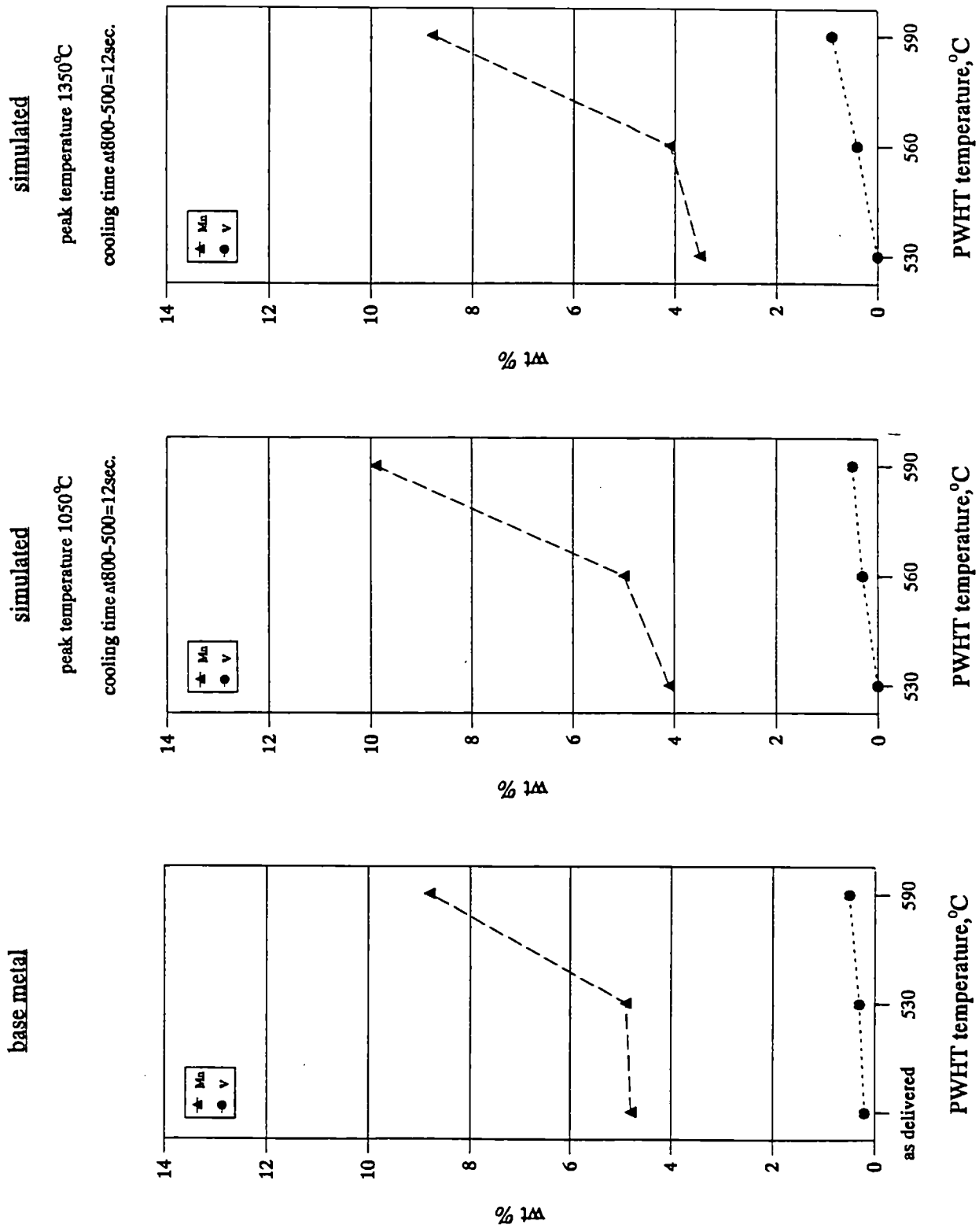

Fig. 4.119 The chemical composition of the grain boundary carbides in material TM in the as delivered condition, after weld thermal simulation and after PWHT.

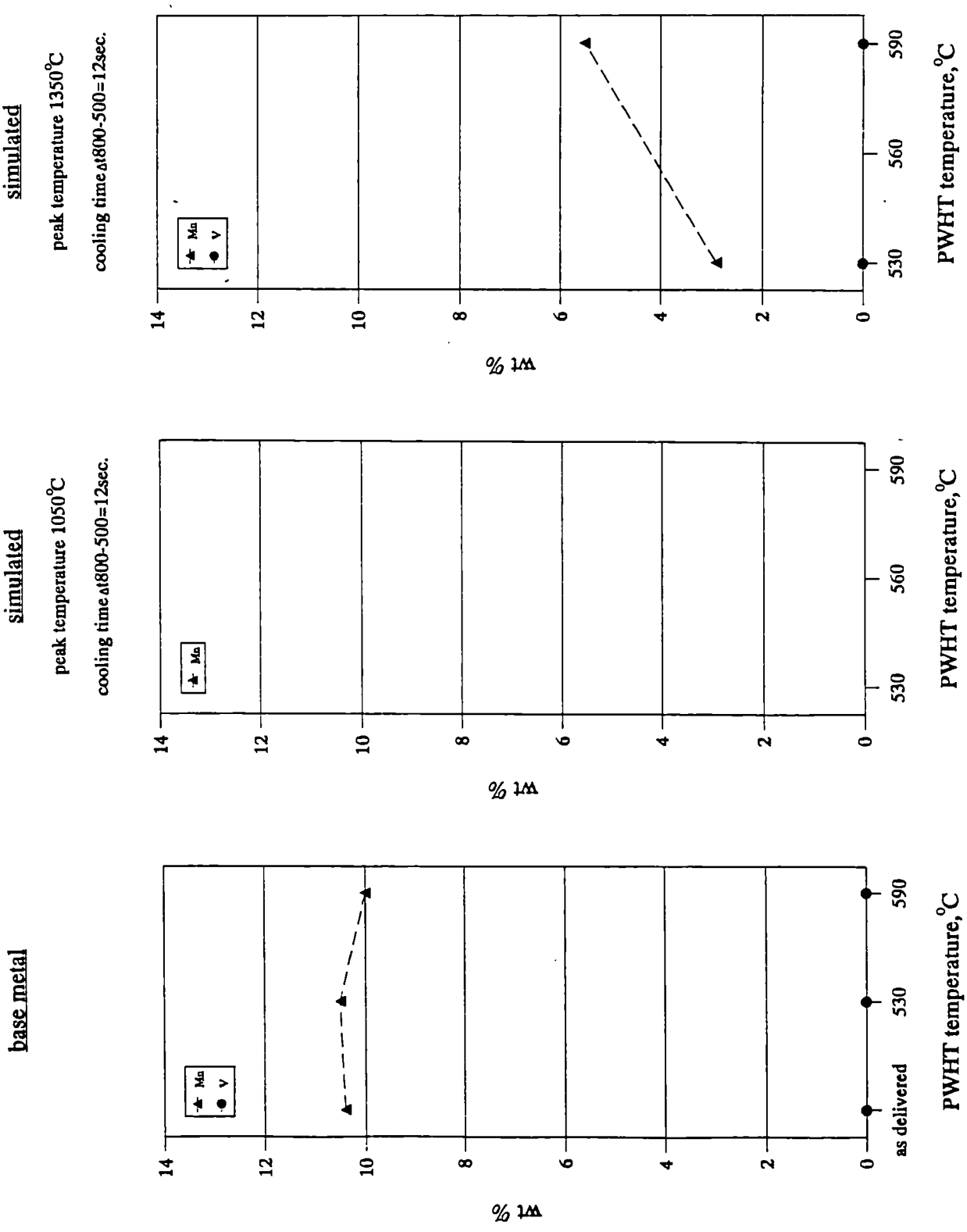

Fig. 4.120 The chemical composition of the grain boundary carbides in material QT in the as delivered condition, after weld thermal simulation and after PWHT.

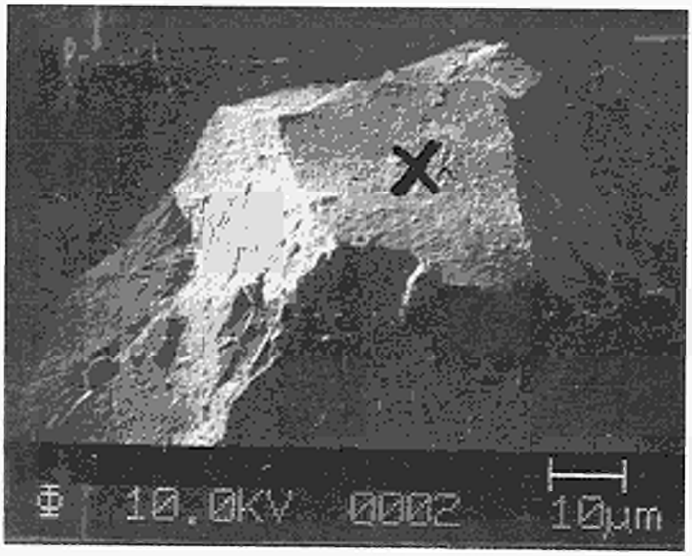

a

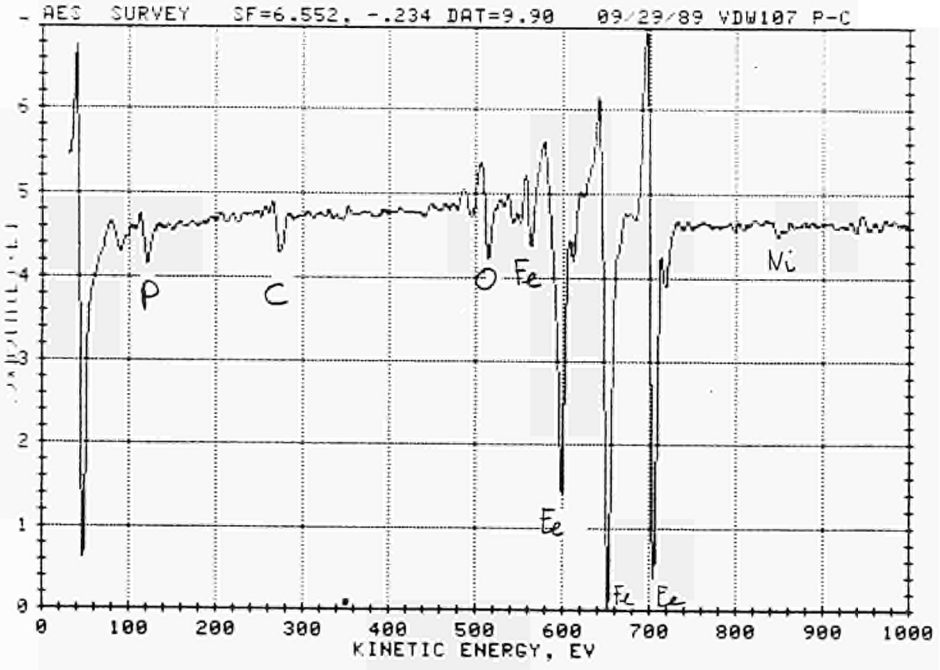

b

Fig. 4.121: Auger analysis of a grain boundary of material N.
Condition: 1350°C/7 sec, PWHT 590°C,
(a) micrograph of the grain boundary
(b) analysis of the fractured surface

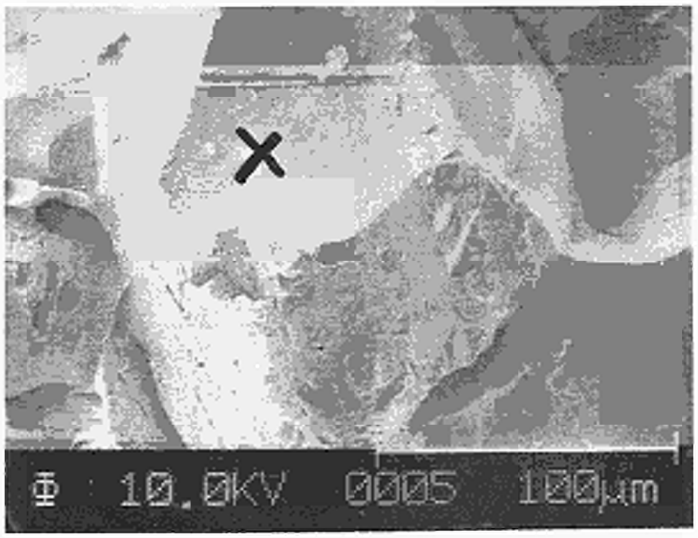

a

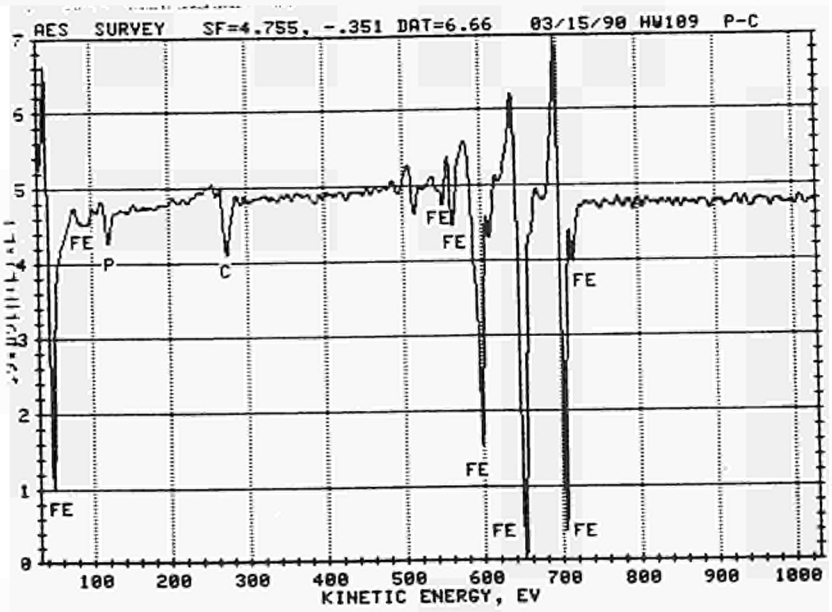

b

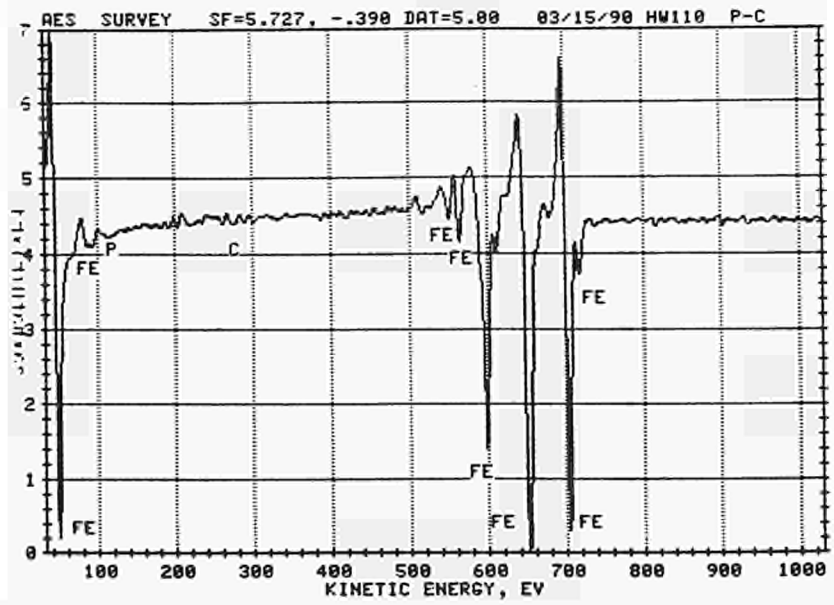

c

Fig. 4.122: Auger analysis of a grain boundary of material TM Condition 1350°C/7 sec, PWHT 590°C,
(a) micrograph of the grain boundary
(b) analysis of the fracture surface
(c) analysis after 2 min sputtering

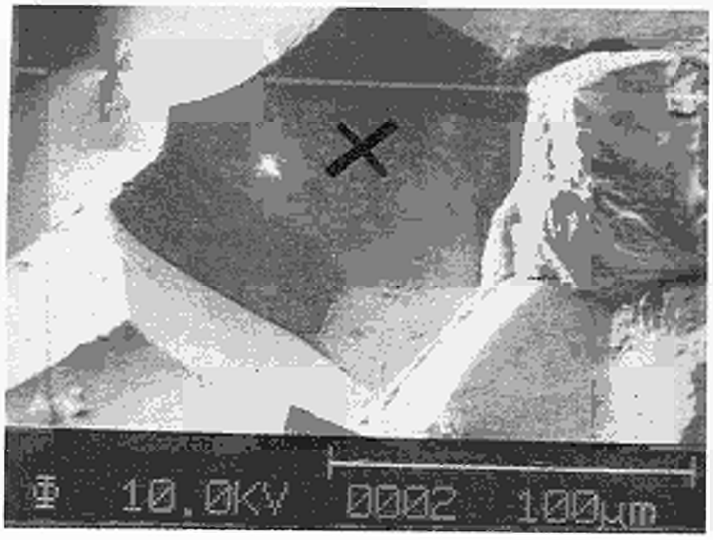

a

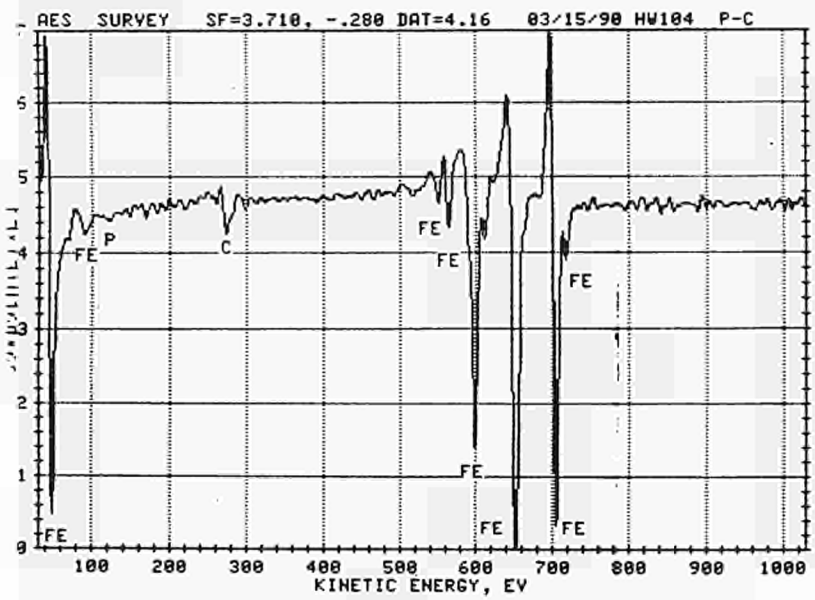

b

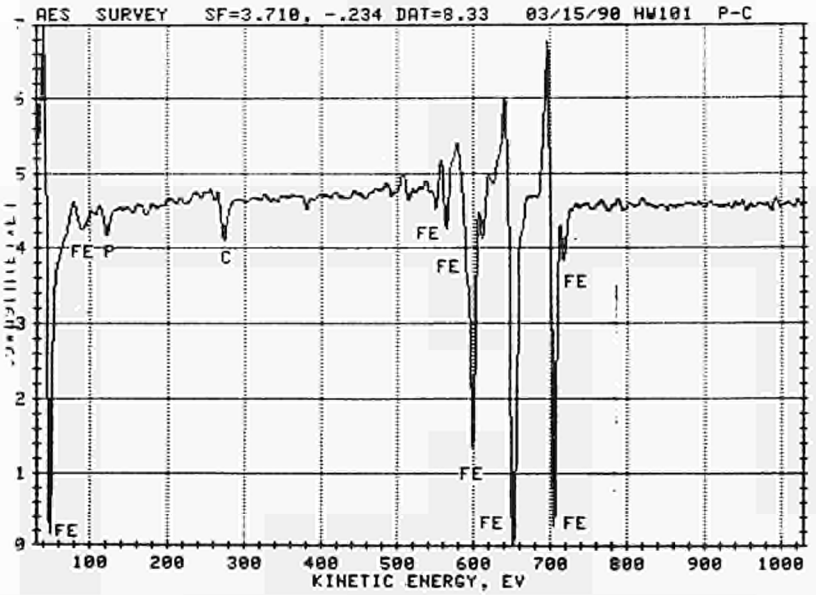

c

Fig. 4.123: Auger analysis of a grain boundary of material QT Condition 1350°C/7 sec, PWHT 590°C,
(a) micrograph of the grain boundary
(b) analysis of the fracture surface
(c) analysis after 2 min sputtering

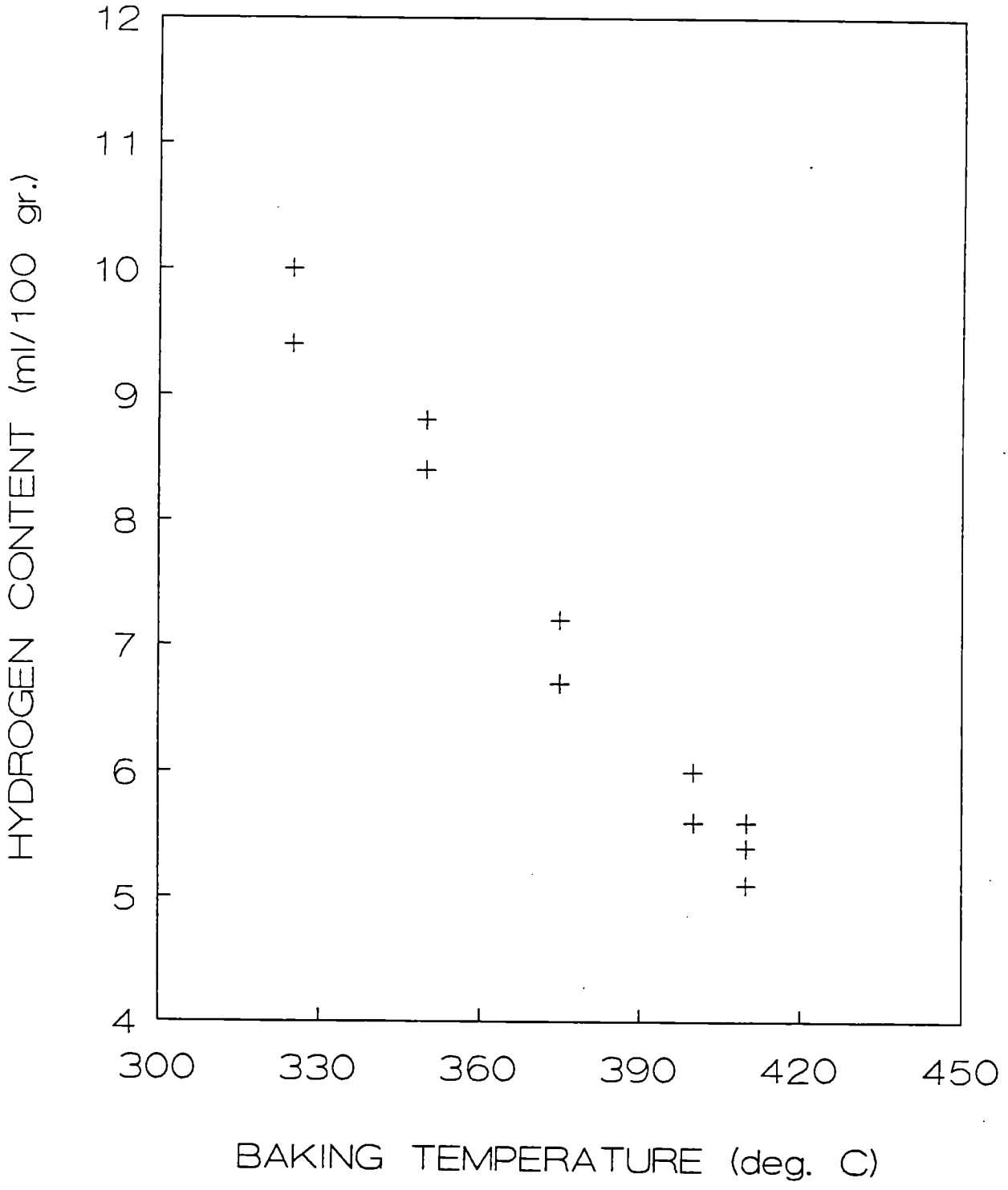

Figure 5.1: Effect of baking temperature of E9018-G SMAW consumables on the diffusable hydrogen content according ISO 3690.

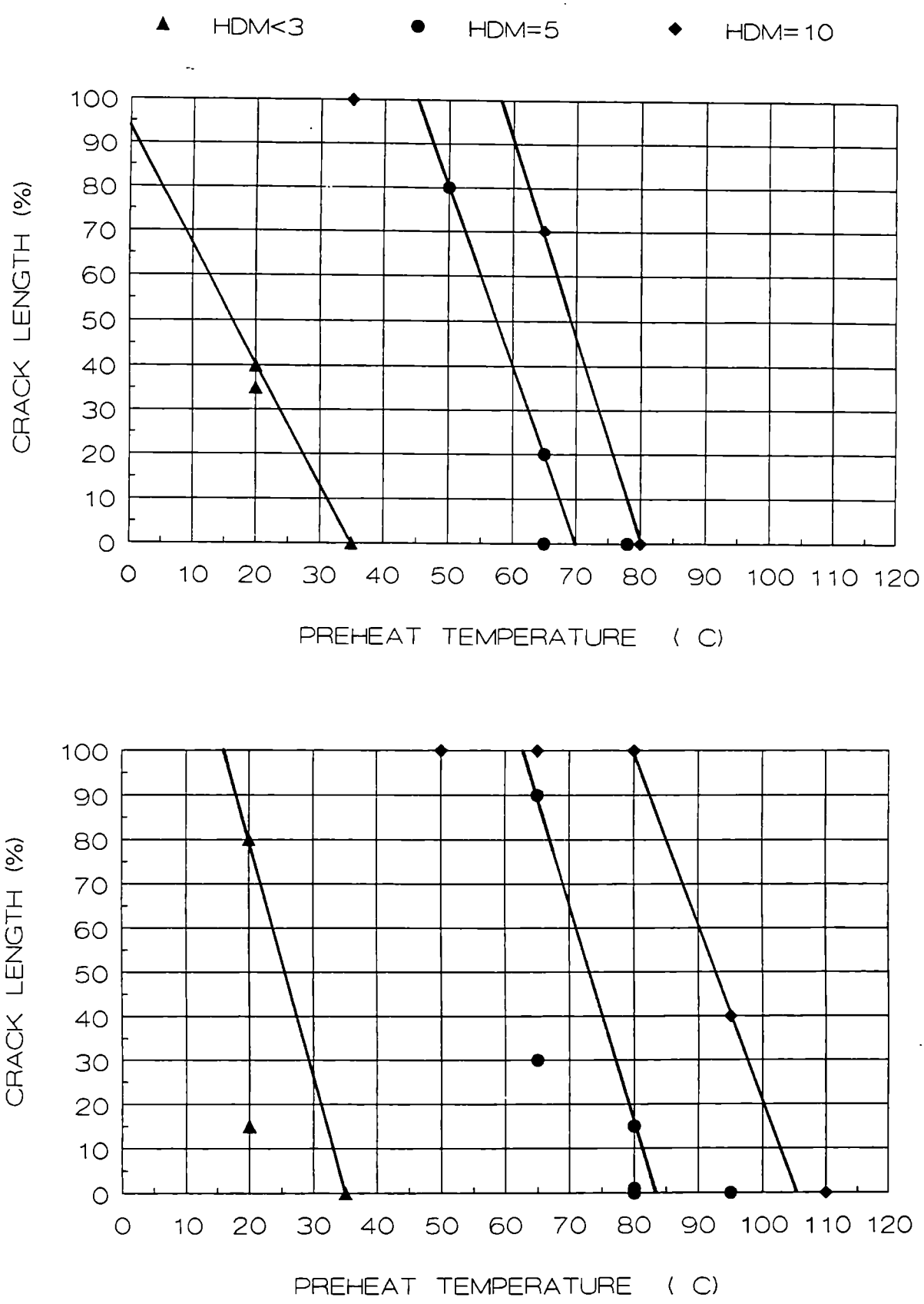

Figure 5.2: Crack length in Tekken test specimens, as a function of pre-heat temperature. Material N
a = 15 mm plate thickness;
b = 50 mm plate thickness

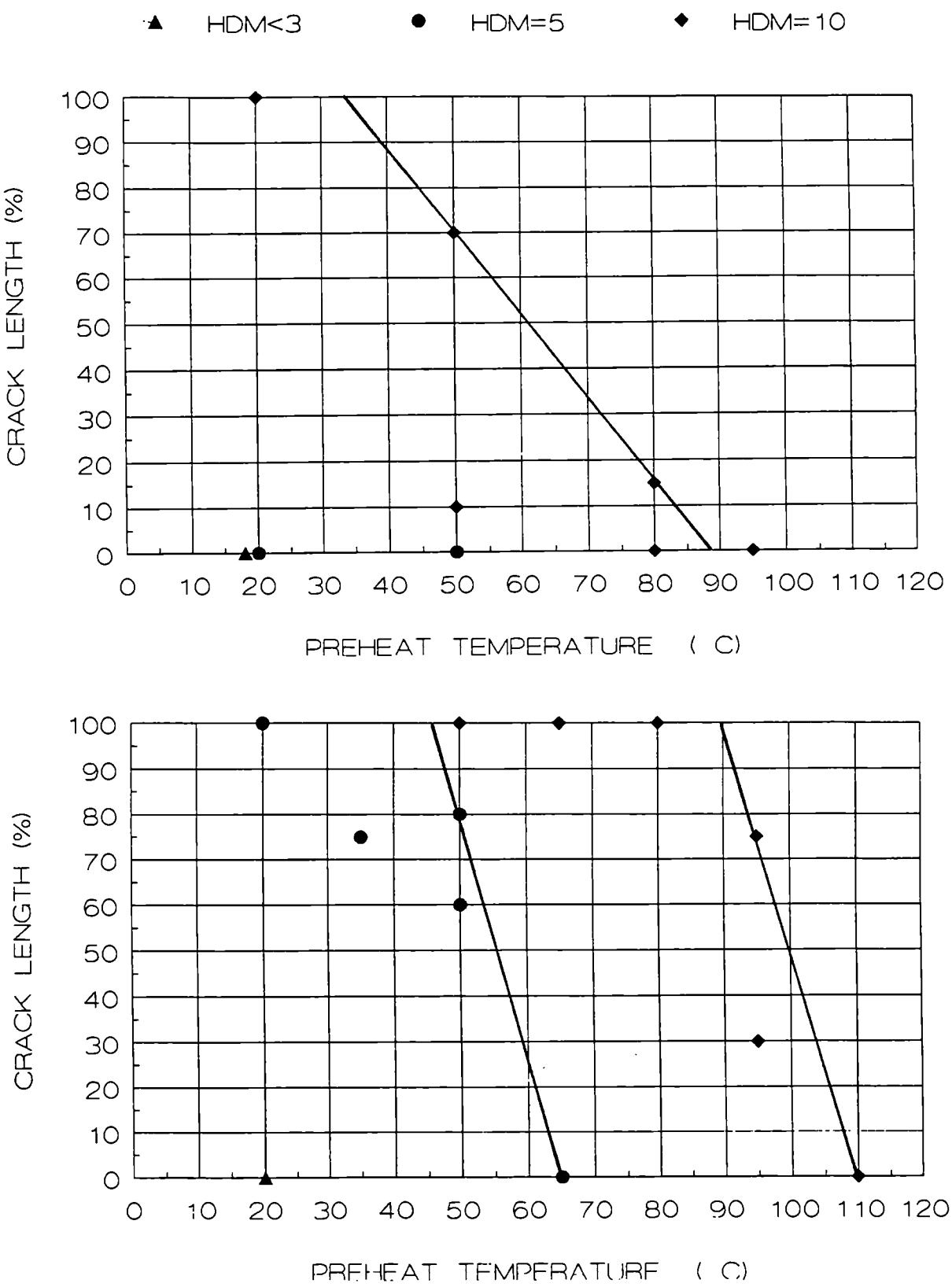

Figure 5.3: Crack length in Tekken test specimens, as a function of pre-heat temperature. Material TM
a = 15 mm plate thickness;
b = 50 mm plate thickness

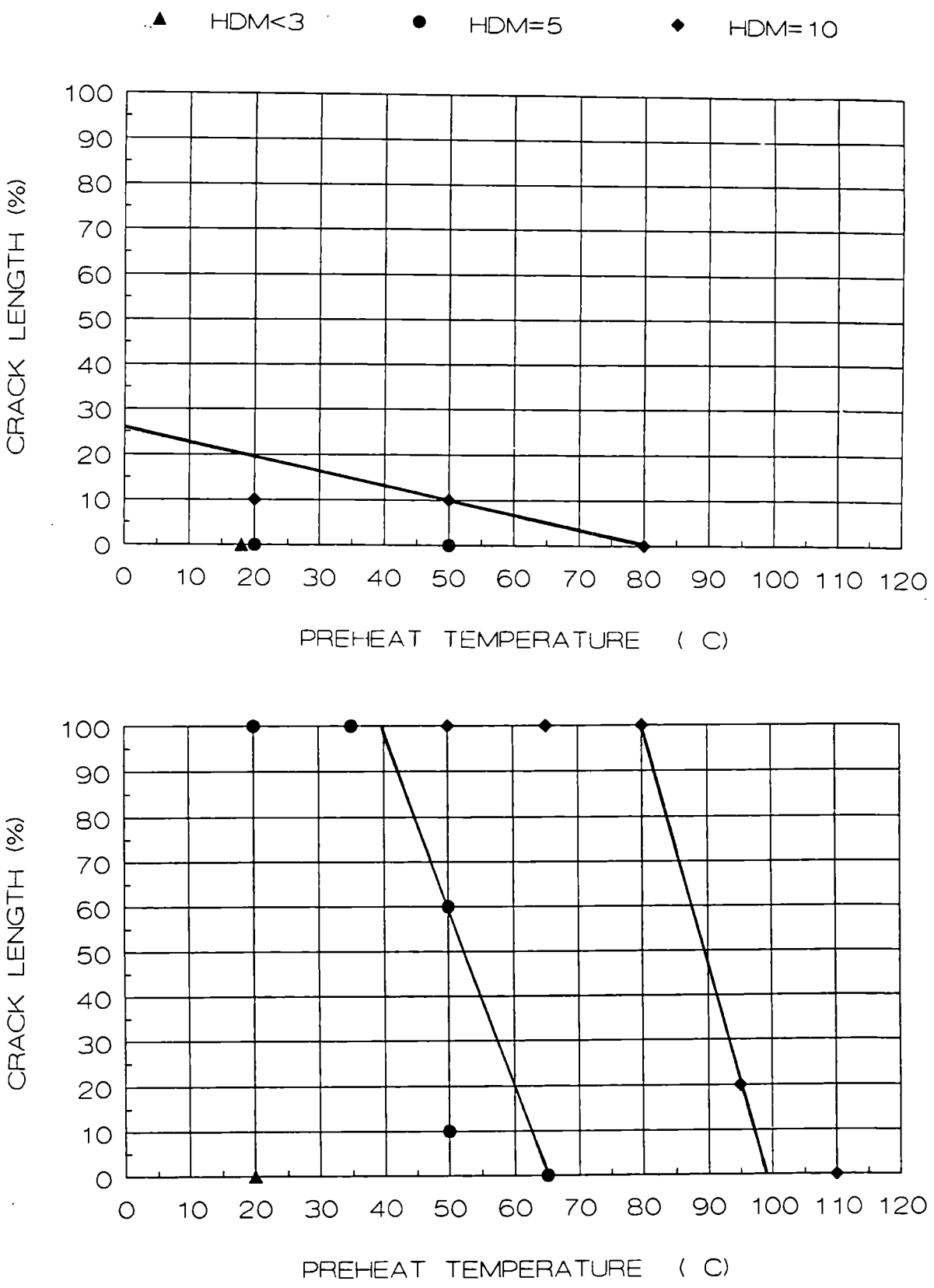

Figure 5.4: Crack length in Tekken test specimens, as a function of pre-heat temperature. Material QT
a = 15 mm plate thickness;
b = 50 mm plate thickness

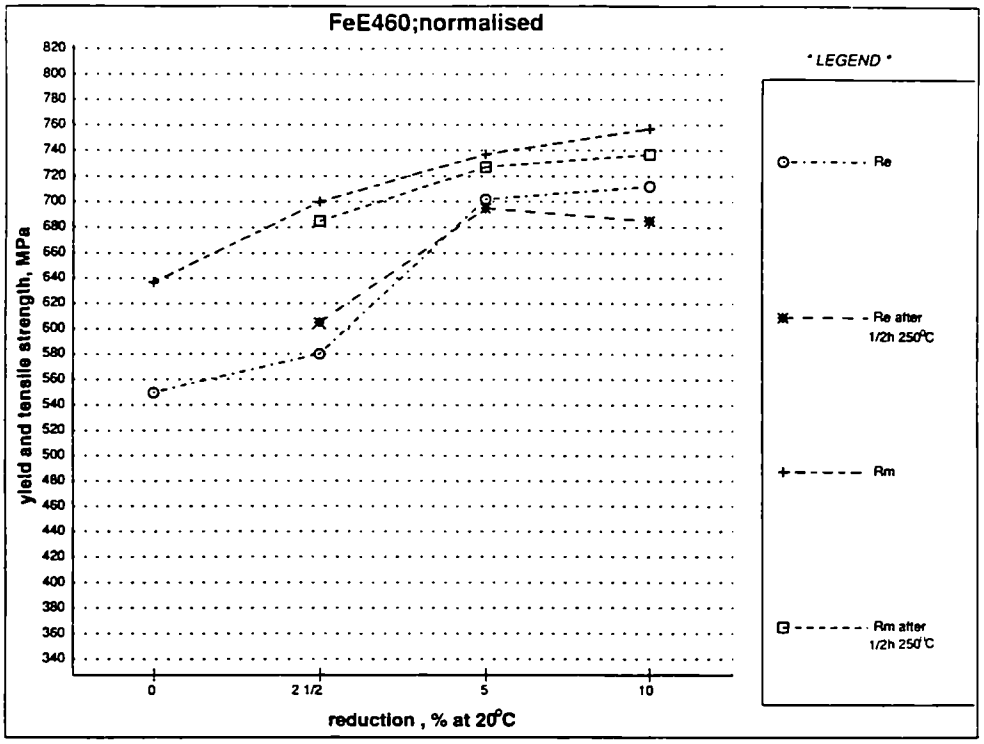

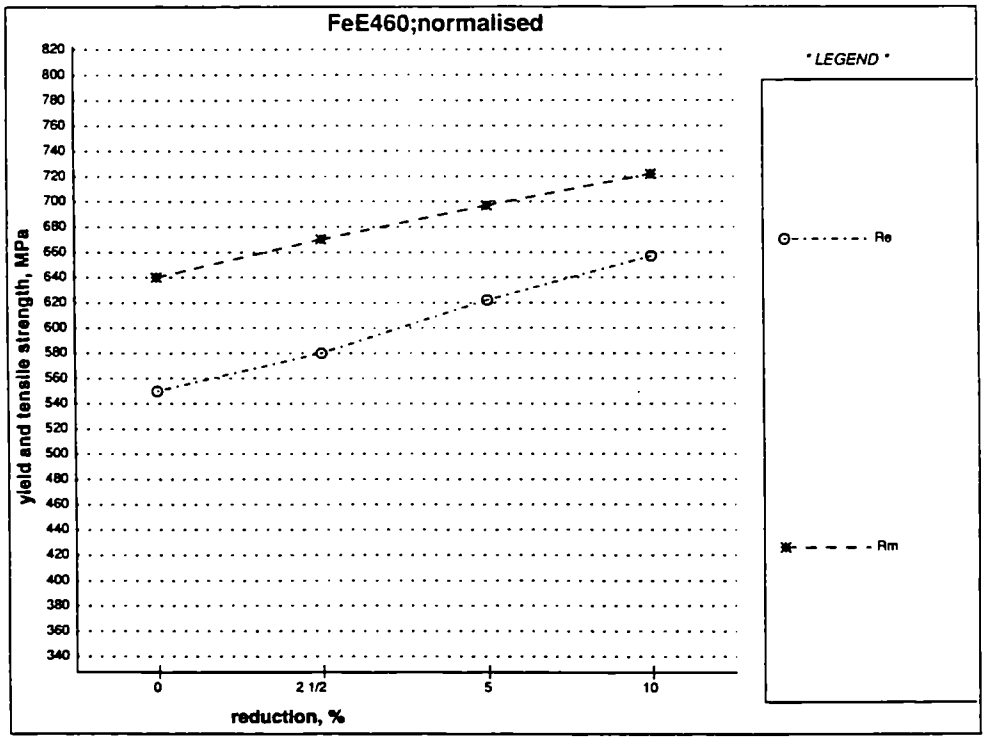

Figure 7.1: Results of the tensile tests on the N material rolled at 20°C (a) and 560°C (b)

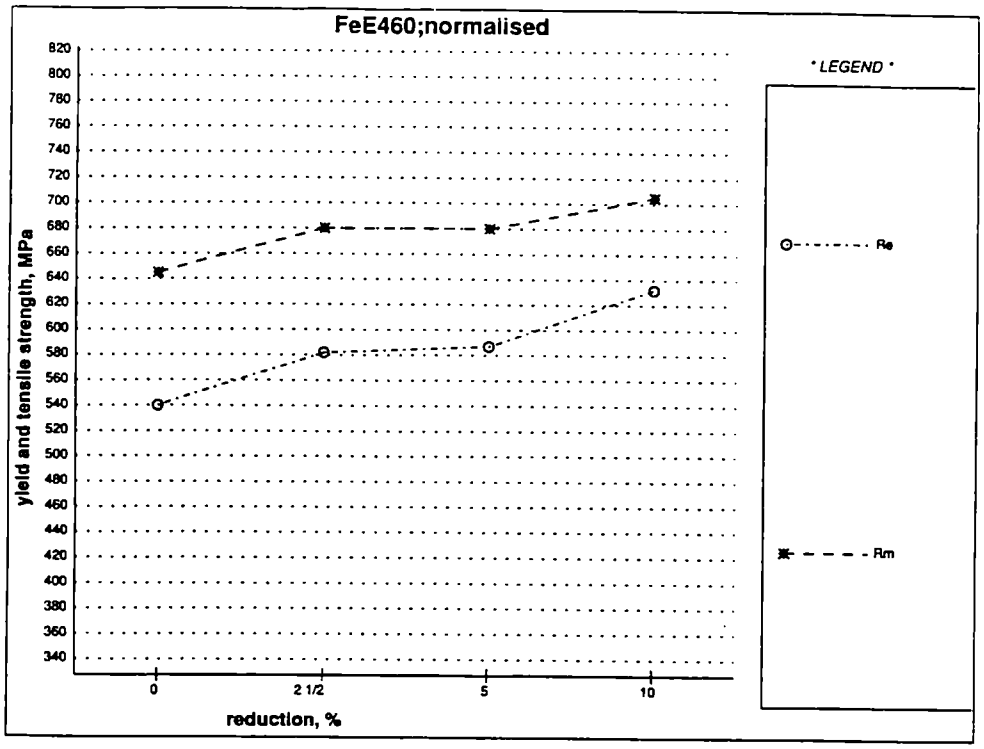

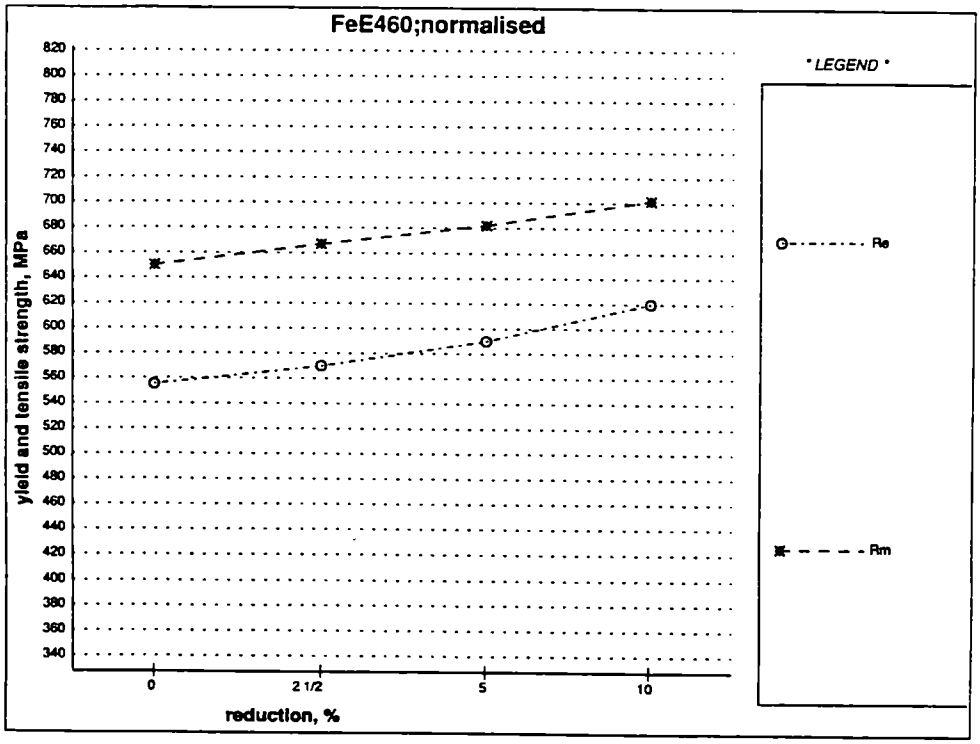

Figure 7.2: Results of the tensile tests on the N material rolled at 590 (a) and 620°C (b)

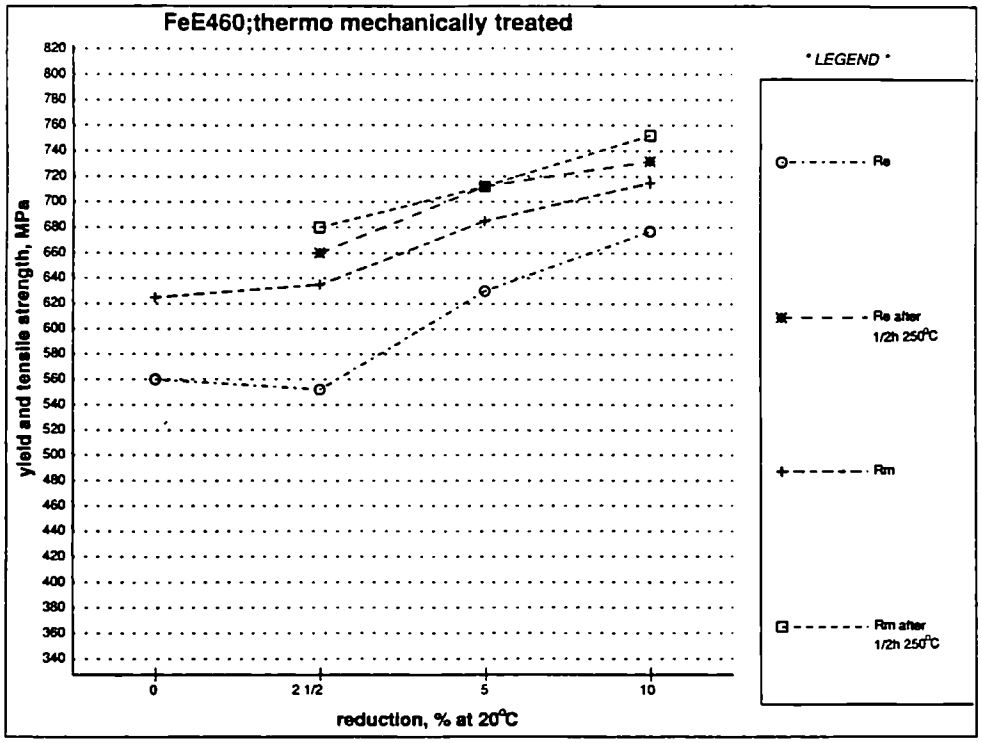

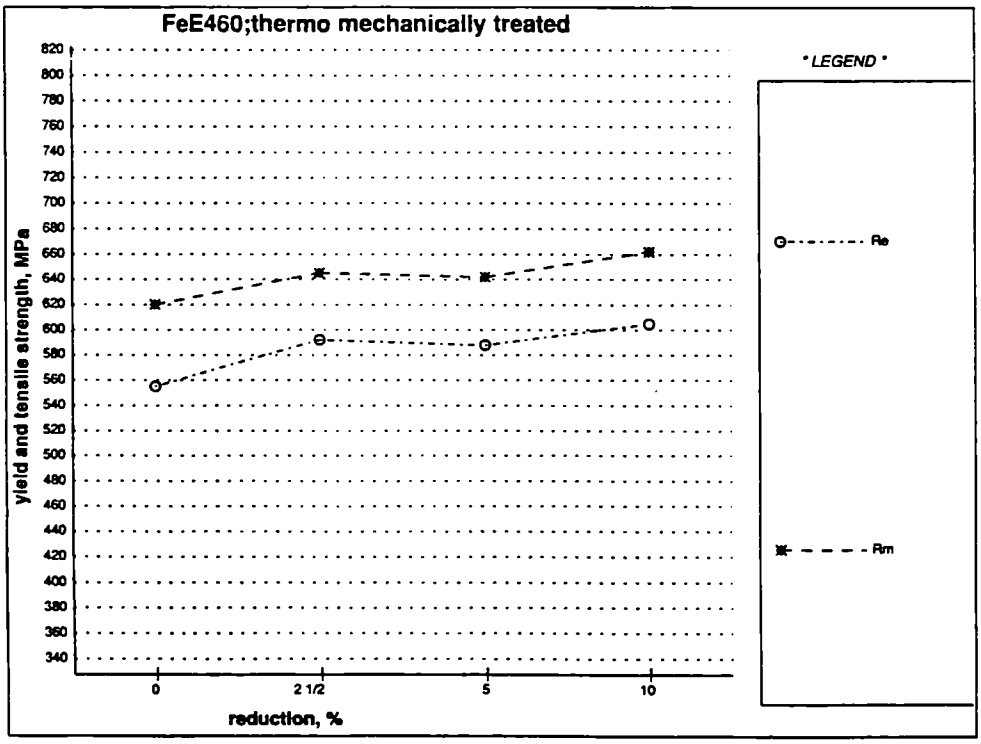

Figure 7.3: Results of the tensile tests on the TM material rolled at 20°C (a) and at 560°C (b)

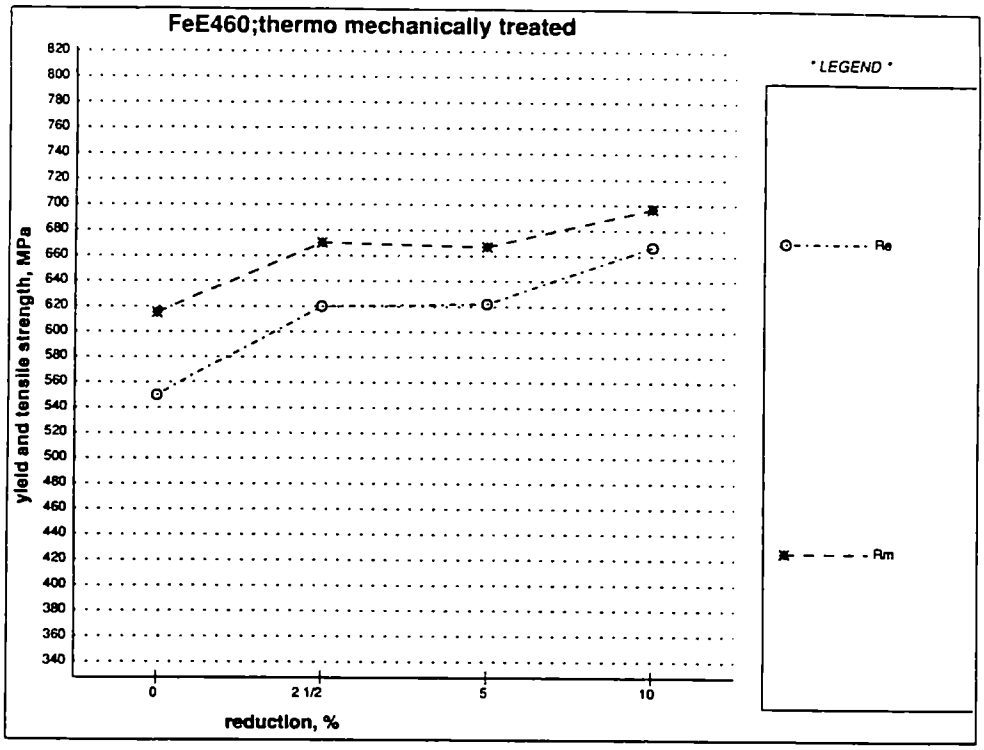

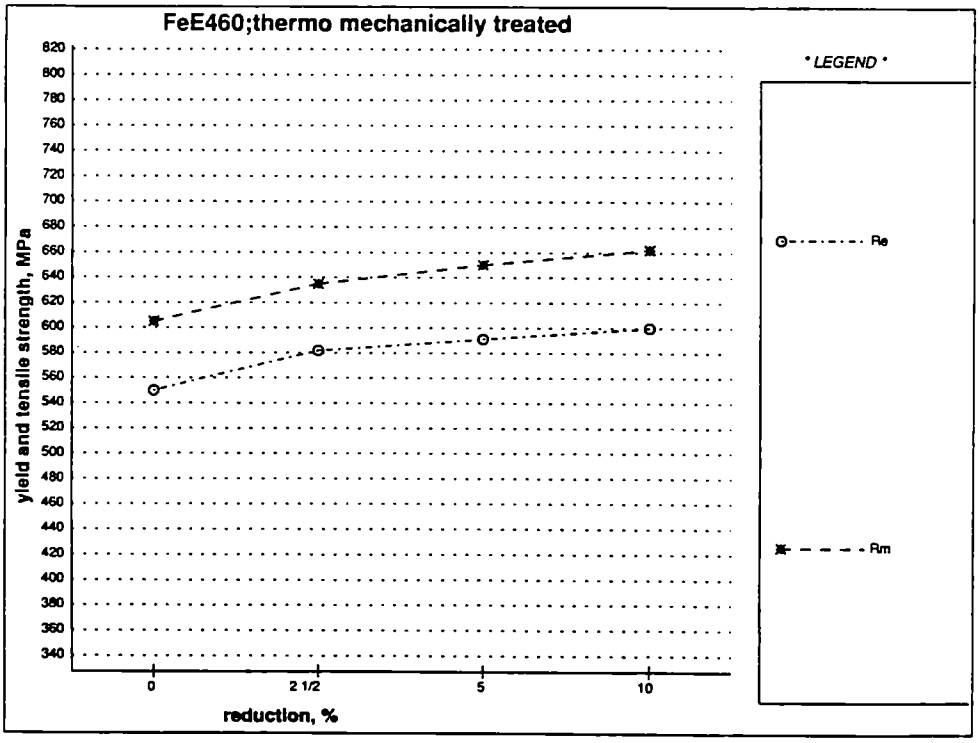

Figure 7.4: Results of the tensile tests on TM material rolled at 590°C (a) and 620°C (b)

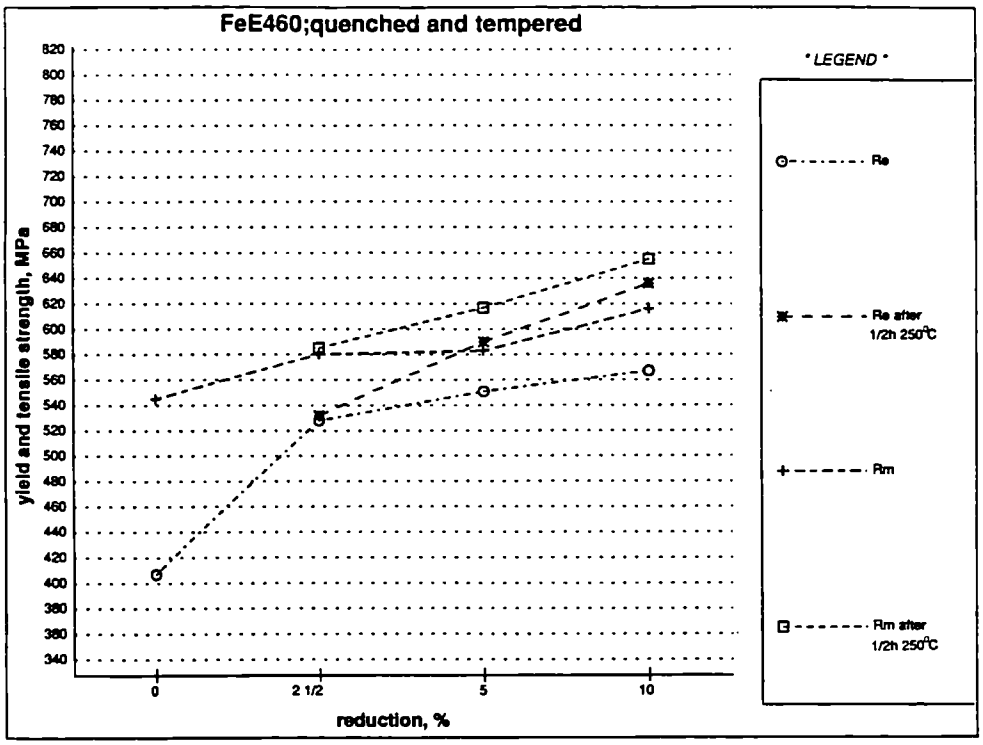

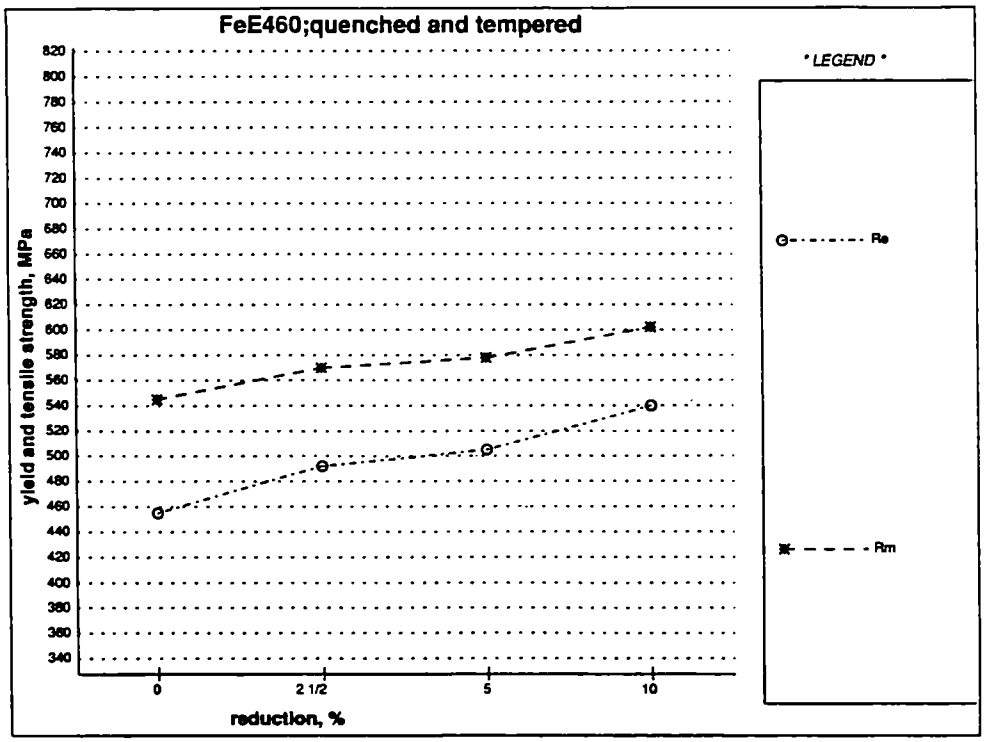

Figure 7.5: Results of the tensile tests on the QT material rolled at 20°C (a) and 560°C (b)

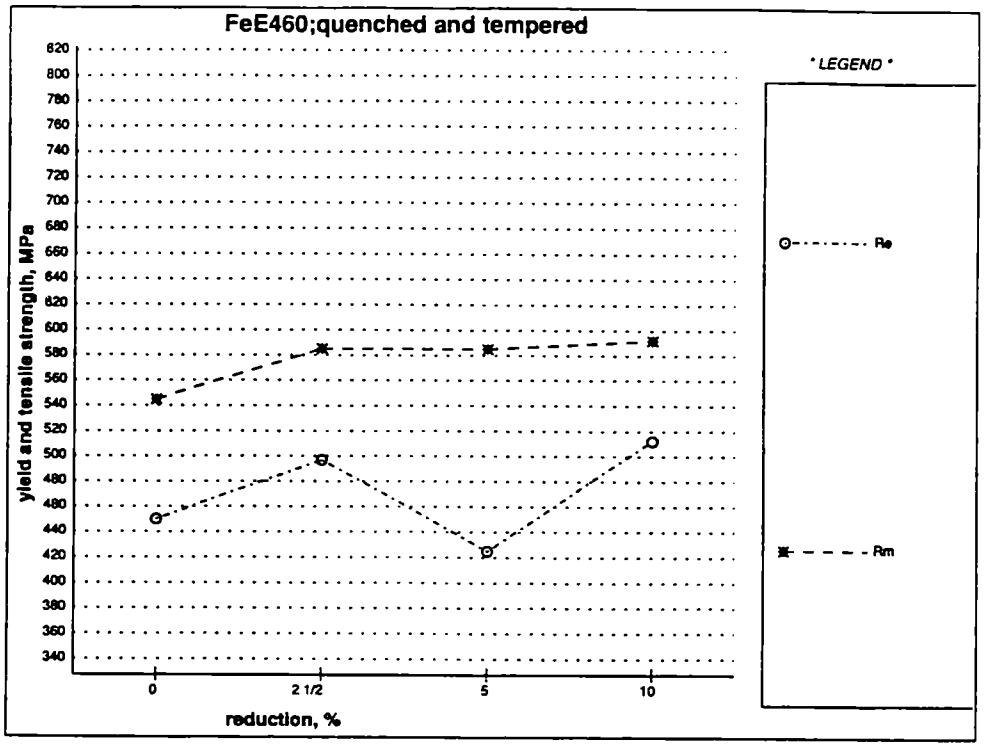

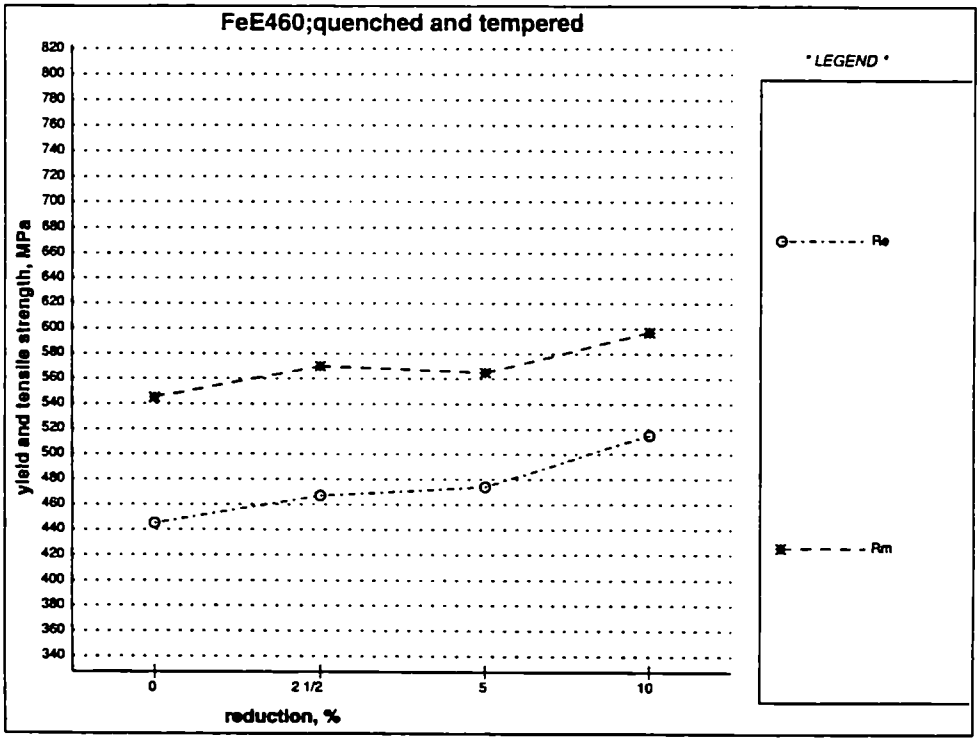

Figure 7.6: Results of the tensile tests on the QT material, rolled at 590°C (a) and 620°C (b)

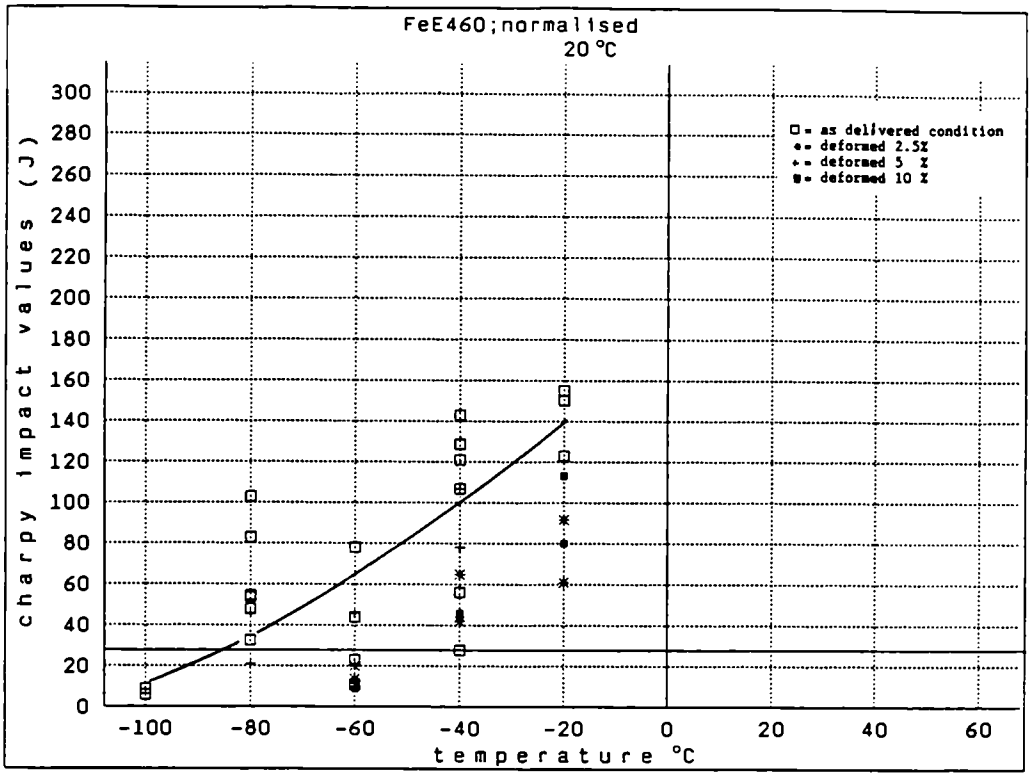

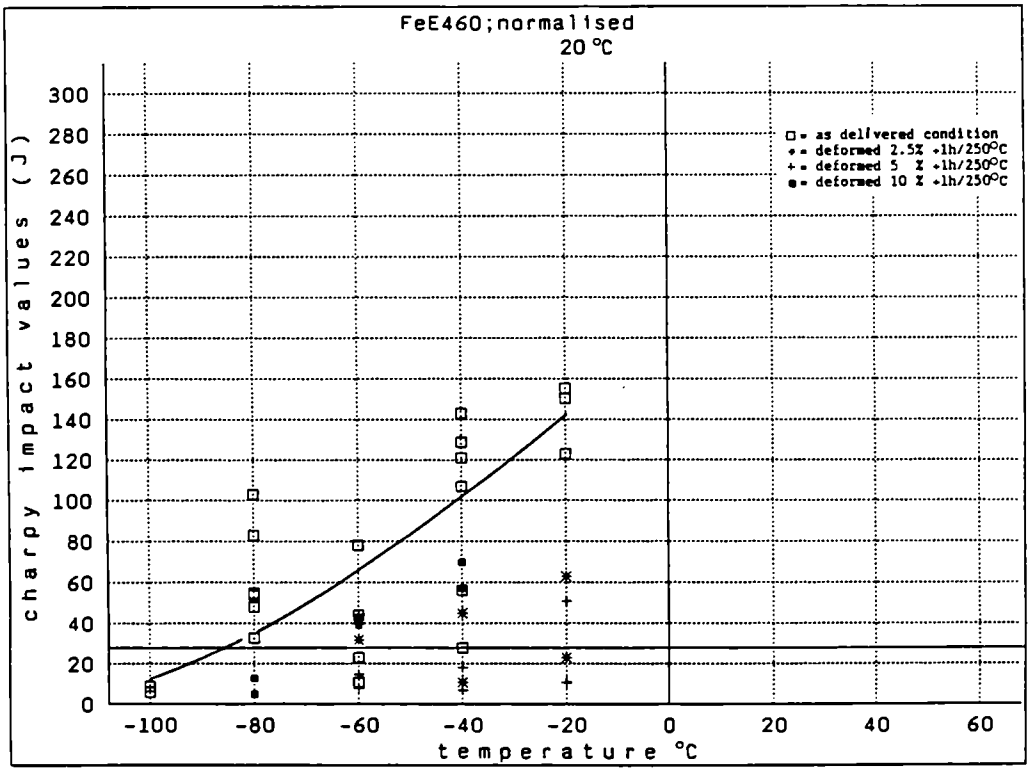

Figure 7.7: Results of the Charpy impact tests on the N material, rolled at 20°C (a) and after strain ageing (b)

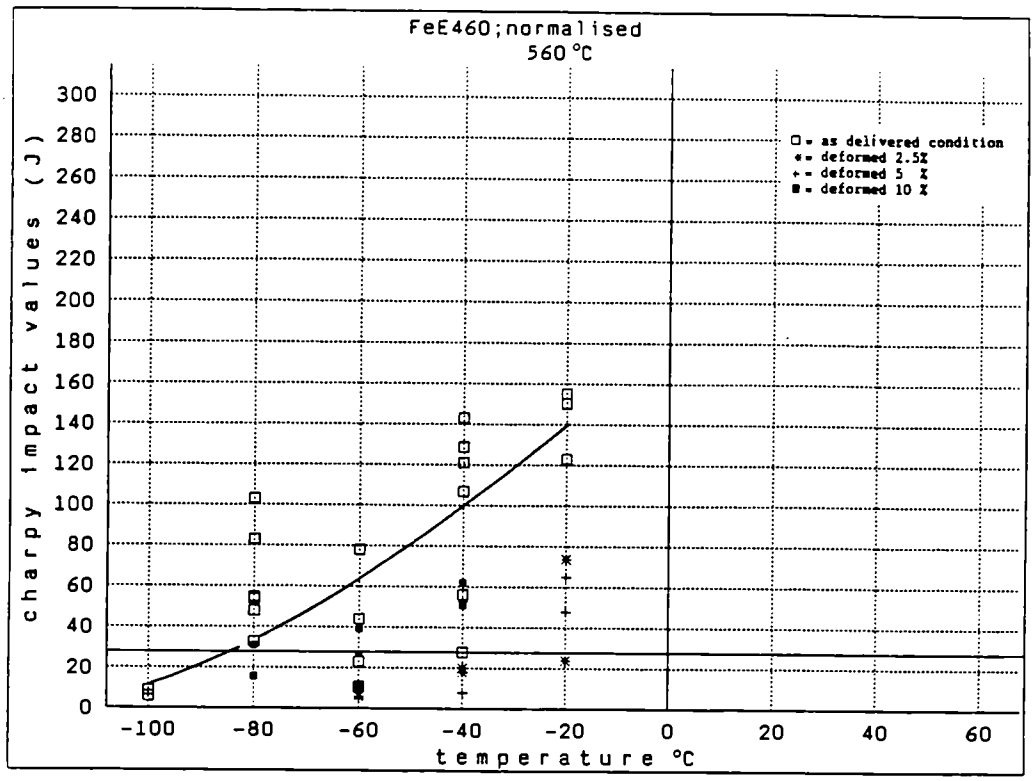

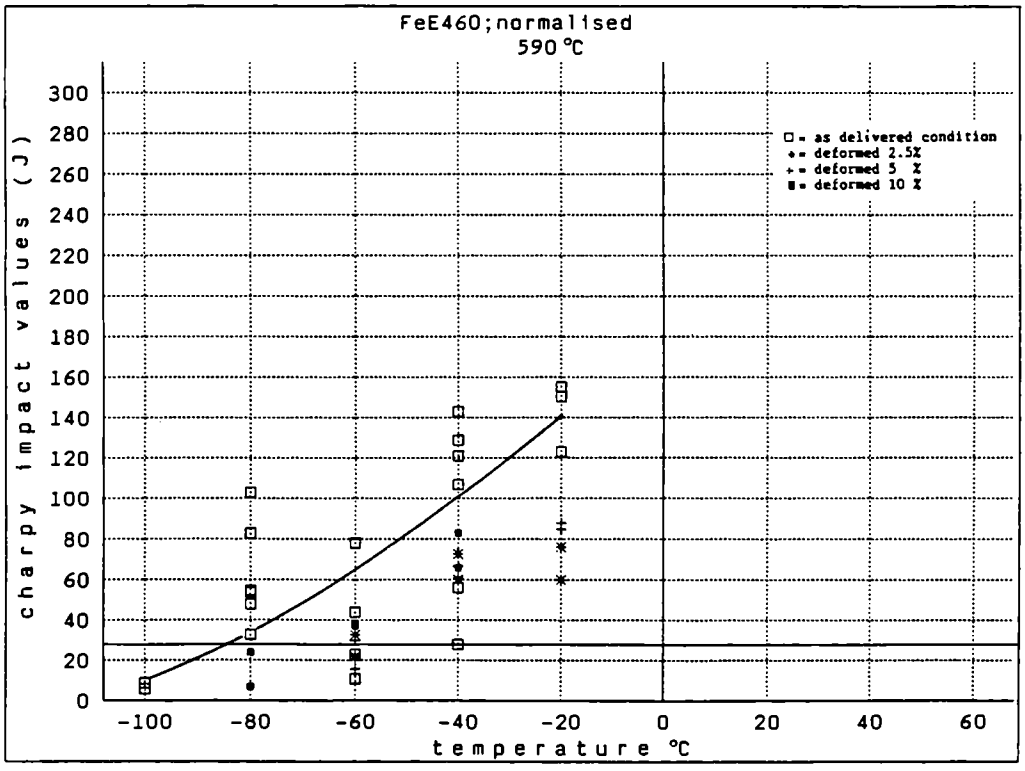

Figure 7.8: Results of the Charpy impact tests on the N material rolled at 560°C (a) and 590°C (b)

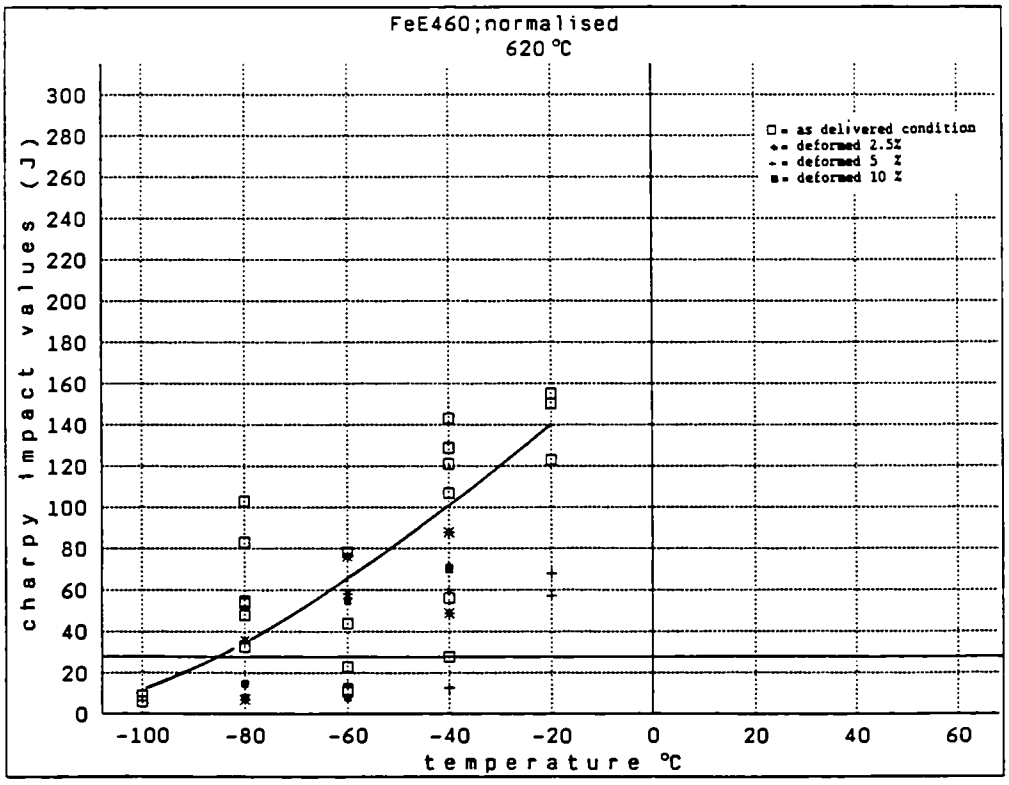

Figure 7.9: Results of the Charpy impact tests on the N material rolled at 620°C

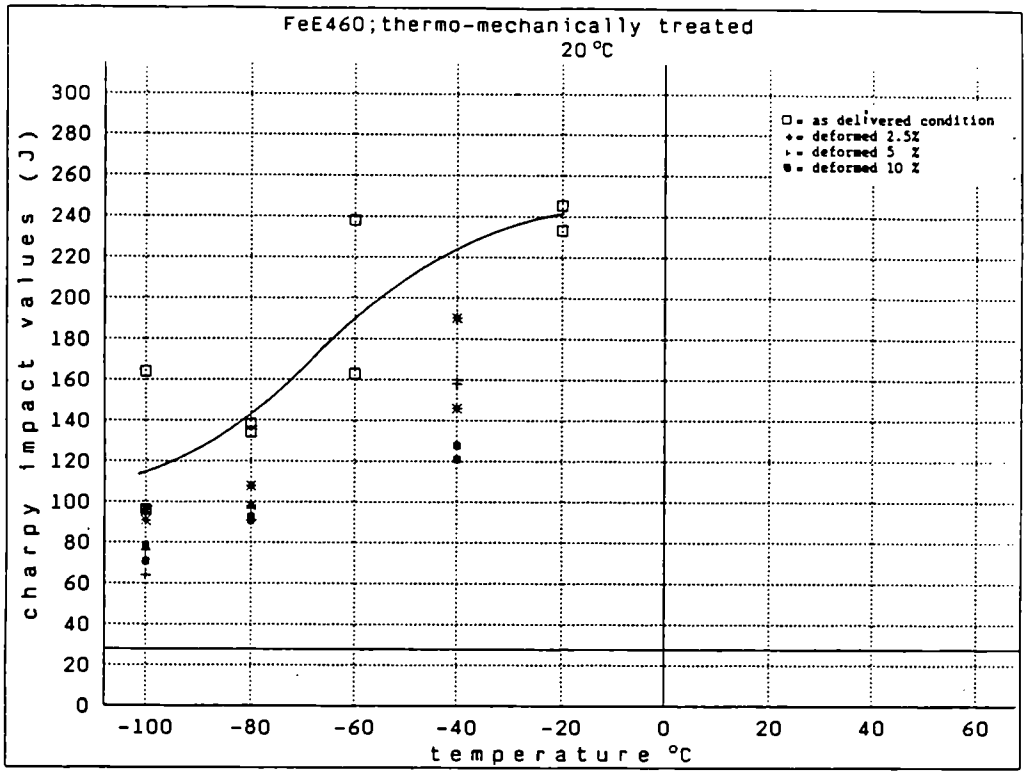

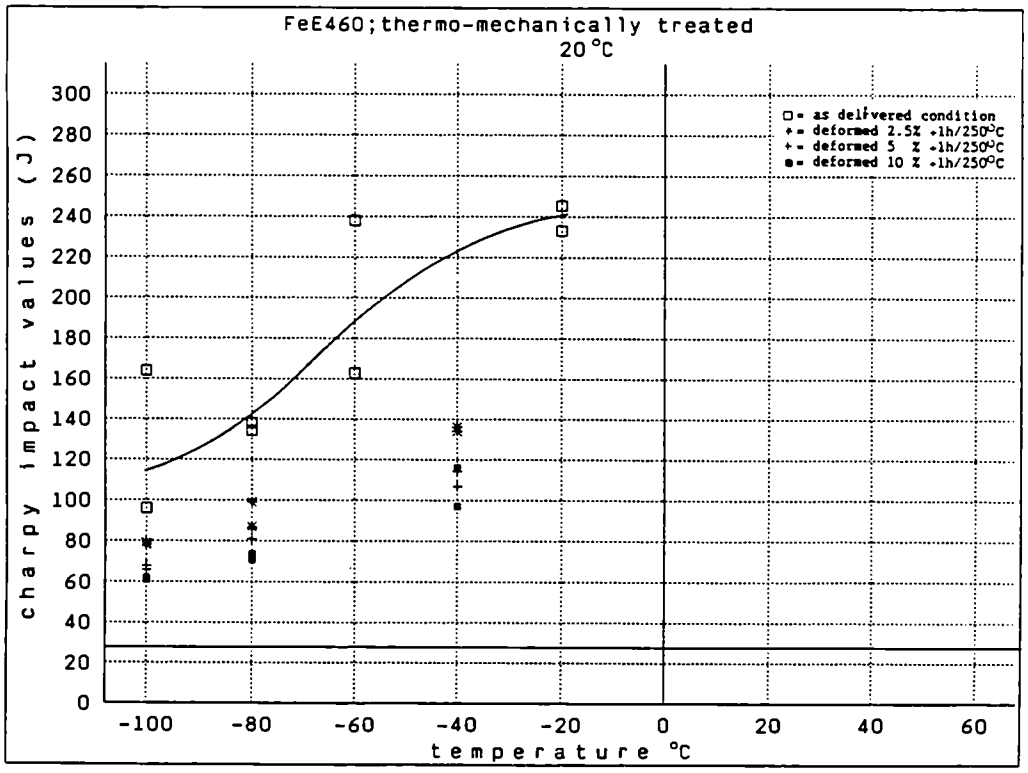

Figure 7.10: Results of the Charpy impact tests on the TM material rolled at 20°C (a) and after strain ageing (b)

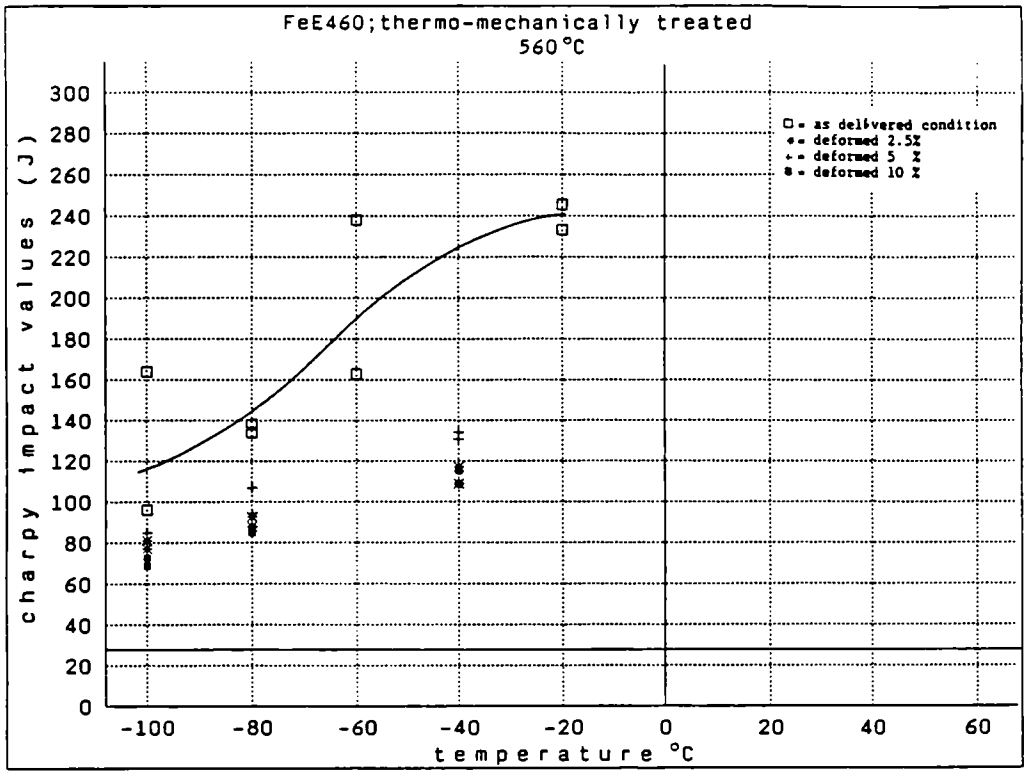

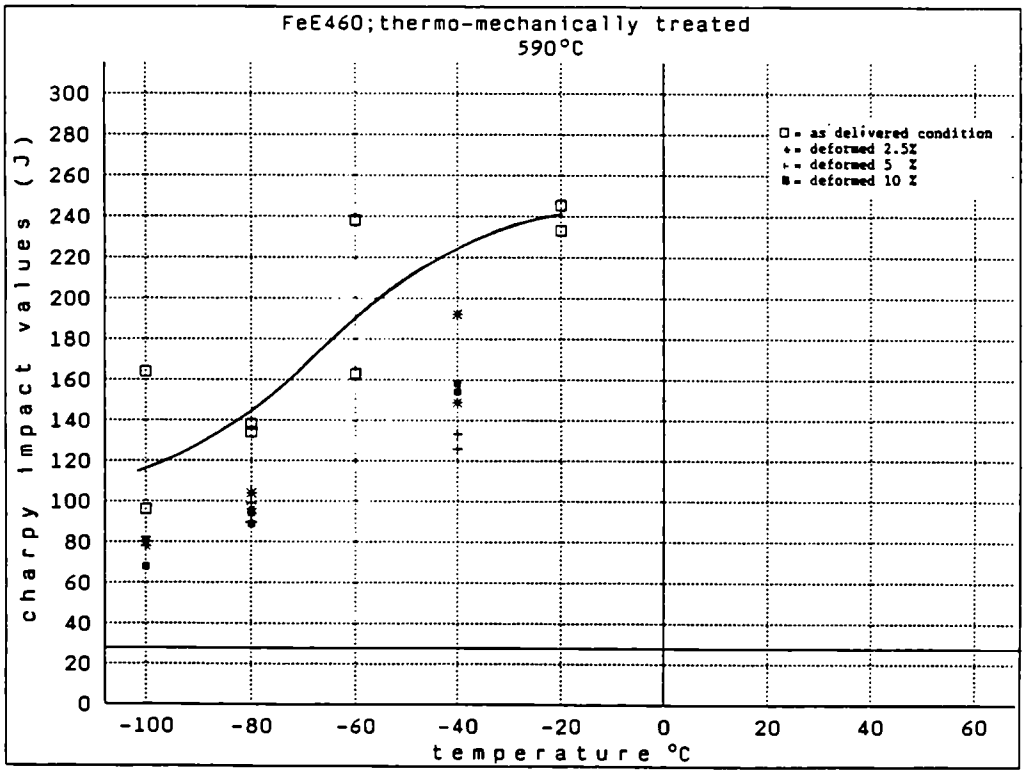

Figure 7.11: Results of the Charpy impact tests on the TM material rolled at 560°C (a) and 590°C (b)

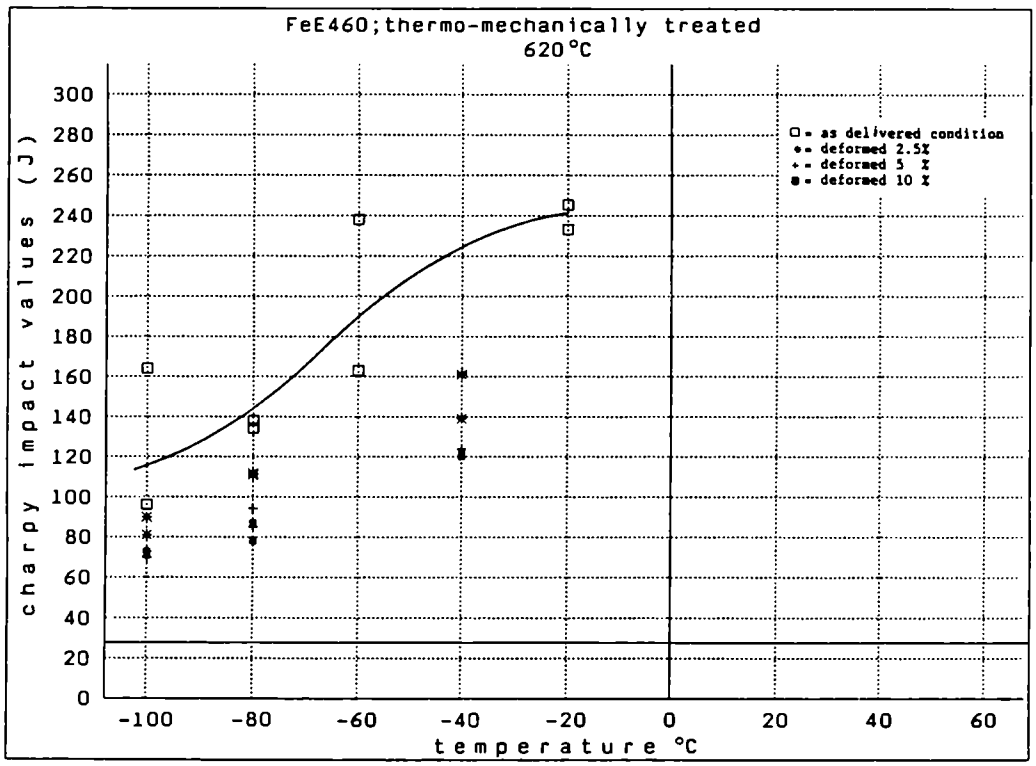

Figure 7.12: Results of the Charpy impact tests on the TM material rolled at 620°C

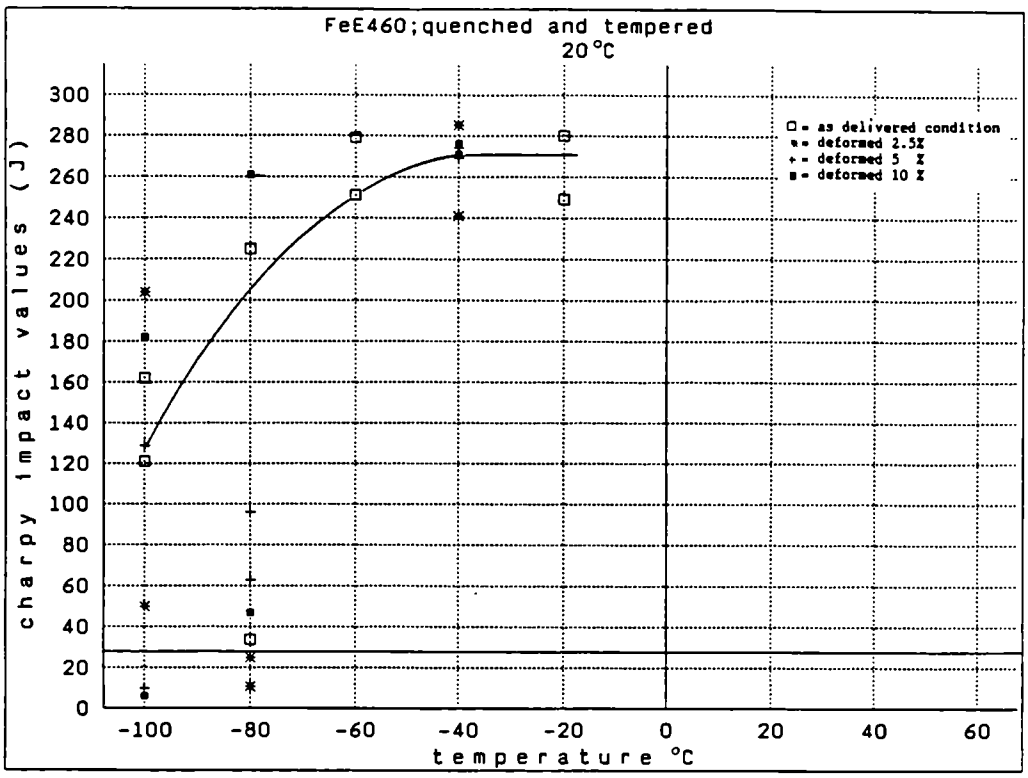

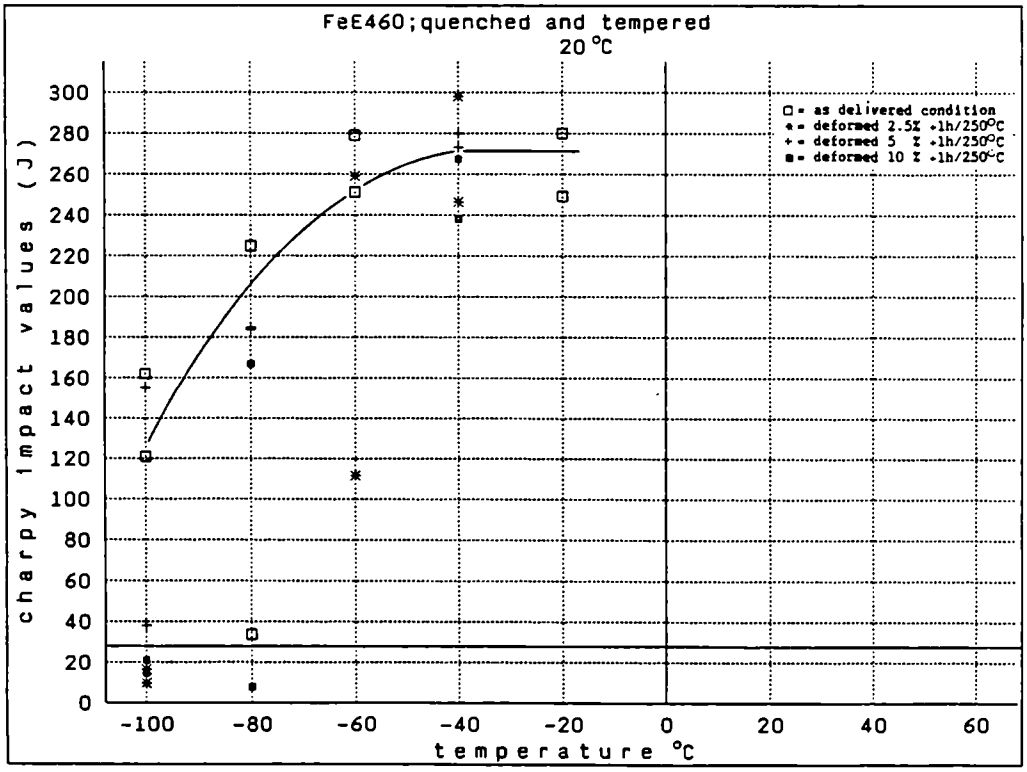

Figure 7.13: Results of the Charpy impact tests on the QT material rolled at 20°C (a) and after strain ageing (b)

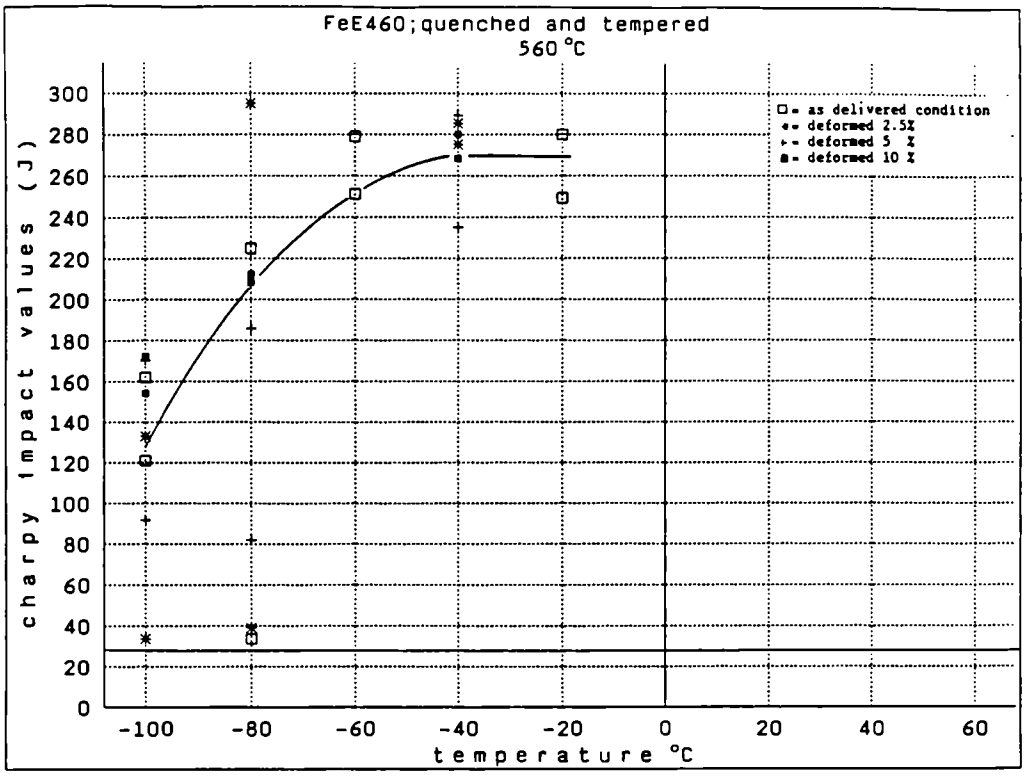

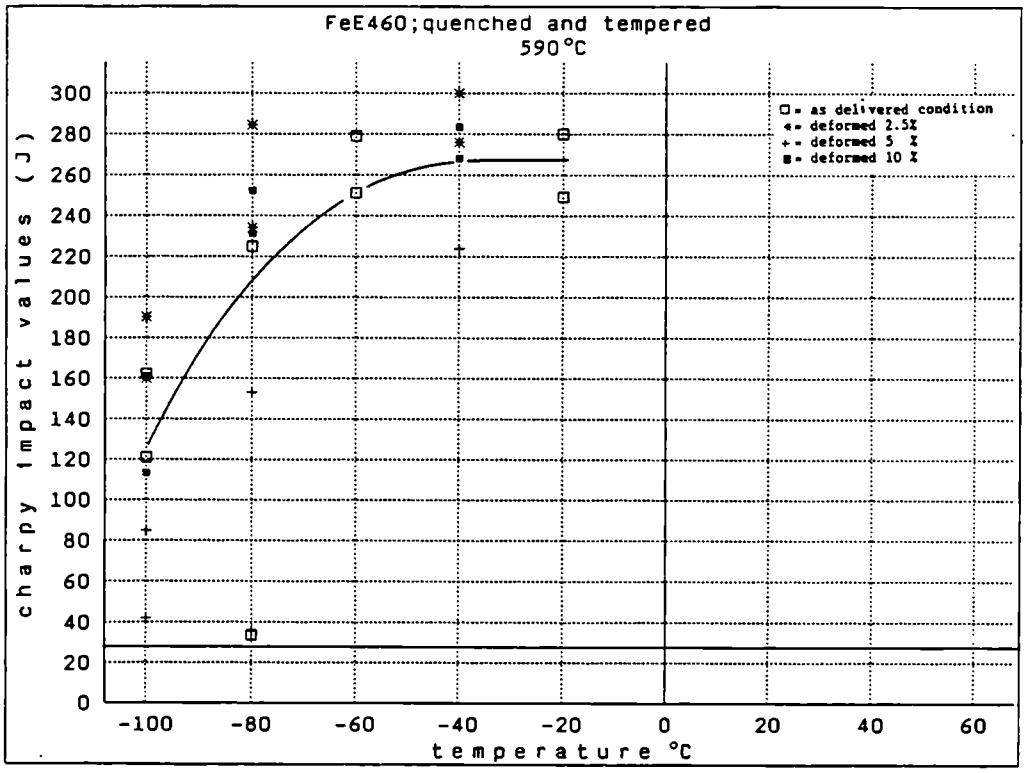

Figure 7.14: Results of the Charpy impact tests on the QT material rolled at 560°C (a) and 590°C (b)

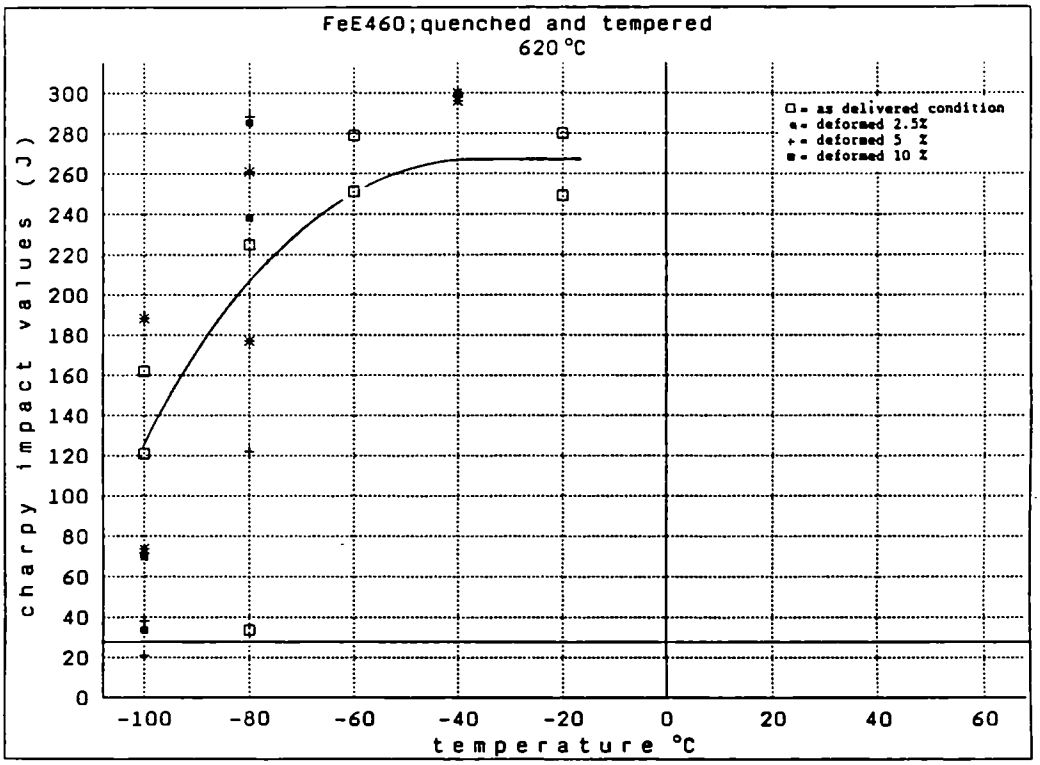

Figure 7.15: Results of the Charpy impact tests on the QT material rolled at 620°C

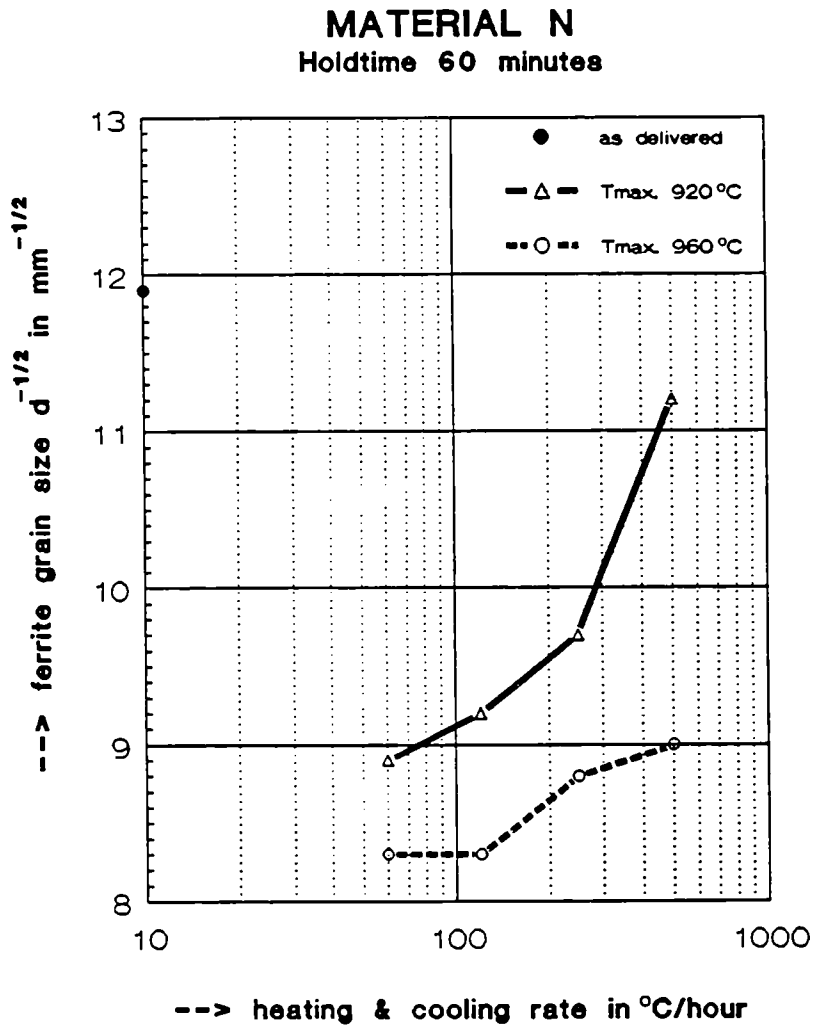

Figure 7.16: The ferrite grain size of material N as a function of the heat cycle

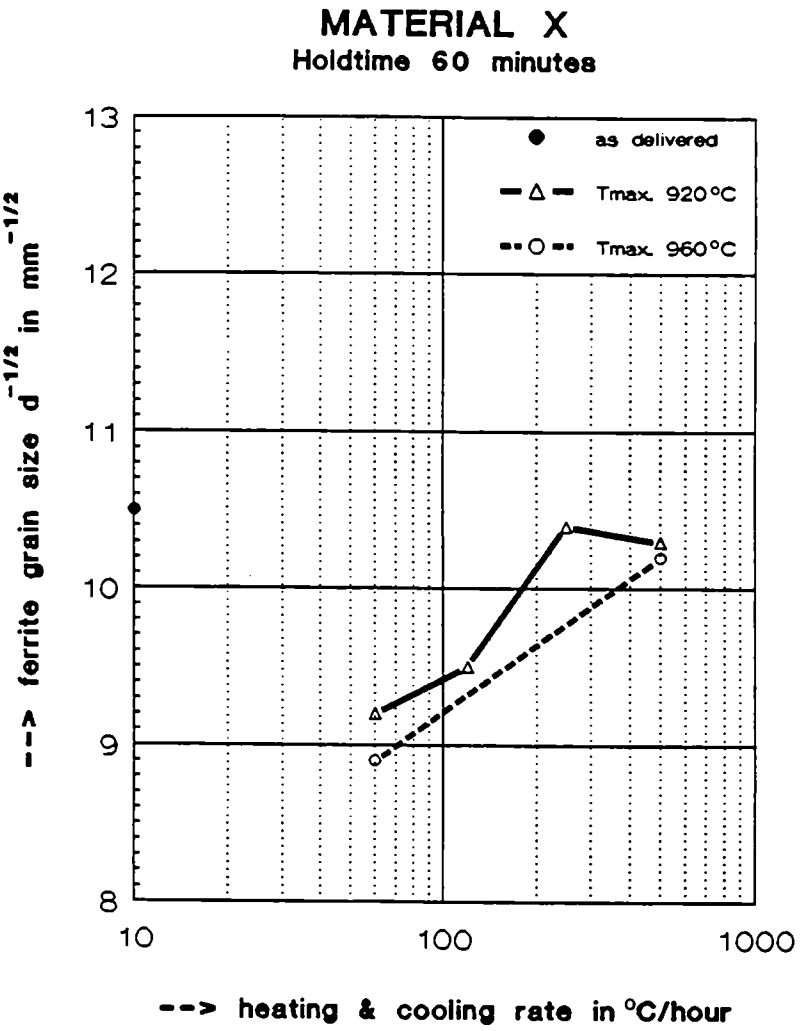

Figure 7.17: The ferrite grain size of material X as a function of the heat cycle

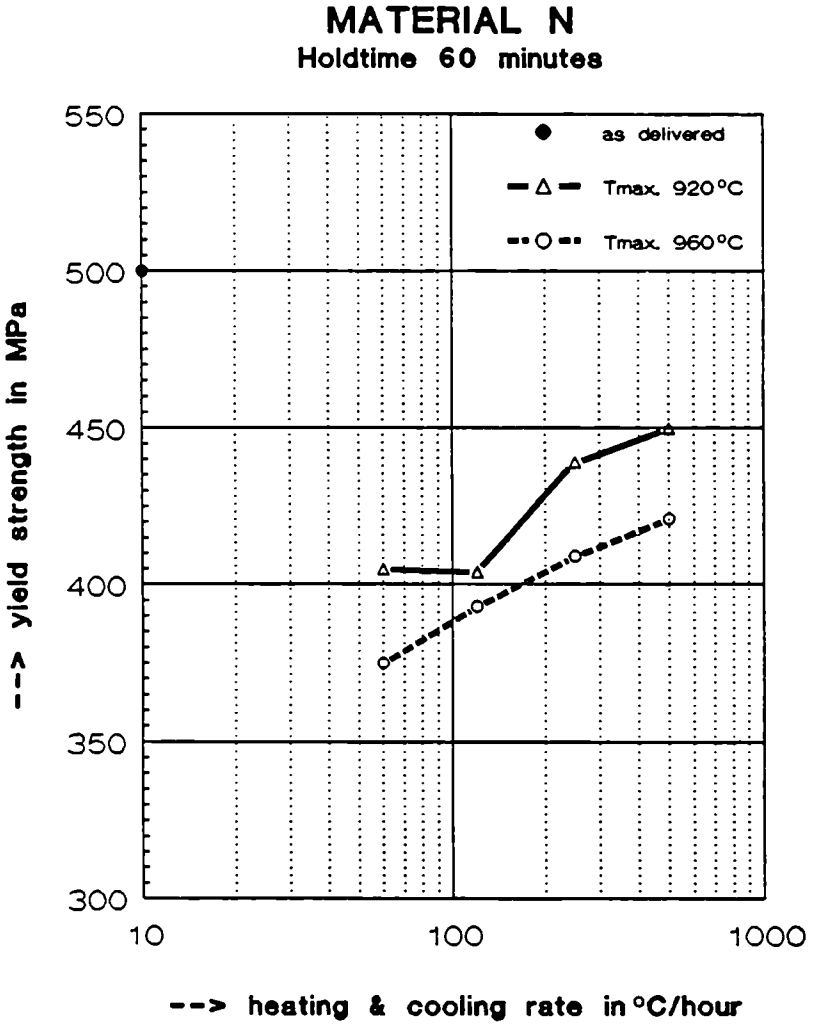

Figure 7.18: The yield strength of material N as a function of the heat cycle.

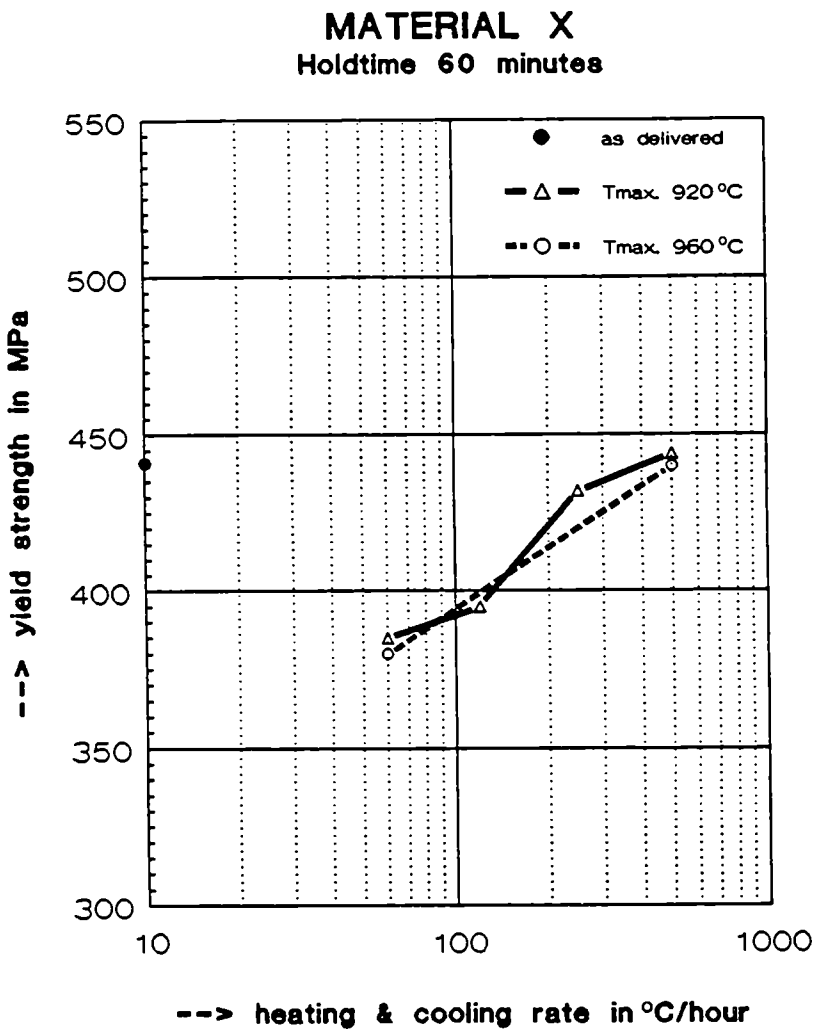

Figure 7.19: The yield strength of material X as a function of the heat cycle

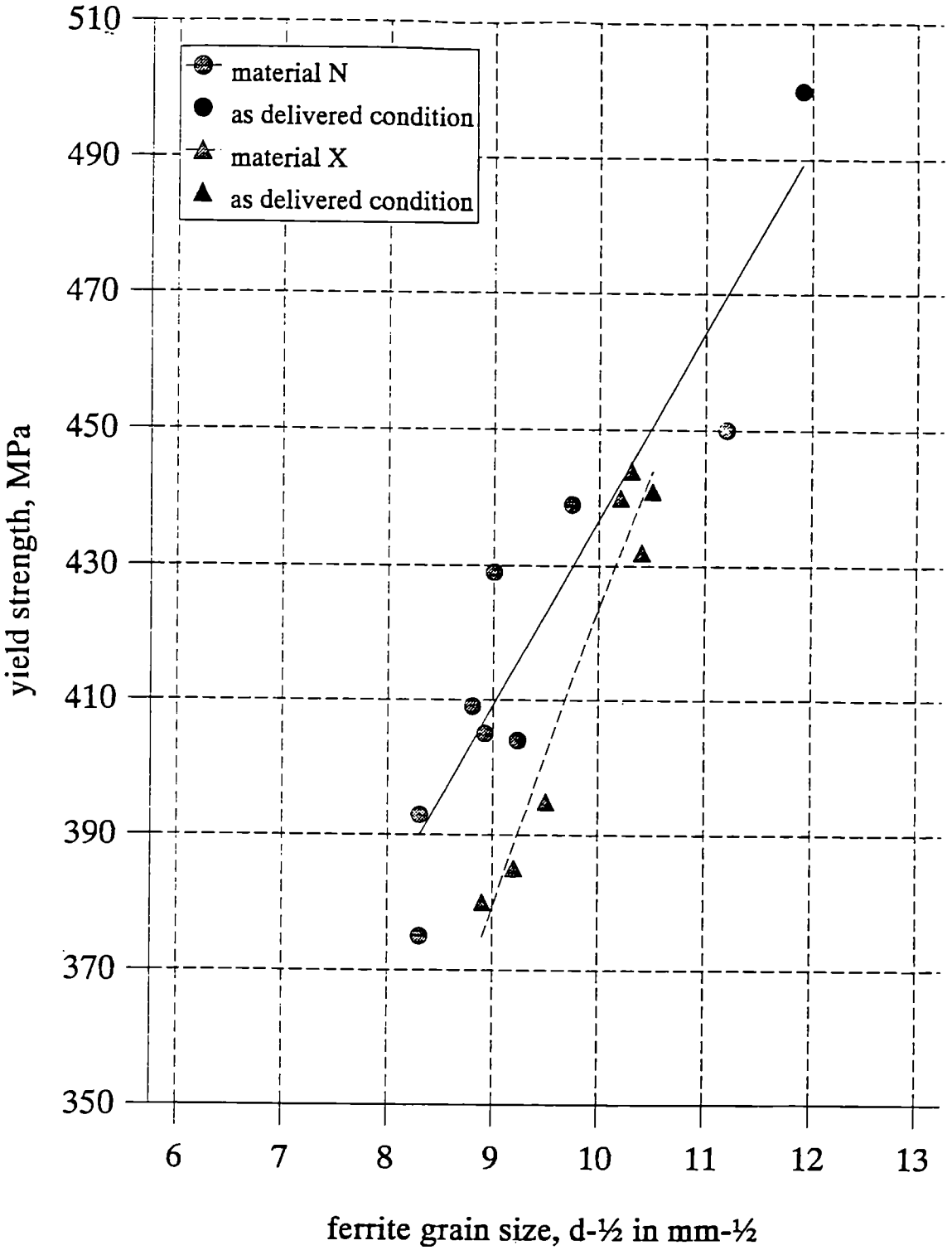

Figure 7.20: The yield strength of material N and X as a function of the ferrite grain size.

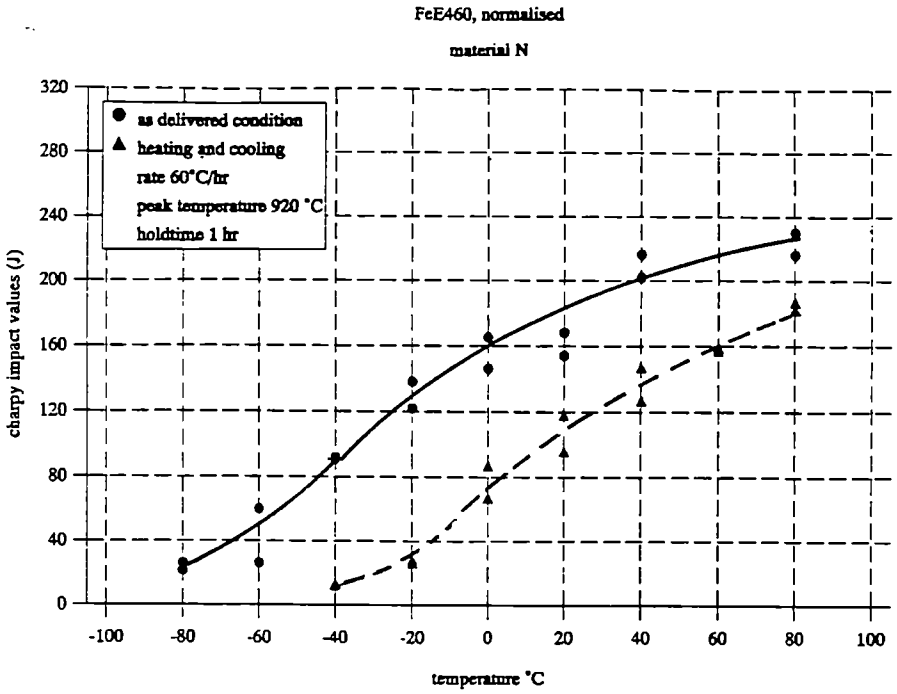

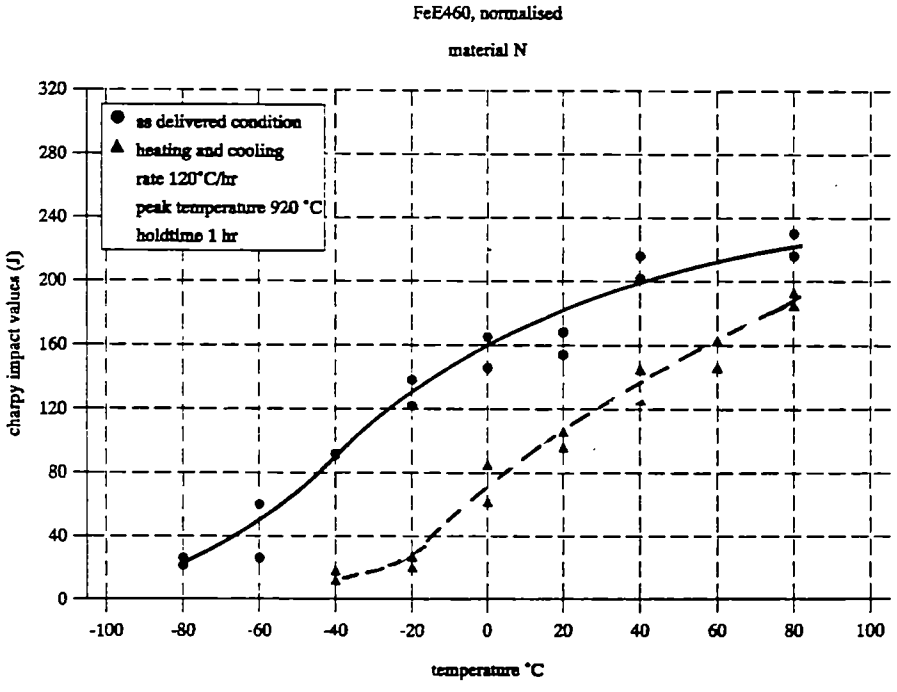

Figure 7.21: Charpy-V transition curves of material N after austenitizing at 920°C with a heating and cooling rate of 60 and 120°C/hr.

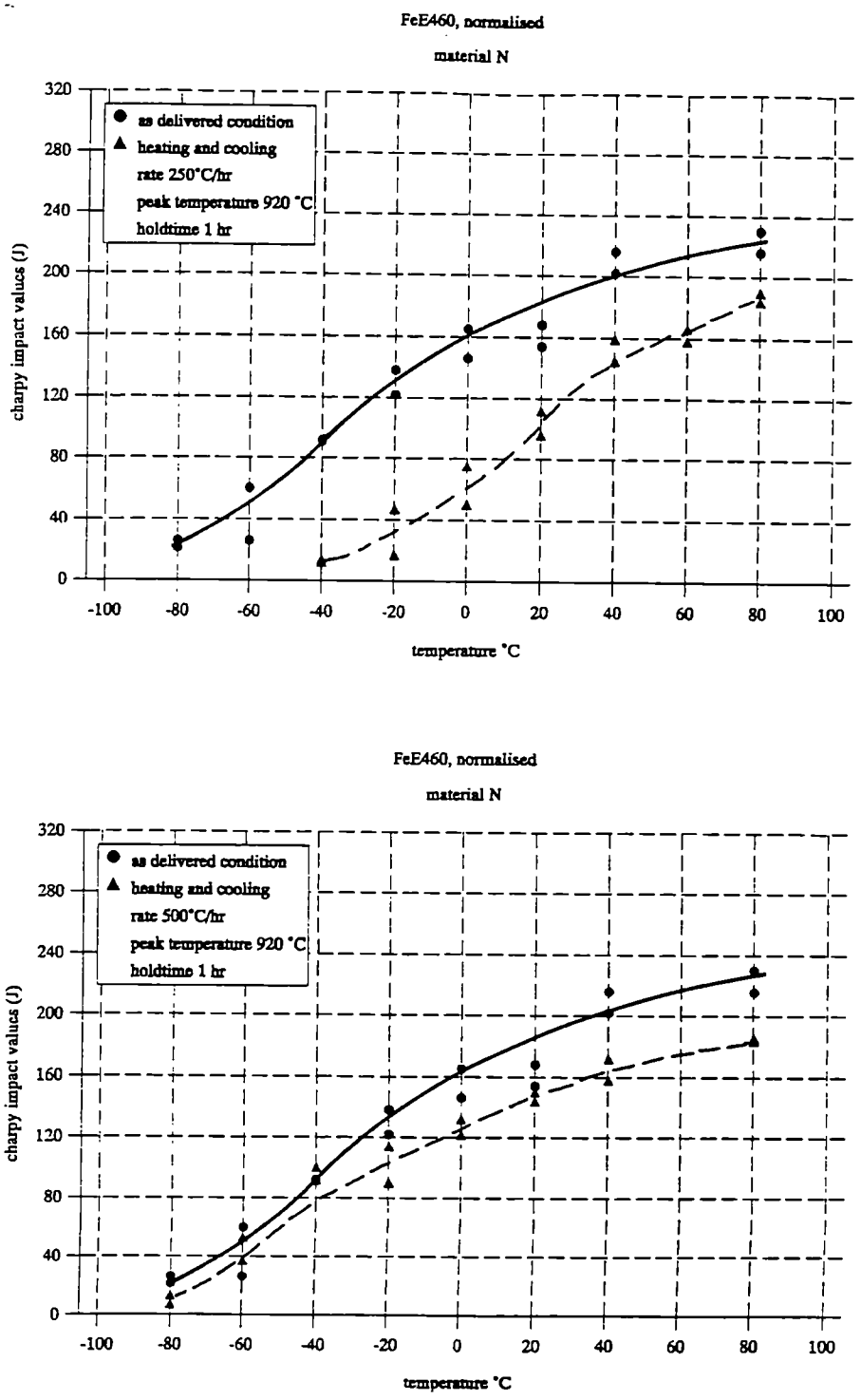

Figure 7.22: Charpy-V transition curves of material N after austenitizing at 920°C with a heating and cooling rate of 250 and 500°C/hr.

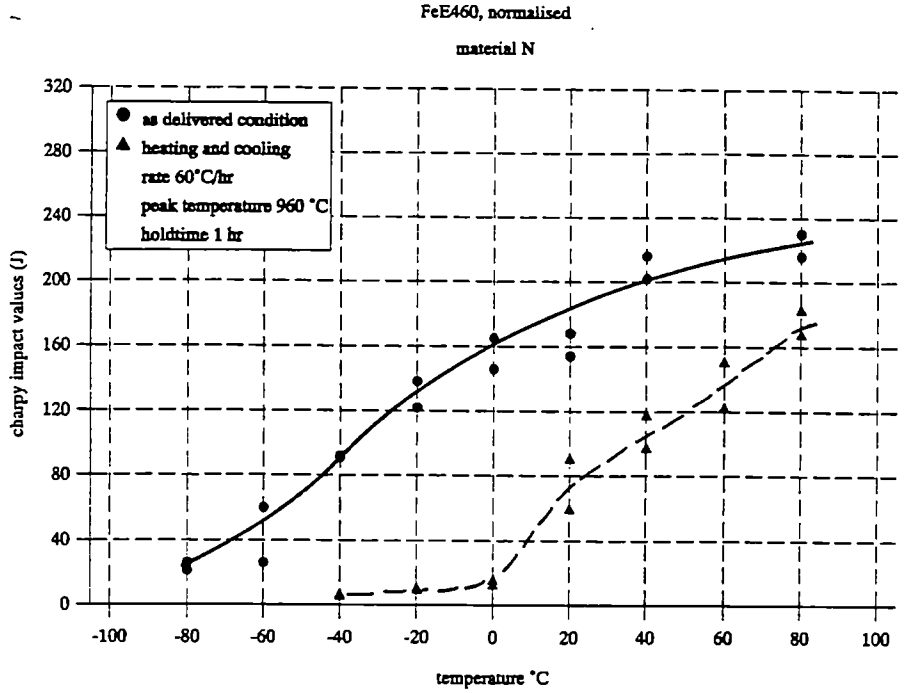

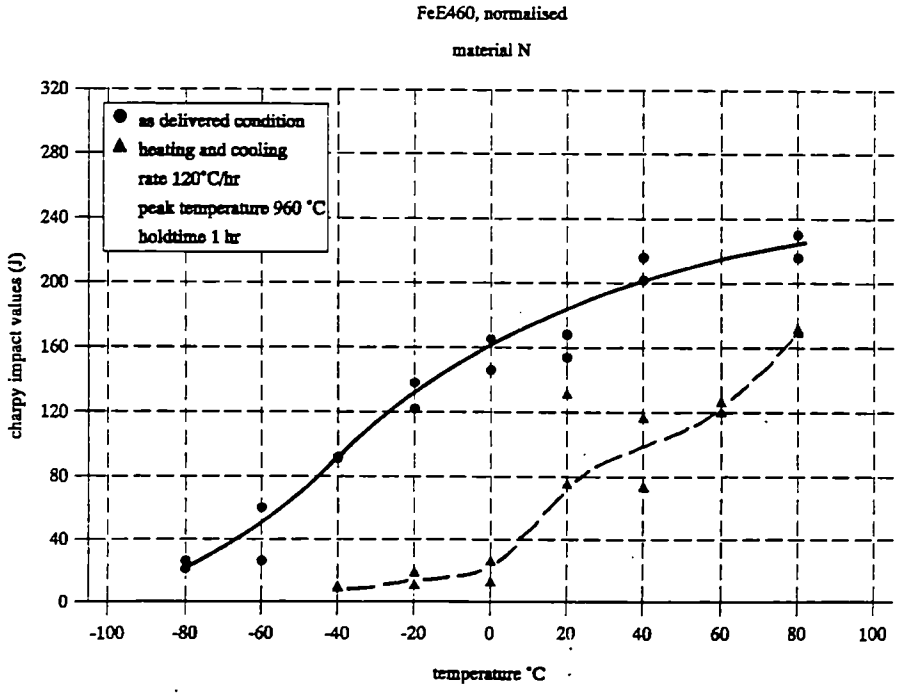

Figure 7.23: Charpy-V transition curves of material N after austenitizing at 960°C with a heating and cooling rate of 60 and 120°C/hr.

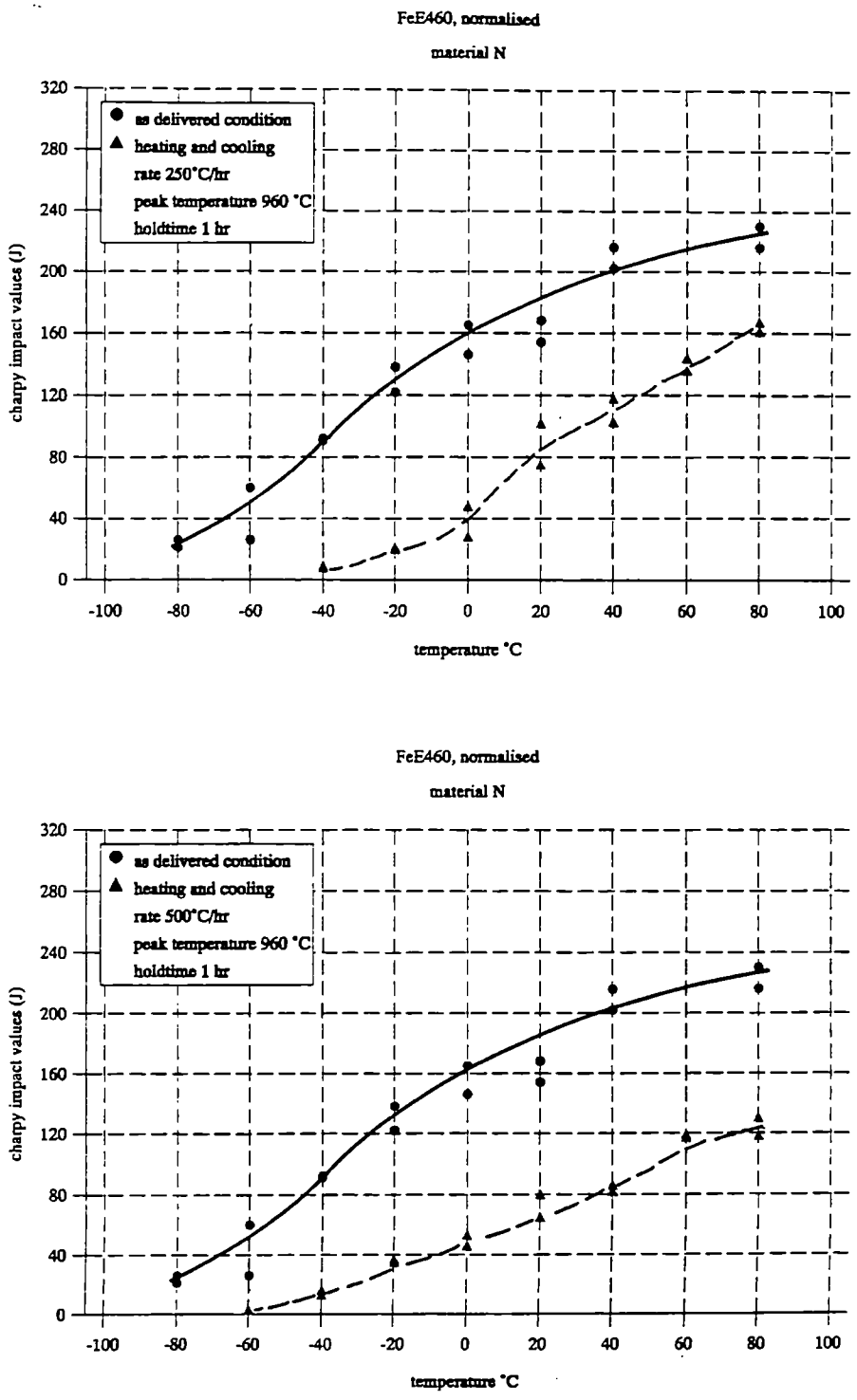

Figure 7.24: Charpy-V transition curves of material N after austenitizing at 960°C with a heating and cooling rate of 250 and 500°C/hr.

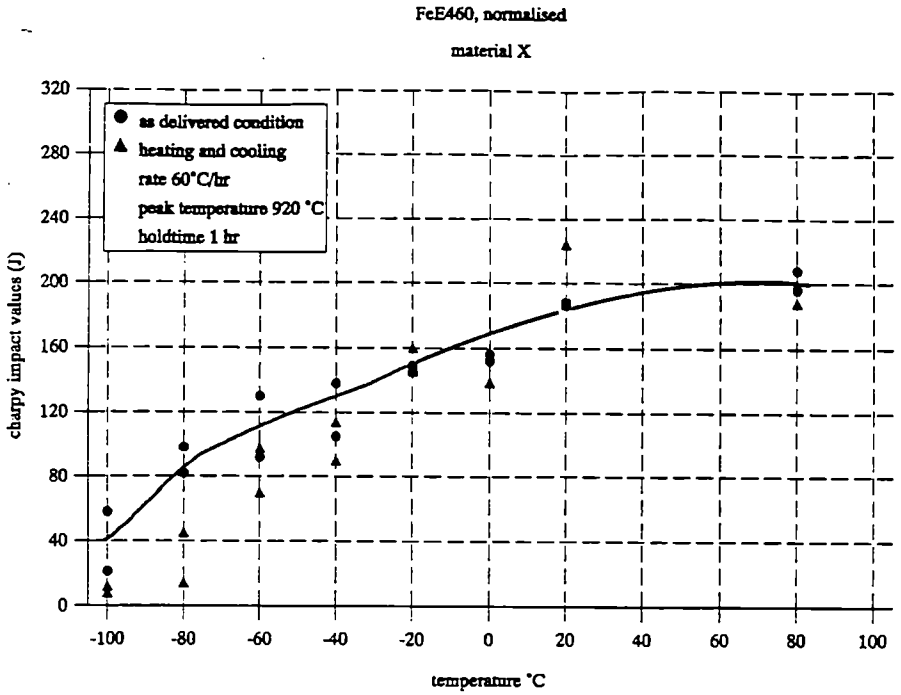

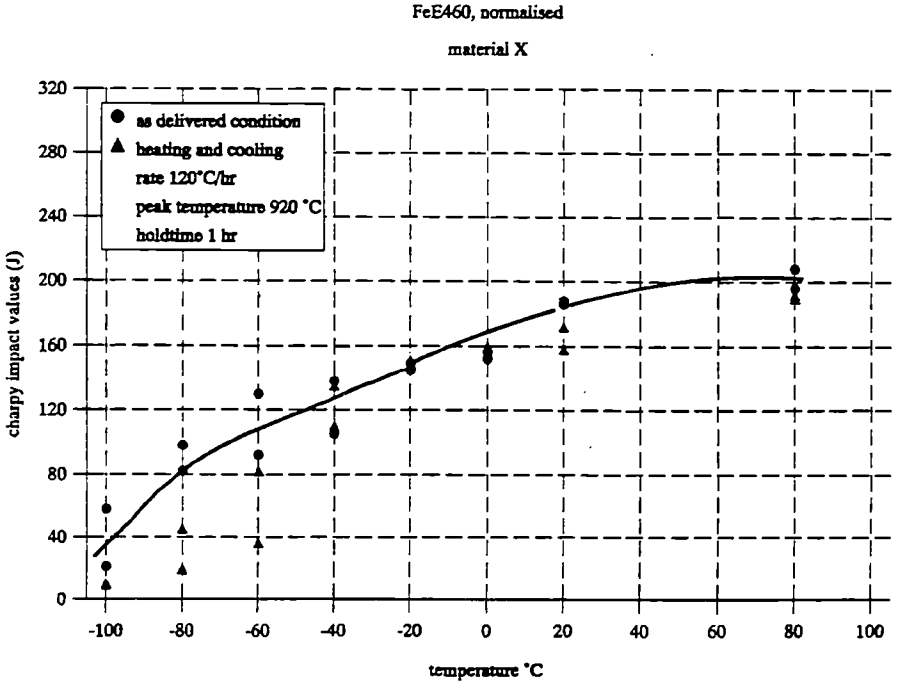

Figure 7.25: Charpy-V transition curves of material X after austenitizing at 920°C with a heating and cooling rate of 60 and 120°C/hr.

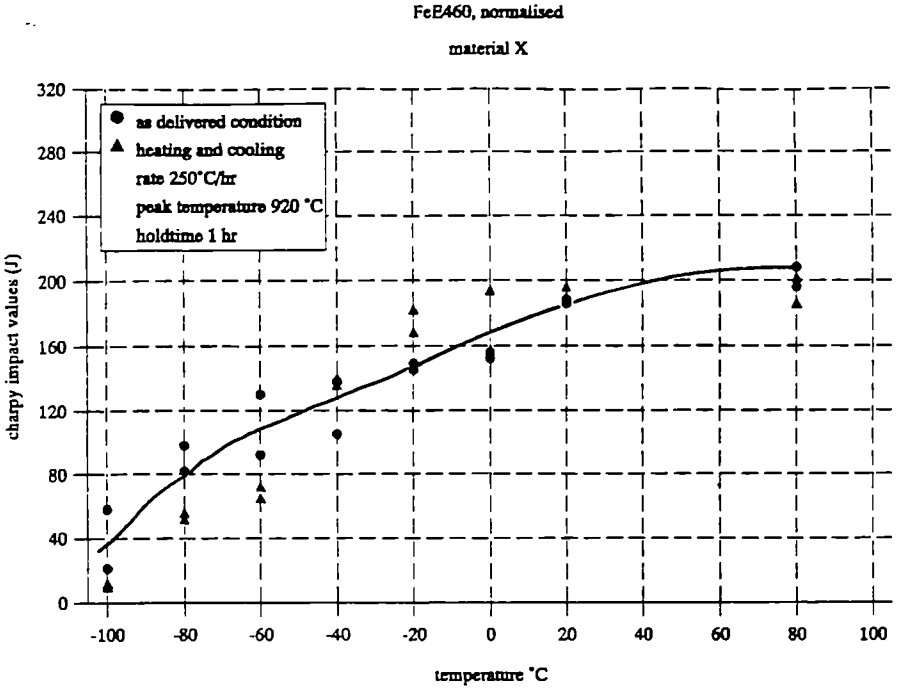

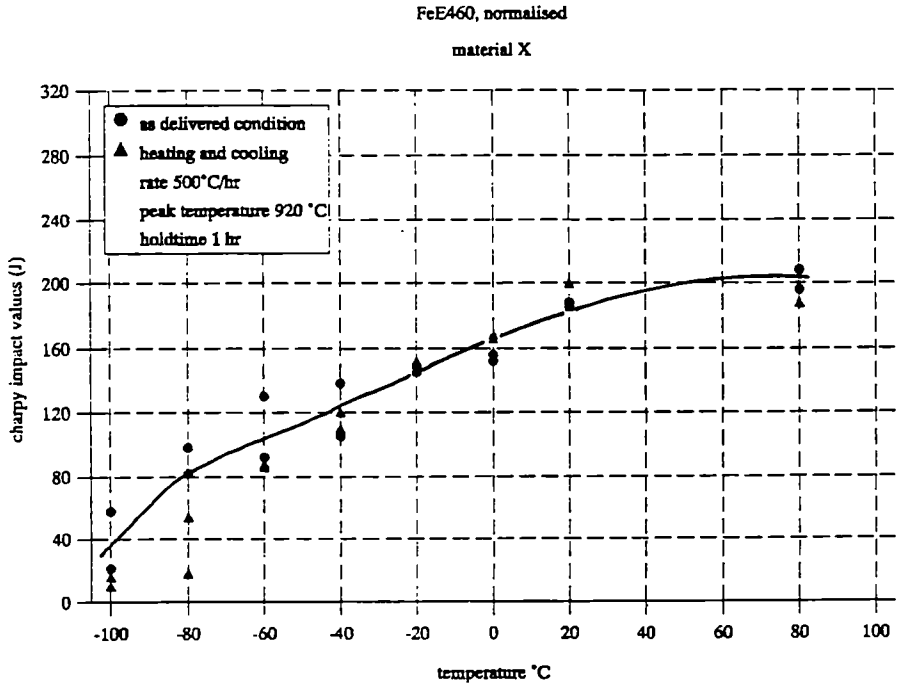

Figure 7.26: Charpy-V transition curves of material X after austenitizing at 920°C with a heating and cooling rate of 250 and 500°C/hr.

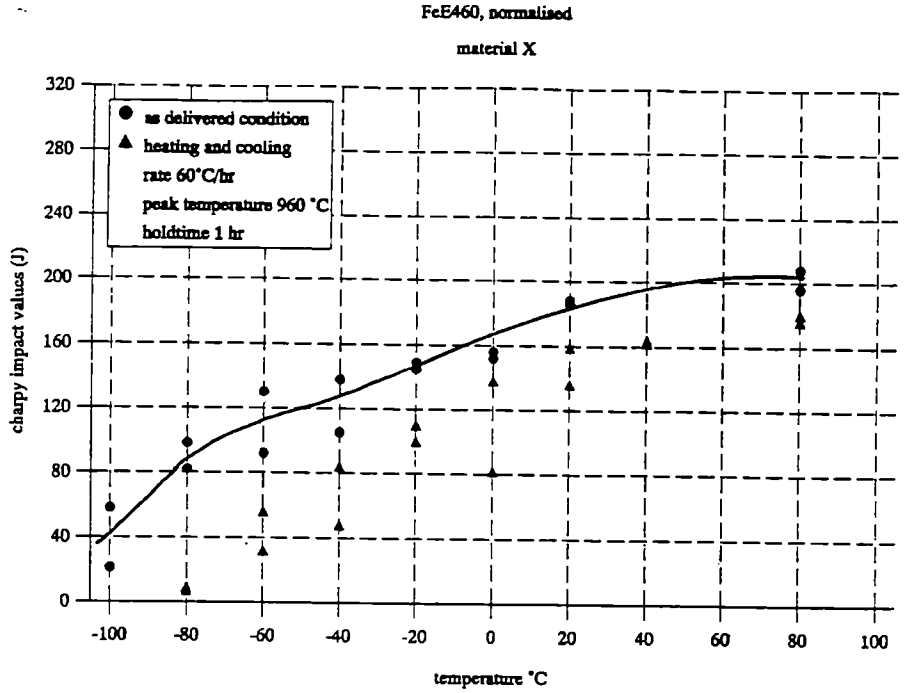

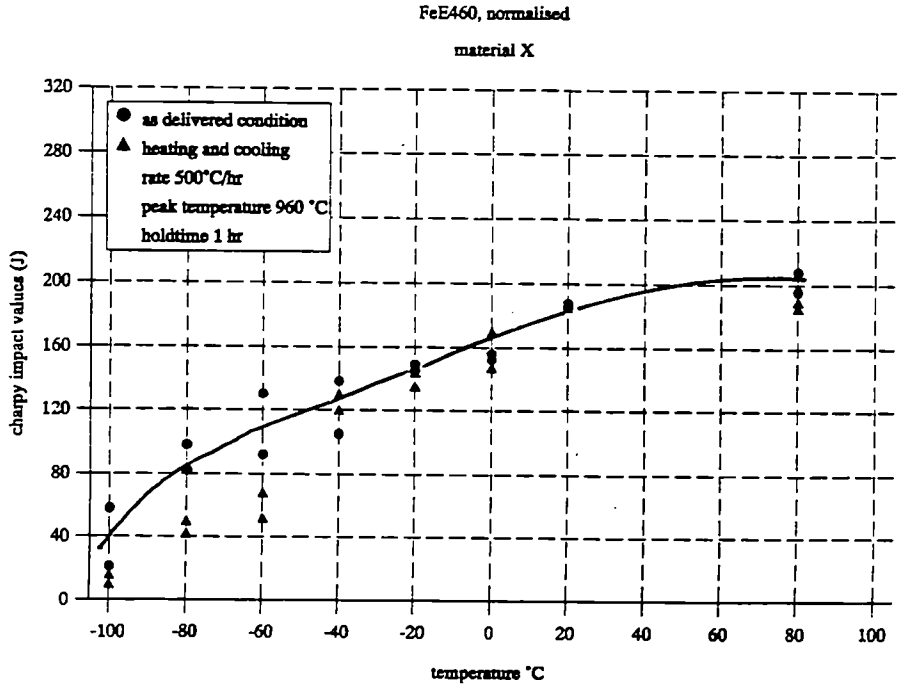

Figure 7.27: Charpy-V transition curves of material X after austenitizing at 960°C with a heating and cooling rate of 60 and 500°C/hr.

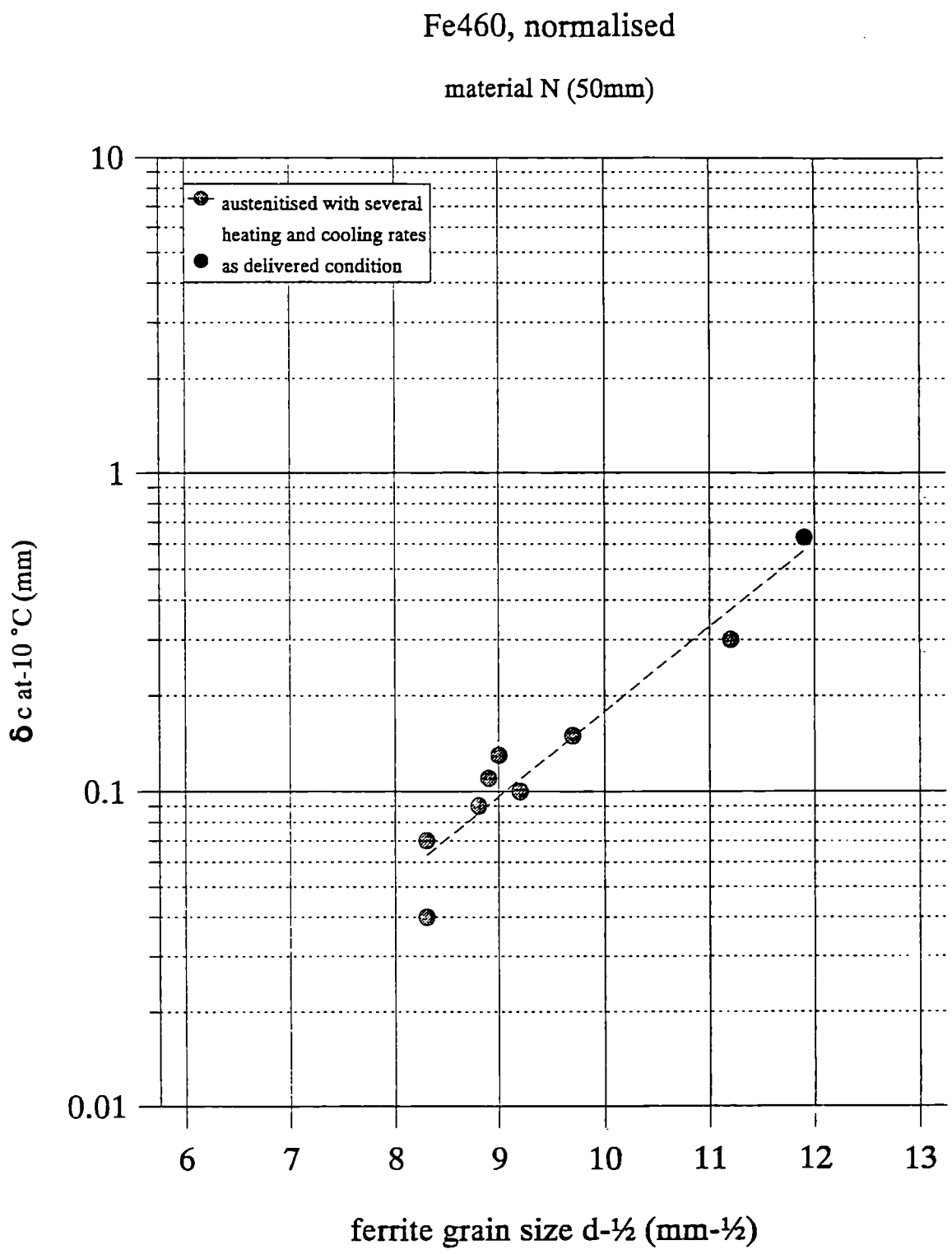

Figure 7.28: CTOD values of material N at -10°C as a function of the ferrite grain size.

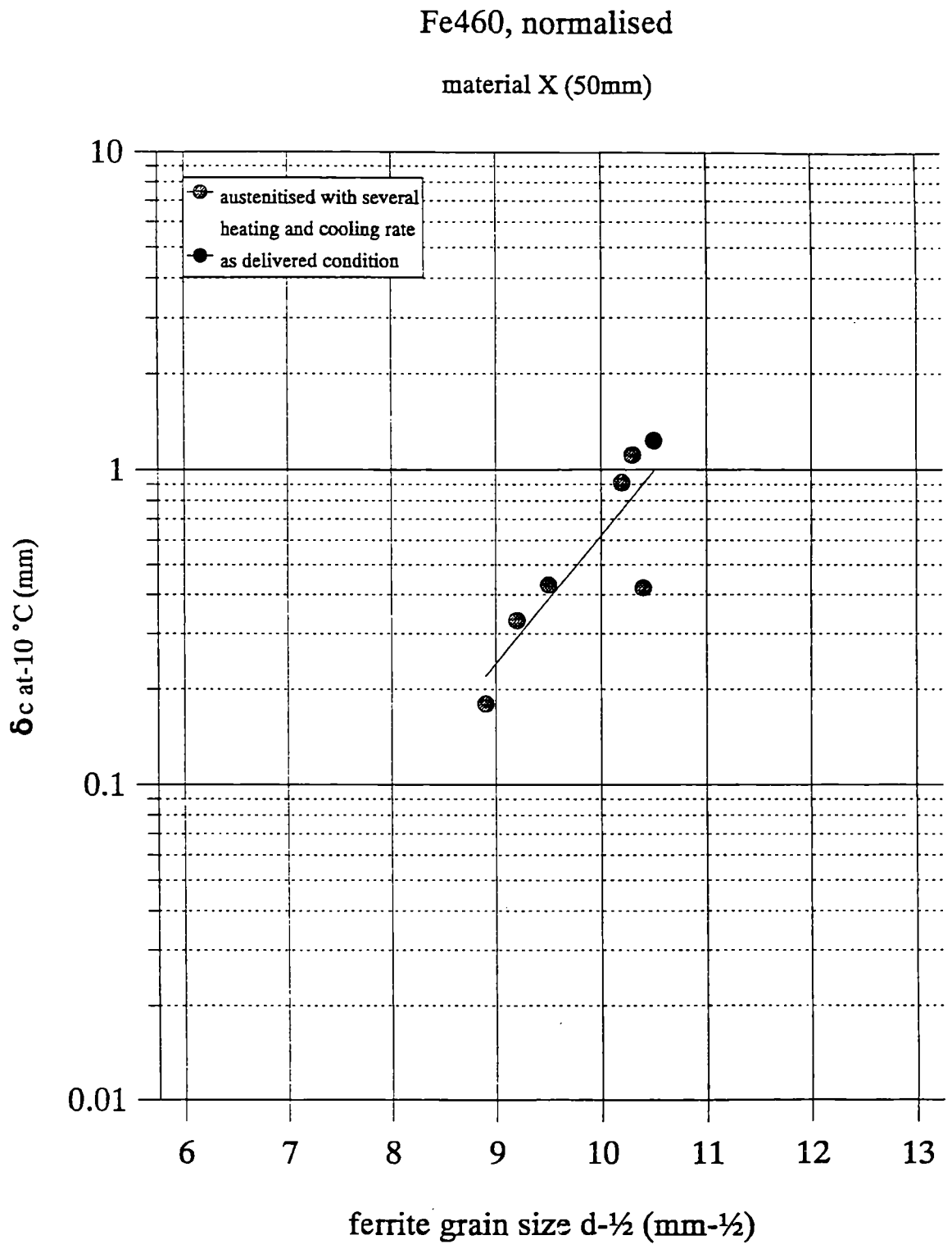

Figure 7.29: CTOD values of material X at -10°C as a function of the ferrite grain size.

APPENDIX 1

WELDING PROCEDURE : 1 **DATE** : 01-10-88
PROJECT : ECSC FeE 460 **PROPOSED BY** : VUIK
PROJECT NUMBER : **CHECKED BY** :
PROJECT LEADER : VUIK **REVISION** : DD - -

Material used : FeE 460 N, TM AND QT
Thickness (mm) : 15
Welding process 1 : SMAW
Welding process 2 : NA
Manual or Machine : MANUAL
Position of welding : 1 G
Filler material 1 spec. : LSN KRYO 2
Filler material 1 class. : AWS SFA5.5 E9018G
Filler material 2 spec. : NA
Filler material 2 class. : NA
Flux : NA
Condition of consumables : VACUUM PACKAGE
Groove preparation : OX. CUTTING + GRINDING
Shielding gas : NA
Backing gas : NA
Welding current : DC
Polarity : ELECTRODE +
Preheat method : GAS
Preheat temperature : MIN. 100 deg. C
Interpass temperature : MAX. 150 deg. C
Check method : THERMO-COUPLE
PWHT : NA

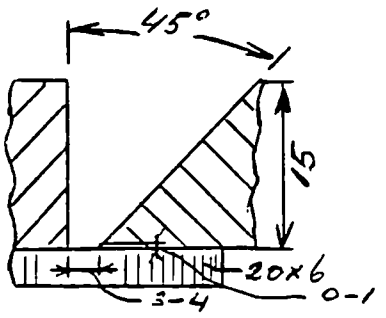

Type of bevel : 1/2 V
Angle (+/- 5 deg.) : 45
Root face (mm) : 0-1
Gap (mm) : 3-4
Flow (l/min) : --
Flow (l/min) : --
Backing strip : STEEL
Back gouging after run : NA
Restraint : MEDIUM
Strongbacks : 400*160*16 mm
a=1/2*t(sb), 3 per m weld
Stick-out SAW : -- mm
Stick-out MIG : -- mm

WELDING SEQUENCE

Pass no.	Process	Electr. size	Electr. param. Amps	Volts	Run out cm.	Travel speed cm/min	Heat input KJ/cm
1	1	3.25	90-100	24-25			13-15
2-N	1	4.0	150-170	25-26			10-12

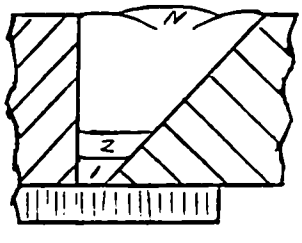

WELDING PROCEDURE : 2 **DATE** : 01-10-88

PROJECT : ECSC FeE 460 **PROPOSED BY** : VUIK

PROJECT NUMBER : **CHECKED BY** :

PROJECT LEADER : VUIK **REVISION** : DD - -

Material used	: FeE 460 N, TM AND QT
Thickness (mm)	: 15
Welding process 1	: SAW
Welding process 2	: NA
Manual or Machine	: MACHINE
Position of welding	: 1 G
Filler material 1 spec.	: OE. SD3Ni1
Filler material 1 class.	: DIN 8557 S3Ni1
Filler material 2 spec.	: NA
Filler material 2 class.	: NA
Flux	: OE. OP 121 TT
Condition of consumables	: AS DELIVERED
Groove preparation	: MACHINING
Shielding gas	: NA
Backing gas	: NA
Welding current	: DC
Polarity	: ELECTRODE +
Preheat method	: NA
Preheat temperature	: MIN. 10 deg. C
Interpass temperature	: MAX. 50 deg. C
Check method	: THERMO-COUPLE
PWHT	: NA

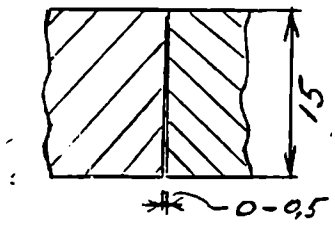

Type of bevel	: I	Flow (l/min)	: --
Angle (deg.)	: --	Flow (l/min)	: --
Root face (mm)	: 15	Backing strip	: NA
Gap (mm)	: 0-0.5	Back gouging after run	: NA
		Restraint	: NONE
		Strongbacks	: NA
		Stick-out SAW	: 30-35 mm
		Stick-out MIG	: -- mm

WELDING SEQUENCE

Pass no.	Process	Electr. size	Electr. param. Amps	Electr. param. Volts	Run out cm.	Travel speed cm/min	Heat input KJ/cm
A1	1	4.0	635-645	32-34		55	23.0
B1	1	4.0	770-780	32-34		60	25.6

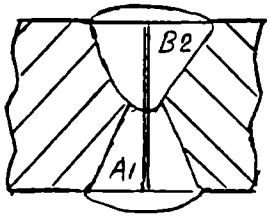

ELDING PROCEDURE	: 3	DATE	: 01-10-88
ROJECT	: ECSC FeE 460	PROPOSED BY	: VUIK
ROJECT NUMBER	:	CHECKED BY	:
ROJECT LEADER	: VUIK	REVISION	: DD - -

aterial used	: FeE 460 N, TM AND QT
ickness (mm)	: 50
elding process 1	: SMAW
elding process 2	: SAW
anual or Machine	: 1: MANUAL 2: MACHINE
osition of welding	: 1 G
iller material 1 spec.	: LSN KRYO 2
iller material 1 class.	: AWS SFA5.5 E9018G
iller material 2 spec.	: OE. SD3Ni1
iller material 2 class.	: DIN 8557 S3Ni1
lux	: OE. OP 121 TT
ondition of consumables	: VACUUM PACK./AS DELIVERED
roove preparation	: OX. CUTTING + GRINDING
ielding gas	: NA
acking gas	: NA
elding current	: DC
olarity	: ELECTRODE +
reheat method	: GAS
reheat temperature	: MIN. 100 deg. C
nterpass temperature	: MAX. 150 deg. C
heck method	: THERMO-COUPLE
WHT	: NA

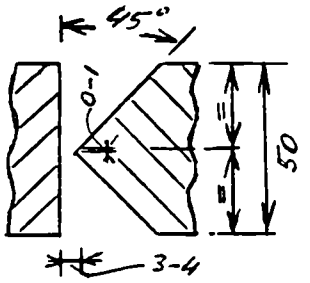

Type of bevel	: K
Angle (+/- 5 deg.)	: 45
Root face (mm)	: 0-1
Gap (mm)	: 3-4
Flow (l/min)	: --
Flow (l/min)	: --
Backing strip	: NA
Back gouging after run	: NA
Restraint	: MEDIUM
Strongbacks	: 600*250*25 mm
a=1/2*t(sb), 3 per m weld	
Stick-out SAW	: 30-35 mm
Stick-out MIG	: -- mm

ELDING SEQUENCE

Pass no.	Process	Electr. size	Electr. param. Amps	Volts	Run out cm.	Travel speed cm/min	Heat input KJ/cm
A1	1	3.25	100-110				20-25
A2,3	1	4.0	175-190	26-27			13-16
A4	2	4.0	460-480	26-27		50	15-16
A5-N	2	4.0	570-580	30-31		50	20-21
GRINDING, 3-4 MM DEEP							
B1	2	4.0	570-580	26-27		50	18
B2	2	4.0	570-580	28-29		50	19-20
B3-M	2	4.0	570-580	30-31		50	20-21

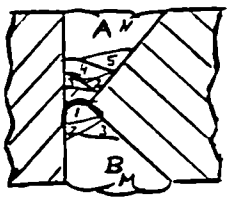

WELDING PROCEDURE	**: 4**	**DATE**	**: 01-10-88**
PROJECT	**: ECSC FeE 460**	**PROPOSED BY**	**: VUIK**
PROJECT NUMBER	**:**	**CHECKED BY**	**:**
PROJECT LEADER	**: VUIK**	**REVISION**	**: DD - -**

Material used	: FeE 460 N, TM AND QT
Thickness (mm)	: 50
Welding process 1	: SMAW
Welding process 2	: SAW
Manual or Machine	: 1: MANUAL 2: MACHINE
Position of welding	: 1 G
Filler material 1 spec.	: LSN KRYO 2
Filler material 1 class.	: AWS SFA5.5 E9018G
Filler material 2 spec.	: OE. SD3Ni1
Filler material 2 class.	: DIN 8557 S3Ni1
Flux	: OE. OP 121 TT
Condition of consumables	: VACUUM PACK./AS DELIVERED
Groove preparation	: OX. CUTTING + GRINDING
Shielding gas	: NA
Backing gas	: NA
Welding current	: DC
Polarity	: ELECTRODE +
Preheat method	: GAS
Preheat temperature	: MIN. 150 deg. C
Interpass temperature	: 200 deg. C
Check method	: THERMO-COUPLE
PWHT	: NA

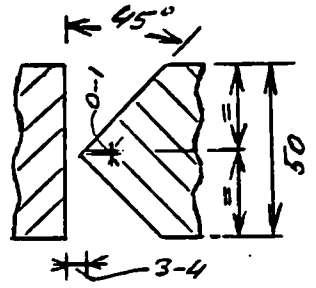

Type of bevel	: K
Angle (+/- 5 deg.)	: 45
Root face (mm)	: 0-1
Gap (mm)	: 3-4
Flow (1/min)	: --
Flow (1/min)	: --
Backing strip	: NA
Back gouging after run	: NA
Restraint	: MEDIUM
Strongbacks	: 600*250*25 mm
a=1/2*t(sb), 3 per m weld	
Stick-out SAW	: 30-35 mm
Stick-out MIG	: -- mm

WELDING SEQUENCE

Pass no.	Process	Electr. size	Electr. param. Amps	Volts	Run out cm.	Travel speed cm/min	Heat input KJ/cm
A1	1	3.25	100-110				20-25
A2	1	4.0	175-190	26-27			20-25
A3	2	4.0	460-480	26-27		50	15-16
A4-N	2	4.0	650-670	30-31		35	34-35
GRINDING, 3-4 MM DEEP							
B1	2	4.0	650-670	27-28		35	31-32
B2-M	2	4.0	650-670	30-31		35	34-35

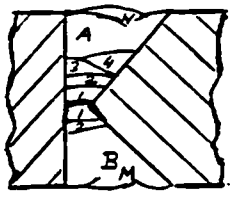

ELDING PROCEDURE	: 5	**DATE**	: 01-09-89
ROJECT	: ECSC FeE 460	**PROPOSED BY**	: VUIK
ROJECT NUMBER	:	**CHECKED BY**	:
ROJECT LEADER	: VUIK	**REVISION**	: DD - -

aterial used	: FeE 460 N, TM AND QT
hickness (mm)	: 50
elding process 1	: SAW
elding process 2	: NA
anual or Machine	: MACHINE
osition of welding	: 1 G
iller material 1 spec.	: OE. SD3Ni1
iller material 1 class.	: DIN 8557 S3Ni1
iller material 2 spec.	: NA
iller material 2 class.	: NA
lux	: OE. OP 121 TT
ondition of consumables	: AS DELIVERED
roove preparation	: MACHINING
hielding gas	: NA
acking gas	: NA
elding current	: DC
olarity	: ELECTRODE +
reheat method	: GAS
reheat temperature	: MIN. 100 deg. C
nterpass temperature	: MAX. 150 deg. C
heck method	: THERMO-COUPLE
WHT	: NA

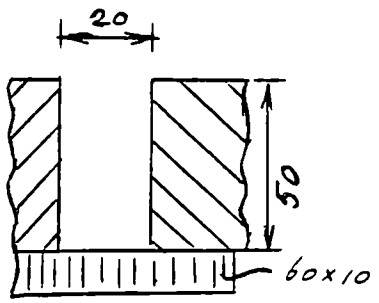

Type of bevel	: I
Angle (deg.)	: --
Root face (mm)	: 50
Gap (mm)	: 20
Flow (l/min)	: --
Flow (l/min)	: --
Backing strip	: NA
Back gouging after run	: NA
Restraint	: MEDIUM
Strongbacks	: 600*250*25 mm
a=1/2*t(sb), 3 per m weld	
Stick-out SAW	: 30-35 mm
Stick-out MIG	: -- mm

ELDING SEQUENCE

Pass no.	Process	Electr. size	Electr. param. Amps	Volts	Run out cm.	Travel speed cm/min	Heat input KJ/cm
A1-N	1	4.0	570-580	30-31			20-21

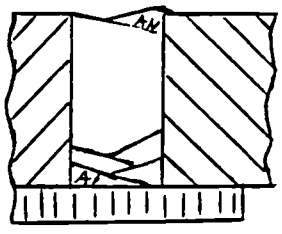

WELDING PROCEDURE : 6 **DATE** : 01-09-89

PROJECT : ECSC FeE 460 **PROPOSED BY** : VUIK

PROJECT NUMBER : **CHECKED BY** :

PROJECT LEADER : VUIK **REVISION** : DD - -

Material used	: FeE 460 N, TM AND QT
Thickness (mm)	: 50
Welding process 1	: SAW
Welding process 2	: NA
Manual or Machine	: MACHINE
Position of welding	: 1 G
Filler material 1 spec.	: OE. SD3Ni1
Filler material 1 class.	: DIN 8557 S3Ni1
Filler material 2 spec.	: NA
Filler material 2 class.	: NA
Flux	: OE. OP 121 TT
Condition of consumables	: AS DELIVERED
Groove preparation	: MACHINING
Shielding gas	: NA
Backing gas	: NA
Welding current	: DC
Polarity	: ELECTRODE +
Preheat method	: GAS
Preheat temperature	: MIN. 150 deg. C
Interpass temperature	: 200 deg. C
Check method	: THERMO-COUPLE
PWHT	: NA

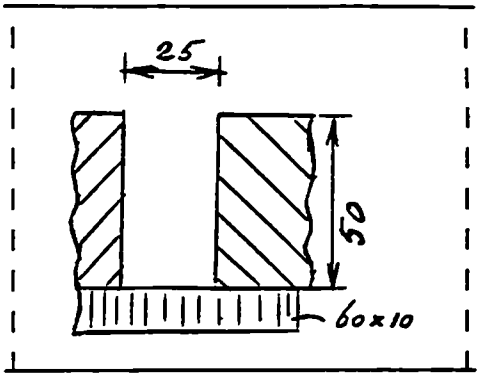

Type of bevel	: I
Angle (deg.)	: --
Root face (mm)	: 50
Gap (mm)	: 25
Flow (l/min)	: --
Flow (l/min)	: --
Backing strip	: NA
Back gouging after run	: NA
Restraint	: MEDIUM
Strongbacks	: 600*250*25 mm
	a=1/2*t(sb), 3 per m weld
Stick-out SAW	: 30-35 mm
Stick-out MIG	: -- mm

WELDING SEQUENCE

Pass no.	Process	Electr. size	Electr. param. Amps	Volts	Run out cm.	Travel speed cm/min	Heat input KJ/cm
A1-N	1	4.0	650-670	30-31			34-35

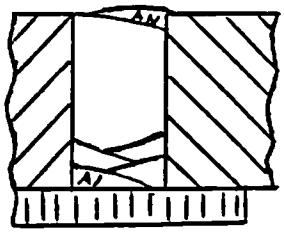

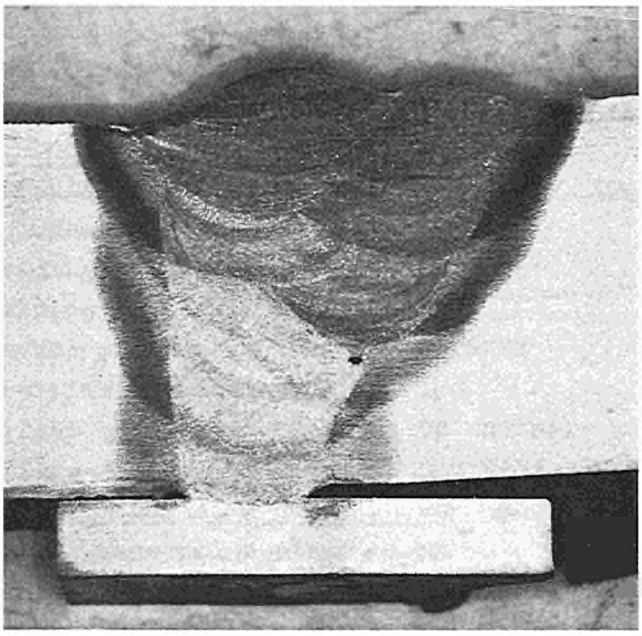

a

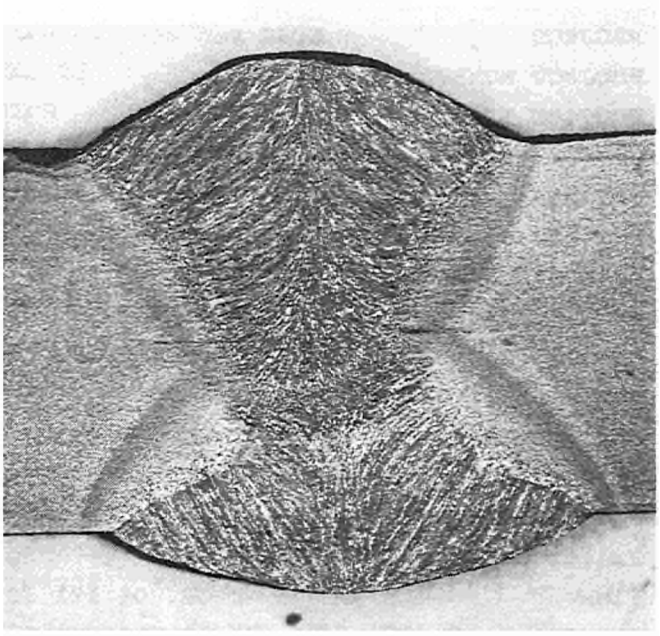

b

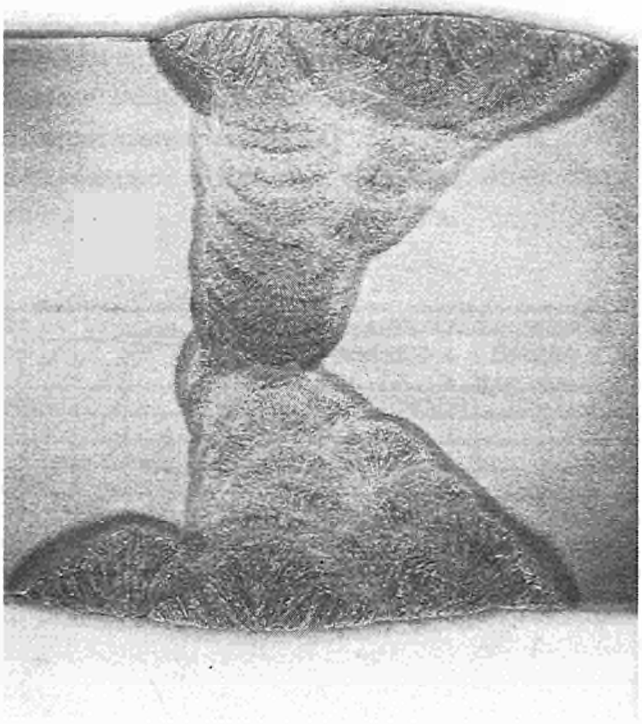

c

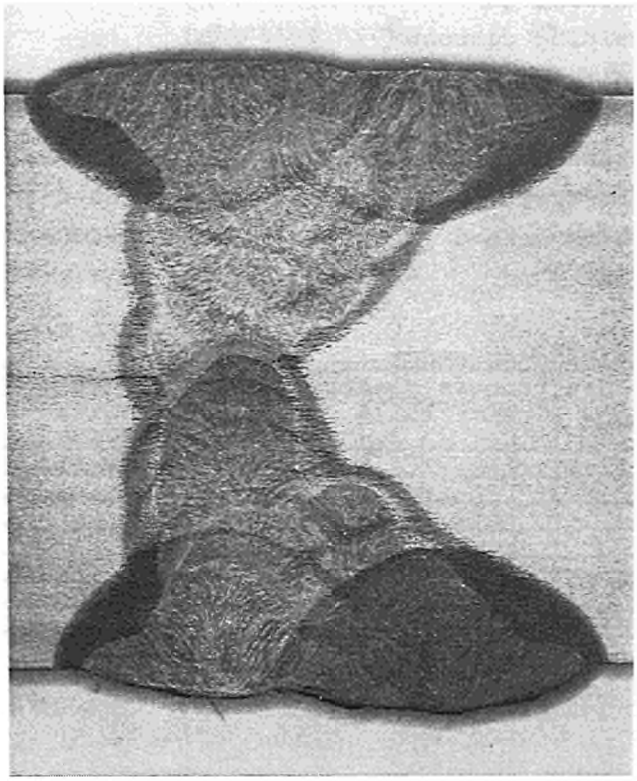

d

Figure A1: Examples of macrostructures of the testwelds:
a = SMAW, N, 15 mm b = SAW, QT, 15 mm
c = SAW, N, 50 mm, 22 kJ/cm d = SAW, QT, 50 mm, 35 kJ/cm

APPENDIX 2

Pressure Vessel 1.

Pressure vessel 1 is designed to withstand an internal pressure of 3.85 MPa (38.5 bar) at a service temperature of 100°C. The vessel will be erected on site, and has therefore been equipped with a skirt.
All calculations have been performed according to "Dienst voor het Stoomwezen", the Dutch certifying authority for boilers and pressure vessels. The rules of "Dienst voor het Stoomwezen" prescribe Post Weld Heat Treatment for wall thicknesses over 32 mm.

Data concerning the vessel:

Diameter (Di)	: 3500 mm
Length	: 32000 mm
Wall thickness cylinder	: based on calculations using the Re and Rm values at 100°C: Re = 294 Mpa Rm = 490 Mpa Allowable stress: minimum of 0,67*Re or 0,5*Rm => 197 Mpa => wall thickness = 34,6 mm + 3 mm corrosion allowance => wall thickness used = 38 mm
Manholes	: 2 : 24" diameter
Nozzles	: 4 : 18" diameter 4 : 8" diamete 2 : 4" diameter
NDT	: 100% Radiograph testing + 100% Ultrasonic testing before PWHT, 100% Ultrasonic testing after PWHT

Recalculation* of the wall thicknes of the cylinder is be manufactured in FeE 460, leads to a wall thickness of 27,6 mm. This value is based on Re (100°C) = 402 Mpa, and Rm (100°C) = 560 Mpa.
Adding the corrosion allowance, the wall thickness in FeE 460 amount to 31 mm.

*: As the vessel in FeE 460 will not be post weld heat treated, only the minimum value of 0,67*Re and 0,44*Rm is allowed as operating stress.

Pressure vessel 2.

Pressure vessel 2 is an upright standing vessel, designed to withstand 11 MPa internal pressure at an operating temperature of 200°C.

Data concerning the vessel:

Diameter (Di)	: 2350 mm
Length	: 29663 mm
Wall thickness cylinder:	based on Re(200°C) = 235 Mpa
	Rm(200°C) = 470 Mpa
	wall thickness = mm
	+ 3 mm corrosion allowance
	=> wall thicknes used = 89 mm
Manhole	: 1 : 20" diameter
Nozzles	: 2 : 16" diameter
NDT	: 100% Ultrasonic testing before PWHT,
	100% Ultrasonic testing after PWHT

Recalculation of the wall thickness of the cylinder is be manufactured in FeE 460, leads to a wall thickness of 57,8 mm. This value is based on Re(200°C) = 343 Mpa, and Rm(200°C) = 560 Mpa. Adding the corrosion allowance, the wall thickness in FeE 460 amounts to 61 mm.

Pressure vessel 3.

Pressure vessel 3 is designed to withstand an internal pressure of 3,5 MPa at a service temperature of 100°C. Like vessel 1 and 2, is an upright standing vessel.

Data concerning the vessel

Diameter (Di)	: 2500 mm
Length	: 20000 mm
Wall thickness cylinder:	based on Re(100°) = 304 Mpa
	Rm(100°) = 490 Mpa
	Wall thickness = 21,8 mm
	+ 3 mm corrosion allowance
	=> wall thickness used = 25 mm
Manhole	: 1 x 20" diameter
Nozzles	: 2 x 20" diameter
	2 x 18" diameter
	4 x 12" diameter
	6 x 4" diameter
NDT	: 100% Radiograph testing +
	100% Ultrasonic testing

Recalculation of the wall thickness of the cylinder manufactured in FeE 460 leads to a wall thickness of 17,9 mm.
This value is based on Re = 402 MPa
Rm = 560 MPa.
Adding the corrosion allowance, the wall thickness in FeE 460 amounts to 21 mm.

Re and Rm values of StE355 and StE460 (DIN 17102) as a function of wall thickness and temperature.

Temperature	Steel type	Re/Rm	Re and Rm values as a function of wall thickness: wall thickness (mm)								
			≤16	≤ 35	≤ 50	≤ 60	≤ 70	≤ 85	≤100	≤125	≤150
RT	StE355	Re	≥355	≥355	≥345	≥335	≥335	≥325	≥315	≥305	≥295
		Rm	490-630	490-630	490-630	490-630	490-630	480-620	470-610	460-600	450-590
	StE460	Re	≥460	≥450	≥440	≥430	≥420	≥410	≥400	≥390	≥380
		Rm	560-730	560-730	560-730	560-730	560-730	550-720	540-710	530-700	520-690
100°C	StE355	Re	≥304	≥304	≥294	≥294	≥294	≥284	≥275	≥265	≥255
	StE460	Rm	≥402	≥402	≥392	≥392	≥392	≥382	≥373	≥363	≥353
200°C	StE355	Re	≥255	≥255	≥255	≥255	≥255	≥245	≥235	≥226	≥216
	StE460	Rm	≥343	≥343	≥343	≥343	≥343	≥333	≥324	≥314	≥304

Rm values are considered not to be effected by temperatures up to 200°C.

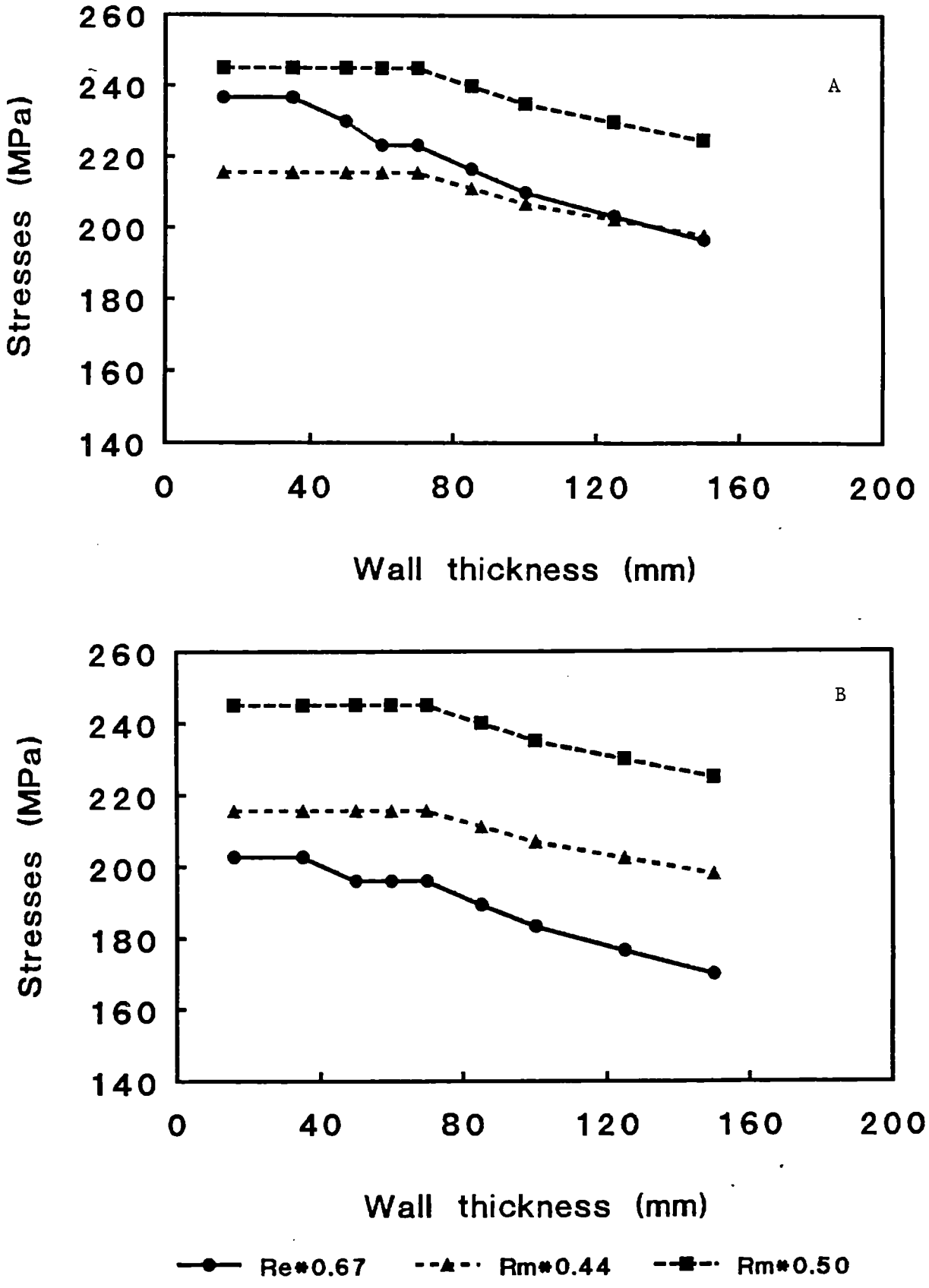

Figure A3.1: Stresses to be used in the calculations for FeE 355 at 20°C (A) and 100°C (B).

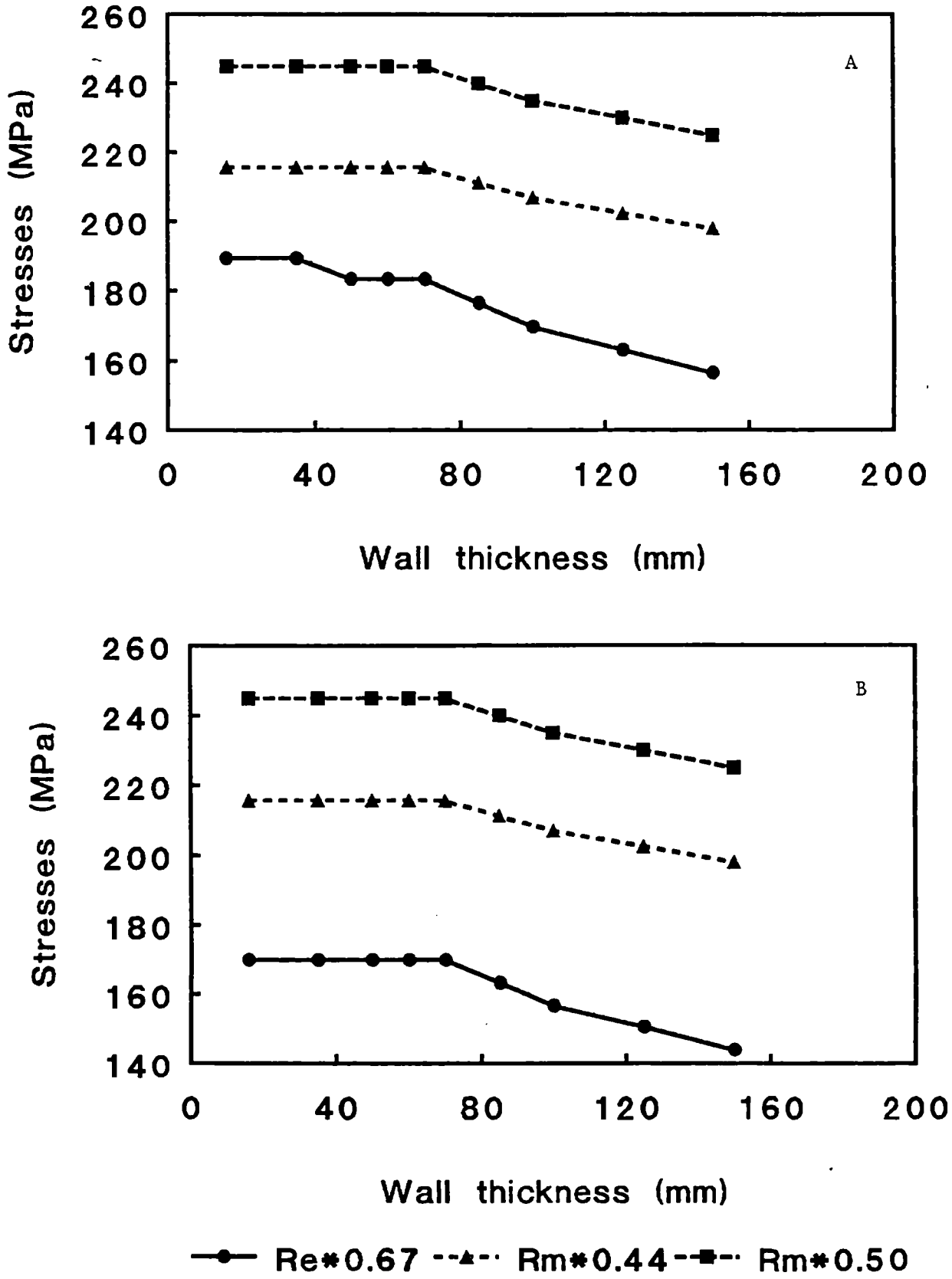

Figure A3.2: Stresses to be used in the calculations for FeE 355 at 150°C (A) and 200°C (B).

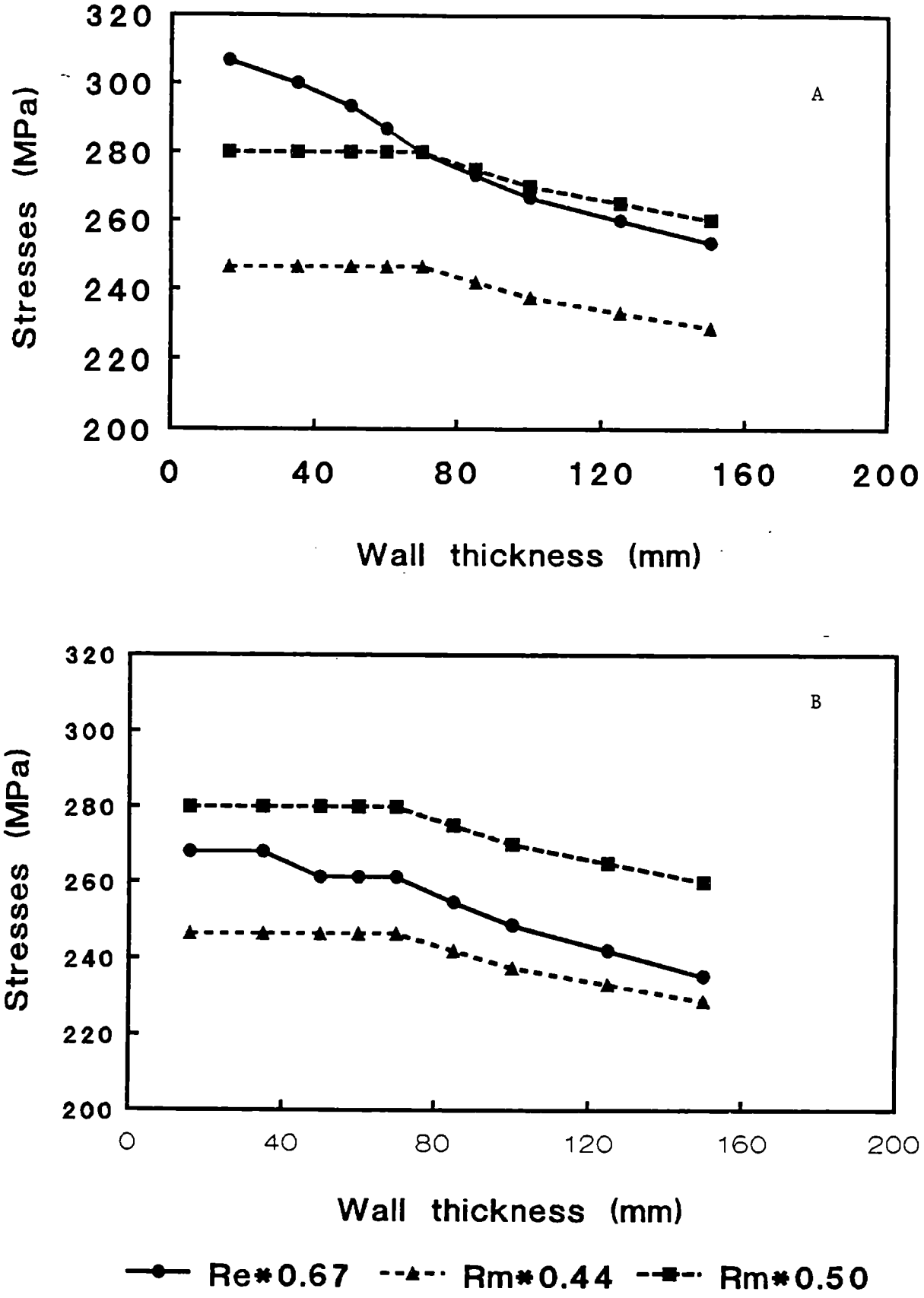

Figure A3.3: Stressess to be used in the calculations for FeE 460 at 20°C (A) and 100°C (B).

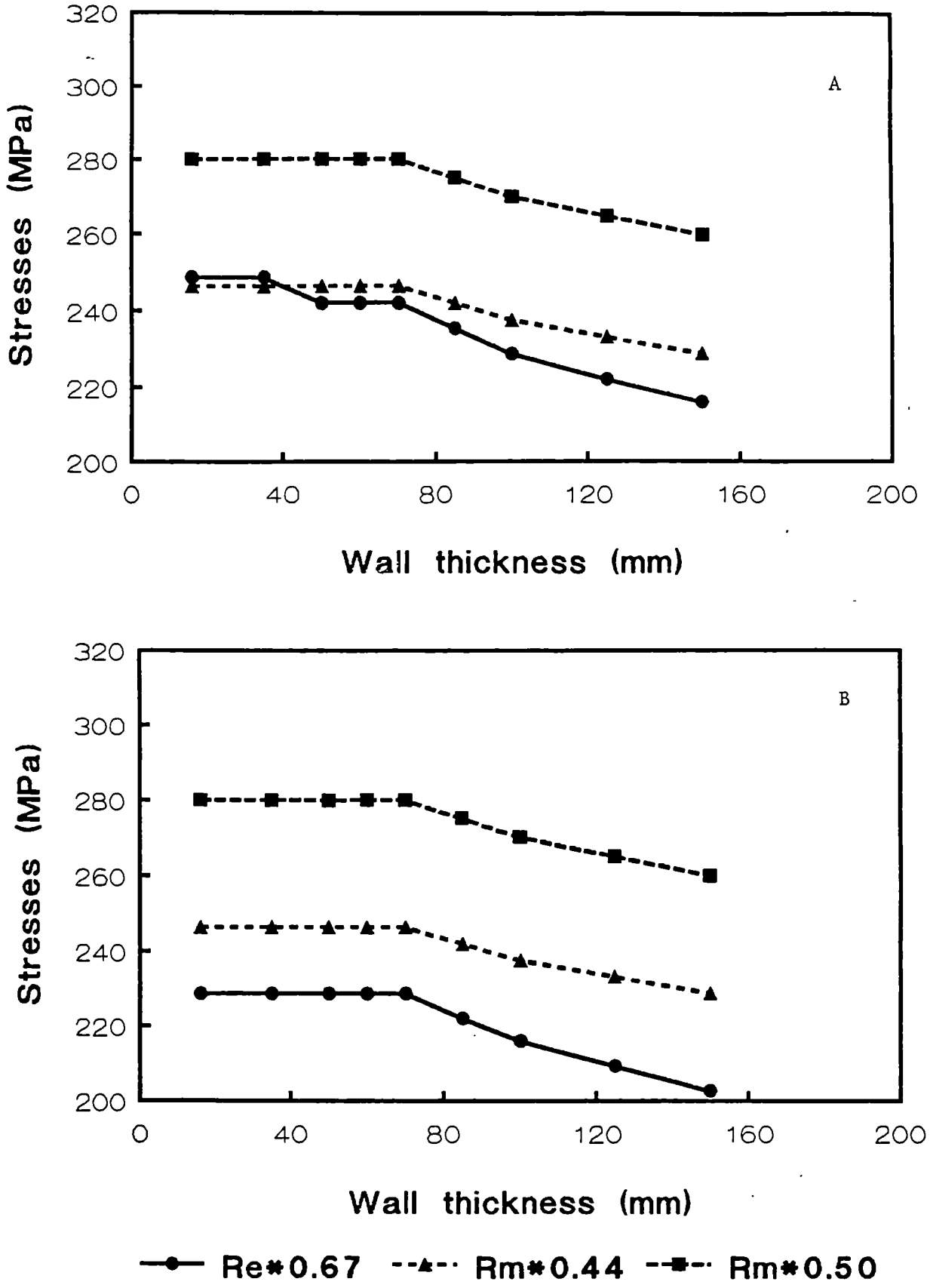

Figure A3.4: Stresses to be used in the calculations for FeE 460 at 150°C (A) and 200°C (B).

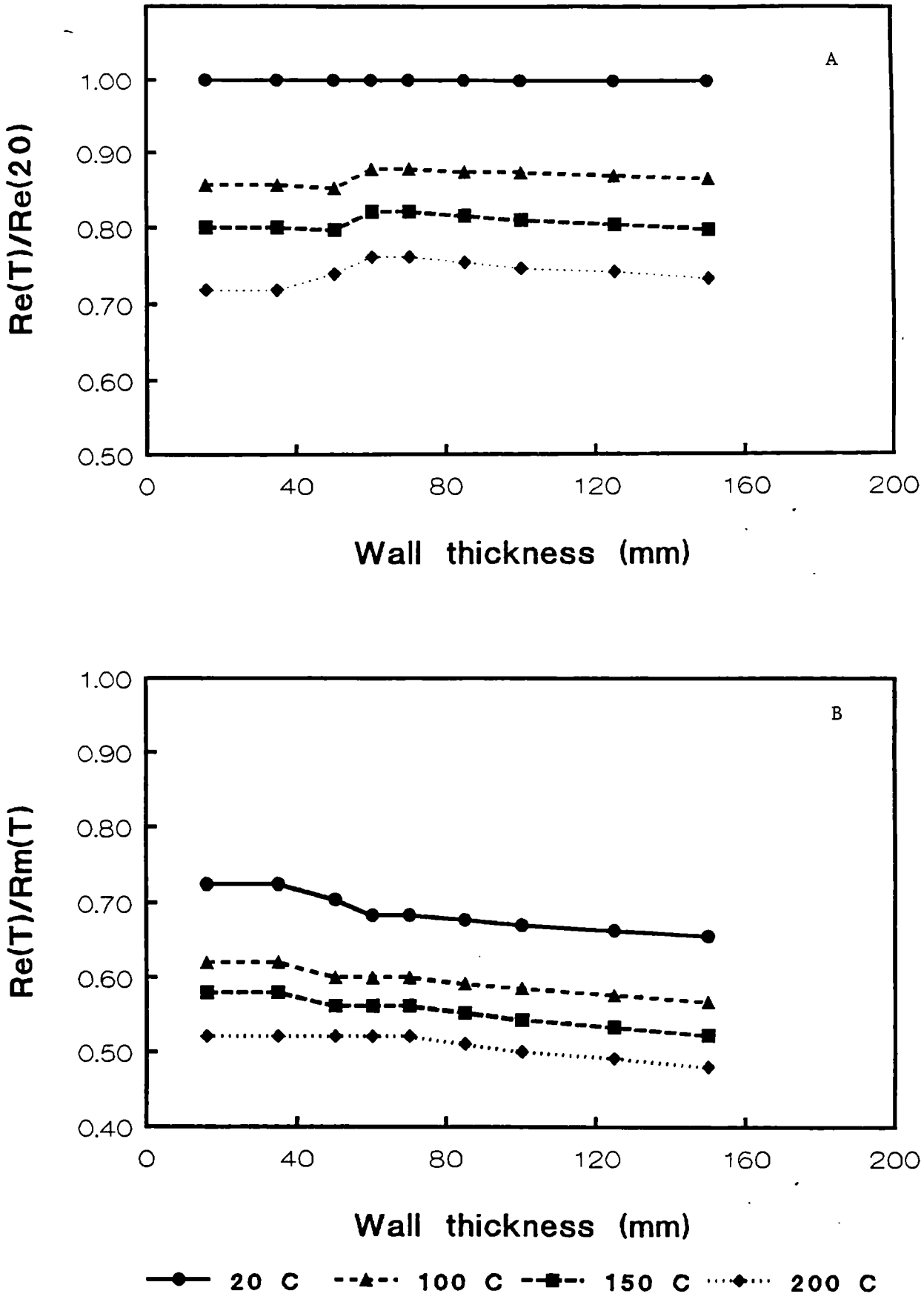

Figure A4.1: Re(T)/Re(20) (A) and Re(T)/Rm(T) (B) as a function of wall thickness and temperature for FeE 355.

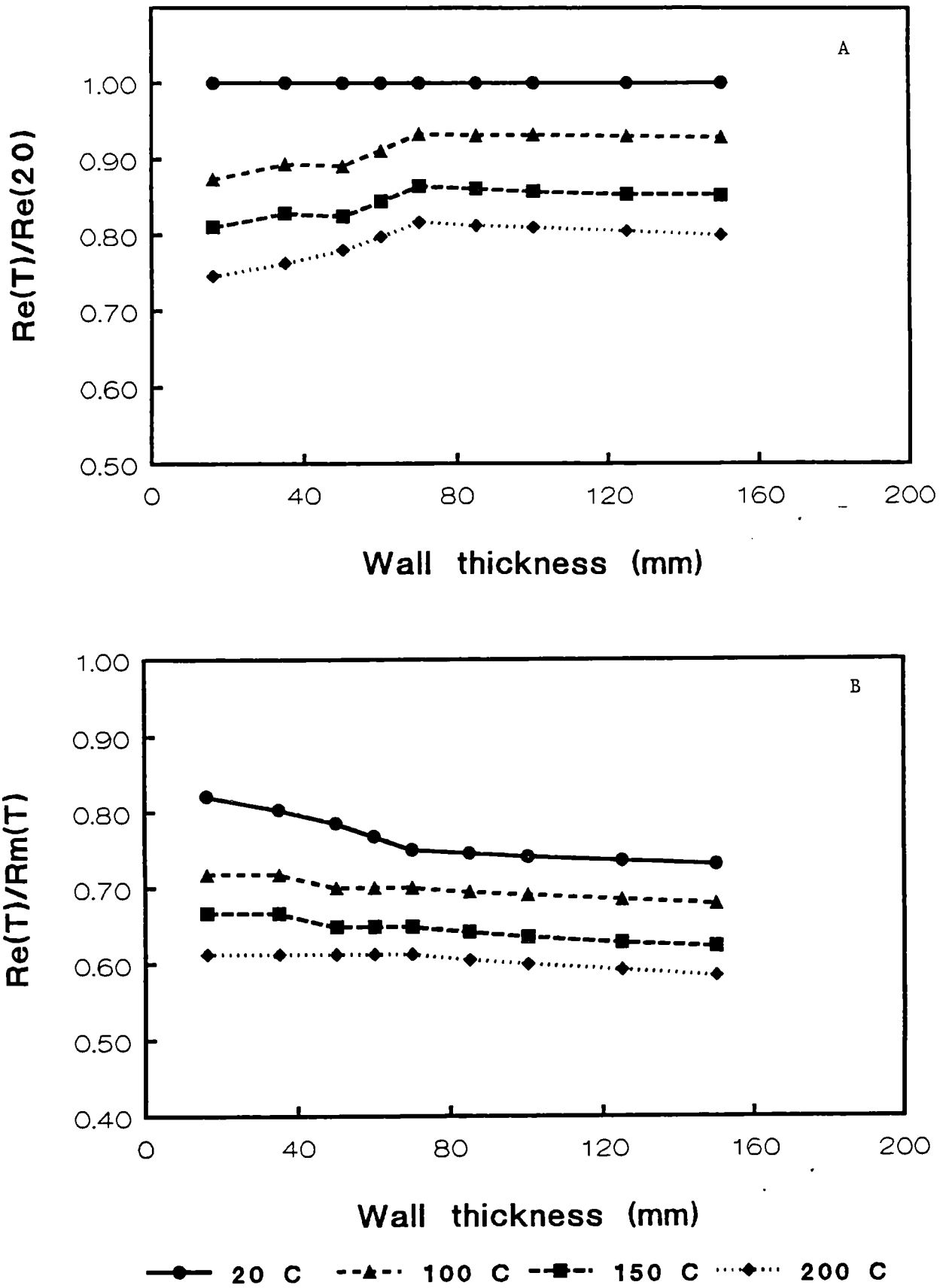

Figure A4.2: Re(T)/Re(20) (A) and Re(T)/Rm(T) (B) as a function of wall thickness and temperature for FeE 460.

APPENDIX 5

Applications of High Strength Steel in Bridges

Introduction

A research programme is carried out at the TNO Metals Research Institute on High Strength Steel. The programme consisted of activities concerning the quality of and the welding with High Strength Steel as well as activities concerning the application of this type of steel in various types of structures.

To test the advantages and disadvantages of High Strength Steel in different type of structures, some company's were asked to make comparative designs with steel FeE 355 and with HSS FeE 450 QT. Rijkswaterstaat Directie Bruggen was asked to make this comparison for bridges.

In order to do so, an actual design project was chosen, in which two details of the structure were redesigned in High strength Steel.

The project chosen is the design of the bridge over the river the Waal near Zaltbommel. The design of the bridge has been split into two parts. The first part is the crossing of the river, the second part is the crossing of the outer arches.

For both parts designs are being made. A main span in steel and an outer march crossing in steel-concrete composite.

For both designs a redesign was made wherein some of the FeE355 details were replaced by FeE 450 QT with a reduced area.

Application of High Strength Steel in the main span

The main span design is a cable stayed bridge with a total length of 384 meters, a mid span of 256 meters and two side spans of 64 meters (see figure 1).

The design of the different main-construction-parts, the deckplate, the longitudinal stiffeners of the deckplate, the crossbeams, the main beams, the stay cables and the pylons is based upon the design criteria strength, fatigue, stability and stiffness. The use of High Strength Steel is most effective when strength is the main design criterium. In steel bridges, however, in most parts strength is not or not alone the main design criterium.

The lower flange and the web of the crossbeams were chosen in this study, because strength is the main design criterium for these parts. Stability and fatigue however, are also of importance. To use the higher yield strength of the FeE 460, the cross section of the lower flange was reduced to 75% (355/460 = 0.77) of this original cross section. The web thickness was kept constant.
The results of this study are as follows:

- An increase of the stress range in the cross beams by approximately 20%. Based on an estimation of the actual traffic loads, the fatigue life of the cross beams decreases from 150 years in the FeE 355 design to 65 years in the HS-steel design. The required lifetime of the bridge is 75 years.
- The decrease of the stiffness of the cross beam leads to larger relative deflections in the deck and thus to a greater change of problems with the asphalt wearing surface.
- The decrease of the stiffness of the cross beams leads to a 5% larger stress range in the longitudinal stiffness of the deckplate which gives a decrease in the fatigue life of about 15%. The longitudinal stiffness have already been designed for fatigue, so this leads to a redesign (thicker materials) of these constructional parts.
- When both the flange and the web are replaced by FeE 450 QT there is no positive price effect due to the fact that the reduced area multiplied by the increased material price remain constant in comparison with the FeE 355 design.
- The zero price effect is caused by the fact that the web of the cross beam also has to be made in FeE 450 QT to meet the safety requirements of the Dutch standards. When the web could be made of FeE 360, the total project cost would decrease appr. 0.2%.

The conclusion of this part of the study is that the use of High Strength Steel in these cross beams has no advantages.

Application of High Strength Steel in the composite outer marches spans

An study of the use of High Strength Steel in composite bridges has been made.

The structure consists of eleven parallel simply supported steel beams with a span of appr. 60 meters in the length of the structure with a concrete deck. The connection between the steel beams and the concrete is made by studs (see figure 2).

The original design has been based on FeE 355. An alternative design was made based on a reduced cross section of the lower flange to 80% (ratio between the yield strengths of the two materials) of the original value and the same web thickness, but using High Strength Steel FeE 450 QT for both. This design shows a more or less similar load deflection behaviour (see figure 3) which means that the safety on collapse remains constant. Taking into account a higher price for the High Strength Steel the total cost rise 0.4%. The negative price effect is caused by the fact that the web of the beams also has to be made in FeE 450 QT to meet the safety requirements of the Dutch standards. When the web could be made of FeE 360, the total project cost would decrease appr. 1%.
An additional cost factor was that during the redesigning it came out that the decrease of the lower flange led to an increase in the thickness of the concrete deck.

The conclusion of this part of the investigation can be that the use of High Strength Steel in this composite design does not give great advantages.

LOAD DEFLECTION DIAGRAM STEEL CONCRETE BRIDGE

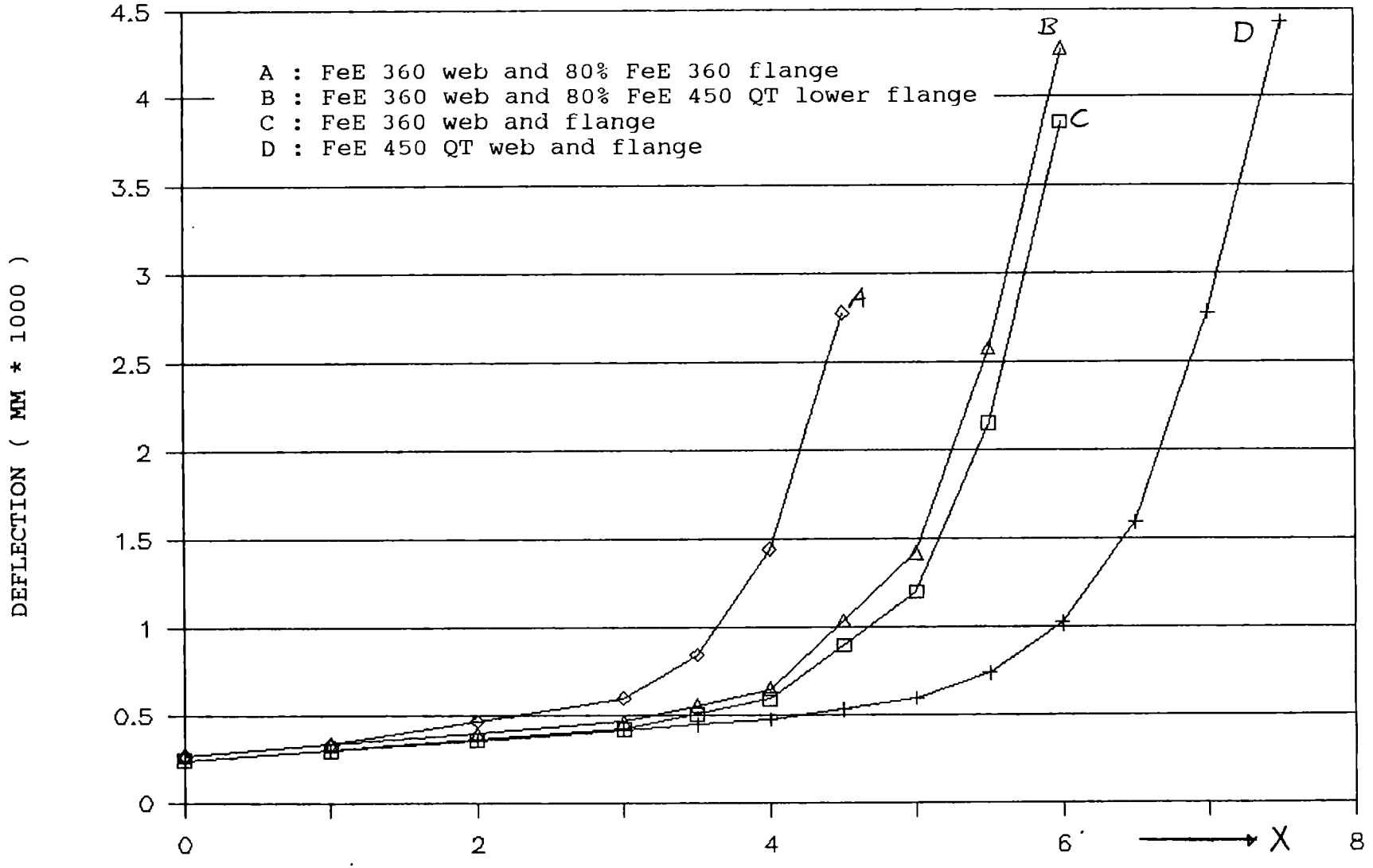

FIGURE 3

DEAD LOAD + VEHICLE LOAD + X * TRAFFIC LOAD

European Commission

EUR 15807 — Properties and service performance
Application of FeE460, a comparative investigation towards normalized, quenched and tempered, and thermomechanically treated steel types

J. Vuik, J. Van Wortel

Luxembourg: Office for Official Publications of the European Communities

1996 — XIV, 220 pp. — 21.0 x 29.7 cm

Technical steel research series

ISBN 92-827-7200-4

Price (excluding VAT) in Luxembourg: ECU 23

In this summary, the items that have been investigated and the main results of the research contract 7210/KA/607-F1.3/88, 'Application of FeE460, a comparative investigation towards normalized, quenched and tempered, and thermomechanically treated steel types' are described.

The steels mentioned before have been investigated (in plate thicknesses 15 and 50 mm) on the items:

a) mechanical properties and microstructure after a weld thermal simulation;

b) cold cracking susceptibility;

c) mechanical properties of test welds;

d) mechanical properties after deformation at different temperatures;

e) calculation of the price-effect of application of FeE460 instead of FeE355.

The results of the weld thermal simulation programme established that acceptable hardness values and good Charpy-V notch toughness properties can be obtained with all three steels. PWHT at temperatures of 560° or 590° C reduced the fracture energies of the QT material, and deteriorated the properties of the N and TM material. An acceptable PWHT temperature is 530° C. At high PWHT temperatures, all materials fractured intergranulaly (at low test temperatures). This has been associated with segregation of P to former austenite grain boundaries. At higher test temperatures the presence of V carbonitrides further reduces the Charpy-V fracture energy for the materials TM and N.

Venta • Salg • Verkauf • Πωλήσεις • Sales • Vente • Vendita • Verkoop • Venda • Myynti • Försäljning

BELGIQUE / BELGIË

Moniteur belge/
Belgisch Staatsblad

Rue de Louvain 42/Leuvenseweg 42
B-1000 Bruxelles/B-1000 Brussel
Tél. (02) 512 00 26
Fax (02) 511 01 84

Jean De Lannoy

Avenue du Roi 202/Koningslaan 202
B-1060 Bruxelles/B-1060 Brussel
Tél. (02) 538 51 69
Fax (02) 538 08 41

Autres distributeurs/
Overige verkooppunten:

Librairie européenne/
Europese boekhandel

Rue de la Loi 244/Wetstraat 244
B-1040 Bruxelles/B-1040 Brussel
Tél. (02) 231 04 35
Fax (02) 735 08 60

Document delivery:

Credoc

Rue de la Montagne 34/Bergstraat 34
Boîte 11/Bus 11
B-1000 Bruxelles/B-1000 Brussel
Tél. (02) 511 69 41
Fax (02) 513 31 95

DANMARK

J. H. Schultz Information A/S

Herstedvang 10-12
DK-2620 Albertslund
Tlf. 43 63 23 00
Fax (Sales) 43 63 19 69
Fax (Management) 43 63 19 49

DEUTSCHLAND

Bundesanzeiger Verlag

Postfach 10 05 34
D-50445 Köln
Tel. (02 21) 20 29-0
Fax (02 21) 2 02 92 78

GREECE/ΕΛΛΑΔΑ

G.C. Eleftheroudakis SA

International Bookstore
Nikis Street 4
GR-10563 Athens
Tel. (01) 322 63 23
Fax 323 98 21

ESPAÑA

Mundi-Prensa Libros, SA

Castelló, 37
E-28001 Madrid
Tel. (91) 431 33 99 (Libros)
431 32 22 (Suscripciones)
435 36 37 (Dirección)
Fax (91) 575 39 98

Boletín Oficial del Estado

Trafalgar, 27-29
E-28071 Madrid
Tel. (91) 538 22 95
Fax (91) 538 23 49

Sucursal:

Librería Internacional AEDOS

Consejo de Ciento, 391
E-08009 Barcelona
Tel. (93) 488 34 92
Fax (93) 487 76 59

Librería de la Generalitat
de Catalunya

Rambla dels Estudis, 118 (Palau Moja)
E-08002 Barcelona
Tel. (93) 302 68 35
Tel. (93) 302 64 62
Fax (93) 302 12 99

FRANCE

Journal officiel
Service des publications
des Communautés européennes

26, rue Desaix
F-75727 Paris Cedex 15
Tél. (1) 40 58 77 01/31
Fax (1) 40 58 77 00

IRELAND

Government Supplies Agency

4-5 Harcourt Road
Dublin 2
Tel. (1) 66 13 111
Fax (1) 47 52 760

ITALIA

Licosa SpA

Via Duca di Calabria 1/1
Casella postale 552
I-50125 Firenze
Tel. (055) 64 54 15
Fax 64 12 57

GRAND-DUCHÉ DE LUXEMBOURG

Messageries du livre

5, rue Raiffeisen
L-2411 Luxembourg
Tél. 40 10 20
Fax 49 06 61

NEDERLAND

SDU Servicecentrum Uitgeverijen

Postbus 20014
2500 EA 's-Gravenhage
Tel. (070) 37 89 880
Fax (070) 37 89 783

ÖSTERREICH

Manz'sche Verlags-
und Univeraitätsbuchhandlung

Kohlmarkt 16
A-1014 Wien
Tel. (1) 531 610
Fax (1) 531 61-181

Document delivery:

Wirtschaftskammer

Wiedner Hauptstraße
A-1045 Wien
Tel. (0222) 50105-4356
Fax (0222) 50206-297

PORTUGAL

Imprensa Nacional — Casa da Moeda, EP

Rua Marquês Sá da Bandeira, 16-A
P-1099 Lisboa Codex
Tel. (01) 353 03 99
Fax (01) 353 02 94/384 01 32

Distribuidora de Livros
Bertrand, Ld.ª

Grupo Bertrand, SA

Rua das Terras dos Vales, 4-A
Apartado 37
P-2700 Amadora Codex
Tel. (01) 49 59 050
Fax 49 60 255

SUOMI/FINLAND

Akateeminen Kirjakauppa

Akademiska Bokhandeln
Pohjoisesplanadi 39 / Norra esplanaden 39
PL / PB 128
FIN-00101 Helsinki / Helsingfors
Tel. (90) 121 4322
Fax (90) 121 44 35

SVERIGE

BTJ AB

Traktorvägen 11
Box 200
S-221 00 Lund
Tel. (046) 18 00 00
Fax (046) 18 01 25

UNITED KINGDOM

HMSO Books (Agency section)

HMSO Publications Centre
51 Nine Elms Lane
London SW8 5DR
Tel. (0171) 873 9090
Fax (0171) 873 8463

ICELAND

BOKABUD
LARUSAR BLÖNDAL

Skólavördustíg, 2
IS-101 Reykjavik
Tel. 551 56 50
Fax 552 55 60

NORGE

NIC Info a/s

Boks 6512 Etterstad
0606 Oslo
Tel. (22) 57 33 34
Fax (22) 68 19 01

SCHWEIZ/SUISSE/SVIZZERA

OSEC

Stampfenbachstraße 85
CH-8035 Zürich
Tel. (01) 365 54 49
Fax (01) 365 54 11

BĂLGARIJA

Europress Klassica BK Ltd

66, bd Vitosha
BG-1463 Sofia
Tel./Fax (2) 52 74 75

ČESKÁ REPUBLIKA

NIS ČR

Havelkova 22
CZ-130 00 Praha 3
Tel./Fax (2) 24 22 94 33

HRVATSKA

Mediatrade

P. Hatza 1
HR-4100 Zagreb
Tel./Fax (041) 43 03 92

MAGYARORSZÁG

Euro-Info-Service

Európa Ház
Margitsziget
H-1138 Budapest
Tel./Fax (1) 111 60 61, (1) 111 62 16

POLSKA

Business Foundation

ul. Krucza 38/42
PL-00-512 Warszawa
Tel. (2) 621 99 93, 628 28 82
International Fax&Phone (0-39) 12 00 77

ROMÂNIA

Euromedia

65, Strada Dionisie Lupu
RO-70184 Bucuresti
Tel./Fax 1-31 29 646

RUSSIA

CCEC

9,60-letiya Oktyabrya Avenue
117312 Moscow
Tel./Fax (095) 135 52 27

SLOVAKIA

Slovak Technical
Library

Nàm. slobody 19
SLO-812 23 Bratislava 1
Tel. (7) 52 204 52
Fax (7) 52 957 85

CYPRUS

Cyprus Chamber of Commerce
and Industry

Chamber Building
38 Grivas Dhigenis Ave
3 Deligiorgis Street
PO Box 1455
Nicosia
Tel. (2) 44 95 00, 46 23 12
Fax (2) 36 10 44

MALTA

Miller Distributors Ltd

PO Box 25
Malta International Airport LQA 05 Malta
Tel. 66 44 88
Fax 67 67 99

TÜRKIYE

Pres AS

Dünya Infotel
TR-80050 Tünel-Istanbul
Tel. (1) 251 91 90/251 96 96
Fax (1) 251 91 97

ISRAEL

Roy International

17, Shimon Hatarssi Street
P.O.B. 13056
61130 Tel Aviv
Tel. (3) 546 14 23
Fax (3) 546 14 42

Sub-agent for the Palestinian Authority:

INDEX Information Services

PO Box 19502
Jerusalem
Tel. (2) 27 16 34
Fax (2) 27 12 19

EGYPT/ MIDDLE EAST

Middle East Observer

41 Sherif St.
Cairo
Tel/Fax (2) 393 97 32

UNITED STATES OF AMERICA/ CANADA

UNIPUB

4611-F Assembly Drive
Lanham, MD 20706-4391
Tel. Toll Free (800) 274 48 88
Fax (301) 459 00 56

CANADA

Subscriptions only
Uniquement abonnements

Renouf Publishing Co. Ltd

1294 Algoma Road
Ottawa, Ontario K1B 3W8
Tel. (613) 741 43 33
Fax (613) 741 54 39

AUSTRALIA

Hunter Publications

58A Gipps Street
Collingwood
Victoria 3066
Tel. (3) 9417 53 61
Fax (3) 9419 71 54

JAPAN

Procurement Services Int. (PSI-Japan)

Kyoku Dome Postal Code 102
Tokyo Kojimachi Post Office
Tel. (03) 32 34 69 21
Fax (03) 32 34 69 15

Sub-agent:

Kinokuniya Company Ltd
Journal Department

PO Box 55 Chitose
Tokyo 156
Tel. (03) 34 39-0124

SOUTH and EAST ASIA

Legal Library Services Ltd

Orchard
PO Box 0523
Singapore 9123
Tel. 243 24 98
Fax 243 24 79

SOUTH AFRICA

Safto

5th Floor, Export House
Cnr Maude & West Streets
Sandton 2146
Tel. (011) 883-3737
Fax (011) 883-6569

ANDERE LÄNDER OTHER COUNTRIES AUTRES PAYS

Office des publications officielles
des Communautés européennes

2, rue Mercier
L-2985 Luxembourg
Tél. 29 29-1
Télex PUBOF LU 1324 b
Fax 48 85 73, 48 66 17

CG-NA-15807-EN-C

NOTICE TO THE READER

All scientific and technical reports published by the European Commission are announced in the monthly periodical **'euro abstracts'**. For subscription (1 year: ECU 63) please write to the address below.

Price (excluding VAT) in Luxembourg: ECU 23

ISBN 92-827-7200-4

OFFICE FOR OFFICIAL PUBLICATIONS
OF THE EUROPEAN COMMUNITIES

L-2985 Luxembourg